

Master's thesis: Humanoid robot for sign language

Candidates: Guy Fierens, Stijn Huys, Jasper Slaets

Thesis supervisors

Internal	Ing. Erwin Smet
External	Dr. Joost Van Dinther

2014-2015

Masterproef tot het behalen van het diploma

Master of Science in de industriële wetenschappen: Elektromechanica

Master's thesis: Humanoid robot for sign language

Candidates: Guy Fierens, Stijn Huys, Jasper Slaets

Thesis supervisors

Internal	Ing. Erwin Smet
External	Dr. Joost Van Dinther

2014-2015

Masterproef tot het behalen van het diploma

Master of Science in de industriële wetenschappen: Elektromechanica

Abstract

In Flanders, one in a thousand children is born deaf. Together with the people who become deaf by a medical condition like head traumas, meningitis or sudden changes of pressure when flying or diving we get a continuously growing group in our society, currently consisting of more than 60.000 people in Flanders. Expanding this thought to a global level, we can see that the deaf society represents 70 million people according to the World Federation of the Deaf.

In order to reduce the communication gap between the hearing and the deaf this paper will discuss the design of a humanoid robot which can serve as a sign language translator between the two communities. By studying state of the art technologies a design will be created that is:

- easy to assemble,
- not too expensive,
- usable for people with a minimal knowledge level in robotics.

A first phase of the project will consist of building one single arm in order to spell words of the Flemish sign language and count from one to ten. After this, the setup can be expanded to a dual arm robot in order to perform the complete Flemish sign language. This work will handle the design of the single arm robot.

Assignments

GUY FIERENS

Universiteit Antwerpen

Opdrachtomschrijving Masterproef

Elektronische aansturing en modelvorming van een humane robot voor gebarentaal

Probleemstelling en motivatie

In Vlaanderen wordt 1 op 1000 kinderen doof geboren. Hierbij komen ook de mensen door een aandoening doof worden, wat de dovengemeenschap een groeiende bevolkingsgroep maakt die momenteel 60 000 mensen telt. (bron Fevlado) Om de communicatiekloof tussen doven en horenden te verkleinen willen wij een goedkope en makkelijk te gebruiken robotarm bouwen. Deze robot kan dan gebarentolk zijn tussen beide partijen. Door een kinematisch bewegingsmodel te ontwerpen kunnen we de robot via een microcontroller aansturen. Mechanisch wordt de robot ontworpen door 2 medestudenten.

Doelstellingen

- Studie naar de anatomie van de menselijke arm (gewrichten, spieren en botten). Nadruk ligt hier bij vrijheidsgraden en constraints. (eind september 2014)
- Kiezen van een geschikte wiskundige oplosmethode. (midden oktober 2014)
- Analyse naar de werking van de gekozen oplosmethode. (eind oktober 2014)
- Onderzoek naar elektronische aansturing (stuklijst, schakelingen). (februari 2015)
- Opstellen van het kinematisch model en het testen hiervan in simulatiesoftware. (midden maart 2015)
- Testen en implementeren van het bewegingsmodel in de mechanisch afgewerkte robotarm. (april/mei 2015)
- Monteren van elektronica (sensoren en controller). (april/mei 2015)

Deliverables

- een analyse van de anatomische opbouw van de menselijke arm
- een grondige literatuurstudie
- een gevalideerd model, methodiek...
- een animatie
- een prototype

Opdrachtschrijving Masterproef

Mechanische realisatie van een humane robot voor gebarentaal

Probleemstelling en motivatie

Voor doven is het niet altijd even gemakkelijk om deel te nemen aan dagdagelijkse activiteiten. Door middel van de robotarm willen wij het mogelijk maken om doven, bijvoorbeeld in een normale klas, les te laten volgen zonder dat hier een extra tolk moet bij zijn. Alles zal zo ontworpen worden dat de gehele arm afgedrukt kan worden met behulp van een 3D-printer zodat het ook mogelijk is voor gezinnen, die geen ervaring hebben met gebarentaal, om onze robot zelf goedkoop en eenvoudig in elkaar te steken en zo makkelijker met het dove familielid te kunnen (leren) communiceren. Op wetenschappelijk en technisch vlak willen we vooral kijken naar de mogelijkheden qua snelheid, duidelijkheid en juistheid van de gebaren. Mijn taak zal bestaan uit het onderzoek naar verschillende bestaande modellen van robotarmen en makkelijke productie- en assemblagemogelijkheden. Aan de hand van die opgedane kennis zal ik onze eigen robot zo goedkoop en efficiënt mogelijk ontwerpen, rekening houdend met bijvoorbeeld materiaalbesparing, materiaaleigenschappen en een enigszins beperkte sterktesimulatie. Samen met de 2 medestudenten zullen we, mits er de nodige sponsoring wordt gevonden, daarna een eerste model beginnen bouwen.

Doelstellingen

- Studie naar reeds bestaande modellen en technologieën binnen het kader van robotarmen (eind oktober 2014)
- Studie naar de meest geschikte 3D-printtechniek en een daar bijhorende 3D-printer met mogelijkheid tot het printen van het juiste materiaal, passend bij ons project (eind oktober 2014)
- Studie naar makkelijke assemblagemogelijkheden (eind oktober 2014)
- Zoektocht naar een gemotiveerde sponsor voor het project en opstart van webpagina en sociale media (eind november 2014)
- Eerste prototypetekening (midden december 2014)
- (Enigszins beperkte) sterktesimulatie (eind september 2014)
- Prototype aanpassen zodat de onderdelen van de andere teamleden correct geplaatst kunnen worden, mogelijke materiaalbesparingen toepassen en pijnpunten uit de sterktesimulatie aanpakken (midden februari 2015)
- Aangepaste 3D-tekeningen afdrukken met aangekochte 3D-printer (eind februari 2015)
- Assemblage en testperiode (eind maart 2015)
- Optimalisatie, aanpassingen en aanpak van problemen (midden mei 2015)
- Afwerken van het naar buiten te brengen prototype (eind mei 2015)

Opdrachtomschrijving masterproef

Mechanische aansturing van een humane robot voor gebarentaal

Probleemstelling en motivatie

Het is bewezen dat 1 op 1000 kinderen doof geboren worden. Daar komen dan ook nog eens mensen bij die doof worden door een aandoening. Omdat deze groep mensen in aantal blijft toenemen, is het noodzakelijk dat ook zij kunnen blijven deelnemen aan de bevolkingsgemeenschap. Een robot die spraak omzet naar gebarentaal zou hiervoor al een oplossing kunnen bieden. Niet alleen in thuisomgeving, maar ook op openbare plaatsen kan het de communicatie sterk verbeteren. Dit zonder dat men extra personeel moet aanwerven die als tolk functioneert. Om deze robot te kunnen realiseren hebben we het werk in 3 delen opgesplitst: Structuur, aansturing en een kinematisch model. Het is naderhand logisch dat een robot kan niet alleen functioneren met een structuur en een kinematisch model. Het is dus noodzakelijk dat we naar een efficiënte manier van aansturen gaan zoeken. Onderzoek doen naar verschillende methoden, met zijn eigen voor- en nadelen is dus een 'must'. Ook gebruiksgemak en betaalbaarheid zijn belangrijke factoren bij het bepalen van de aansturing. Hulpmiddelen zoals "Gravity compensation" worden ook naderhand bekeken of ze al dan niet kunnen toegepast worden.

Doelstellingen

- Studie naar anatomie van de menselijke arm (botten, gewrichten en spieren) in verband met noodzakelijke, te realiseren bewegingen. (eind september 2014)
- Studie naar Vlaamse gebarentaal + analyse van elke letter apart. (eind september 2014)
- Onderzoek naar voordeel en/of nut van "Gravity compensation" (eind oktober 2014)
- Onderzoek naar methode van aansturing + analyse op voor- en nadelen (eind november 2014)
- Testen op aansturing robotarm (eind februari 2015)
- Realisatie robotarm (eind april 2015)

Deliverables

- een grondige literatuurstudie
- een grondige studie naar de gebarentaal
- een analyse van "Gravity compensation"
- een gevalideerde aanstuur methodiek
- een prototype

Introduction

With the continuously growing population of hearing impaired, a new way of communication between the two populations needs to be presented in order to reduce the current communication barrier. As an open source, affordable and easy to use application, the Aslan robot presents a solution for this problem. By limiting the cost of a functional humanoid robot, the product stays accessible for the broad public.

The Aslan robot can serve in a number of application as a sign language translator ranging from applications in health care to applications at in classes or at home.

Only recently, a standardized version of the Flemish sign language has been created. But due to the lack of teachers and sign language courses, the spreading and integration of the standardized Flemish sign language knows a moderate progress. In many cases, for example when hearing parents have a deaf child, the family develops a form of sign language themselves. For domestic use, the personal sign language suffices, but when trying to communicate with third parties the communication will deteriorate.

In combination with its use as a sign language translator, the Aslan robot can serve as a sign language teacher. When combined with a human teacher, the robot can perform the right symbols, enabling the teacher of a more personal guidance of the students. This will improve the overall quality of the course, as well as enabling to teach the sign language to a larger number of people without extra teachers.

We would like to thank the following persons for being a part of this newly introduced project:

Erwin Smet – For the knowledge, guidance, support and feedback throughout the year.

Joost Van Dinther – For his trust and belief in our project, and for making this project possible.

Bram Vanderborcht – For his guidance, advice and knowledge in the first weeks of the project.

Sanne Van Der Donck – For the introduction into the Flemish sign language.

MobilAnt – For the information regarding the deaf community.

Felix Rijkers – For his help with designing the website.

Trideus/Jesse Buteneers – For sponsoring printing materials.

Walter Janssens, Frank Haemels, Laurent Keersmaeckers, Augustinus De Winter, Jean-Pierre Smet – For support regarding questions about their specific fields of research.

In order to guide the reader through the design process, the chapters have been put in an order which describes the aspects of the design chronologically. A brief content of the different chapters can be found below.

Chapter 1: Human anatomy of the upper extremities – Guy Fierens

In the first chapter of this work we will take a look at the mother of all designs regarding humanoid robotics: the human body itself. By analyzing the bone structure, as well as the different joints and the muscles we get a general idea of how to build a humanoid robot arm.

Chapter 2: Convention and abbreviations used in this work– Guy Fierens

This chapter handles the different coordinate systems in our setup. Local and global coordinate systems are defined for the arm as well as an index convention of the different joints.

Chapter 3: Flemish sign language alphabet – Jasper Slaets

This chapter gives an introduction to the Flemish sign language alphabet. The signs will be analyzed and translated to the necessary degrees of freedom. To simplify the actuation it is vital to reduce the amount of degrees of freedom.

Chapter 4: Inverse kinematics – Guy Fierens

Using inverse kinematics, a mathematical model can be created to control the robot arm. After explaining the inverse kinematic problem, this part will compare six commonly used solving methods and evaluate these regarding our application.

Chapter 5: Mechanics – Jasper Slaets

To understand the mechanics behind the application, it is necessary to choose the right actuation method, actuation structure and actuators. For this reason these aspects will be extensively handled. Because a remote actuation cable system seems best, cables will be discussed as well.

Chapter 6: Communication and position feedback – Guy Fierens

The human arm has a large number of degrees of freedom. In order to show all the gestures of the Flemish sign language, a lot of these need to be actuated. To be able to use a large amount of motors, in combination with the appropriate sensors, multiple devices will have to cooperate. Chapter 6 will discuss the I²C network, a frequently used networking protocol, in combination with the decision analysis regarding the electrical components responsible for reading the sensors.

Chapter 7: Prototyping and rapid modeling – Stijn Huys

This chapter handles the different types of fabrication to create the robotic arm, going from milling to 3D-printing. The best method and machine will be determined to fabricate and shape every piece. Once the fabrication method has been chosen, the settings and environment will be discussed.

Chapter 8: Mechanical design – Stijn Huys

This chapter covers the complete process of designing the complete humanoid arm. Research will be done to learn more about existing robotic hands, all parts will be dimensioned and everything will be optimized to create a working product.

Chapter 9: System architecture and programming – Guy Fierens

When designing and writing a complex, extensive program it is important to maintain a well-defined structure in order to keep the program as clear as possible. In chapter 9, this design or architecture is explained. Besides the system architecture this chapter will also handle the programming of the robot, including the different movement functions and a symbolic table.

Chapter 10: Electrical design - Guy Fierens

In addition to the software, the hardware of the Aslan robot needs to be designed. Chapter 10 will discuss the electrical design of the robot. This implies the integration of all the hardware components like the Arduino microcontroller, the servo controller, fuses and a stabilized power supply. All these components shall be discussed and then selected.

Chapter 11: Organization of the project

Since this is a completely new project for the University of Antwerp, a lot of arrangements had to be made in order to make the physical realization of the robot possible. The organization of the project has been a time-consuming part of the project, and is therefore definitely worth mentioning in this paper.

TABLE OF CONTENTS

Abstract	4
Assignments	5
Guy Fierens.....	5
Stijn Huys.....	7
Jasper Slaets	9
Introduction.....	11
List of images.....	21
List of tables	25
List of symbols	27
List of abbreviations	27
List of symbols.....	28
List of programming variables.....	29
1. Human anatomy of the upper extremities.....	30
1.1 Introduction.....	30
1.2 Glossary of terms [1]	30
1.3 Bones in the upper extremities [1], [2]	31
1.3.1 Humerus	31
1.3.2 Ulna and radius.....	31
1.3.3 Carpus.....	32
1.3.4 Metacarpus.....	32
1.3.5 Phalanges.....	32
1.4 Joints in the human body [1], [2]	33
1.5 Movements in synovial joints [1]	34
1.6 Types of synovial joints [1]	35
1.7 Most important synovial joints in our setup [1], [2]	36
1.8 Constraints in the upper extremities. [4]	37
1.9 Muscles and tendons in the upper extremities [1], [2].....	39
1.10 Conclusion	39
2. Convention and abbreviations used in the further course of this work [2], [3].....	40
2.1 Introduction.....	40
2.2 Global coordinate system.....	40
2.3 Local coordinate system.....	40
2.4 Joint indices	41
2.5 Conclusion	41
3. The Flemish sign language alphabet	43

3.1	Introduction.....	43
3.2	Some fundamental characters	43
3.3	degrees of freedom Analysis	44
3.4	Reducing degrees of freedom	44
3.5	Conclusion	45
4.	Inverse Kinematics.....	46
4.1	Introduction.....	46
4.2	List of frequently used symbols.....	46
4.3	Inverse kinematics.....	46
4.4	Redundancy.....	47
4.5	Different solving methods.....	48
4.5.1	Algebraic methods.....	48
4.5.2	Iterative methods.....	48
4.6	Conclusion	51
5.	Mechanics.....	52
5.1	Introduction.....	52
5.2	Movement system.....	52
5.2.1	Methods	52
5.2.2	Joints [13]	55
5.2.3	Actuation Architecture [10].....	57
5.2.4	Conclusion	59
5.3	Pre-calculations	60
5.3.1	Introduction.....	60
5.4	Actuators	62
5.5	Requirements electrical motors.....	62
5.5.1	Choosing the right electrical motor.....	62
5.5.2	Stepper motors [15]	63
5.5.3	RC Servomotors	66
5.5.4	Conclusion	71
5.6	Post-calculations.....	71
5.6.1	Transmission.....	71
5.6.2	Force on cables and locations [22].....	72
5.6.3	Real values.....	73
5.7	Conclusion	75
5.8	Cables	75
5.8.1	Kind of material	75

5.8.2	Extension [28].....	77
5.8.3	Extension & reduction in the system	79
5.8.4	Actual system reduction & extension	82
5.8.5	Designing the cable system	82
5.8.6	Conclusion	88
6.	Communication and position feedback	89
6.1	Introduction.....	89
6.2	I ² C- bus communication	89
6.3	Position feedback	91
6.3.1	Defining every option	92
6.3.2	Conclusion: Choosing the best option.....	94
7.	Prototyping and rapid modeling	95
7.1	Introduction.....	95
7.2	Milling.....	95
7.3	3D-printing.....	96
7.3.1	Introduction.....	96
7.3.2	Types of additive manufacturing.....	97
7.3.3	Stereolithography.....	97
7.3.4	Polyjet.....	98
7.3.5	Selective Laser Sintering.....	99
7.3.6	Fused Deposition Modeling.....	100
7.3.7	Conclusion	105
7.4	Final conclusion of the research.....	105
7.5	Choice of additive fabrication and device	105
7.6	Attending RapidPro: 3D-printing convention.....	106
7.7	Properties chosen printer.....	107
7.8	Cura software	108
7.9	Development of the settings.....	109
7.10	Design rules for 3D-printing	110
7.11	Printing times	113
7.12	Material	113
7.13	Filament.....	114
7.14	Print bed	115
7.15	Problems.....	115
7.16	Meshmixer.....	117
7.17	Final conclusion	118

8.	Mechanical design.....	119
8.1	Introduction.....	119
8.2	Existing humanoid arms	119
8.2.1	Introduction.....	119
8.2.2	Anthromorphic 20-DOF Robotic Hand	119
8.2.3	TBM–Hand.....	120
8.2.4	DLR Arm Hand System.....	120
8.2.5	Tuat/Karlsruhe hand.....	121
8.2.6	Gifu III Hand.....	121
8.2.7	IH2 Azzurra Hand.....	122
8.2.8	Open Hand Project	122
8.2.9	Inmoov Robot	123
8.2.10	MA-I Hand.....	123
8.2.11	Conclusion	123
8.3	Adapting existing technologies	124
8.3.1	Introduction.....	124
8.3.2	Adapting a prosthetic arm.....	124
8.3.3	Adapting a robotic spider	125
8.3.4	Conclusion	125
8.4	Dimensions of the human arm.....	126
8.4.1	Introduction.....	126
8.4.2	General	126
8.4.3	Conclusion	126
8.5	Mechanical design of Project Aslan.....	127
8.5.1	Introduction.....	127
8.5.2	Dimensions of the parts	127
8.5.3	Snap-on joints.....	130
8.5.4	Design of the thumb.....	131
8.5.5	Design of the adduction and abduction of the index finger	132
8.5.6	Design of the wrist.....	133
8.5.7	Open design with lids	135
8.5.8	Assembling the arm.....	135
8.6	Simulations	136
8.7	Conclusion	136
9	System architecture and programming.....	137
9.1	Introduction.....	137

9.2	General system architecture	137
9.3	Flemish sign language.....	140
9.3.1	Movement timing.....	140
9.3.2	Gesture decomposition	140
9.4	Software safety.....	141
9.5	Programming.....	141
9.5.1	List of used symbols.....	141
9.5.2	Programming log	142
9.5.3	Programming with the Designer Systems DS-DSX18.S servo driver	142
9.6	Conclusion	142
10	Electrical design.....	143
10.1	Introduction.....	143
10.2	Components	143
10.2.1	Microcontroller.....	143
10.2.2	Servo controller	144
10.2.3	Stabilized power supply.....	145
10.2.4	Servo motors and position feedback.....	145
10.3	Practical realisation of the I ² C network.....	146
10.4	Electrical design.....	146
10.4.1	Fuses	146
10.4.2	Heat dissipation.....	147
10.4.3	Connectors	147
10.5	Casing design	149
10.6	Servo motor distribution	151
10.7	Conclusion	151
11	Organization of the project	152
11.1	Introduction.....	152
11.2	Naming the project.....	152
11.2.1	Naming the project.....	152
11.2.2	Designing a logo	152
11.3	Determination of the budget	153
11.4	Sponsorship	153
11.4.1	Finding a sponsor.....	153
11.4.2	About our sponsor.....	153
11.4.3	Sponsorship and contracts	154
11.4.4	Planning of our time in the Skillslab	154

11.4.5	Sponsoring by Trideus	154
11.5	Public relations	154
11.5.1	Website.....	154
11.5.2	Demo model at the open house.....	155
11.6	Placing/tracking Orders and financial matters.....	155
11.7	Conclusion	155
Conclusion	156
Annexes	166
Annex 1: muscles in the upper extremities.....		166
Muscles responsible for shoulder movement.....		166
Muscles responsible for elbow movement		166
Muscles responsible for wrist movement		167
Muscles responsible for hand movement.....		167
Annex 2: Flemish sign language alphabet.....		168
Annex 3: Volume experiment.....		179
Annex 4: torque Estimation.....		181
Annex 5: RC servo motors		182
Annex 6: Estimated minimum distances		184
Annex 7: Properties Dyneema, nylon and stainless steel		185
Dyneema.....		185
Nylon 6.....		187
Stainless steel		190
Annex 8: Details measurements PIP joint little finger.....		191
Annex 9: Details measurement MCP joint pointer finger		193
Annex 10: Detail measurements TMC joint thumb.....		196
Annex 11: Location actuators.....		198
Annex 12: Design cable system in arm.....		199
Annex 13: Control by approach.....		210
Annex 14: Stereolithography: Properties and materials.....		218
Annex 15: Polyjet: Properties and materials		224
Annex 16: ABS and PLA properties [66]		225
Annex 17: Specific printing times		230
Annex 18: Joint angles.....		231
Annex 19: Ranked positions		232
Annex 20: Programming log		234
Software safety.....		234

Aslan	234
Motor calibration	235
Servo testing.....	235
Annex 21: Decision analysis	236
21.1 Decision matrix Fused Deposition Modeling printer.....	236
21.2 Analytical Hierarchy Process with Saaty's scale of relative importance	237
Annex 22: Datasheets.....	241
22.1 Designer Systems DS-SCX18.S servo controller.....	241
22.2 TDK Lambda LS 100-5 Power Supply	249
22.3 Texas Instruments CD74HCT4015E multiplexer	251
22.4 Sunon cooling fan	255
22.5 Ultimaker 2	258
Annex 23: Schematics.....	259
Annex 24: Limited movability of Batan micro servo motor	266
Introduction.....	266
Hypothesis 1	266
Hypothesis 2	268
Hypothesis 3	271
Annex 25: Unexpected behavior of servo motors	272
Introduction.....	272
Hypothesis 1	272
Hypothesis 2	273
Annex 26: Bill of Materials	275
Annex 27: Portfolio.....	276

List of images

FIGURE 1: DIRECTION INDICATORS [OPERATIE-INZICHT.NL]	31
FIGURE 2: ANATOMY OF THE HUMAN ARM [OPERATIE-INZICHT.NL]	32
FIGURE 3: ANATOMY OF THE HUMAN HAND [OPERATIE-INZICHT.NL].....	33
FIGURE 4: STRUCTURAL CLASSIFICATION OF JOINTS [OPERATIE-INZICHT.NL].....	33
FIGURE 5: TYPES OF MOVEMENT [OPERATIE-INZICHT.NL]	34
FIGURE 6: SYNOVIAL JOINTS [OPERATIE-INZICHT.NL].....	35
FIGURE 7: FINGER AND WRIST MOVEMENT [HANDSURGERY.COM]	38
FIGURE 8: ELBOW AND SHOULDER MOVEMENT [OANDPLIBRARY.ORG].....	38
FIGURE 9: COORDINATE SYSTEMS OF THE HUMAN ARM	42
FIGURE 10: CHARACTER "A"	43
FIGURE 11: CHARACTER "B"	43
FIGURE 12: CHARACTER "C"	43
FIGURE 13: CHARACTER "R"	44
FIGURE 14: CHARACTER "Y"	44
FIGURE 15: FORWARD AND INVERSE KINEMATICS [ROBOT ARMS – A. REHIARA].....	47
FIGURE 16: CONFIGURATIONS OF A REDUNDANT ROBOT [PATENT US4999553A].....	47
FIGURE 17: JACOBIAN INVERSION METHOD [7]	49
FIGURE 18: EXTENDED STATE – SINGULARITY [7]	49
FIGURE 19: ILL CONDITIONED STATE [7]	50
FIGURE 20: SOLVING A KINEMATIC MODEL USING THE JACOBIAN TRANSPOSE METHOD [7]	51
FIGURE 21: DIRECT DRIVEN ACTUATION	52
FIGURE 22: LINK-HOSTED ACTUATION	53
FIGURE 23: REMOTE ACTUATION	53
FIGURE 24: SME CRYSTALLINE STRUCTURE [11]	54
FIGURE 25: ACTIVE JOINTS CONNECTIONS.....	55
FIGURE 26: EXAMPLE PASSIVE JOINT [13].....	56
FIGURE 27: CABLE CONNECTIONS.....	56
FIGURE 28: A) PASSIVE SINGLE-ACTING B) ACTIVE SINGLE-ACTING [10].....	58
FIGURE 29: REMOTE ACTUATION CONNECTIONS [10]	58
FIGURE 30: TORQUE CALCULATION EXAMPLE FINGER	61
FIGURE 31: CROSS SECTION STEPPER MOTOR [DESIGNWORLDONLINE.COM]	63
FIGURE 32: PERMANENT MAGNET STEPPER MOTOR [15].....	64
FIGURE 33: PM STEPPER MOTOR 24 POLES [15]	65
FIGURE 34: VR STEPPER MOTOR 30° STEP [17].....	65
FIGURE 35: A RC SERVO MOTOR [PRINCETON.EDU]	66
FIGURE 36: LORENTZ FORCE DC-MOTOR [19].....	67
FIGURE 37: LEFT HAND RULE [WIKIPEDIA.ORG]	67
FIGURE 38: SERVO MOTOR WIRING [ADAFRUIT.COM]	68
FIGURE 39: COMMAND SIGNAL SERVO MOTOR [PRINCETON.EDU].....	68
FIGURE 40: ANALOG CONTROL SERVO MOTOR [SAILSERVO.CO.UK]	69
FIGURE 41: GENERAL RC SERVO MOTOR CONTROL [14].....	70
FIGURE 42: INPUT SIGNAL DUTY CYCLE < 50% [SAILSERVO.CO.UK]	70
FIGURE 43: STATEMENT 1 & 2.....	72
FIGURE 44: MECHANICAL CONSTRAINTS.....	72
FIGURE 45: STRUCTURE DIFFERENCE [23].....	75
FIGURE 46: GENERAL STRESS-STRAIN DIAGRAM [24]	76
FIGURE 47: TWISTED FIBER CABLE	78
FIGURE 48: EXTENSION AND REDUCTION	79
FIGURE 49: INFLUENCE SHAPE JOINT.....	80
FIGURE 50: GENERAL CALCULATION POSITION 1	80
FIGURE 51: GENERAL CALCULATION POSITION 2	81

FIGURE 52: EXTENSION & REDUCTION DOUBLE ACTUATION.....	82
FIGURE 53: CROSS SECTION LITTLE FINGER	82
FIGURE 54: FLEXOR CABLE MAXIMUM POSITION.....	83
FIGURE 55: FLEXOR CABLE MINIMUM POSITION	83
FIGURE 56: EXTENSOR CABLE MINIMUM POSITION	84
FIGURE 57: EXTENSOR CABLE MAXIMUM POSITION.....	84
FIGURE 58: MINIMUM POSITION TMC	85
FIGURE 59: MAXIMUM POSITION TMC	85
FIGURE 60: PATH THROUGH THE PALM OF THE HAND.....	86
FIGURE 61: EXTRA BAR WRIST JOINT	86
FIGURE 62: LOCATION ACTUATORS IN THE ARM	87
FIGURE 63: "EIGHT KNOT"	87
FIGURE 64: SITUATION METHOD EQUAL EXTENSION AND REDUCTION	88
FIGURE 65: APPROACH OF THE EXACT CALCULATION	88
FIGURE 66: ONE I ² C MASTER WITH MULTIPLE SLAVES [PHILIPS SEMICONDUCTORS I ² C HANDBOOK].....	89
FIGURE 67: MASTER/MASTER COMMUNICATION [PHILIPS SEMICONDUCTORS I ² C HANDBOOK]	90
FIGURE 68: A MASTER WRITES DATA TO A SINGLE SLAVE [30].....	90
FIGURE 69: MASTER READS DATA FROM A SLAVE [30]	91
FIGURE 70: MASTER READS OR WRITES DATA TO MULTIPLE SLAVES [30].....	91
FIGURE 71: SERVO MECHANISM [32]	92
FIGURE 72: MULTIPLEXER PRINCIPLE [ARDUINO.CC].....	93
FIGURE 73: PDIP AND SOIC CHIP VERSION.....	93
FIGURE 74: GENERAL REPRESENTATION OF ADDITIVE MANUFACTURING TYPES	97
FIGURE 75: BASIC SET-UP OF A STEREO LITHOGRAPHY-BASED PRINTER [36].....	98
FIGURE 76: BASIC SET-UP OF A POLYJET PRINTER [38]	99
FIGURE 77: BASIC SET-UP OF SELECTIVE LASER SINTERING [39]	99
FIGURE 78: BASIC SET-UP OF FUSED DEPOSITION MODELING [40].....	100
FIGURE 79: ULTIMAKER 2 (MOVING EXTRUDER) [41].....	103
FIGURE 80: BEETHEFIRST (MOVING BED) [42]	103
FIGURE 81: BIOHAZARD DELTABOT [43]	103
FIGURE 82: ULTIMAKER 2.....	106
FIGURE 83: 'PRINT ALL AT ONCE'-FUNCTION.....	108
FIGURE 84: 'PRINT ONE AT A TIME'-FUNCTION.....	108
FIGURE 85: VISUAL COMPARISON OF EVERY SETTING. FROM LEFT TO RIGHT: FAST PRINT, NORMAL PRINT, HIGH QUALITY, ULTI-QUALITY AND OUR CUSTOM SETTINGS.....	110
FIGURE 86: EXAMPLE FOR SUPPORT SETTINGS	110
FIGURE 87: FOREARM WITH A LOT OF SUPPORT MATERIAL	111
FIGURE 88: ORIENTATION FOR GOOD FUNCTIONAL SURFACES.....	111
FIGURE 89: SLICED VIEW OF A 3D-PRINT STRUCTURE	111
FIGURE 90: ABDUCTION AND ADDUCTION JOINT OF THE INDEX FINGER	112
FIGURE 91: ORIENTATION OF FUNCTIONAL AXES	112
FIGURE 92: USED SPOOLS OF FILAMENT	114
FIGURE 93: USED PAINTER'S TAPE	115
FIGURE 94: BADLY WRAPPED SPOOL OF FILAMENT.....	115
FIGURE 95: SCRAPED FILAMENT.....	115
FIGURE 96: DISASSEMBLED AND ASSEMBLED FEEDER	116
FIGURE 97: DISASSEMBLED ULTIMAKER 2 AND BROKEN SENSOR	116
FIGURE 98: THE NEW TEFLON TUBE AND THE OLD ONE.....	117
FIGURE 99: TREE-LIKE SUPPORT STRUCTURE CREATED BY MESHMIXER [47]	117
FIGURE 100: OUR ULTIMAKER 2 WHILE PRINTING	118
FIGURE 101: ASSEMBLED ANTHROMORPHIC 20-DOF ROBOTIC HAND WITH VISIBLE JOINTS [48].....	119
FIGURE 102: FINAL PRODUCT OF THE ANTHROMORPHIC 20-DOF ROBOTIC HAND [48]	119
FIGURE 103: SNAP-ON JOINTS OF THE ANTHROMORPHIC 20-DOF ROBOTIC HAND [48].....	120
FIGURE 104: COMPOSITION OF ONE FINGER OF THE TBM-HAND [49]	120

FIGURE 105: COMPOSITION OF THE THUMB OF THE TBM-HAND [49]	120
FIGURE 106: FINAL PRODUCT OF THE TBM-HAND [49]	120
FIGURE 107: THE DLR ARM HAND SYSTEM [50].....	120
FIGURE 108: THE TUAT/KARLSRUHE HAND [51]	121
FIGURE 109: DESIGN OF A FINGER OF THE TUAT/KARLSRUHE HAND [51]	121
FIGURE 110: THE GIFU III HAND [52]	121
FIGURE 111: THE IH2 AZZURRA HAND [53].....	122
FIGURE 112: EXPLODED VIEW OF THE OPEN HAND PROJECT [54].....	122
FIGURE 113: INMOOV ROBOT [55]	123
FIGURE 114: MA-I HAND [56].....	123
FIGURE 115: BEBIONIC [57].....	124
FIGURE 116: T8X ROBOTIC SPIDER [58]	125
FIGURE 117: TOP VIEW OF THE DISTAL PHALANX OF THE RING FINGER	127
FIGURE 118: GENERAL DIMENSIONS OF THE PALM	128
FIGURE 119: DIMENSIONS OF THE FOREARM.....	129
FIGURE 120: SHAPE OF THE FOREARM	129
FIGURE 121: BALL AND SOCKET SNAP-FIT [59]	130
FIGURE 122: UNREINFORCED C-SHAPE	131
FIGURE 123: REINFORCED C-SHAPE	131
FIGURE 124: ASSEMBLY OF THE THUMB	131
FIGURE 125: THE MOST EXTREME POSITIONS OF THE THUMB.....	132
FIGURE 126: JOINT FOR ADDUCTION/ABDUCTION OF THE INDEX FINGER	132
FIGURE 127: THE LETTER R FORMED BY A HUMAN HAND (LEFT) AND BY OUR ROBOTIC HAND (RIGHT).....	133
FIGURE 128: BALL CHAINS: DIN 5280 [60]	133
FIGURE 129: FIXED ATTACHMENT ON THE PALM FOR WRIST EXTENSION AND FLEXION	134
FIGURE 130: GEAR ON THE MOTOR FOR WRIST EXTENSION AND FLEXION	134
FIGURE 131: TENSION MECHANISM USED FOR THE BALL CHAIN	134
FIGURE 132: FULLY ASSEMBLED ARM (INVENTOR RENDERING).....	135
FIGURE 133: FULLY ASSEMBLED ARM (FINISHED PRODUCT).....	136
FIGURE 134: GENERAL SYSTEM ARCHITECTURE	138
FIGURE 135: PROGRAM EXAMPLE	139
FIGURE 136: ARDUINO DUE [62]	144
FIGURE 137: DESIGNER SYSTEMS DS-SCX18.S [DESIGNERSYSTEMS.CO.UK]	145
FIGURE 138: TDK LAMBDA LS 100-5 [US.TDK-LAMBDA.COM]	145
FIGURE 139: POWER SUPPLY EXTERNAL FUSE RATING [63]	146
FIGURE 140: IEC60320 MATING [SCHURTER.COM]	148
FIGURE 141: ORGANIZATION OF THE COMPONENTS	150
FIGURE 142: THE LOGO OF PROJECT ASLAN	152
FIGURE 143: EUROPEAN INSTITUTE FOR OTORHINOLARYNGOLOGY - HEAD & NECK SURGERY LOGO	153
FIGURE 144: DEMO SET-UP SHOWN AT THE OPEN HOUSE	155
FIGURE 145: FRONT VIEW "A"	170
FIGURE 146: LEFT SIDE VIEW "A"	170
FIGURE 147: FRONT VIEW "B"	170
FIGURE 148: LEFT SIDE VIEW "B"	170
FIGURE 149: FRONT VIEW "C"	170
FIGURE 150: LEFT SIDE VIEW "C"	170
FIGURE 151: FRONT VIEW "D".....	171
FIGURE 152: LEFT SIDE VIEW "D"	171
FIGURE 153: FRONT VIEW "E"	171
FIGURE 154: LEFT SIDE VIEW "E".....	171
FIGURE 155: FRONT VIEW "F"	171
FIGURE 156: LEFT SIDE VIEW "F"	171
FIGURE 157: FRONT VIEW "G"	172
FIGURE 158: LEFT SIDE VIEW "G"	172

FIGURE 159: FRONT VIEW “H”	172
FIGURE 160: LEFT SIDE VIEW “H”	172
FIGURE 161: FRONT VIEW “I”	172
FIGURE 162: LEFT SIDE VIEW “I”	172
FIGURE 163: FRONT VIEW “J”	173
FIGURE 164: LEFT SIDE VIEW “J”	173
FIGURE 165: FRONT VIEW “K”	173
FIGURE 166: LEFT SIDE VIEW “K”	173
FIGURE 167: FRONT VIEW “L”	173
FIGURE 168: LEFT SIDE VIEW “L”	173
FIGURE 169: FRONT VIEW “M”	174
FIGURE 170: LEFT SIDE VIEW “M”	174
FIGURE 171: FRONT VIEW “N”	174
FIGURE 172: LEFT SIDE VIEW “N”	174
FIGURE 173: FRONT VIEW “O”	174
FIGURE 174: LEFT SIDE VIEW “O”	174
FIGURE 175: FRONT VIEW “P”	175
FIGURE 176: LEFT SIDE VIEW “P”	175
FIGURE 177: FRONT VIEW “Q”	175
FIGURE 178: LEFT SIDE VIEW “Q”	175
FIGURE 179: FRONT VIEW “R”	175
FIGURE 180: LEFT SIDE VIEW “R”	175
FIGURE 181: FRONT VIEW “S”	176
FIGURE 182: LEFT SIDE VIEW “S”	176
FIGURE 183: FRONT VIEW “T”	176
FIGURE 184: LEFT SIDE VIEW “T”	176
FIGURE 185: FRONT VIEW “U”	176
FIGURE 186: LEFT SIDE VIEW “U”	176
FIGURE 187: FRONT VIEW “V”	177
FIGURE 188: LEFT SIDE VIEW “V”	177
FIGURE 189: FRONT VIEW “W”	177
FIGURE 190: LEFT SIDE VIEW “W”	177
FIGURE 191: FRONT VIEW “X”	177
FIGURE 192: LEFT SIDE VIEW “X”	177
FIGURE 193: FRONT VIEW “Y”	178
FIGURE 194: BOTTOM VIEW “Y”	178
FIGURE 195: FRONT VIEW “Z”	178
FIGURE 196: BOTTOM VIEW “Z”	178
FIGURE 197: ARCHIMEDES [64]	180
FIGURE 198: EXPERIMENT	180
FIGURE 199: DETAILS LOWER CABLE MAXIMUM POSITION	191
FIGURE 200: DETAILS LOWER CABLE MINIMUM POSITION	191
FIGURE 201: DETAILS UPPER CABLE MAXIMUM POSITION	192
FIGURE 202: DETAILS UPPER CABLE MINIMUM POSITION	192
FIGURE 203: DETAILS LOWER CABLE ADDUCTION MINIMUM POSITION	193
FIGURE 204: DETAILS LOWER CABLE ABDUCTION MAXIMUM POSITION	193
FIGURE 205: DETAILS LOWER CABLE MCP MINIMUM POSITION	194
FIGURE 206: DETAILS LOWER CABLE MCP MAXIMUM POSITION	194
FIGURE 207: DETAILS UPPER CABLE MCP MINIMUM POSITION	195
FIGURE 208: DETAILS UPPER CABLE MCP MAXIMUM POSITION	195
FIGURE 209: DETAILS MINIMUM DISTANCE TMC	196
FIGURE 210: DETAILS MEASUREMENT UPPER CABLE TMC MAXIMUM POSITION	197
FIGURE 211: DETAILS LOWER CABLE TMC MAXIMUM POSITION	197
FIGURE 212: LOCATION ACTUATOR IN ARM	198

FIGURE 213: LOCATION ACTUATORS IN THE PALM OF THE HAND	198
FIGURE 214: SITUATION EXACT CALCULATION	209
FIGURE 215: PWM CONTROL OF AN ANALOG SERVO MOTOR [SERVO CITY.COM]	266
FIGURE 216: MINIMUM AND MAXIMUM PULSE WIDTH [SERVO CITY.COM]	266
FIGURE 217: HYPOTHESIS 1 LIMITED MOVABILITY SCHEMATIC	267
FIGURE 218: SERVO BLOCK DIAGRAM [65]	268
FIGURE 219: MECHANICAL CONSTRAINT ON THE SERVO POTENTIOMETER AXIS	269
FIGURE 220: HYPOTHESIS 2 LIMITED MOVABILITY SCHEMATIC	269
FIGURE 221: HYPOTHESIS 3 LIMITED MOVABILITY	270
FIGURE 222: CONTROL REGISTERS	273

List of tables

TABLE 1: LIST OF ABBREVIATIONS	27
TABLE 2: LIST OF SYMBOLS	28
TABLE 3: TYPES OF MOVEMENT	34
TABLE 4: JOINTS IN THE UPPER EXTREMITIES	36
TABLE 5: CONSTRAINTS IN THE UPPER EXTREMITIES	37
TABLE 6: JOINT INDICES	41
TABLE 7: RESULTS SIMPLIFICATION DOFS	45
TABLE 8: LIST OF FREQUENTLY USED SYMBOLS	46
TABLE 9: ACTIVE AND PASSIVE JOINTS	57
TABLE 10: ESTIMATED VOLUMES	60
TABLE 11: SEQUENCE VR STEPPER MOTOR 30° STEP	66
TABLE 12: MINIMUM LOCATION FORCES ESTIMATED	73
TABLE 13: WEIGHED MASS	73
TABLE 14: TORQUE WEIGHED PARTS	74
TABLE 15: MINIMUM LOCATION REAL FORCES	74
TABLE 16: GENERAL PHYSICAL PROPERTIES	76
TABLE 17: PHYSICAL PROPERTIES USED MATERIALS	76
TABLE 18: EXTENSION RESULTS	77
TABLE 19: DECISION TABLE	94
TABLE 20: PROS AND CONS OF USING MILLING MACHINES	95
TABLE 21: MAIN PROPERTIES OF ABS	101
TABLE 22: MAIN PROPERTIES OF PLA	102
TABLE 23: MAIN PROPERTIES OF PVA	102
TABLE 24: MOST IMPORTANT VALUES OF VARIOUS PRINTING SETTINGS	109
TABLE 25: BRIEF LIST OF PRINTING TIMES	113
TABLE 26: AVERAGE HAND DIMENSIONS GATHERED FROM BRITISH ADULTS	126
TABLE 27: LENGTHS OF FINGER MEASURED FROM AXIS TO C-SHAPE	128
TABLE 28: NUMBER OF POSITIONS FOR EACH FUNCTION	140
TABLE 29: ARDUINO DUE SPECIFICATIONS	144
TABLE 30: FUSE RATINGS	146
TABLE 31: COMPONENT OPERATING TEMPERATURES	147
TABLE 32: SERVO MOTOR DISTRIBUTION	151
TABLE 33: MUSCLES RESPONSIBLE FOR SHOULDER MOVEMENT	166
TABLE 34: MUSCLES RESPONSIBLE FOR ELBOW MOVEMENT	166
TABLE 35: MUSCLES RESPONSIBLE FOR WRIST MOVEMENT	167
TABLE 36: LIST OF DESCRIPTIONS	168
TABLE 37: LIST OF IMAGES	170
TABLE 38: ESTIMATED VOLUMES	180
TABLE 39: ESTIMATED TORQUE	181
TABLE 40: ESTIMATED MINIMUM DISTANCES	184

TABLE 41: EXACT CALCULATIONS DEPENDING IN DISTANCE UNTIL GUIDANCE	199
TABLE 42: SOLUTION LEFT PART OF THE EQUATION	200
TABLE 43: SOLUTION RIGHT PART OF THE EQUATION.....	202
TABLE 44: MAXIMUM AND MINIMUM ANGEL DEPENDING ON THE SHAPE OF THE DISC.....	208
TABLE 45: APPROACH ANGLES ALPHA AND BETA	210
TABLE 46: APPROACH Y' AND BETA'	212
TABLE 47: APPROACH X' AND S'	214
TABLE 48: DEVIATION FROM EXACT CALCULATION	216
TABLE 49: RANKED POSITIONS FOR FINGER MOVEMENT.....	232
TABLE 50: RANKED POSITIONS FOR THUMB MOVEMENT	232
TABLE 51: RANKED POSITIONS FOR WRIST MOVEMENT.....	232
TABLE 52: RANKED POSITIONS FOR ELBOW MOVEMENT.....	233
TABLE 53: RANKED POSITIONS FOR SHOULDER MOVEMENT	233
TABLE 54: PULSE WIDTH TEST RESULTS.....	267
TABLE 55: ACTUAL MINIMUM OF DIFFERENT SERVO MOTORS	271
TABLE 56: ACTUAL MAXIMUM OF DIFFERENT SERVO MOTORS.....	271
TABLE 57: CONTROL REGISTER TEST RESULTS	274

List of symbols

LIST OF ABBREVIATIONS

Table 1: List of abbreviations

Abbreviation	Meaning
ABS	Acrylonitrile Butadiene Styrene
DIP	Distal interphalangeal joint
DOF	Degree of freedom
E	Index for the elbow joint
FDP	Fused Deposition Modeling
FFF	Fused Filament Fabrication
IP	Interphalangeal joint, specifically used for the thumb
MCP	Metacarpophalangeal joint
MPD	Molten Polymer Deposition
PIP	Proximal interphalangeal joint
PLA	PolyLactic Acid
PM	Permanent Magnet
PVA	PolyVinyl Alcohol
RC	Radio Controlled
RU	Index for the radio-ulnar joint
S	Index for the shoulder joint
SL	Stereolithography
SLA	Stereolithography
SMA	Shape Memory Alloy
SME	Shape Memory Effect
TMC	Trapezometacarpal joint
VR	Variable Reluctance
W	Index for the wrist joint

LIST OF SYMBOLS

Table 2: List of symbols

Symbol	Meaning
E	Positioning error
R	Radius
$f(\Theta)$	Forward kinematics function
A	Surface
B	Induction
D_g	Ball diameter
D_k	Socket opening diameter
E	Youngs modulus
$E(\Theta)$	Error function
F	Force
I	Current
J^\dagger	Moore-Penrose pseudoinverse jacobian
$J(\Theta)$	Jacobian matrix
L	Length
M	Amount of actuators
M	Mass
N	Amount of degrees of freedom
P	Desired position of the end-effector $P(x,y,z,\delta x, \delta y, \delta z)$
T	Torque
V	Volume
X	Cartesian position of the end-effector $X(x,y,z,\delta x, \delta y, \delta z)$
\dot{X}	Lineair velocity vector of the end-effector $(dx/dt, dy/dt, dz/dt)$
α	Angle
α	Gain
σ	Tension
ϵ	Elongation
ϵ	Extension
ρ	Density
Θ	Joint states $\Theta(\theta_1,\theta_2,\dots,\theta_n)$
$\dot{\theta}$	Joint rotational velocity

LIST OF PROGRAMMING VARIABLES

...control

Suffix of integer value used to write variables to the servo motors control register. Prefix of the variable is one of the before mentioned joint indices.

...position

Suffix of integer value used to write variables to the servo motors position register. Prefix of the variable is one of the before mentioned joint indices.

**abduction(int pos)
address**

Function for the abduction of the index finger
Integer value to describe which servo driver needs to be accessed

elbow(int pos)

Function for the two DOF movement of the elbow

finger

Integer value describing which finger needs to be moved.

finger(int finger, int pos)

Finger movement function, first variable describing the finger that needs to be moved while the second variable defines the position.

l

Integer length of spell.

pos

Integer value describing the position.

Register

Register value to write variables to a servo Driver

shoulder(int pos)

Function for the simplified shoulder movement

spell

String variable entered with the keyboard.

symbol[l]

Spell converted to an array of characters.

thumb(int pos)

Movement function for the thumb.

Value

Value used to send to the servo driver

wrist(int pos)

Movement function for the thumb.

WriteRegister(int address, byte Register, byte Value)

Function to write variables to the different servo drivers.

1. Human anatomy of the upper extremities

1.1 INTRODUCTION

Guy Fierens - When designing a humanoid robot, it is important to study state of the art technologies and designs. In the field of humanoid robotics the mother of designs is the human body itself. In the following chapter the key aspects of the human arms will be discussed:

- The muscles actuating the human arm and hand.
- The bones responsible for the strength and structure.
- The different joints necessary for precise and robust movements.

1.2 GLOSSARY OF TERMS [1]

In the course of the next chapter, a number of terms will be used frequently.

Degrees of freedom: A degree of freedom is defined as an independent parameter to define the configuration of a mechanical system. E.g. a joint with one degree of freedom is only able to move/rotate in one single direction.

Proximal and distal (Figure 1): Describes the position of a limb, bone,... with respect to a specific point of attachment. Proximal is closer to that specific point, distal further. The upper arm is for example located distal from the shoulder.

Medial and lateral (Figure 1): Describes the position relative to the center line. Medial is close the center line while lateral is further from the center line and closer to the sides of the body.

Anterior and posterior (Figure 1): These terms describe the location of a bone or limb relative to the body. Anterior or ventral is closer to the front of the body, while posterior or dorsal is closer to the back.

Anatomical position and write mode: The anatomical position as seen on the left side of Figure 1 is the default position used in medical literature, used because of its accuracy and consistency. In the anatomical position the described person is standing upward with his/her head facing forward, arms alongside the body and the palms of his/her hands facing forwards. The writing mode describes solely the position of the palm of the hand and is the opposite of the anatomical position with the palm facing down.

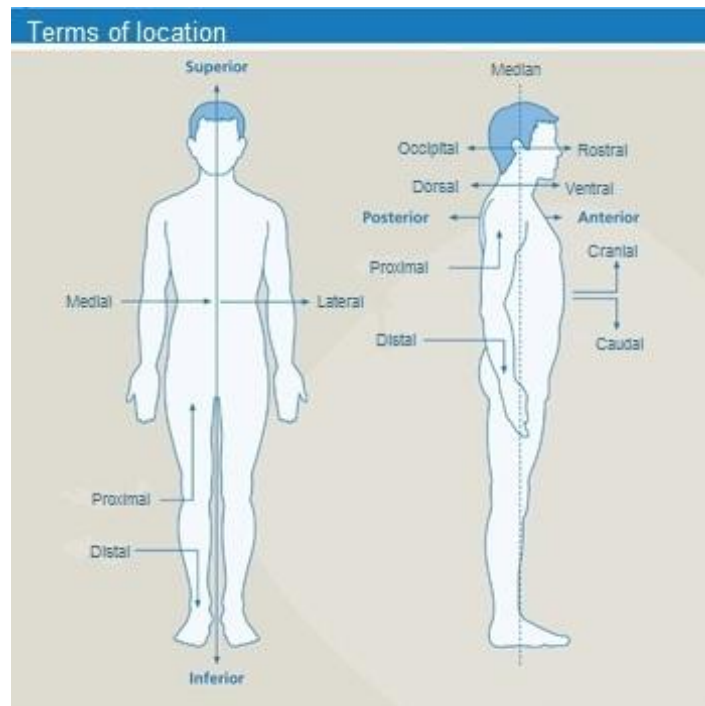


Figure 1: Direction indicators [Operatie-inzicht.nl]

1.3 BONES IN THE UPPER EXTREMITIES [1], [2]

Between the shoulder joint and fingers are 30 different bones, each connected by means of joints. Each of these bones has its own function, which will be discussed below. This gives us a clear picture of the structure of the upper limbs or extremities of the human body. The different bones will be described downwards starting from the shoulder joint.

1.3.1 Humerus

The humerus or upper arm is connected on its proximal side to the shoulder blade and with its distal side to the elbow joint (Figure 2).

1.3.2 Ulna and radius

These two bones are commonly known as the underarm. At its proximal side, the ulna forms a one degree of freedom hinge joint together with the humerus enabling the flexion and extension of the underarm. The joint between the radius and humerus is a two degrees of freedom ball joint, also enabling flexion and extension in combination with the pronation and supination of the hand (rotating around the ulna). See Figure 2.

The ulna and radius are also connected to each other on their axis which stabilizes the combination, maintaining a relative position to each other. When in anatomical position the ulna and radius are parallel to each other, while in write mode the radius will cross the ulna.

1.3.3 Carpus

The carpus or os metacarpi form the base structure of the human hand (Figure 3). This combination of eight different bones is ordered in two rows of four bones: a distal and a proximal row.

These bones are packed close to each other and held in place by ligaments, which only allow limited movement. The bones in the proximal row together with the radius form the wrist, while the distal row work together with the metacarpal bones. At the bottom, the carpus bones form a tunnel, guiding the tendons responsible for finger movements.

1.3.4 Metacarpus

The metacarpus or os metacarpi are numbered from thumb side to little finger starting with the roman number I. Metacarpus II to V form joints with limited movability with the carpus on its proximal side and form two degree of freedom joints with the phalanges. Metacarpus I, located in the thumb forms a saddle joint with the trapezium, enabling movement in two degrees of freedom.

1.3.5 Phalanges

The phalanges are the fourteen remaining bones in the human hand as seen in Figure 3. These fourteen bones are divided over the five fingers, giving two to the thumb and three to each other finger. The phalanges are connected to each other with hinge joints.

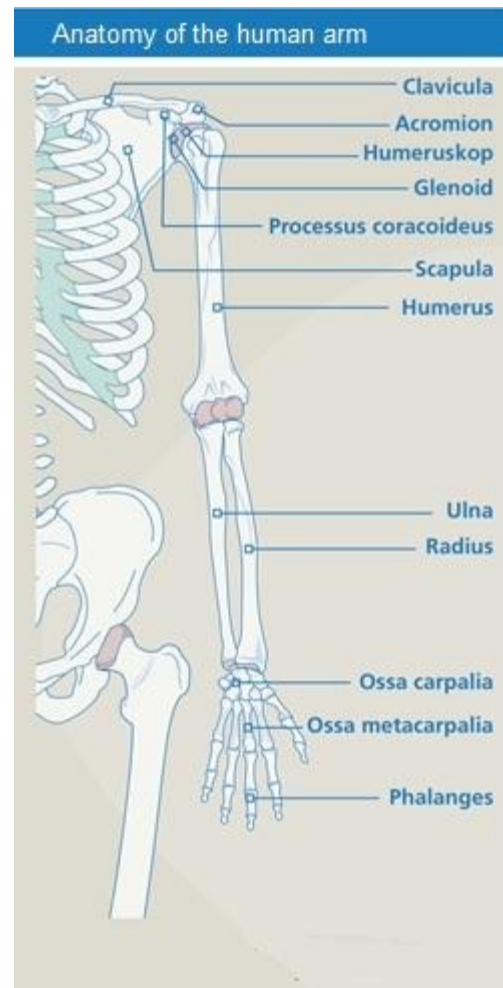


Figure 2: Anatomy of the human arm [Operatie-inzicht.nl]

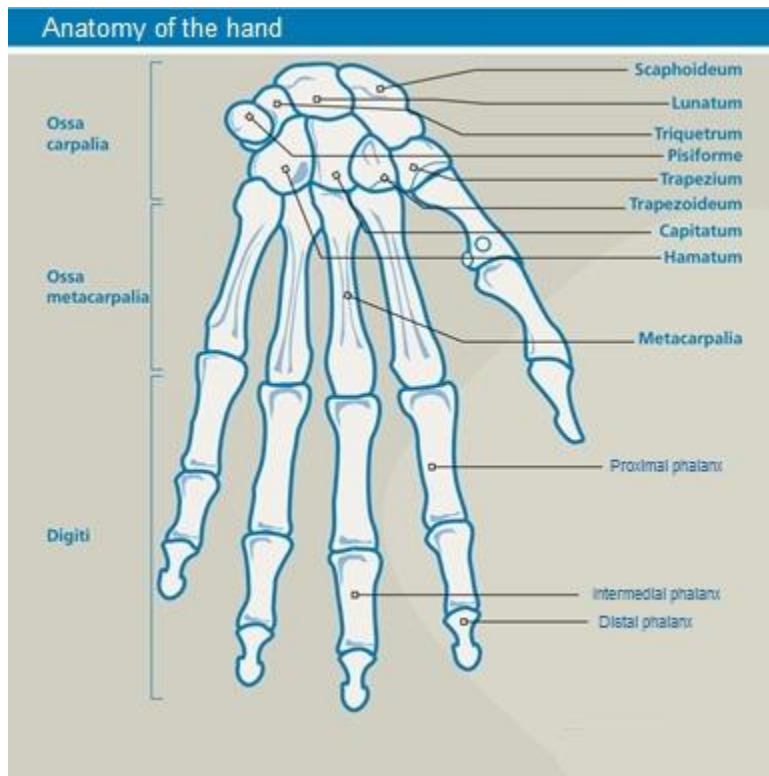


Figure 3: Anatomy of the human hand [Operatie-inzicht.nl]

1.4 JOINTS IN THE HUMAN BODY [1], [2]

Synovial joints consist of a joint chapel and a joint cavity between the articulated bones. It is this type of joint responsible for the human movement. In addition to the synovial joints, the human body also consists of fibrous (which are immobile, like the joints connecting the bones of our skull) and cartilage joints who allow a limited mobility, like the joints in our spine. Because only the synovial joints are relevant in our setup, only this type of joint will be explained in more detail.

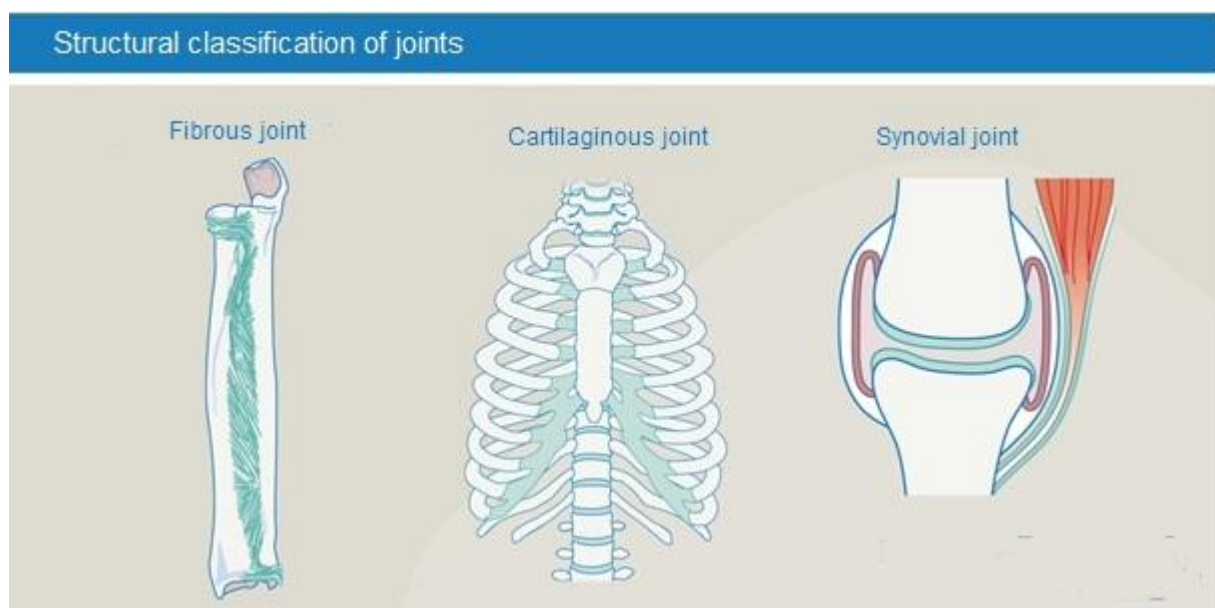


Figure 4: Structural classification of joints [Operatie-inzicht.nl]

1.5 MOVEMENTS IN SYNOVIAL JOINTS [1]

Table 3: Types of movement

Movement	Opposite movement	Degrees of freedom
Flexion (bending)	Extension	1
Abduction (opening)	Adduction (closing)	1
Pronation (rotate palm of your hand downwards)	Supination (rotate palm of your hand upwards)	1
Circumduction (describing a cone)	/	2
Endorotation (rotate inwards along the longitudinal axis)	Exorotation (rotate outwards along the longitudinal axis)	1
Anteversion (flexion from the anatomical position)	Retroversion (extension from the anatomical position)	1
Dorsiflexion (hand moving towards back hand)	Palmar flexion (hand moving toward the palm) ¹	1

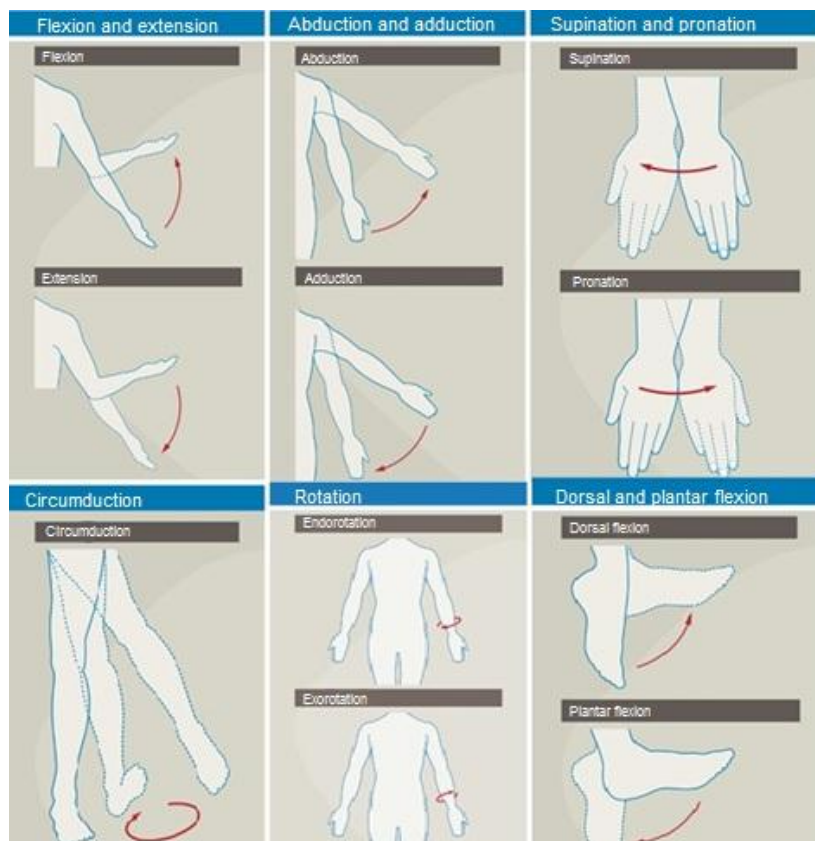


Figure 5: Types of movement [Operatie-inzicht.nl]

¹ Shown in the picture as plantar flexion, which is a movement of the ankle joint.

1.6 TYPES OF SYNOVIAL JOINTS [1]

- **Ball joint:** The head of one bone is ball-shaped and rests in the bowl-shaped part of the other bone. This way, movements are made possible along three axes: flexion-extension, adduction-abduction and internal rotation-external rotation. Example is the shoulder joint.
- **Hinge joint:** By a hinge joint articulated bones can only move relative to each other along a single rotational axis. An example of the hinge joint is the joint between ulna and humerus.
- **Flat joint:** The two articulating bones can only translate relative to each other. Examples are the joints between the ossa carpi in the wrist.
- **Rotary joint:** Rotates a bone along a single axis by pressing it through a loop-shaped ligament to another bone. This joint is not used in our setup, but is mentioned for completeness. Example of this is the rotation of the head.
- **Ellipsoid joint/condyloid joint:** This kind of joint allows flexion-extension, abduction-adduction and circumduction possible by the rest of the condyle (smooth and rounded projection of a bone) to rest in an egg-shaped cavity in another bone. The wrist is an example of a condyloid joint.
- **Saddle joint:** The articulating bones fit together like a man on a saddle. One example is the base of the thumb between the os trapezium of the wrist and the first os metacarpi.

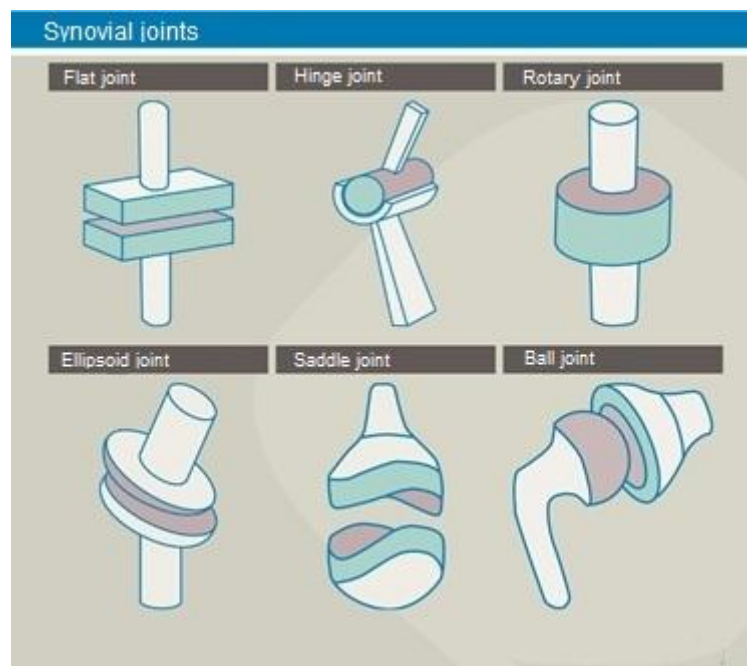


Figure 6: Synovial joints [Operatie-inzicht.nl]

1.7 MOST IMPORTANT SYNOVIAL JOINTS IN OUR SETUP [1], [2]

In Table 4, all the relative joints in our setup are analyzed regarding the type of joint and the number of degrees of freedom.

Table 4: Joints in the upper extremities

Joint	Type of joint	Degrees of freedom	Comments
Shoulder joint	Ball joint	3	
Elbow	Hinge joint	1	Humero-ulnar joint
	Ball joint ²	2	Between radius and humerus, one degree of freedom suppressed by a ligament
Radio-ulnar joint ³	Rotary joint	1	Rotation along longitudinal axis ulna
Wrist radiocarpal	Condyloid joint	2	
Wrist - mediocarpal	Flat joint	2	
Thumb	Saddle joint	3	Makes the thumb opposable
	Hinge joint	1	
	Condyloid joint	2	
Fingers	Condyloid joint	2	
	Hinge joint	1	Connecting phalanges

² The radio-ulnar joint consists of a proximal and a distal part. The proximal part is located near the elbow while the distal part is located near the wrist. The ball joint mentioned is the proximal radio ulnar joint.

³ The rotary joint mentioned is primarily a result of the distal radio ulnar joint, which connects the ulna, radius and the ossa carpi.

1.8 CONSTRAINTS IN THE UPPER EXTREMITIES. [4]

All joints mentioned above only have a limited freedom of movement, often limited by the shape of the joint itself but also partly by the supporting and actuating muscles. See the attached images for joint angle references.

Table 5: Constraints in the upper extremities

Joint	Movement	Angle	Opposite movement	Angle	Figure
Shoulder joint	Abduction (elevation)	90°	Adduction (depression)	40°	Figure 8
	Anteversion (flexion)	90°	Retroversion (extension)	40°	Figure 8
	Endorotation (rotation medial)	60°	Exorotation (rotation lateral)	70°	Figure 8
Shoulder and clavicle joint	Abduction	180°	Adduction	40°	Figure 8
	Anteversion	170°	Retroversion	40°	Figure 8
	Endorotation	90°	Exorotation	100°	Figure 8
Elbow	Extension	10°	Flexion	150°	Figure 8
	Pronation	90°	Supination	90°	Figure 8
Wrist	Ulnar abduction	30°	Radial abduction	30°	Figure 7
	Dorsal extension	60°	Palmar flexion	60°	Figure 7
Saddle joint thumb	Extension	30°	Flexion	40°	/
	Abduction	10°	Adduction	40°	/
Metacarpophalangeal joint ⁴	Dorsal extension	30°	Palmar flexion	90°	Figure 7
	Ulnar abduction-	20°-40°	Radial abduction	20°-40°	Figure 7
Proximal interphalangeal joint ⁵	Palmar flexion	100°	/	/	/
Distal interphalangeal joint ⁶	Palmar flexion	90°	/	/	/

⁴ Joint between metacarpals and phalanges.

⁵ Joint between first two phalanges. Palmar flexion is the only movement possible.

⁶ Joint between the last two phalanges. Palmar flexion is the only movement possible.

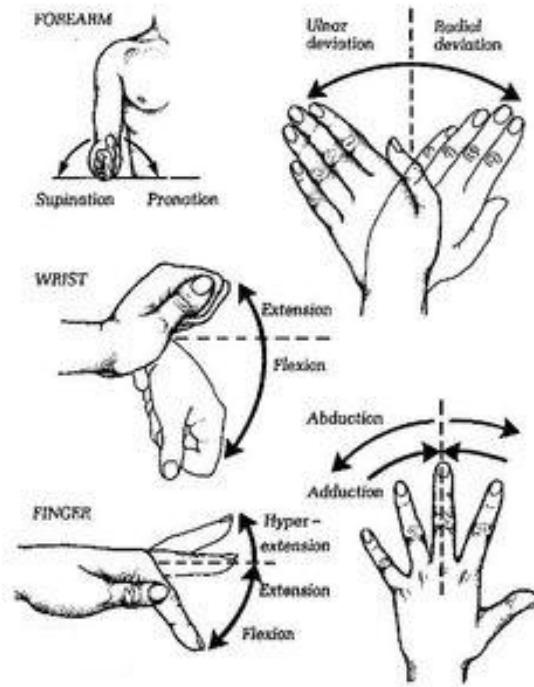


Figure 7: Finger and wrist movement [handsurgery.com]

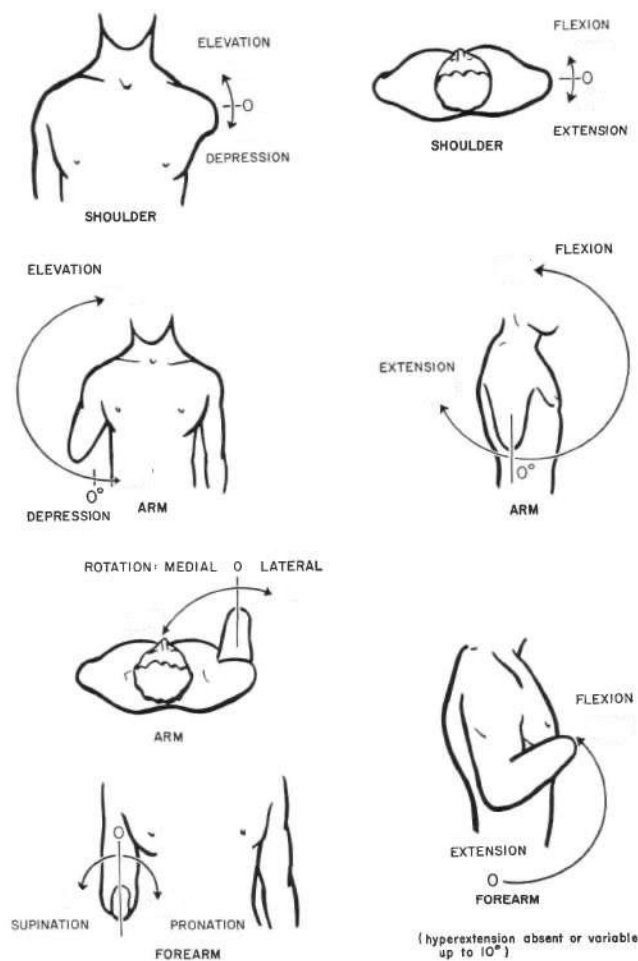


Figure 8: Elbow and shoulder movement [oandplibary.org]

1.9 MUSCLES AND TENDONS IN THE UPPER EXTREMITIES [1], [2]

Analyzing the tables in Annex 1, we can see that the human body uses numerous muscles that often help each other to perform certain movements. These muscles are often large and powerful, allowing them to lift or move heavy loads. Different muscles are grouped according to their function, placing the flexors anterior while the extensors are located posterior in the body. All of this can be of importance in the design of the mechanical robot arm, where we can start using one single actuator for each degree of freedom.

The muscles responsible for the movement of the fingers can be found in the hand as well as in the forearm, using tendons to get to the fingers. The muscles in the forearm provide force and powerful movements while the muscles located inside the hand provide precise movements like handling a pen for example.

The tendons actuating the fingers have their origin in the respective muscle and their insertion at the base of the fingers they need to actuate. E.g. the tendon responsible for the flexion of the proximal interphalangeal joint of the index finger has its insertion at the base of the intermedial phalanx. Each of the four fingers is actuated by a combination of five tendons, two for extension and three for flexion. The extension of the proximal and distal interphalangeal joint is provided by a single tendon while the flexion of these joints is provided for by two tendons.

The tendons for the movement of the hand are guided from their origin in the forearm to their insertion in the hand, through synovial sheaths containing synovial fluid to reduce friction. Two retinacula or ligaments guide the tendons through the wrist. One on the dorsal side of the hand to guide the tendons responsible for extension and one on the palmar side of the hand to guide the tendons responsible for flexion.

In the kinematic chain from shoulder to fingertip of the thumb, the human arm counts a total of 12 degrees of freedom spread across a chain of six joints. In total, the human arm counts 28 degrees of freedom. Considering this is a very complex setup, the following sections will handle the necessary movements and degrees of freedom for single-hand sign language.

1.10 CONCLUSION

A couple of key elements, relevant to designing a humanoid robot were stated. To conclude, a brief summary of these aspects will be given.

First of all, and also a very important element is the general architecture of the upper extremity. The bones connecting each joint, but more importantly the joints themselves. The different kind of joints with their respective degrees of freedom and the constraints imposed by the ligaments and cartilage.

A second element is the movement of the different joints by the muscles and the position of these muscles in the arm. For powerful hand movements the muscles are positioned in the upper arm while muscles responsible for precise hand movement are located in the hand itself. Also, since the distal joints of the fingers are passive and move relative to the proximal joint in the human hand, these joints will also be designed to be passive in the robot. This saves us four motors to control the robot. The muscles actuating the wrist, elbow and shoulder are located proximal to their respective joint and have connection points proximal and distal to the joint.

2. Convention and abbreviations used in the further course of this work [2], [3]

2.1 INTRODUCTION

Guy Fierens - In the remainder of this paper a general convention will be used regarding the used joints. This does not only make it easier for the reader to grasp the overall picture, but it will also make the calculations clearer given the created recognizable index.

The structure of the convention is inspired by [3] and is based on the clinical terms used in medical literature such as [2] and [4]

2.2 GLOBAL COORDINATE SYSTEM

The global coordinate system or base coordinate system is chosen to be located at the shoulder joint. This coordinate system is fixed and all desired coordinates will be described using this coordinate system. When describing rotations, the position and orientation of the local coordinate system of the end-effector will be compared to the base coordinate system.

The orientation of the different axis of the base coordinate system will be chosen according to the Denavit-Hartenberg convention. The convention states that the z-axis must be oriented along the axis of rotation of the link it describes. Because this is a fixed coordinate system and therefore doesn't rotate, the z-axis will be chosen along the first axis of rotation of the shoulder joint. The x-axis will be along the longitudinal axis, pointing to the front of the body. Finally the y-axis will complete the right handed coordinate system.

2.3 LOCAL COORDINATE SYSTEM

Both for the end effector (fingertips) and each joint, a local coordinate system can be defined according to the Denavit-Hartenberg convention. As mentioned above the z-axis is oriented along the axis of rotation of link $i+1$. The x-axis is oriented perpendicular to both z_i and z_{i-1} . The y-axis again completes the right handed coordinate system.

2.4 JOINT INDICES

In calculations, when talking about joint variables (joint coordinate systems or joint angles) an index will be added to the variable to make clear which joint is described. The used indices are explained in Table 6.

Table 6: Joint indices

Joint	Index
Shoulder joint	S
Elbow	E
Radio-ulnar joint ⁷	RU
Wrist	W
Metacarpophalangeal joint	MCP
Proximal interphalangeal joint	PIP
Distal interphalangeal joint	DIP
Interphalangeal joint ⁸	IP
Trapezometacarpal joint	TMC

For example a rotation angle in the shoulder along the x-axis: Θ_{sx}

2.5 CONCLUSION

This brief chapter defines a clear convention for further use in this work. Using this convention, it is always clear to the reader which part of the robot is addressed through the index of the variable. The definition of the joints coordinate systems shall be of further use in the next chapter on kinematics.

As a result of this chapter, Figure 9 shows the coordinate systems for the human arm. Since the coordinate systems of the little, ring, middle and index finger are identical, only the coordinate systems of the little finger are displayed.

⁷ Anatomically a part of both the elbow and the wrist, mechanically not necessarily

⁸ Specifically for the joint in the thumb

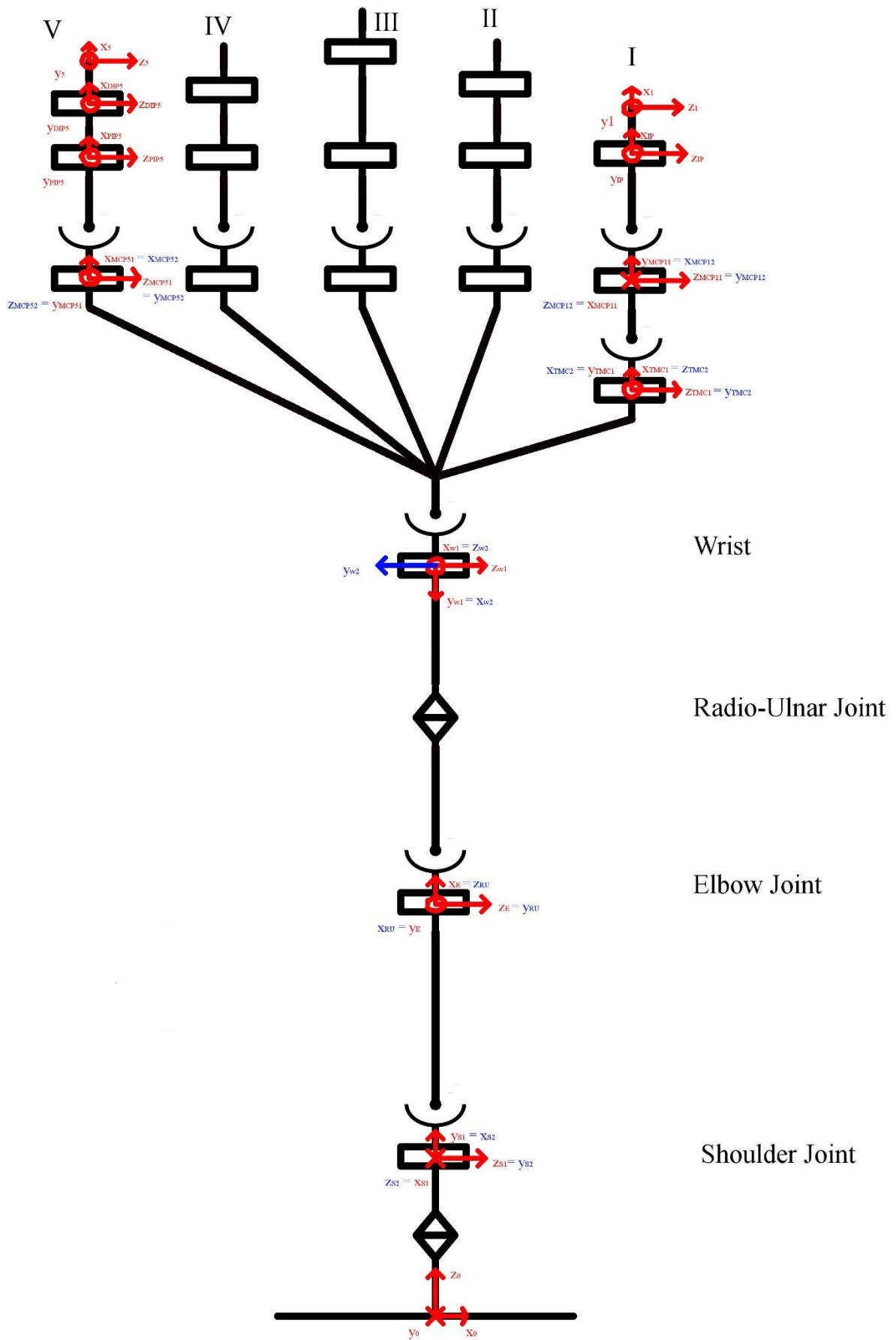


Figure 9: Coordinate systems of the human arm

3.The Flemish sign language alphabet

3.1 INTRODUCTION

Jasper Slaets - The Flemish sign language is too complex to deal with at the start of the project, so we limit ourselves (on advice of MobilAnt) to the Flemish sign language alphabet and counting from one to ten. This way, we can gradually add more complexity to our robot. In Annex 2 a list of each letter of the hand alphabet can be found. There is also a description of the finger movements for each character. Some fundamental characters will be described in following paragraph. Next an analysis regarding the degrees of freedom of the Flemish sign language alphabet will be made and at the end an overall conclusion.

3.2 SOME FUNDAMENTAL CHARACTERS

To understand the movements as a result of the sign language alphabet, a few fundamental characters will be explained. The reason they are fundamental is because these character are a result from basic movements (flexion, extension, adduction, abduction, rotation TMC, W, RU, E, S). This explanation is based on the previous mentioned coordinate systems and chosen joint indices.

The first character of the Flemish sign language alphabet, "A", looks like a fist with an extended thumb. Translated to chosen joint indices results in flexion for MCP, PIP and DIP joints (fingers) and extension for MCP and IP joint (thumb). This character is visualized in Figure 10.

Character "B" is the counterpart of character "A". All fingers are extended and the thumb is flexed. This results in extension for MCP, PIP, DIP joint (fingers) and flexion for MCP and IP joint (thumb). This character is visualized in Figure 11.

Character "C" is something between character "A" and "B". The fingers and thumb are half flexed, half extended and the thumb is rotated perpendicular to the palm of the hand. This results in half flexion, half extension for MCP, PIP, DIP joints (fingers) and for MCP, IP joint (thumb). The TMC joint will be subjected to rotation of 90 ° relative to the palm of the hand (Figure 12).

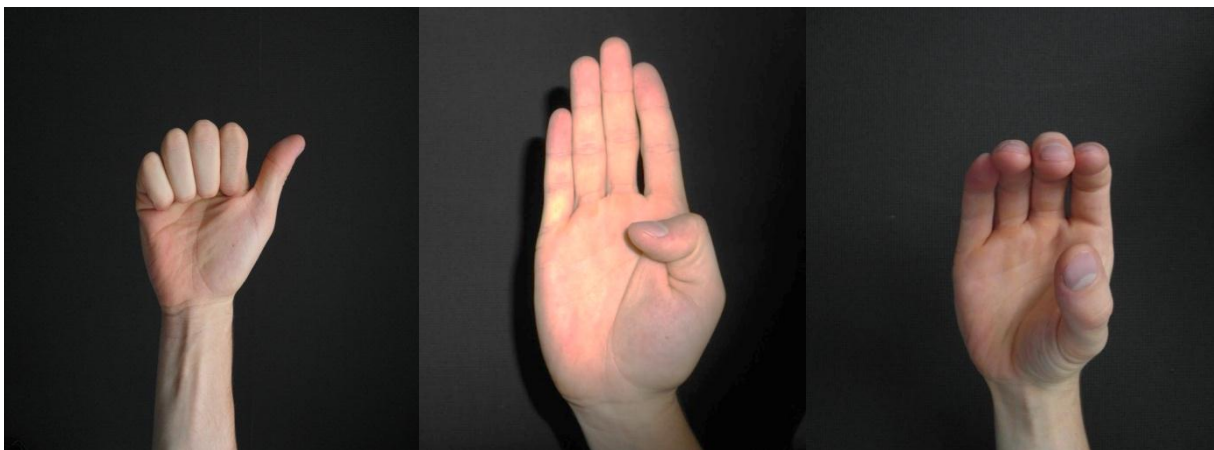


Figure 10: Character "A"

Figure 11: Character "B"

Figure 12: Character "C"

Character "R", visualized in Figure 13, is an example of adduction and abduction for the index finger. Little, ring finger and thumb are flexed and middle and pointer finger are extended. Middle and pointer finger also need to be crossed, which is a result from abduction. These movements results in flexion for MCP, PIP, DIP joints (little and ring finger) and MCP, IP joint (thumb), extension for MCP, PIP, DIP joints (middle and pointer finger) and abduction for MCP joint (pointer finger).

Character "Y", visualized in Figure 14, is an example of the characters for which movements of wrist, elbow and shoulder are necessary to complete. Ring, middle and pointer finger are flexed and little finger and thumb are extended. In order to complete the character, the hand must go down. This results in an additional flexion and extension in E joint (elbow) and W joint (wrist).

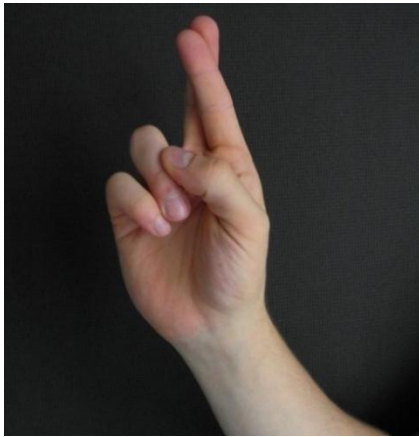


Figure 13: Character "R"

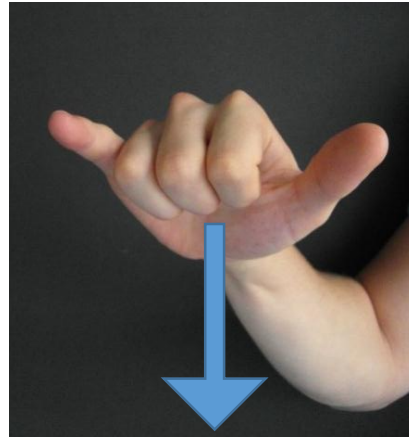


Figure 14: Character "Y"

3.3 DEGREES OF FREEDOM ANALYSIS

As explained, each character has its movements. How the movements are realized can be explained as follows. Joints on their own can't move, but when combined with muscles the result will be actual movement. Each joint represents a degree of freedom (DOF). As shown in Figure 9: the shoulder has 3 DOFs, the elbow has 2 DOFs, the wrist has 2 DOFs, saddle joint has 2 DOFs, the thumb has 3 DOFs and each of the remaining fingers has 4 DOFs. The total sum of the DOFs is 28 DOFs. It is necessary for our application to exclude as many DOFs as possible, because the more DOFs we have the more complex the application will become.

3.4 REDUCING DEGREES OF FREEDOM

To determine the DOFs that can be excluded, an analysis of the Flemish sign language alphabet had to be done. The method to determine the needed DOFs is explained below:

Take the first character: "A". It takes 3 DOFs for each finger to flex except for the thumb. So 12 DOFs in total. Next take the second character: "B". It takes 2 DOFs to form this letter. Now are already 14 DOFs in use. Next take the third character: "C". It takes 3 DOFs for each finger to flex, thumb included. Then compare the used DOFs of character "C" with the used DOFs of characters "A" and "B". In total it takes 15 DOFs for character "C" and 14 DOFs for characters "A" and "B". When taking a closer look at the DOFs, it can be seen that the 14 DOFs used for characters "A" and "B" are exactly the same 14 DOFs used for character "C". So, 1 DOF more is needed to form character "C" and the total used DOFs are increased by 1 from 14 to 15.

This method can be repeated for each character. The results of the analysis can be found in Table 7.

Table 7: Results simplification DOFs

Part	Joint	DOFs	Excluded	Result	Amount
Fingers	MCP ⁹	2	1	1	3
	PIP	1	0	1	4
	DIP	1	0	1	4
Thumb	TMC	2	1	1	1
	MCP	2	1	1	1
	IP	1	0	1	1
Wrist	W	2	1	1	1
Elbow	E	1	0	1	1
	RU	1	0	1	1
Shoulder	S	3	0	3	1
Total		28	6	22	

The analysis has pointed out that 2 DOF in the thumb can be excluded by giving the thumb a different offset, 3 DOFs in little, ring and middle finger (abduction/adduction) can be excluded and 1 DOF in the wrist can be excluded which we can compensate by using other DOFs. This results in a total reduction of 6 DOFs from 28 DOFs to 22 DOFs.

3.5 CONCLUSION

It can be seen that the Flemish sign language alphabet already is very complex. The analysis done to exclude as many DOF as possible approves this by leaving a result of 6 DOFs that can be reduced from 28 DOFs in total to 22 DOFs. It is not much, but it simplifies our application a bit.

Practical, more DOFs will be excluded due a lack of time. 2 DOFs in the shoulder will be excluded and the remaining DOF (abduction and adduction) will be executed at the elbow, so the elbow has 3 DOFs instead of 2 DOFs.

⁹ The MCP joint of the pointer finger still has 2 DOFs.

4. Inverse Kinematics

4.1 INTRODUCTION

Guy Fierens - Controlling a robot to move it to a goal position, a set of joint positions have to be calculated. To do this, inverse kinematics are used. During the past few years, a lot of research has been done on inverse kinematic algorithms for robot manipulators.

In the following chapter the topic of inverse kinematics will be discussed. Six of the most frequently used solving methods are presented and evaluated regarding our topic.

4.2 LIST OF FREQUENTLY USED SYMBOLS

Table 8: List of frequently used symbols

Symbol	Meaning/connotations
X	Cartesian position of the end-effector $X(x,y,z,\delta x, \delta y, \delta z)$
P	Desired position of the end-effector $P(x,y,z,\delta x, \delta y, \delta z)$
Θ	Joint states $\Theta(\theta_1, \theta_2, \dots, \theta_n)$
\dot{X}	Linear velocity vector of the end-effector $(dx/dt, dy/dt, dz/dt)$
$J(\theta)$	Jacobian matrix
J^\dagger	Moore-Penrose pseudoinverse Jacobian
$\dot{\theta}$	Joint rotational velocity
$E(\Theta)$	Error function
e	Positioning error
F	Force
$f(\Theta)$	Forward kinematics function
α	Gain

4.3 INVERSE KINEMATICS

As we concluded the research on the human anatomy in chapter 1, we can model the human skeleton as a structure consisting of a serial chain where joints are linked to each other through the human bones. The origin of this structure is defined to be right before the shoulder. This way we have a fixed base origin without losing the degrees of freedom of the shoulder.

When trying to model this system, a first step is to define the forward kinematic model where the position X is determined from known joint angles Θ using a function $f(\Theta)$. (Equation 1) The next, and more complex step of the process is inverting this function to calculate joint angles for a given position. (Equation 2) The complexity in this step lies in the inversion of non-linear equations or the inversion of a redundant system, which we will discuss later.

$$X = f(\theta)$$

Equation 1

$$\theta = f^{-1}(X)$$

Equation 2

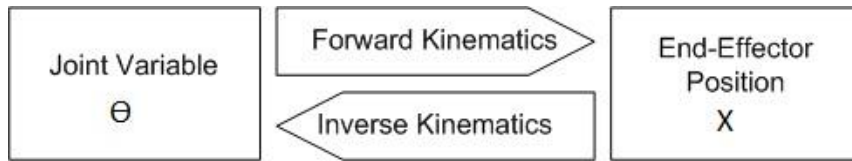


Figure 15: Forward and inverse kinematics [Robot Arms – A. Rehiara]

As we learned in chapter 2, each joint has its own coordinate system. Using different reference techniques, transformation matrices can be created. These matrices describe the transformation of the joints coordinate system relative to the coordinate system of the previous joint or the base coordinate system. [5] The combination of these matrices leads to the forward kinematic function f .

4.4 REDUNDANCY

When a robot has more degrees of freedom than the ones necessary to define the position of its end-effector it is kinematical redundant. In the kinematic chain we will model, there are eleven degrees of freedom from shoulder till one of the fingertips. To define the position of the end-effector we only need six degrees of freedom: x , y , z and rotations about these three axis, what makes our system kinematical redundant.

The order of redundancy determines the amount of configurations a robot can describe. As we see in Figure 16 the robot can reach multiple configurations without moving the end-effector. The obvious advantage of a redundant robot is increased functionality and performance. A major disadvantage is the increased complexity of the kinematic system. Calculating times increase due to the inversion problem, making the robot slower.

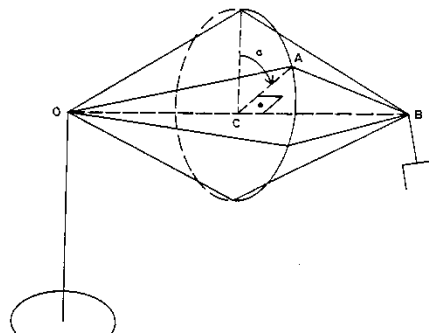


Figure 16: Configurations of a redundant robot [Patent US4999553A]

4.5 DIFFERENT SOLVING METHODS

To solve redundant systems, literature offers numerous solutions. Generally speaking we can divide these solutions into two categories: explicit and implicit solutions. When solving a problem explicitly the robot is considered as a whole whereas the implicit method will divide the robot in different non-redundant pieces. The implicit method is frequently used in the modelling of mobile manipulators, where the mobile platform and the surmounted robot arm are considered different parts.

Because we are studying and analyzing a solid kinematic chain, we will be using the explicit method to keep our calculations structured. In the following paragraphs some frequently used explicit solving methods will be weighed against each other.

4.5.1 Algebraic methods

The most graphical and easy to understand way to solve a kinematic system is to use the analytical method [6], [7]. By using a graphical representation of the robot setup and basic geometrics we can easily calculate the coordinates for a given joint rotation. After some extra calculations, the inverse equations can be easily derived.

The analytical method is mostly used in short, serial mechanical chains in a two dimensional space. When analytically solving a more complex setup an overview becomes more difficult to preserve, which makes this method not suitable for longer serial chains in 3D space.

4.5.2 Iterative methods

The more complex setups are mostly solved using iterative solution methods where we gradually work towards an optimal solution. The most-used frequently used solving methods described in [7] are compared in the following paragraphs.

4.5.2.1 Jacobian

The Jacobian matrix of a robot $J(\Theta)$ creates a transition between the joint space and the Cartesian space or 'task space' from the end-effector. Looking at Equation 3, we can see this transition is carried out by linking the time-derivatives of both variables.

$$\dot{X} = J(\theta)\dot{\theta}$$

Equation 3

Most of the mentioned solution methods use the Jacobian matrix. However the Jacobian not always offers a ready-to-solve equation. When calculating redundant systems, the Jacobian cannot be inverted to calculate the joint rotations for a desired end-effector position (Equation 5). The Jacobian is rectangular for redundant systems, making this matrix impossible to invert.

As mentioned above, the Jacobian matrix creates a transition between joint space and Cartesian space. This transition becomes more clear in the definition of the Jacobian matrix itself. In [8] the Jacobian matrix is described as a function of Θ . Each term of the matrix describes the change of a coordinate ∂X in function of a changed joint angle $\partial\theta_j$:

$$J(\theta) = \left(\frac{\partial X}{\partial \theta_j}\right)_{i,j}$$

Equation 4

4.5.2.2 Jacobian inversion method

To calculate the joint rotations starting from Equation 3, we have to invert the Jacobian to get to:

$$\dot{\theta} = J^{-1}(\theta)\dot{X}$$

Equation 5

Starting from this equation the Jacobian inversion method consists of two stages, as shown in Figure 17. In the first phase we look at the problem using Equation 3. The purpose of this first phase is to calculate the Jacobian matrix and the location of the end-effector using the current joint angles. The second phase consists of the inversion of the Jacobian matrix and adjusting the joint angles according to Equation 5. This process is repeated until an optimal result is reached.

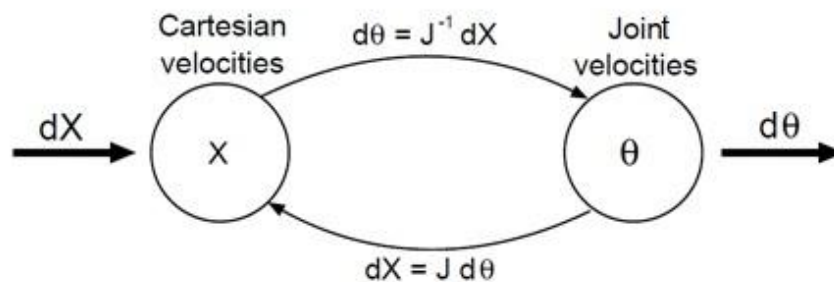


Figure 17: Jacobian inversion method [7]

The biggest obstacle solving a problem with this method is the inversion of the Jacobian matrix. When the number of degrees of freedom of X is not equal to the number of DOF θ (what happens in redundant kinematic chains), the Jacobian matrix is rectangular and therefore not invertible. To deal with this problem, the Jacobian's Moore-Penrose pseudoinverse [9] is often calculated. This leads to a square matrix which we can use to calculate X. Since this method is an approximate and local solution numerical errors can appear, leaving us stranded without a solid solution.

Another problem arises when the rank of the Jacobian is not equal to the required DOFs and the matrix cannot be inverted. This happens when some rows of the Jacobian are linearly dependent, often occurring when joints are in an extended position relative to each other. In this singular state shown in Figure 18 a change in either the first or the second joint will result in the same movement of the end-effector. This can be resolved by preventing these states using constraints.

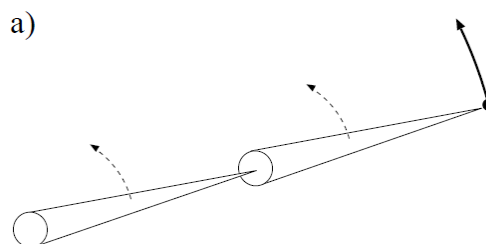


Figure 18: Extended state – Singularity [7]

Related to the problem with singularities are the “ill conditioned states”. These states occur when the robot is in a configuration between singular and non-singular. When a robot is in an ill conditioned state a distance in Cartesian space can be small, while the distance in joint space is rather large as seen in Figure 19, comparing configuration I and II.

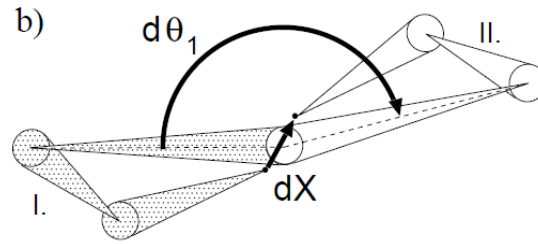


Figure 19: Ill conditioned state [7]

4.5.2.3 Optimization based method

The principle of the optimization based method starts from Equation 2 which is looked at as a minimization problem. We rewrite this equation to the following error function $E(\Theta)$ where P is the desired end-effector position and X the current position:

$$E(\theta) = (P - X)^2$$

Equation 6

Using this function, standard optimization methods can be used to minimize the error function.

4.5.2.4 Cyclic coordinate descent (CCD)

The CCD method is similar to the optimization based method. The main difference between these two methods is that the CCD methods uses the minimization process from Equation 6 on each joint separately. The kinematic chain is calculated from the most distant joint back to the first joint from the base. Each time the chain is calculated only a single joint value is changed. This way the problem is approached in a more analytical way, what makes it faster to solve.

This method is better not used for longer kinematic chains, because the algorithm calculates each joint individually in each loop. An increasing number of joints will increase the computation time drastically. Also by changing just a single value each time the algorithms calculates all the joints, makes the movement less natural.

4.5.2.5 Genetic algorithms

The fifth frequently used solving method are the genetic algorithms who can be divided in a local and a global solution. The local solution can also be used as a minimization process using Equation 6.

The main difference between the local and the global approach lies in the way the end-effector travels before reaching a certain configuration. The local approach only focuses on the end-effector position whereas the global approach also takes in mind the way the end-effector has to travel to reach its desired position. This implies that more complex movements like walking or jumping can be calculated using the global approach.

As the name suggests, genetic algorithms partially work as the algorithms controlling our body. Through a couple of parameters a calculated solution is evaluated and compared with other solutions to select the best solution. The next generation will then be a mutation of the best solutions and the process can be repeated, until a satisfying solution is found.

Although complex movements can be realized using genetic algorithms, the calculation is not only time-consuming but it is also not always certain that an appropriate solution can be found.

4.5.2.6 Jacobian transpose method

The transpose Jacobian method solves the problem of inverting the Jacobian when dealing with redundant systems. To do this we need to use the principle of virtual work and generalized forces. An external force vector consisting of a pulling force and a twist force which is applied to the end-effector generating forces and torques in each joint, leading to:

$$\dot{\theta} = J^T F$$

Equation 7

This equation can be used in combination with the error function $E(\theta)$ (Equation 6) leading to:

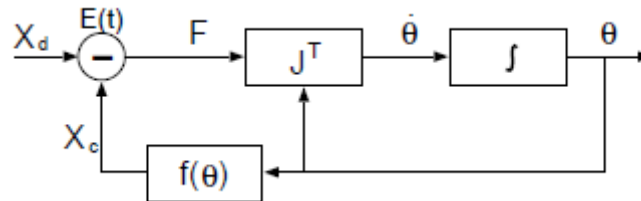


Figure 20: Solving a kinematic model using the Jacobian transpose method [7]

Using the transpose Jacobian method instead of the Jacobian inverse method solves the problem of the Jacobian inversion. But other bottlenecks like singularities and ill conditioning remain.

4.6 CONCLUSION

When trying to spell words using the alphabet of the Flemish sign language it is sufficient to program the sequences and joint angles of the different movements. The same is true for counting from one to ten and some one hand word symbols.

The desired joint positions can be calculated with Cartesian coordinates for each letter of the alphabet using the techniques mentioned above, but this unnecessarily creates a more complex model.

At the moment the project will be expanded to a dual hand robot and the complete Flemish sign language will be performed it might come in handy to define each position using Cartesian coordinates. The option of simply programming the sequences still stands, but might require more functions or code to program each static word. When programming words where the two hands need to interact with each other dynamically, a mathematical model becomes more interesting. Using a mathematical model in this situation, trajectory planning can be implemented and the interaction between the two arms becomes more clear to define.

5. Mechanics

5.1 INTRODUCTION

Jasper Slaets - In this chapter the overall mechanics behind our application will be explained. First the movement system will be handled, to see which possibilities there are to execute the right movement. Second, there will be a pre-calculation to estimate how big the acting forces and torques will be. Third, the right electro motors will be chosen based on the pre-calculations. Fourth, when the electro motors are chosen it is possible to calculate the acting forces and torques based on them. The final part of mechanics is choosing the right cables based on the chosen movement system. In this last part, the material, structure, extension in the cable extension as result of the construction will be handled.

5.2 MOVEMENT SYSTEM

First must be looked at the possible bottlenecks, to decide which movement system can be used. Those bottlenecks were first of all, the mass of the structure. The more weight as result of increasing mass is a problem to actuate the construction properly. The further away the point representing the mass of the structure is from the joint, the bigger the needed torque will be to move the structure. Second, the accuracy of the movements, which is directly connected to previous bottleneck and the actuation system. Third, the movement system must fit in the construction, so the shape of the structure is also very important.

In next paragraph, the different methods to control a joint will be handled. Next, the different joints will be explained. After these two paragraphs, there will be room for actuation architecture and at the end an overall conclusion considering the movement system.

5.2.1 Methods

There are currently three methods to control joints. In-site actuation, remote actuation with cables or belts or shape memory alloys (SMA). In the following paragraphs these different methods are described.

5.2.1.1 In-site actuation [10]

In-site actuation can be described as the actuator is located inside on of the two links related to the joint which must be actuated or is located directly inside the joint. This method can be achieved in two different ways. First, direct-drive actuation: the actuator is placed inside the joint without any transmission components (Figure 21). Second, link-hosted actuation: the actuator is placed inside one of the two links related to the joint (Figure 22). But either way the joint is driven, so it's called an active joint.

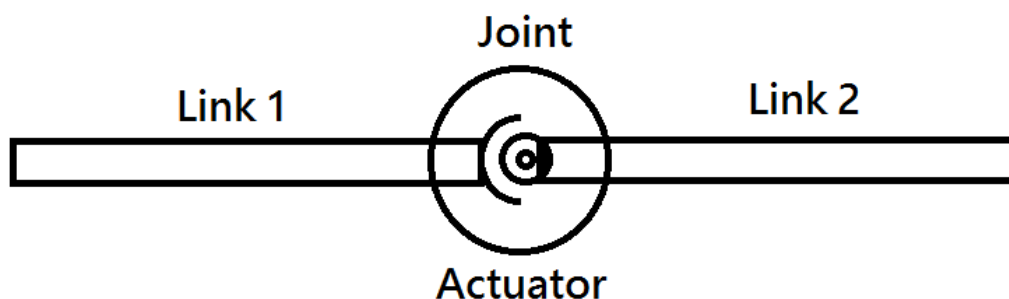


Figure 21: Direct driven actuation

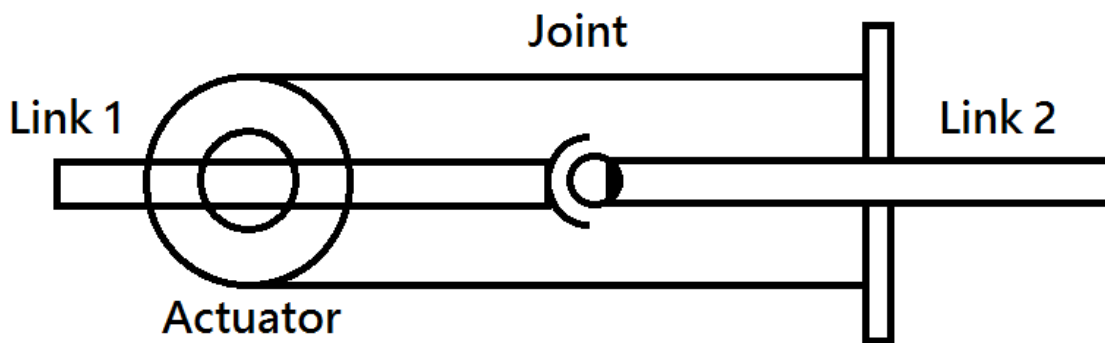


Figure 22: Link-hosted actuation

Direct driven actuation is regularly used in industrial robots, because it simplifies the transmission chain. Actually there is no transmission at all when the actuator is directly connected to the joint axis. Unless the transmission is located inside the actuator. In this case it's possible to move heavy robot arms, like industrial robots. There are also negative aspects about this method. The mass of the actuator is focused on the joint itself. If the joint needs to be moved as well (along with the mass of the actuator), it takes more power in the previous joint. Another issue is the wiring. The cables from the actuator in the joint also produce a relative large torque disturbance in the previous joint.

Link-hosted actuation is almost the same as the previous actuation. The only difference is that now there is some kind of transmission between the actuator and the joint, because the actuator is placed on one of the two links connected to the joint. The advantages and disadvantages are for this method the same as for the direct-drive actuation method.

5.2.1.2 Remote actuation [10]

Because of the previous mentioned method's disadvantages, it is necessary to look for alternatives. Remote actuation is one of the two alternatives. The actuator is now placed outside the two links that are connected to the joint (Figure 23). For this reason, transmission is necessary. This transmission can be anything, but basically they can be divided into two groups: flexible-link transmission and rigid-link transmission.

Flexible-link transmission is based on deformable connections. Translation and rotation can be provided by changing the transmission path.

Rigid-link transmission is mainly based on articulated linkages (mainly gear trains). These transmissions can be divided into two groups: parallel and non-parallel axes gear trains. Respectively a car transmission or worm gears.

Rigid-link transmission isn't possible for our application because of the weight that comes along with it. Flexible-link transmission is a very good alternative, because we can compensate weight by using light weighted cables or belts.

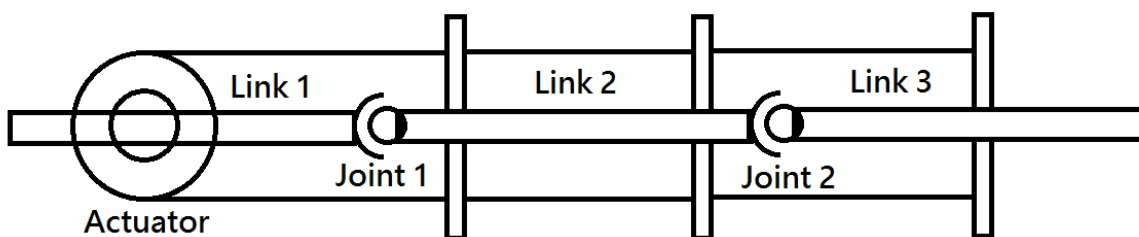


Figure 23: Remote actuation

5.2.1.3 Shape memory alloy [11]

A last method to control joints is shape memory alloys (SMA's). This method can be seen as a whole new type of actuation or as direct driven actuation. The difference between both views is where the SMA's are used in the structure. When the SMA is used only on the joint it can be seen as direct driven actuation. When whole the structure is a SMA it can be seen as a new form of actuation.

The SMA's are alloys or groups of metallic materials that have the ability to return to a previous defined shape of size when subjected to a specific thermal process.

This process is called: shape memory effect (SME). The SME occurs due to a temperature and stress dependent shift in the material's crystalline structure. There are two different phases called Martensite and Austenite. Martensite is the low temperature phase of iron and is relatively soft. Austenite is the high temperature phase of iron and is relatively hard.

In order to understand this phenomenon, it is useful to consider the simplified two-dimensional representation of the material's crystalline arrangement shown in Figure 24.

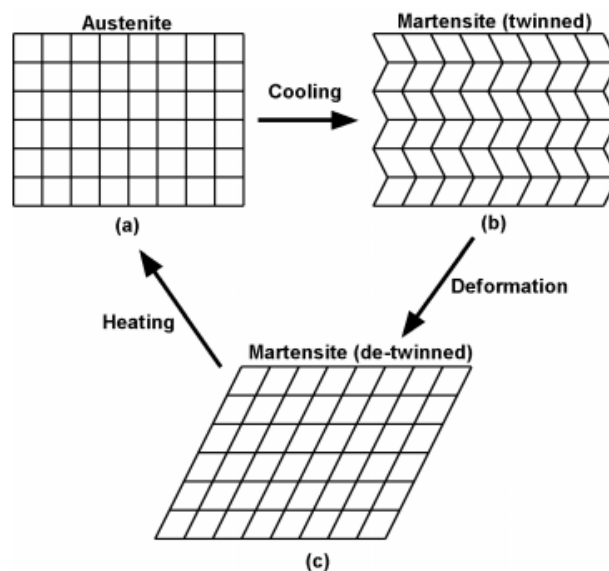


Figure 24: SME crystalline structure [11]

SME can also be created by applying a certain voltage. Not with metallic materials or any alloys, but with polymers. Actuators made from polymers seems to provide many advantages over traditional actuation. Some crucial aspects such as feasibility, stability and durability are still being questioned. However, considering the development progress, the debate might not be the limitation or failure of the technology but the consequences for improvement. But this technology is still in a research phase, which means that it would take a lot of time before this method can actually applied. [12]

These methods can also be used to control joints or in best case there is no need for joints anymore because the SMA remembers any position it was given before. There are so much possibilities with this SMA but it is still in a research phase. Precise control of joints or positioning in general is not possible at this present day. For this reason SMA are not suitable for our application.

5.2.2 Joints [13]

As told in the previous paragraph, it is recommended to use the remote control system, so the mass is reduced at all the points furthest away from the shoulder joint. Since chains and belts are too big and too heavy, so cables will be the lightest and most compact solution to actively move a joint.

The next thing needed to take a look at, is which movement the fingers need to make. In chapter 3 is talked about the DOFs of the fingers. Each finger had four DOFs, of which three are actively moved and one passively. For flexion and extension only three DOFs are needed of which are two actively moved (MCP and PIP) and one passively (DIP). The difference between an actively and a passively moved joint will be explained in next two paragraphs.

5.2.2.1 Active joint

An active joint is a joint which is driven. As previously mentioned in paragraph 5.2.2.1, there are three different ways to move a joint. For example if an axis is directly connected to a motor or when one of the two links that are connected to the joint is driven by cables (Figure 25), the joint is actively driven. As can be seen in Figure 25, joints MCP and PIP are actively controlled by cables with force F_1 and F_2 . For flexion, upper forces F_1 and F_2 are used. For extension, lower forces F_1 and F_2 are used.

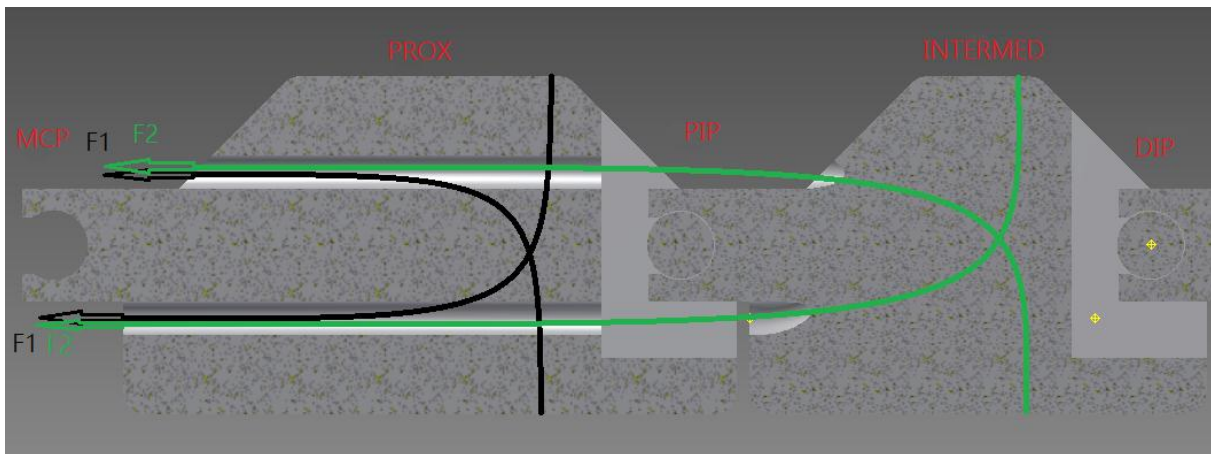


Figure 25: Active joints connections

5.2.2.2 Passive joint

A passive joint is a joint that moves as a result from another joint and isn't directly controlled. An example from a paper related to this subject is given in Figure 26. In this figure, cables T4 and T3 represents the connection for the actively moved joints and cable T5 represents the connection for the passive joint. T5 starts at the opposite side of the end of T3 and T4 end on the opposite side of the end of T5. This is because first there must be a cable extension, otherwise there won't get any movement from the passive joint. If the finger is about to flex, T3 will be pulled and there will be a cable extension on the opposite side of the joint in T5 in the PIP joint. This extension needs to be compensated by a cable reduction that will occur in the DIP joint. This cable reduction has the effect that a pulling force will occur. All parts of the finger will flex. So the DIP joint will be the passive controlled one and the PIP joint is the active controlled one. Same explanation can be given for the extension of the finger. Only the active controlled joint is the DIP joint and the passive controlled joint is the PIP joint.

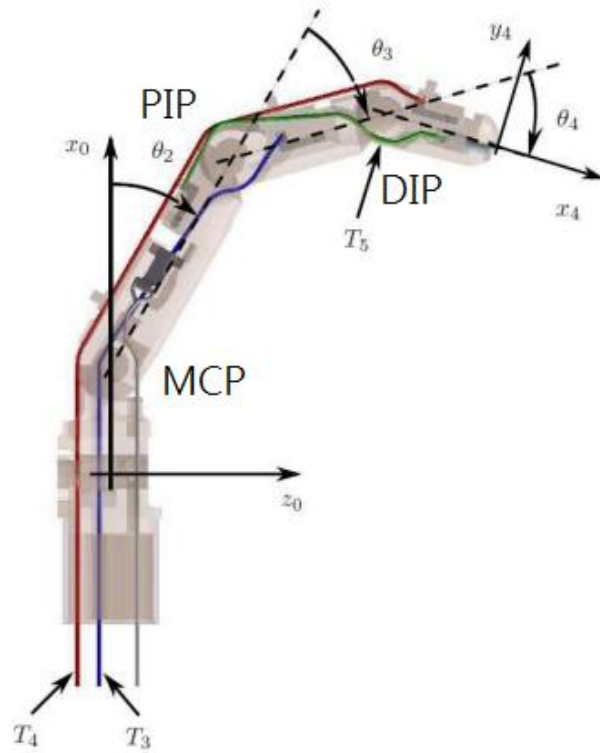


Figure 26: Example passive joint [13]

In our application there is one major difference. The proximal and intermedial part need to be actively controlled because of the movements we want to make. This includes the passive joint (DIP) for flexion and extension is the same. Therefore a connection from the proximal part to the distal part of the finger is needed for the passive movement. The principle of the passive movement is the same as previously mentioned.

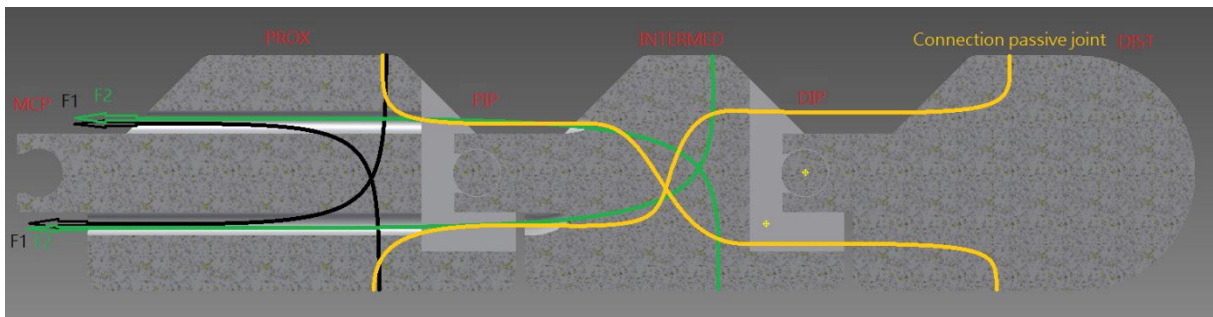


Figure 27: Cable connections

5.2.2.3 Active and Passive joints

In Table 9 can be seen which joints of the human hand and arm need to be actively or passively driven based on analyzing the motion of the human hand and arm. All excluded DOF are also excluded in this table (chapter 3).

Table 9: Active and passive joints

Part	Joint	DOFs	Active or passive	Part	Joint	DOFs	Active or passive
Fingers	DIP	1	Passive	Thumb	DIP	1	Active
	PIP	1	Active		MCP	1	Active
	MCP ¹⁰	1	Active		Saddle	1	Active
Wrist		1	Active	Shoulder		3	Active
Elbow		2	Active				

5.2.3 Actuation Architecture [10]

All previous mentioned methods to control a joint can be applied according to different types of structure. For example by using more than one actuator the joint can be controlled differently.

In general, a number N can be considered for all the joint in a robotic hand and a number M for all the actuators that are used to drive the joints in any way. There are three main categories of actuation schemes:

- $M < N$: some joints are passive, coupled, or under actuated;
- $M = N$: each joint has its own actuator and there are no passive, coupled or under actuated joints;
- $M > N$: more than one actuator is operating on a single joint.

These configurations depend on the type of actuators, in this case type of motors. Two main actuation modalities can be recognized: single-acting actuators and double-acting actuators.

Single-acting actuators are motors which can generate a controlled motion in one direction only. The reverse motion must be generated by an external action. This external action can be passive or active. Respective examples are a spring and an antagonistic actuator (Figure 28).

Double-acting actuators are motors which can generate a controlled motion in two directions. Such actuators can be used to drive a joint all by itself. But when such actuators are used, they can be combined as well. This functional redundancy can allow sophisticated drive techniques, like a complex push-pull system.

¹⁰ The MCP joint of the pointer finger has two DOF that are actively driven.

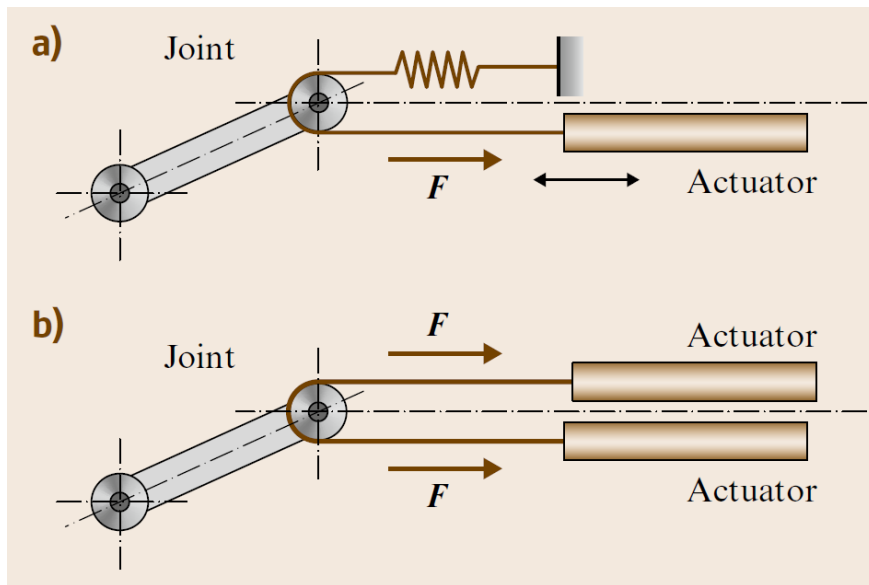


Figure 28: a) Passive single-acting b) Active single-acting [10]

The biggest advantage of this system is the flexibility, because of the compensation of different path length in case of remote control. The biggest disadvantage is feedback from the actuators. It is difficult to host two actuators. In other words a higher control complexity is necessary which results in a greater cost. For remote controlled systems, three different configurations can be used. Two for single-acting actuators (Figure 29b & c) and one for double-acting actuators (Figure 29a).

To minimize the control complexity and to use as less actuators as possible to reduce mass and volume, double-acting actuators will be used. For this reason an N-type architecture will be used.

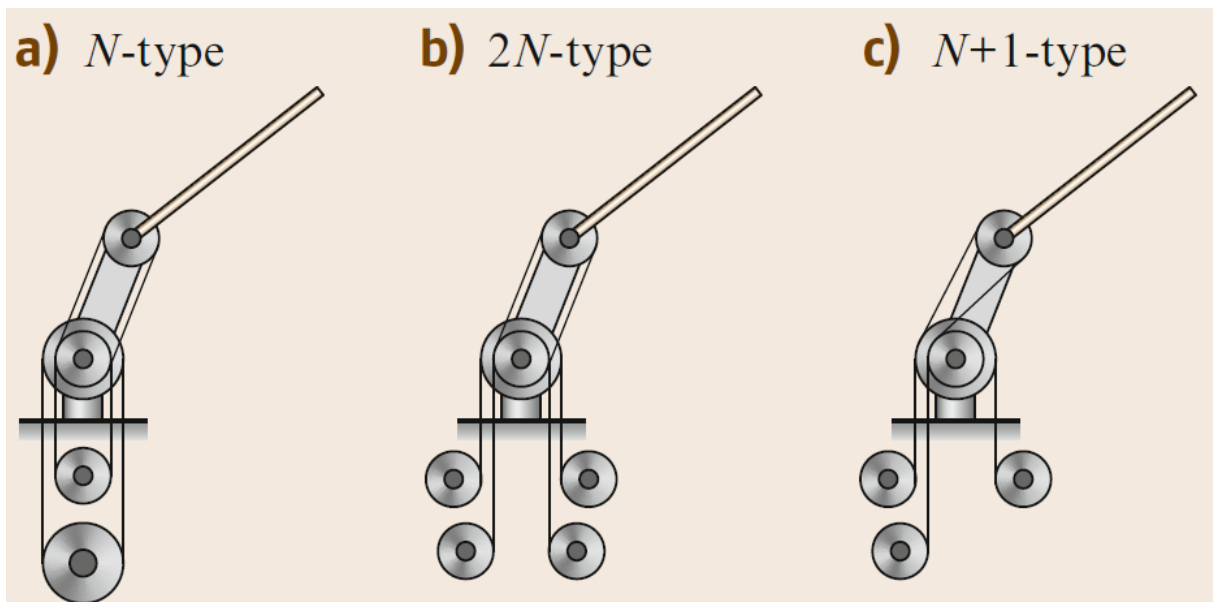


Figure 29: Remote actuation connections [10]

5.2.4 Conclusion

In previous paragraphs is told what possibilities there are to obtain the most optimal movement system for our application. The only bottleneck that appeared was the mass. The mass need to be as less as possible and it must be centered as close as possible to the shoulder. This is necessary to reduce the motors power that is directly proportional the size of the motors. In other words, the joints controlled on the axis of the joint itself is not an option here. The SMA's and electroactive polymers are still in a research phase, therefore this method cannot be used.

For these two reasons and the fact that chains and belts are too big and heavy, it is recommended to use remote actuation with lightweight cables. Though there is one exception. The saddle joint, which is simplified in our application to one DOF instead of two, will be in-site actuated. This is because it simplifies the rotational control of the thumb.

When decided which joint needs to be actively or passively driven, it is possible to choose the most optimal actuation architecture. As can be seen in Table 9, the actuation architecture for the four fingers is $M < N$. This is because there are three or four joints to control with only 2 or 3 actuators. The remaining joints have an $M = N$ architecture because they are actively driven and most of the time in depended from each other.

Because everything in our application needs to be as light and compact as possible, it is recommended to use as less actuators as possible. Which lead to integrate double-acting actuators. This results in an N configuration for the cable system. The only disadvantage to this configuration is the fact that the actuation in both directions need to be the same, but this will be handled more specific in paragraph 5.8.3.

When the optimal configuration is chosen, it is possible to proceed with pre-calculations to decide which actuators can be used.

5.3 PRE-CALCULATIONS

5.3.1 Introduction

In order to decide the actuation of our application, some pre-calculations had to be done. These pre-calculations will be based on an estimation, because a point to start from is needed. The volume of every part of the finger will be estimated. When this information is obtained, the torque on each joint can be calculated. From these calculated torques it is possible to search the right category of actuator to actuate our application.

5.3.1.1 Estimation

In an estimation it is usual to take average values for all the used factors.

The average density of PLA and ABS is approximately 1230 kg/m³ and 1110 kg/m³ (paragraph 7.3.6.3). These average densities are needed, because these are the only materials that can be printed with. Because of reducing the mass, it is logical to take into account an average degree of filling (50%). Of this 50% is 80% printing material and a remaining small percentage of 20% steel cable. This is because when the mass of an object is so little that the mass of the cables through the object will matter, it is necessary to take this mass also in account.

The average lengths of the fingers, the palm of the hand, the lower arm and the upper arm are also given. The only element remaining to calculate the estimated torque is the volume. Therefore a volume experiment was needed and explained in Annex 3. The results of this experiment can be seen in Table 10.

Table 10: Estimated volumes

Pointer finger	Distal	5	cm ³	Middle finger	Distal	4	cm ³
	Medial	5	cm ³		Medial	9	cm ³
	Proximal	10	cm ³		Proximal	11	cm ³
Ring finger	Distal	5	cm ³	thumb	Distal	8	cm ³
	Medial	5	cm ³		Proximal	8	cm ³
	Proximal	6	cm ³		TMC	50	cm ³
Little finger	Distal	3	cm ³	Palm of the hand		373	cm ³
	Medial	3	cm ³	Lower arm		580	cm ³
	Proximal	4	cm ³	Upper arm		843	cm ³

5.3.1.2 Calculation estimated torque

Now it is easy to calculate the mass of each part of the hand and arm. Physics tells us that the mass of an object is equal to the volume of the object multiplied by the density of the used material Formula:

$$m_{object} = V_{object} * \rho_{object}$$

Equation 8: Mass object

Because the fingers, hand and arm are going to be 3D-printed, it is needed to take into account a certain degree of filling. To keep it average, the degree of filling will be 50%. Of that 50% is 80% PLA or ABS and 20% steel, as previously mentioned. With all these factors chosen, it is possible to calculate the mass of each part. With Equation 8, it is possible to convert this mass to weight.

When the weight is calculated it is possible to calculate torque, because the weight and the average length (Table 27) of each part is given. For the remaining joints it is necessary to take the weight of the previous part in account to have realistic torque calculation. This calculations is schematically represented in Figure 30 for each joint in a finger. Same calculation can be applied to the wrist elbow and shoulder joint.

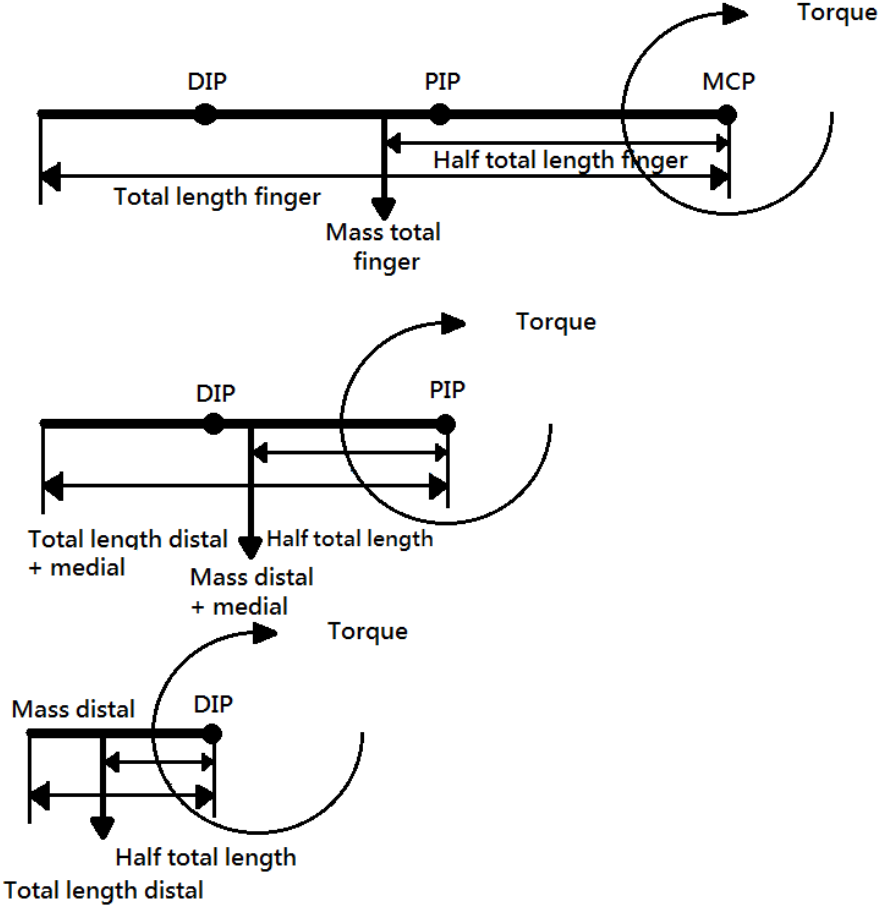


Figure 30: Torque calculation example finger

To continue with the example, take the distal part of the pointer finger and the two previous mentioned configurations. Configuration one (80% PLA, 20% steel) gives a mass of 6.3 g. The average length of the distal part is 2.5 cm. These two factors result in a torque of 0.00077 Nm (\approx 0.0079 kgcm) for the DIP joint. Same can be done for configuration two (80% ABS, 20% steel). The mass of the distal part is 6.1 g and the average length is 2.5 cm. This two factors result in a torque of 0.00074 Nm (\approx 0.0076 kgcm) for the DIP joint. The reason to convert Nm to kgcm is the fact that some small electro motors have this unit for torque. All the results of the estimated torques can be found in Annex 4.

5.4 ACTUATORS

When the pre-calculations are done, it is possible to take a look at which actuators could be used. In our case it will be electrical motors, because other types of actuation are too “industrial sized” to apply. For example pneumatic or hydraulic actuation. When chosen electrical motors it can be predicted that these actuators must meet certain requirements. With these requirements it is significant to choose the right electrical motor. Two types of electrical motors turn out to meet these requirements and will be explained and compared in next paragraphs.

5.5 REQUIREMENTS ELECTRICAL MOTORS

The electro motors needed for our application meet certain conditions. Low voltage is the first one. For this reason only one power supply can be used for the chosen motors and the control of them. The electro motors also need to be small, because there isn't much space in our arm structure. They also need to be light because otherwise the structure will become too heavy for the electro motors to handle. Next, the electro motors need to have a reasonable torque to be able to move the construction. Also a holding torque is required to hold the construction in the right position. The last condition is that the motors needed for our application must be controllable. It is necessary to achieve the right positions. In next paragraph all these requirements will be compared with each electrical motor to choose the best possibility for our application.

5.5.1 Choosing the right electrical motor

To start this chapter it is necessary to know what types of electrical motors there are. As known, there are a lot of electrical motors, different sizes, controllable or not, high speed / low speed and so on. But most of the times they are divided into three groups. The first group of electrical motors includes the alternating current-motors (AC-motors). These motors can be directly connected to the electric grid. The second group includes the direct current-motors (DC-motors). These motors can be directly connected to a battery or a DC-source like the power supply of a computer. The third group includes the stepper motors.

AC-motors are often used in industrial applications, which involve high power motors because a constant rotational torque and speed is required to control large loads, for example pumps or motors in electric cars. Light duty DC-motors and stepper motors are often used for position control, micro processing and robotic circuits. [14]

The motors needed for our application must be controllable, specifically angular controllable. For this reason the speed of the motors is not significant, but the position of the motor axis is. When the position of the motor axis can be controlled, the right angle and respectively the right motion can be achieved. As previously mentioned, only light duty DC-motors and stepper motors suitable for our application. These two types of electrical motors are explained in next paragraphs, starting with stepper motors and followed by light duty DC-motors.

5.5.2 Stepper motors [15]

5.5.2.1 Introduction

All stepper motors can be viewed as brushless motors. Because the rotor has no windings, brushes or commutator, they are robust and inexpensive. The rotor is cylindrical and has external poles. The rotor often includes a permanent magnet. The stator has electromagnets, these windings are disposed in laminated steel. Only the can stack structure is an exception. There are no disposed windings here. The number of windings can change from 2 to 5. A winding is also called a "phase" (Figure 31).

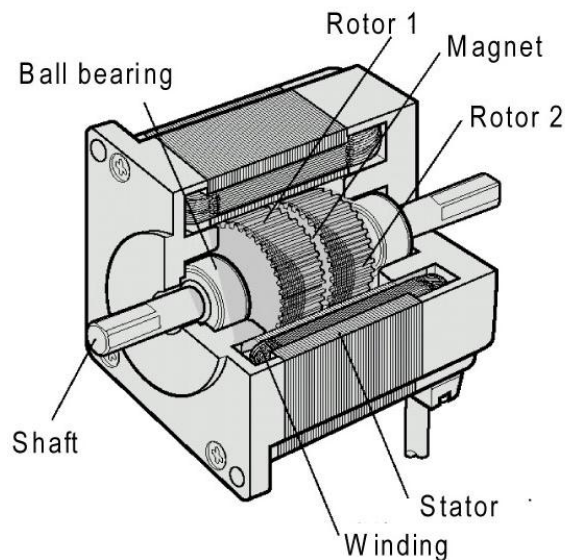


Figure 31: Cross section stepper motor [designworldonline.com]

Stepper motors work differently from other motors. Rather than voltage being applied and the rotor spinning smoothly, stepper motors rotate in response to individual control pulses applied to its windings. Every change in this process, moves the motor by an exact angle. These small angle increments are called "steps", hence the name "stepper motor". The motor can be held in any fixed position as well.

The order in which those electromagnets are activated determines the rotation direction. Each step covers a specific range of "swing". The step angle is related to motor construction details: number of coils, number of poles or number of teeth. It can be from 90° to 0.75° , corresponding to 4 to 500 steps per rotation. Typically a stepper motor has 200 steps/rot, or 1.8 degrees per step.

To move the rotor, the electric magnets on the motor must be activated in the right order. This commutation is handled externally by the stepper motor controller. One digital input pulse to the controller corresponds to one step. The frequency of the digital input signal controls the speed of the motor. The rotation speed is low, normally below 300-350 rpm. The very maximum speed limit is about 2000 rpm.

5.5.2.2 Types of stepper motors

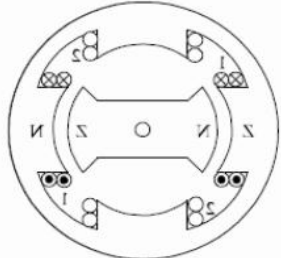
Stepper motors come in three variations, permanent magnet (PM), variable reluctance (VR) and hybrid (combination of both PM and VR) stepper motors. When there is no label on the stepper motor that tells us which kind of stepper motor it is, it is still possible to determine which motor it is. When no voltage is applied, it is possible to feel the difference by manually rotating the motor's axis. If it is a PM stepper motor, it tends to "cog" because of the residual magnetism in the rotor.

If it is a VR stepper motor, it will spin freely. They may “cog” a little bit because of a little residual magnetism. Another difference between PM and VR stepper motors is the amount of windings they have. A VR stepper motor regularly have three (or more) windings, with a common return and PM stepper motors regularly have two independent windings, with or without center taps. [16]

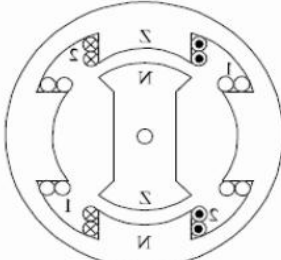
In next paragraphs only PM and VR stepper motors will be discussed, because the hybrid version is a combination from both types.

5.5.2.3 Permanent magnet

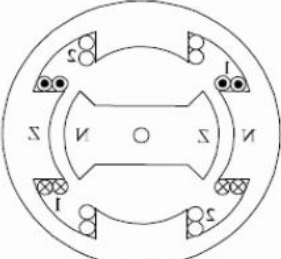
A permanent magnet type stepper motor, has a cylindrical permanent magnet rotor. The stator usually has two windings as previously mentioned. In the Figure 32 you can find the basic principles of a PM stepper motor, with one pole pair in the rotor and one pole pair per phase in the stator. The stator has two phases, divided into two parts (one per pole), which are connected in series. The rotor is a permanent magnet with two poles. The step angle will be 90 degrees.



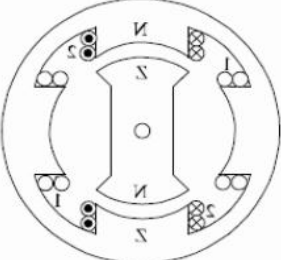
If phase 1 is actuated the rotor has set itself according to the axis line of this phase: different magnetic poles attract each other so the poles of the stator electromagnet brings the permanent rotor magnet in a horizontal position.



If phase 2 is actuated, the rotor will focus according to the vertical axis of this phase. The rotor has been rotated clockwise through an angle of 90 °.



If phase 1 is actuated with a negative current, the poles of the electromagnet will be magnetized opposed to the position 1 and the rotor rotates further clockwise 90 °.



Finally, when phase 2 is actuated with a negative current, the rotor rotates clockwise another 90 °.

Figure 32: Permanent magnet stepper motor [15]

This principle can be applied to PM stepper motors with a larger number of poles to result in a smaller step angle. Figure 33 shows a PM stepper motor with twenty-four poles, but with only two windings (the same as previous example). Each winding is wrapped in a mild steel shell, with fingers brought to the center. These alternating north-south fingers will attract the PM rotor. When the polarity of the phase is reversed, the rotor would jump $360^\circ / 24 \text{ poles} = 15^\circ$. The direction is not known, which is not efficient. But, if phase 2 is energized directly after phase 1, the rotor will move 7.5° . This is due to the offset of 7.5° of phase 2 relative to phase 1.

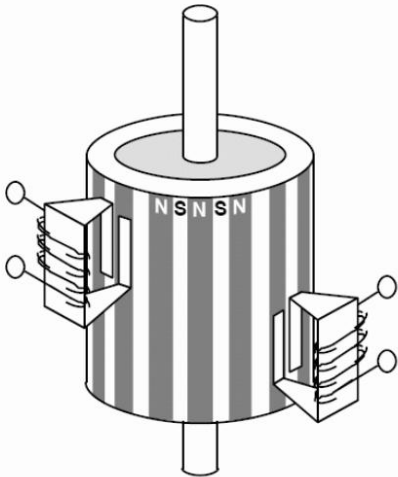


Figure 33: PM stepper motor 24 poles [15]

5.5.2.4 Variable reluctance [17]

The VR stepper motor usually has three (or more) windings and are typically connected as shown in Figure 34. The end of each winding is connected to a common terminal. When used, the common terminal is typically connected to the positive side of the power supply and the windings are energized in sequence.

The cross section shown in Figure 34 is of 30 degree per step variable reluctance motor. The rotor in this motor has 4 teeth and the stator has 6 poles. Each winding is wrapped around two opposite poles.

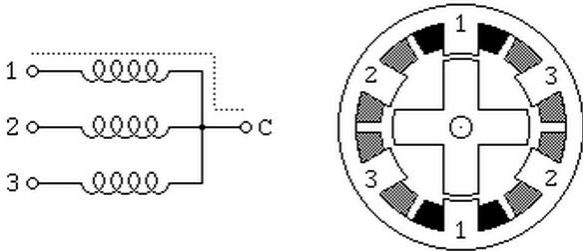


Figure 34: VR stepper motor 30° step [17]

The working sequence is as follows:

When winding 1 is energized, the rotor teeth (marked with X) are attracted to winding 1 its poles. When winding 2 is energized after winding 1, the rotor will rotate 30 degrees clockwise so that the teeth (marked with Y) will line up with winding 2 its poles. If this process is continued to winding 3 and start over from winding 1, the stepper motor will continuously rotate clockwise. In Table 11 is the applied sequence shown, with a logic 1 (current applied to winding) and a logic 0 (no current applied to winding) for 12 steps or 1 revolution.

Table 11: Sequence VR stepper motor 30° step

Steps =>	1	2	3	4	5	6	7	8	9	10	11	12
Winding 1	1	0	0	1	0	0	1	0	0	1	0	0
Winding 2	0	1	0	0	1	0	0	1	0	0	1	0
Winding 3	0	0	1	0	0	1	0	0	1	0	0	1

There are also VR stepper motors with four and five windings which requires five or six wires (four or five windings plus one common terminal wire). These motors are driven with the same principle as previously mentioned. But it is very important to work out the correct sequence of energizing the windings so the motor will step nicely.

The VR stepper motor with 30 degrees per step, uses the fewest number of rotor teeth and stator poles that performs nicely. When more motor poles and more rotor teeth are used, it is possible to make smaller steps. Toothed faces on each motor pole and a respectively toothed rotor allows for step angles as small as a few degrees.

5.5.3 RC Servomotors

5.5.3.1 Introduction [18]

The basic principles of the 'radio controlled' servo motors are based on the same principles as a regular, controlled brushless DC-motor. Except a servo motor has 2 components: a brushless DC-motor and a gearbox to reduce the speed (Figure 35).



Figure 35: A RC servo motor [Princeton.edu]

A brushless DC-motor is a machine that converts DC-energy to rotating mechanical energy. A DC-motor is based on the Lorentz-force. When current flows through a conductor in a magnetic field, a force will occur. The direction of the force can be found by 'the left hand rule' (Figure 37). This force will push the conductor out of the magnetic field. The amplitude of the force depends on the amplitude of the magnetic induction (B), the length of the conductor (L) and the amplitude of the current through the conductor (I) (Figure 36).

$$F = I \cdot L \times B$$

Equation 9: Lorentz force

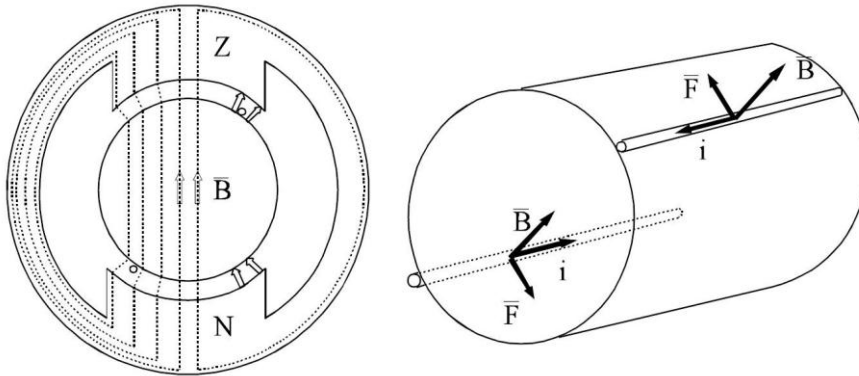


Figure 36: Lorentz force DC-motor [19]

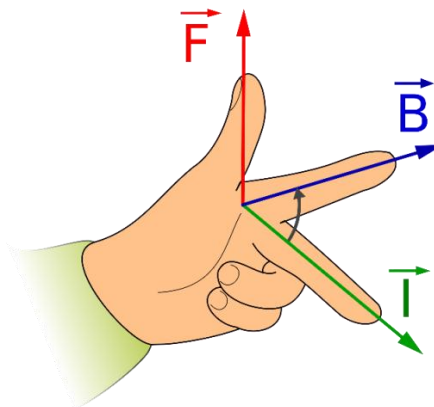


Figure 37: Left hand rule [Wikipedia.org]

Because of the Lorentz force generated by live conductors in a magnetic field on a distance “d” from the center axis in the DC-motor, the DC-motor generates a certain torque T.

$$T = F \cdot d$$

Equation 10: Torque

As told in the previous paragraph, the Lorentz force depends on the amplitude of the magnetic induction (B), the length of the conductor (L) and the amplitude of the current through the conductor (I). For an angle of 90° the sinus will be always 1 (Figure 36):

$$F = B \cdot I \cdot L \cdot \sin(\alpha) = B \cdot I \cdot L \cdot 1$$

Equation 11: Lorentz force simplified

If Equation 10 with Equation 11 are combined, the result is:

$$T = B \cdot I \cdot L \cdot d$$

Equation 12: Torque as result of Lorentz force

Now the crucial factors are known to determine the torque that will be generated. For example how smaller the DC-motor, how smaller the generated torque will be.

5.5.3.2 Servo principle

As told in the introduction, the servo principle is based on a regular, controlled DC-motor. To control the RC servo motor it is needed to know how these RC servo motors are wired. As can be seen in Figure 38, there are 4 wires. A brown, a red, an orange and a white wire. The brown wire is the ground, the red wire is for power ($\pm 5V$), the orange wire is the signal wire and the white wire is for analog positioning feedback.

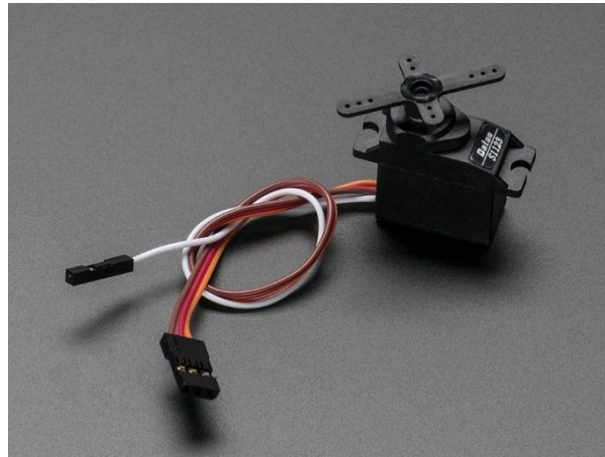


Figure 38: Servo motor wiring [adafruit.com]

The brown and red wire provide the servo of power. The orange and white wire are the signal wires for positioning the servo. The general signal applied to the servo motor is an ordinary logic 'square wave' with a specific wave length. When a 'square wave' with a specific length is applied, the servo goes to a particular angle. In other words:

The wavelength (duty cycle) directly maps to servo angle (Figure 39).

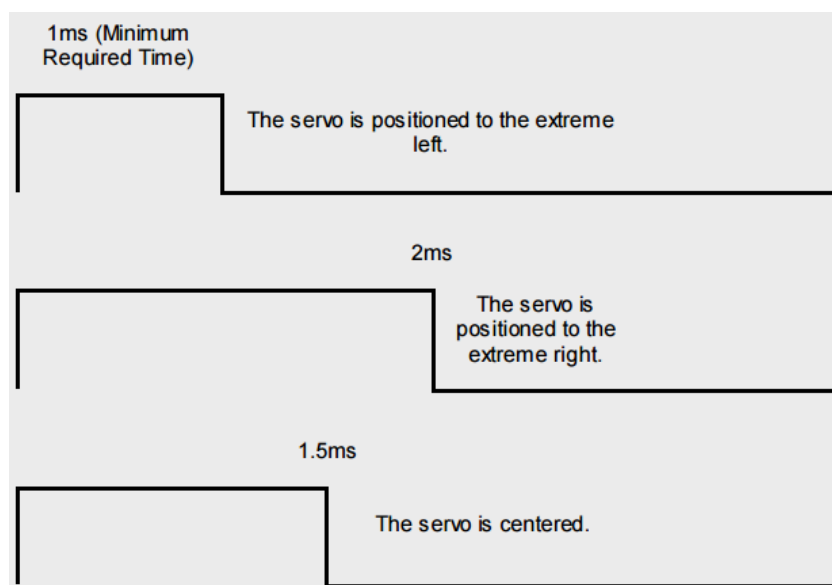


Figure 39: Command signal servo motor [Princeton.edu]

5.5.3.3 Analog VS digital [20]

There are 2 ways to control the servo motor. The first one is the analog way and the second one the digital way. In order to choose which way is the best way for our application, it is necessary to compare them.

5.5.3.4 Analog

An analog controlled servo motor contains several components to convert the incoming signals to a voltage that controls the DC-motor.

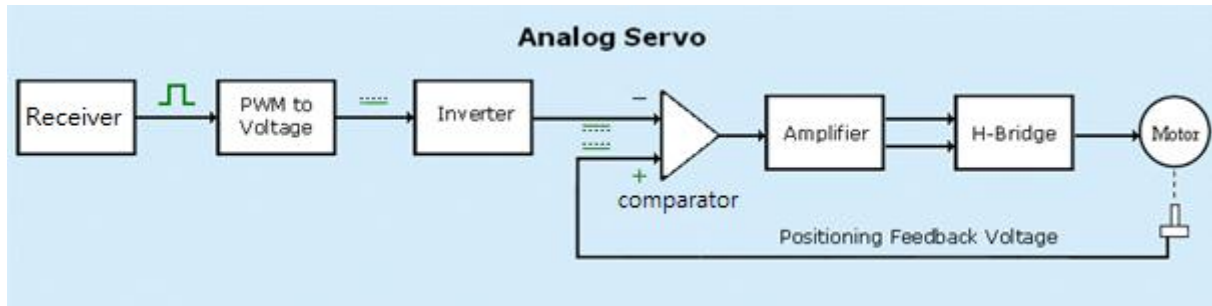


Figure 40: Analog control servo motor [sailservo.co.uk]

As can be seen in Figure 40, the incoming 'square wave' from the receiver is converted into a positive voltage and the inverter inverse it polarity. This way a voltage is presented at the negative side of the comparator. The positive voltage produced by the variable resistor, also called the feedback voltage, represents the servo's axis rotational position. These 2 voltages come together in the comparator.

When these 2 voltages are equal, the comparator will give a zero output. The servo motor remains off. Two unequal voltages will give either a positive or negative voltage output that will result in respectively rotating forwards or backwards. When these two voltages are equal again, the servo motor will turn off.

The amplifier will alter the servo motor's speed when approaching the turn off point to anticipate overshooting. Two output signals are sent to the H-bridge driver to control motor direction and speed.

5.5.3.5 Digital

In a digital controlled servo motor, there is an Integrated Circuit-chip (IC-chip). This IC-chip is actually a microprocessor. The IC-chip normally has a program on board to control the rotation and speed of the servo motor. Some servo motors can be re-programmed with a servo programmer or servo tester for a specific application. The input 'square wave' signal and feedback are converted into numbers. The difference between these numbers is used to modify rotation and speed.

5.5.3.6 RC Servo motor control

The actual control of both digital and analog RC servo motor are the same, as shown in Figure 41. The input signal is compared to the internal feedback signal produced by the position sensor. As result of this comparison the motor will rotate until the input signal and the feedback signal are equal.

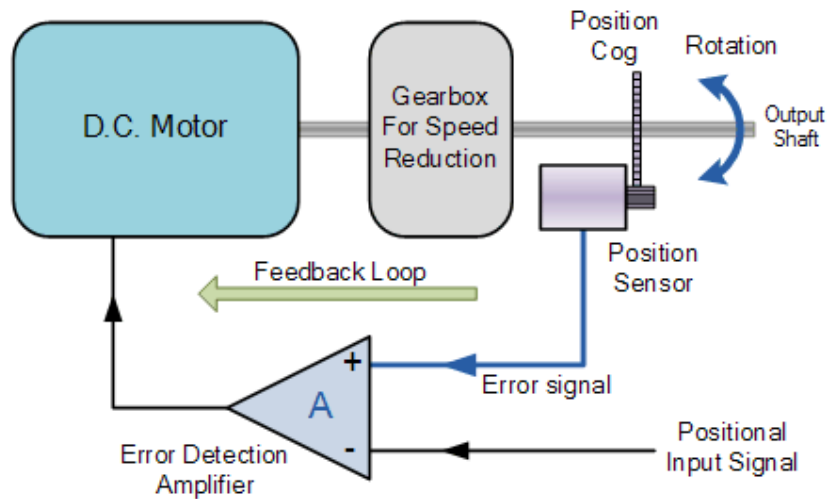


Figure 41: General RC servo motor control [14]

Still there is one difference between both digital and analog RC servo motor. The frequency of pulses that can be applied to the servo motor. The frequency of an analog servo is 50Hz or 50 pulses per second and the frequency of a digital servo motor is maximum 300Hz or 300 pulses per second. This results in a period of 20ms for an analog servo motor and a period of 3,3ms for a digital servo motor. (Figure 42)

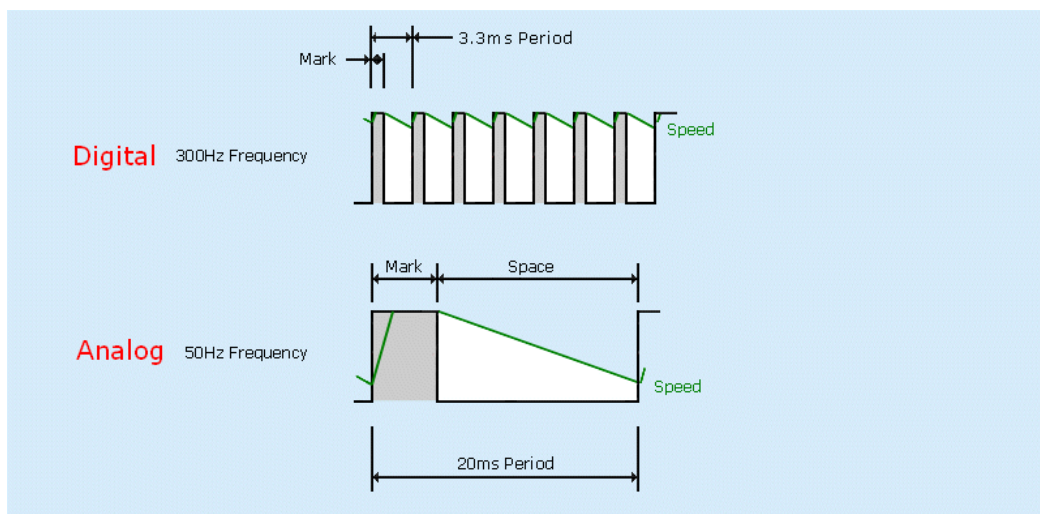


Figure 42: input signal duty cycle < 50% [sailservo.co.uk]

5.5.4 Conclusion

Stepper motors have many advantages: they are relatively cheap and brushless, so no (or less) maintenance is required. It is also simple to control stepper motors. The position is very accurate even when no feedback is required. Another advantage is high torque at low speeds and a relatively high holding torque. And finally they can easily switch from rotation direction.

Stepper motors also have disadvantages. For industrial applications sometimes it is not enough to have a power of 1kW and a maximum speed of 2000 revolutions per minute. They are also less suitable for applications with a strongly varying load torque or large accelerations. Another disadvantage is for small robotic applications as ours, they are quite robust, heavy and big in size. For this reason it is necessary to take a closer look at the servo motors.

The RC servo motors are also cheap and the DC motors inside are also brushless. The control of the RC servo motors is also simple. In this aspect both motor types are the same. But the huge advantage of RC servo motors over stepper motors is the fact that they are not robust, not heavy and not big in size when compared. For this reason it is recommended to use RC servo motors.

In fact there is no big difference between the digital and analog RC servo motor except for the frequency of pulses applied to the internal motor unit. But since an analog feedback signal is required to the controller for future adjustments and more precise control over the needed motions and analog RC servo motors are simpler to control, it is recommended to use analog RC servo motor.

5.6 POST-CALCULATIONS

Now the type of actuators have been chosen, it is necessary to decide which size of RC servo motor can be used in our application. There are a few standard sizes of RC servo motors: micro and standard size [21]. Details can be found in Annex 5. With these specifications it is possible to further work out the remote actuation cable system, starting with the transmission. Then the size and location of the forces on the cables can be determined. And finally the whole calculation will be made again but this time with real values of the prototype that is made.

5.6.1 Transmission

To see which electro motors are able to deliver the needed torque to move the joints, the largest torque from Annex 4 is taken. For the same force the difference in torque will give a difference in distance (Equation 13).

$$F = \frac{T_1}{r_1} = \frac{T_2}{r_2} \leftrightarrow \frac{T_1}{T_2} = \frac{r_1}{r_2}$$

Equation 13: Difference in distance

With T_1 as needed torque on DIP joint, T_2 as applied torque from the possible RC servos and $\frac{r_1}{r_2}$ as the transmission radius.

To calculate the minimum transmission, the smallest RC servo is taken which is the Micro RC servo with torque = 1.6 kgcm (Annex 5) and the largest needed torque (Annex 4). The largest torque is from the MCP joint of the middle finger (≈ 0.16 kgcm). When Equation 13 used the result is a minimum transmission of 1:10 for both configurations (paragraph 5.3.1.2). For example when a radius of 1 cm is taken at the RC servo motor, the radius at the MCP joint of the middle finger will be 0.1 cm (= 1 mm).

These radiuses are small enough to fit into the construction (paragraph 8.5.2). For this reason, to keep it simple and because there are standard discs with this size, a radius of 1 cm at the RC servo motors will be taken.

5.6.2 Force on cables and locations [22]

In this paragraph the acting forces on the cables and the location of them to generate the needed torque will be handled. As calculated in previous paragraph is maximum torque needed for the finger $\approx 0.16 \text{ kgcm}$ ($\approx 0.016 \text{ Nm}$). This torque can be provided by the micro RC servo with a torque of 1.6 kgcm and the standard RC servo with a torque of 6.5 kgcm . Because of the 1 cm radius the force on the cable will be respectively $\approx 16 \text{ N}$ and $\approx 64 \text{ N}$.

To calculate the location of the forces needed to counter the torque of the fingers, it is necessary to make a few statements. First, the X-axis is always the direction of the finger and the Z-axis is always the rotation axis. Second, flexing the fingers is the positive direction of the torque (Figure 43).

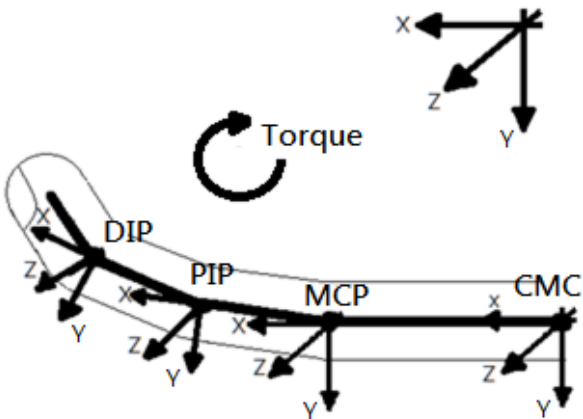


Figure 43: Statement 1 & 2

Third, a joint can take forces and torques in every direction except the rotation axis. This is why the joint is only a rotation point [22]. Fourth, the force on the cable only works in the direction of the cable. Fifth, the applied forces are horizontally constraint, because the singularity [paragraph 4.5.2.2] are compensated by mechanic constraints (Figure 44). The reason for this mechanical constraints is that the motors and cable system are not accurate enough, so this is the safest way to handle the singularities. Therefore, only the Y-component of the location is important (Equation 14).

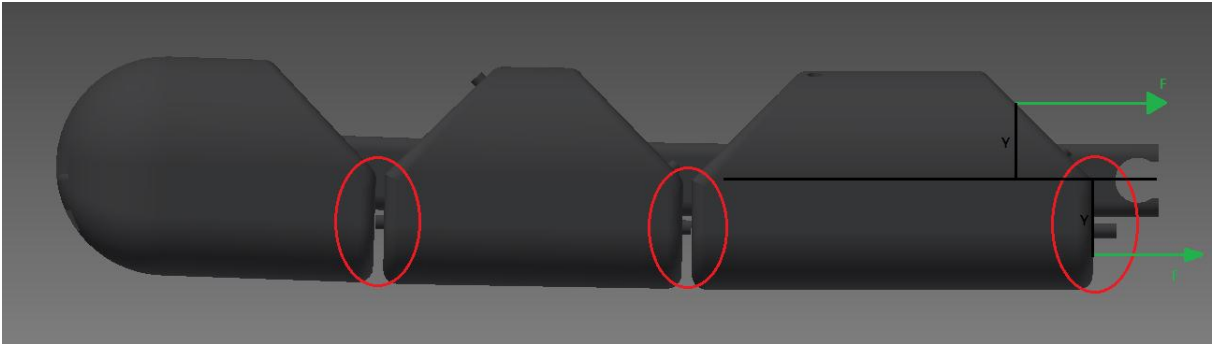


Figure 44: Mechanical constraints

Now the statements are made, so it is possible to calculate the minimum location of the force (Figure 44):

$$Y = \frac{T}{F}$$

Equation 14: Location Force

With Y as the location, T as torque needed to move certain joint and F as the force on the cable provided by the micro RC servo.

In Table 12 are the locations of the forces given for the little finger. When the distances of the two configurations are compared, it can be seen that the difference is not significant. For this reason there is no preference in printing material.

Table 12: Minimum location forces estimated

Location (mm)	MCP	PIP	DIP
80% PLA, 20% steel	0.322	0.138	0.028
80% ABS, 20% steel	0.310	0.133	0.027

In Annex 6 are all the results of the locations of the forces. These locations are minimum values, because when the same force is applied further away from a rotation point, the torque get bigger.

5.6.3 Real values

In this paragraph the exact same calculations will be done as in previous paragraph, but this time with the weight values of the printed parts. This is because an exacter calculation of the acting forces can be made and because it is vital to dimension the motors needed to move arm, elbow and shoulder.

After a few times the little finger is printed, because it is the smallest finger and take less time to print, the mass of the three parts are weighted. The scale used had an accuracy of $\pm 0.001g$, which is necessary because the parts only have a mass of a few grams. The parts are weighted with a piece of the cable equal to the sum of the cables trough the weighted part. An average mass was taken for each part from three printed fingers. Results are shown in Table 13.

Table 13: Weighed mass

PLA printed							
Pointer finger	Distal	0.002433	kg	Middle finger	Distal	0.002433	kg
	Medial	0.003339	kg		Medial	0.003817	kg
	Proximal	0.004195	kg		Proximal	0.004839	kg
Ring finger	Distal	0.002433	kg	Thumb	Distal	0.003339	kg
	Medial	0.003339	kg		Proximal	0.004195	kg
	Proximal	0.004195	kg		TMC	0.020000	kg
Little finger	Distal	0.002433	kg	Palm of the hand		0.127540	kg
	Medial	0.002489	kg				
	Proximal	0.003228	kg				

Table 14: Torque weighed parts

Torque	PLA Printed				
Pointer finger	DIP	0.00030	Nm	0.003042	kgcm
	PIP	0.00101	Nm	0.01026	kgcm
	MCP	0.00332	Nm	0.03385	kgcm
Ring finger	DIP	0.00030	Nm	0.003103	kgcm
	PIP	0.00109	Nm	0.011163	kgcm
	MCP	0.00337	Nm	0.034323	kgcm
Little finger	DIP	0.00028	Nm	0.002848	kgcm
	PIP	0.00084	Nm	0.008608	kgcm
	MCP	0.00223	Nm	0.022753	kgcm
Middle finger	DIP	0.00030	Nm	0.003079	kgcm
	PIP	0.00126	Nm	0.012899	kgcm
	MCP	0.00396	Nm	0.040414	kgcm
Thumb	DIP	0.00047	Nm	0.004743	kgcm
	MCP	0.00191	Nm	0.019469	kgcm
	TMC	0.00786	Nm	0.043682	kgcm
Wrist		0.24754801	Nm	2.524287	kgcm
Elbow		1.611388914	Nm	16.43159	kgcm

Now the mass of every part is calculated, the acting torque of each joint can be determined (Table 14). With the five statements, as in paragraph 5.6.2, it is possible to calculate the location of the forces here. In Table 15 are the results show.

Table 15: Minimum location real forces

Min Distance	PLA Printed						
Pointer finger	Distal	0.019008	mm	Middle finger	Distal	0.019236	mm
	Medial	0.064102	mm		Medial	0.080589	mm
	Proximal	0.211493	mm		Proximal	0.252499	mm
Ring finger	Distal	0.019388	mm	Thumb	Distal	0.029634	mm
	Medial	0.069743	mm		Proximal	0.121642	mm
	Proximal	0.214444	mm		TMC	0.500815	mm
Little finger	Distal	0.017791	mm	Palm of the hand		0.112066	mm
	Medial	0.053783	mm				
	Proximal	0.142158	mm				

5.7 CONCLUSION

As calculated in this paragraph, the torques are very small. For this reason the torques applied by the RC servo's are enough. Due to the radius of 1 cm of the servo arm that was chosen. The acting forces can be horizontally applied, when fingers are mechanically constrained for possible singularities (paragraph 4.5.2.2). This is because the locations of the forces is very small, which is an advantage not only for the structure but also for the applied torque. Remarque: forces are not everything. Cable reduction and extension is also very important. This subject will be discussed in next paragraph.

5.8 CABLES

As previously mentioned a remote actuated cable system will used in our application. To execute the right movements it is vital to make the cable system as accurate as possible. Two bottlenecks that occur are the own extension of the cables and the extension as result of the construction in which the cable system is applied. To determine the grade of influence of the chosen material to the own extension, a comparison will be made between the two fundamental material groups followed by specific examples that could be qualified to use of both fundamental groups in our application. Next the extension as result of the construction will be explained in general, applied to our application and will be calculated. The actuation method is something very important to take into account before the calculation can be made. Finally an overall conclusion concerning the "total extension" will be made.

5.8.1 Kind of material

There are a lot of materials in the world. To choose the right materials, it is recommended to look from a (general) group of materials to specific kinds of materials. This will be done based on certain properties of the materials. To decide which properties are necessary, a few statements will be made. The cable must be strong enough to bear the load on it. A minimum of extension and flexibility are also important. These three demands can be found in the physical properties of the materials.

5.8.1.1 Metallic VS synthetic materials

Materials in general can be divided into two groups. On the one hand there are metals and on the other hand there are synthetic materials. Before comparing the physical properties of these two groups of materials, it is necessary to understand the structure their made of.

Metals are constructed from atoms, which are ranked in a certain grid. Synthetic materials are constructed from macromolecules consisting out of a variety of atoms which are whether or not connected. This is called an amorphous structure. The different structures of metals and synthetic materials are shown in Figure 45.

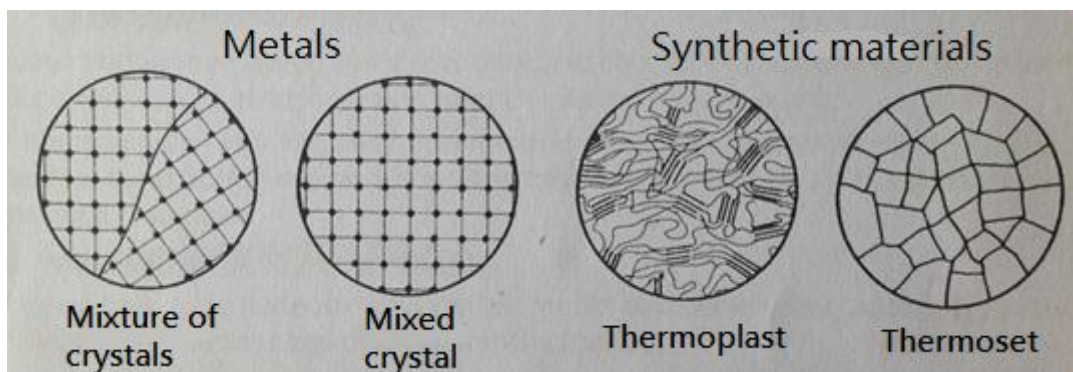


Figure 45: Structure difference [23]

The atoms in a given grid plane of a metal have to move along the atoms in an adjacent grid plane during deformation. This is because of the large primary bonding forces between the atoms, so a large force is needed to move them, which makes metal materials that have good mechanical properties. The molecules in a thermoplast first have to aim for the direction of the force, and then have to move along each other. This is because of the small secondary bonding forces between the molecules, so less force is required. The molecules in a thermoset can't aim for the direction of the force and can move along each other after the bindings are broken, which happens relatively fast. The left diagram in Figure 46 is the general stress-strain diagram for metal and the right diagram is for the synthetic materials.

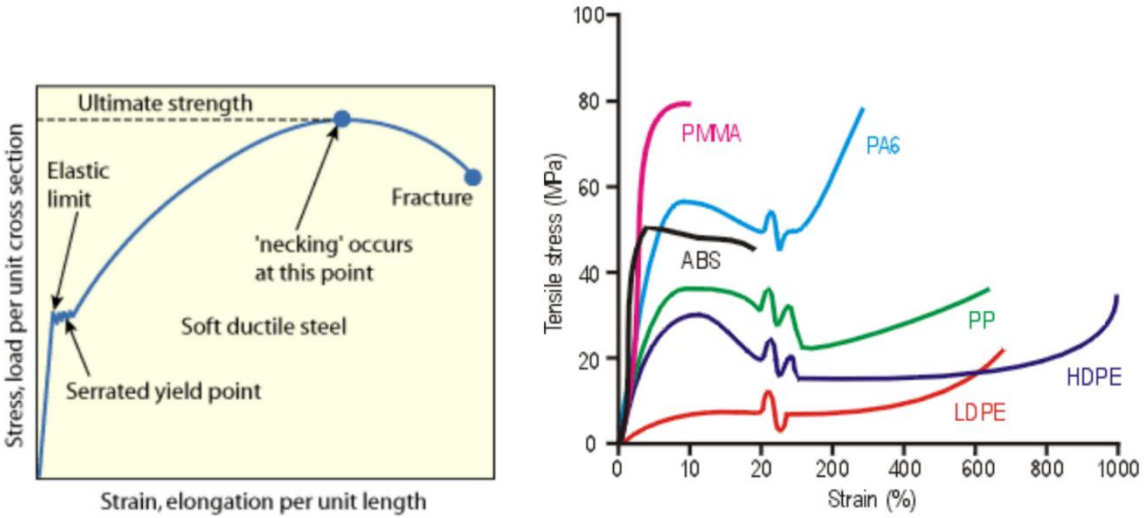


Figure 46: General stress-strain diagram [24]

Now an overview of the physical properties can be made which are useful for our application (Table 16). Because it are cables that are needed, the Young's modulus is the most important property. The Young's modulus is the ratio of stress over strain in the elastic part of the curve. Tensile strength is the strength needed to break the cable. Then there is the specific density, which needs to be as low as possible, to calculate the additional mass to the construction. As previously mentioned, flexibility is also an important factor. The only problem with this factor is that there is no standard physical property for it. It can be deduced from other factors such as structure, density, and diameter. This is why tests of the different materials in the construction are needed.

Table 16: General physical properties

Properties	Metal	Synthetic
Young's modulus (GPa)	Very high	Low, high ¹¹
Tensile strength	Very high	Low, high ¹³
Specific density (kg/m ³)	Very high	Low, high ¹³

The materials used are twisted and non-twisted steel cable, twisted and non-twisted Nylon and twisted Dyneema. The full specifications of these materials can be found in Annex 7. But the useful properties are given in Table 17.

Table 17: Physical properties used materials

¹¹ Depending on which synthetic material

Properties	Steel [25]	Nylon 6 [26]	Dyneema sk65 [27]
Young's modulus	200 GPa	2.8 GPa	116 GPa
Tensile strength	660 MPa	78 Mpa	2.95 GPa
Specific density	7900 kg/m ³	1130 kg/m ³	970 kg/m ³

5.8.2 Extension [28]

When the own extension of the cable is significant, it will result in deviations of the motion in the fingers. This is a result of the own extension of the cable. Because the cable itself also has extension when loaded with a certain force it is necessary to calculate its own extension. Depending on the kind of material the cable is made of (Young's modulus), the extension will be different. To calculate the own extension, two formulas are needed:

$$\sigma = \frac{F}{A}$$

Equation 15: Tension in cable

With σ as tension in the cable, F as loaded force on the cable and A as surface of the cross-section of the cable.

$$\sigma = E * \varepsilon$$

Equation 16: Hooke's Law

With E as Young's modulus and ε as extension.

$$\varepsilon = \frac{F}{A * E}$$

Equation 17: Extension

It can be seen that there is a direct connection between the load F and the extension ε .

To determine the actual extension of the cables, the calculation will be done twice. First, with the force applied from the micro RC servo (=16 N) and second with the force applied from the standard RC servo (=64 N).

When Equation 17 is applied to the physical properties from previous paragraph and to both forces, the results for a cable with a diameter of 1 mm are:

	Steel	Nylon	Dyneema
Extension ε , force 16N (mm)	0.102	7.276	0.176
Extension ε , force 64N (mm)	0.407	29.103	0.702

Table 18: Extension results

As can be seen in Table 18 the extension of Dyneema rivals that of a steel cable, which is almost nothing in comparison to the extension of Nylon. Because the extension needs to be minimized, a Nylon cable is not suitable for our application.

This calculation is only for full cylinders. When the cable exists out of twisted fibers, it will have effect on the own extension of the cable. Figure 47 gives us an example of this twisted fiber cable. In this figure the radius of the big cylinder is three times bigger than the radius of a fiber (green), so $R_1 = 3 * R_2$. To make the comparison between the extension of the fibers and the extension of the cable possible, it is necessary to make some statements. First, same force is applied on both fibers and cable. Second, the force on the fibers can be divided by the number of fibers: $F_1 = 7 * F_2$. Third, the total extension of the fibers is equal to the extension of one fiber. Fourth, the same material is used for both cable and fibers, so $E_1 = E_2 = E$.

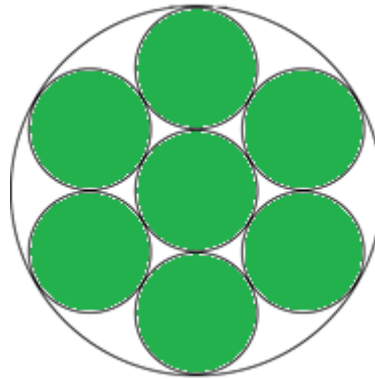


Figure 47: Twisted fiber cable

$$\varepsilon_1 = \frac{F_1}{A_1 * E}$$

Equation 18: Extension Cable

$$\varepsilon_2 = \frac{F_2}{A_2 * E}$$

Equation 19: Extension fibers

When previous statements, Equation 18 and Equation 19 are combined the result will be:

$$\frac{\varepsilon_1}{\varepsilon_2} = \frac{7 * F_2 * \pi * R_2^2}{F_2 * \pi * 9 * R_2^2} = \frac{7}{9} \approx 77.78 \%$$

Equation 20: Difference cable and fibers

It can be seen from Equation 20 that the extension of the fibers is bigger than the extension of the cable. To approach the same extension as the cable, the total sum of surfaces (green) must to be equal to the surface of the cable. The same surface can be achieved by enlarging the number of fibers. The surface of each fiber will be smaller, but the overall sum of the fiber surfaces will approach the surface of the cable.

Now the extension of both fibers and cable is the same, so what is the advantage of the twisted fibers over the regular cable? The answer is flexibility [29]. This is because the fibers can move relative to each other when making a sharp turn. This property is vital for our application, because the cable system needs to fit in the construction.

5.8.3 Extension & reduction in the system

From previous paragraph can be learned that the own extension can be excluded because there are so little in comparison to the construction dimensions. But this is no proof that there will be no extension or reduction at all. It is possible that the construction itself can be the cause of multiple extensions or reductions. In next paragraph will be explained how a construction can be the cause of these “system extensions & reductions”. Then the actual system extensions will be explained and calculated and finally there will be an overall conclusion of the cables extensions.

5.8.3.1 Introduction

When, in our case, cables are used in a remote actuated system, these cables will pass several joints. Every time when a cable passes a joint, this cable can extend or reduce depending on the actuation of each joint. An example is given in Figure 48, which contains a system with two joints and two cables and both cables are fixed at the end. Then the system will be moved (green part) and the effect of the movement on the cables is marked with a red circle. The results are reduction in the upper cable and extension in the lower cable. When the system is moved in the opposite direction, the reduction will be in the lower cable and the extension in the upper cable.

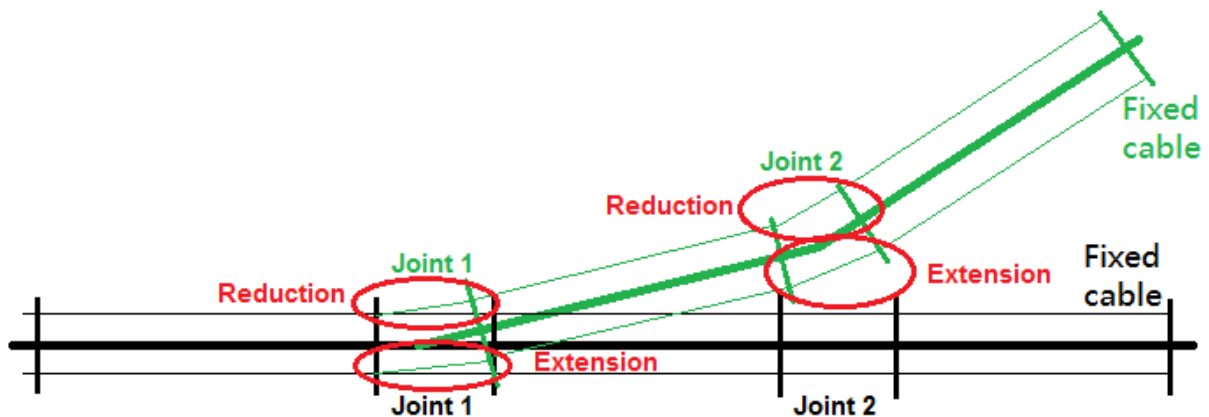


Figure 48: Extension and reduction

It can be seen that the total reduction and extension is the sum of the local reductions and extensions.

5.8.3.2 General calculation

This calculation is an approach to reality, so in other words it means that this calculation can be done very accurately, but in reality it is always different. For this reason it is necessary to take into account a certain tolerance on the calculations. But the greatest factor of influence is the construction itself. The positions of the cables, the shape of the used joints and the movements done in the construction will determine the reduction or extension. Since the cables are situated in the construction, it is clear that the position of the cables only depends on the shape of the construction itself. Next, an example of cable extension depending on the shape of a joint is given in Figure 49. For this reason it is important to choose the shape of the joint wisely. The last factor is the maximum and minimum position of the construction, which is directly connected to the minimum and maximum angle of the joint.

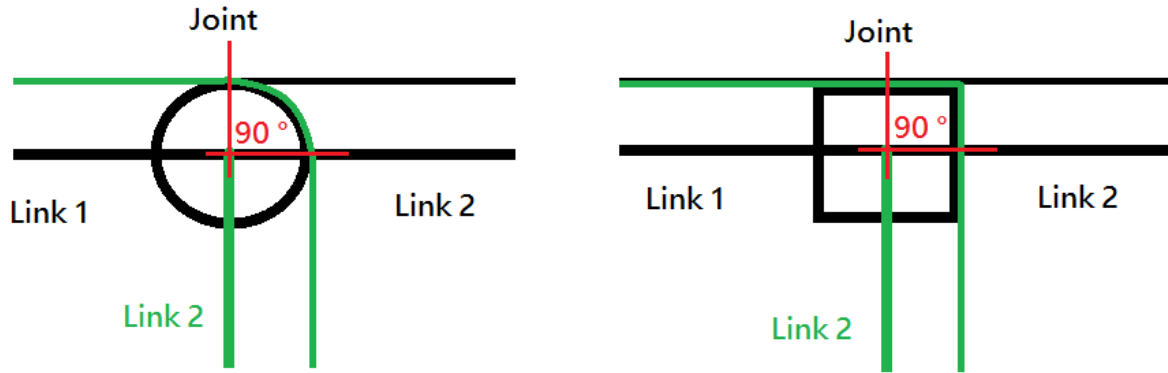


Figure 49: Influence shape joint

Now is known which factors must be taken into account, so the general calculation can be started.

Suppose that link 1 is fixed, link 2 can rotate over a certain angle due to the local joint and the minimum angle is 0° . This situation will be the start position (Figure 50). To simplify the calculation distances Y_1 , Y_2 and X_1 , X_2 will be equal and the joint will be positioned half way X_1 , X_2 . For example: $Y_1 = Y_2 = 5$ mm, $L_1 = L_2 = 10$ mm and the tolerance will be ± 0.01 mm.

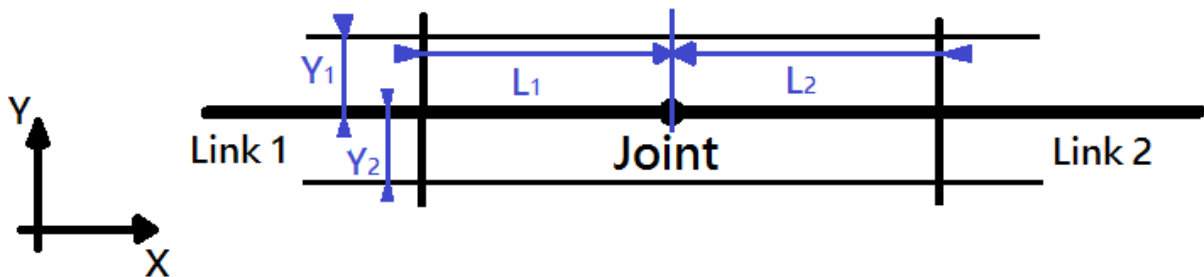


Figure 50: General calculation position 1

Now link 2 will be rotated over a certain angle due to the local joint, in this case 45° (Figure 51). First the reduction in the upper cable will be calculated. Due to geometry, the X, Y component of point P_1 , P_2 can be determined. When these components are known, it is possible to calculate X_{L1} , Y_{L1} and therefore L_1 .

$$X_{L1} = L_1 + \left(\cos\left(\tan^{-1}\left(\frac{Y_1}{L_2}\right) + \alpha\right) * \sqrt{L_2^2 + Y_1^2} \right)$$

Equation 21: X-component upper extension

$$Y_{L1} = \left(\sin\left(\tan^{-1}\left(\frac{Y_1}{L_2}\right) + \alpha\right) * \sqrt{L_2^2 + Y_1^2} \right) - Y_1$$

Equation 22: Y-component upper extension

$$L_1 = \sqrt{X_{L1}^2 + Y_{L1}^2}$$

Equation 23: Total upper extension

In this case $X_{p1} = Y_{p2} = 3.54$ mm and $Y_{p1} = X_{p2} = 10.61$ mm relative to the local joint, so $X_{L1} = 10$ mm + 3.54 mm = 13.54 mm and $Y_{L1} = 10.61$ mm – 5 mm = 5.61 mm. The result for L_1 will be 14.66 mm, which gives a reduction of 5.33 mm in comparison to the start length of 20 mm. Second, the extension in the lower cable will be calculated. This calculation is a little more complex, because the cable will touch the joint (red line in Figure 51), this means that α is greater than $\tan^{-1}\left(\frac{Y_2}{L_2}\right)$. When α is less than $\tan^{-1}\left(\frac{Y_2}{L_2}\right)$, the formulas will be:

$$X_{L2'} = L_1 + \left[\cos\left(\alpha - \tan^{-1}\left(\frac{Y_2}{L_2}\right)\right) \right] * \sqrt{L_2^2 + Y_2^2}$$

Equation 24: X-component lower extension

$$Y_{L2'} = Y_1 + \left[\sin\left(\alpha - \tan^{-1}\left(\frac{Y_2}{L_2}\right)\right) \right] * \sqrt{L_2^2 + Y_2^2}$$

Equation 25: Y-component lower extension

$$L_{2'} = \sqrt{X_{L2'}^2 + Y_{L2'}^2}$$

Equation 26: Total lower extension

When α is equal to $\tan^{-1}\left(\frac{Y_2}{L_2}\right)$, the maximum extension is reached in theory. Following example will proof this. Therefore the calculation will be done in two steps. Step one, from link 1 to joint and step two from joint to point P_2 . Step one is easy to calculate because, $X_{L2} = X_2 / 2 = 10$ mm and $Y_{L2} = Y_2 = 5$ mm. Therefore L_2 will be 11.18 mm. X and Y component of P_2 are necessary to start step two, which are already calculated to determine L_1 . Because the X and Y component of P_2 are calculated relative to the local joint, $X_{L3} = X_{P2} = 10.61$ mm and $Y_{L3} = Y_{P2} = 3.54$ mm. Therefore L_3 will be 11.18 mm, which is exactly the same as L_2 , because maximum extension is reached. The sum of L_2 and L_3 will be 22.36 mm, which results in an extension of 2.36 mm in comparison to the start length of 20 mm. Still the extension depends on the shape of the joint which is used. Due to this shape additional extension could occur.

It is remarkable that there is a difference between the reduction and extension. In this case it was 5.33 mm reduction and 2.36 mm extension, this results in a difference of 2.97 mm. This element could be a very important bottleneck depending on the type of auction (paragraph 5.2.3).

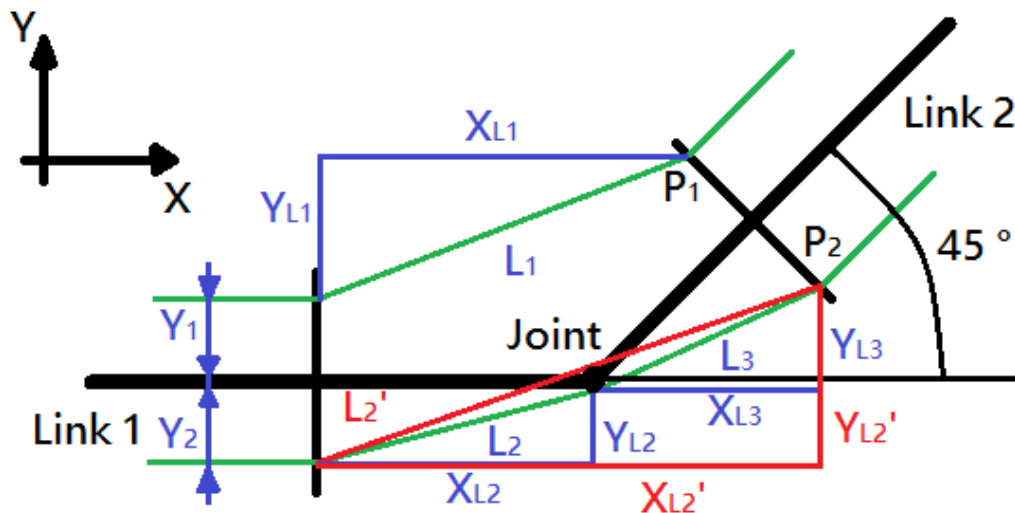


Figure 51: General calculation position 2

5.8.4 Actual system reduction & extension

Previous paragraph mentioned the theory behind the so-called “system extensions and reductions”. This paragraph will explain how the theory has been applied in practice. To encounter the previously mentioned bottleneck, it is vital take a close look at the used actuation architecture (paragraph 0). For several reason a double actuation method was chosen, in other words one RC servo motor is used to execute extension and flexion in the corresponding links (paragraph 3.5). The extension and reduction as result from a double actuation architecture is shown in Figure 52, in which can be seen that L_1' must be equal to L_2' to have an accurate actuation method. If L_1' is not equal to L_2' , one of the two cables will relax and the actuator will move without executing any movement at the corresponding links until the cable is re-strained. For this reason it is necessary to keep the cables strained while executing movement. This can be achieved by ensuring that the cable extension and reduction is the same in each joint the cable passes. This property is most important when designing the actual remote control cable system.

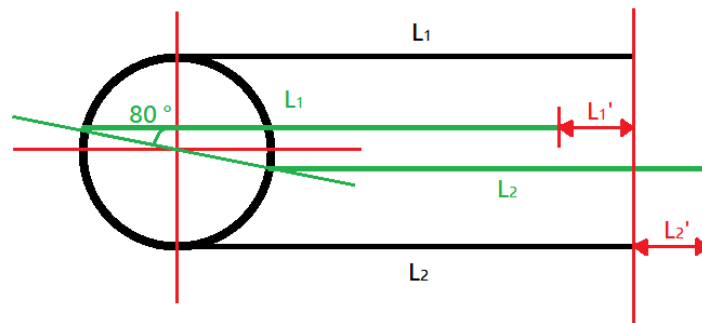


Figure 52: Extension & reduction double actuation

5.8.5 Designing the cable system

The designing will be done from fingertip until the lower arm, starting with the little, ring and middle finger. Next, the MCP joint of the pointer finger will be handled following by the TMC joint of the thumb. When all hand joints are explained, the connection will be made from these joints to the actuators and finally an overall conclusion will be made concerning the design of the cable system.

5.8.5.1 Designing the hand joints

The little, ring and middle finger are the same, because they execute the same movements. The only difference is the length of the proximal and medial part of the fingers. The explanation will be done with the little finger (Figure 53).



Figure 53: Cross section little finger

The minimal angle of the DIP, PIP and MCP joint is 2° and the maximum angle 78° , because of the singularities. Because the position of the force was not significant it is possible to take only the extension and reduction of the cable into account (paragraph 0). Every part of our application is drawn in Autodesk Inventor. This gives a big advantage, because the lengths between the corresponding links of a certain joint can be measured. This way the previous calculations can be simplified to measuring in Autodesk Inventor.

Because of the structure [paragraph 8.5], all the results will have a tolerance of ± 0.01 mm and the shape of the joint with corresponding links will be the same for DIP, PIP and MCP joint. For this reason it is enough to explain only one joint, starting with the reduction in the upper cable. The maximum distance is shown in

Figure 54 and the minimum distance is shown in Figure 55. The results are respectively 9.53 mm and 3.31 mm. Therefore the cable reduction will be 6.22 mm.

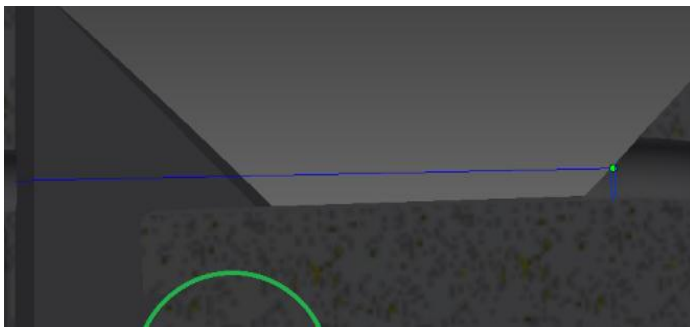


Figure 54: Flexor cable maximum position

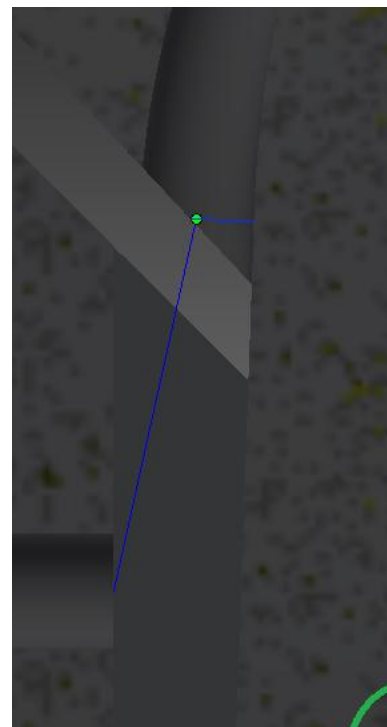


Figure 55: Flexor cable minimum position

Next, the extension of the lower cable will be determined. The minimum distance is shown in Figure 56 and the maximum position is shown in Figure 57. The minimum distance is measured 6.79 mm. As explained in paragraph 5.8.3.2 the maximum distance needs to be calculated in two steps, because the cable will touch the joint. The shape of the joint is a rectangle, for this reason the distance is measured from link 1 to the edge of the joint and from the same edge of the joint to link 2. The results for step one and two are respectively 7.34 mm and 5.72 mm. Therefore the cable extension will be 6.30 mm.

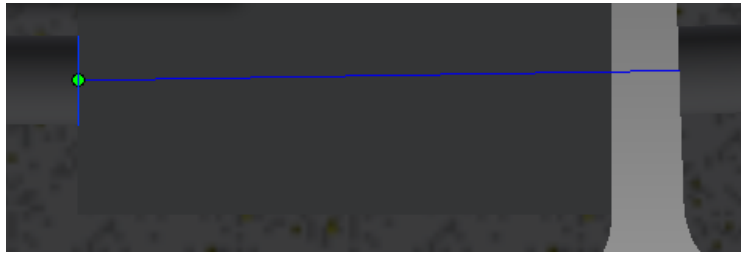


Figure 56: Extensor cable minimum position

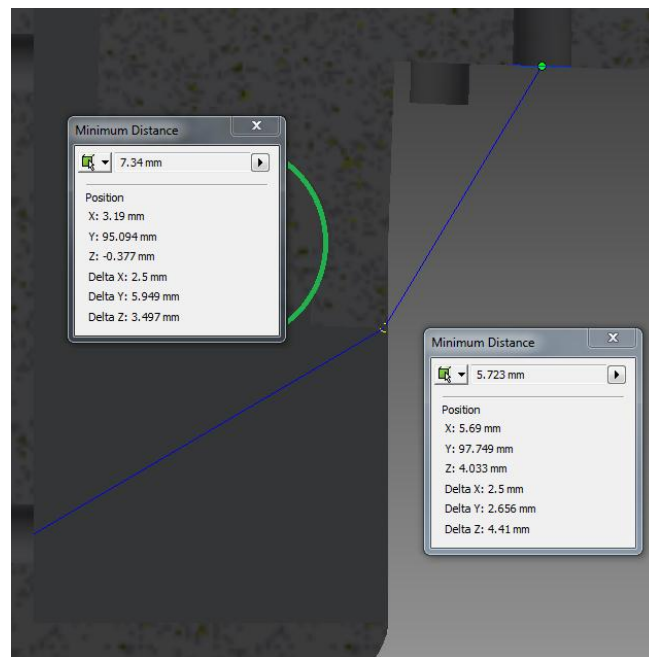


Figure 57: Extensor cable maximum position

When the reduction and extension is calculated, both results can be compared. A reduction of 6.22 mm and an extension of 6.30 mm results in a difference of 0.08 mm, which is almost none. Keep in mind that these are measurements from a 3D-model! Practice has turned out that even when a model gives 0 mm difference, there will always be a small amount of backlash!

Previous measurements are the same for MCP, PIP, DIP joint of the little, ring and middle finger, for PIP, DIP of the pointer finger and MCP, IP for the thumb. Details of these measurements can be found in Annex 8.

Next, the MCP joint of the pointer finger will be handled, because this joint is different compared to previous joints. This joint has 2 DOFs (paragraph 3.5). The MCP joint is partly the same, DOF 1 ensures flexion and extension and DOF 2 ensures the abduction and adduction of the pointer finger (paragraph 1.5). The cable reduction and extension as result from DOF 2 is easy to measure, because the shape of the joint is symmetric and within a boundary of $\pm 20^\circ$ there is a difference in cable length of ± 0.2 mm which is tolerable. DOF 1 is something else, because there is an extra joint between the corresponding links. For this reason it is not possible to use previous method, so an approach was necessary. The best approach was a reduction of 8.77 mm and an extension of 6.28 mm, which results in a difference of 2.49 mm. Details of the measurements can be found in Annex 9. This result is not tolerable, because of the ± 0.01 mm tolerance chosen.

To make this part work properly it is very important to search a method which ensures a minimum of difference between extension and reduction. A solution had not been found due to a lack of time.

To recreate the saddle joint of the thumb, a simplification had to be done. In reality, this joint has two DOFs, but one DOF is compensated by another offset of the thumb structure (paragraph 8.5.4). This DOF is in-site actuated by a RC servo motor, because executing a rotation of 136° from a remote controlled cable system is too complex. The only disadvantage of this solution is the major difference in reduction and extension of the cables to actuate the MCP and IP joint of the thumb. The minimum and maximum position are shown in Figure 58.

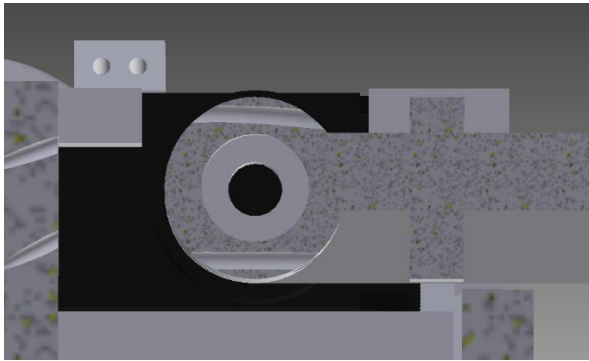


Figure 58: Minimum position TMC

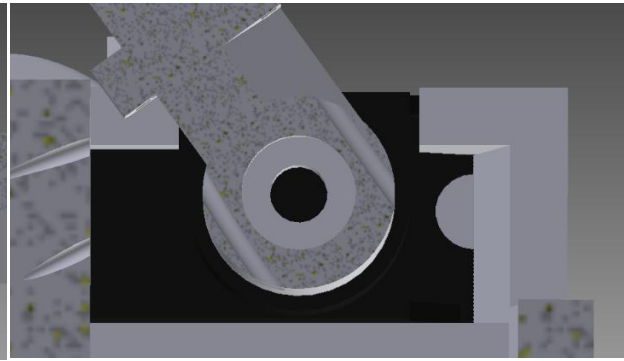


Figure 59: Maximum position TMC

As can be seen in Figure 58 the minimum length of the upper and lower cable are approximately the same ($7.27 \text{ mm} \pm 0.08 \text{ mm}$). When the TMC joint is rotated to maximum position, the upper cable has an extension of 3.15 mm and the lower cable has also an extension of 10.75 mm (8.42 mm added to an arc length of 9.60 mm coming from an arc 110° and a radius is 5 mm which results in 18.02 mm). Details can be found in Annex 10.

Remarkable to this calculation is the fact that there are two extensions instead of an extension and a reduction. For this reason it is not possible to actuate the MCP and IP joint properly. Two possible solutions can be applied: one, use two single actuators instead of using double actuation and two, make a different construction where this bottleneck can be solved. Option one's disadvantage is the complexity of the control and option two's disadvantage is the complexity of the structure. These solutions could not be examined due to a lack of time.

5.8.5.2 Connecting joints to actuators

The actuators of most joints are located in the arm because of several reasons: first, the mass of the actuators must be as close to the shoulder as possible to reduce the necessary torque to move the structure. Second, the actuators could not all fit at the location of the joint with one exception: the TMC joint as previously mentioned. Another exception is the second DOF in the MCP joint of the pointer finger (abduction and adduction). This joint is still remote actuated but from the palm of the hand instead of the arm. Therefore the joint could be more accurately actuated. Detailed images can be found in Annex 11.

The connection from the joints to the actuators must be as smooth as possible to reduce the amount of friction the cable could experience from the structure. Therefore the cable must follow the straightest possible path. The explanation will be done for the little finger because of the longest distance between PIP joint and actuator. The same method is used for all remaining joints. First, the connection from the PIP joint to the palm of the hand will be made. As shown in Figure 53, the cable follows a straight path from the medial part, through the proximal part to the palm of the hand, which is ideal. Next, the cable follows a straight path through the palm of the hand as shown in Figure 60.

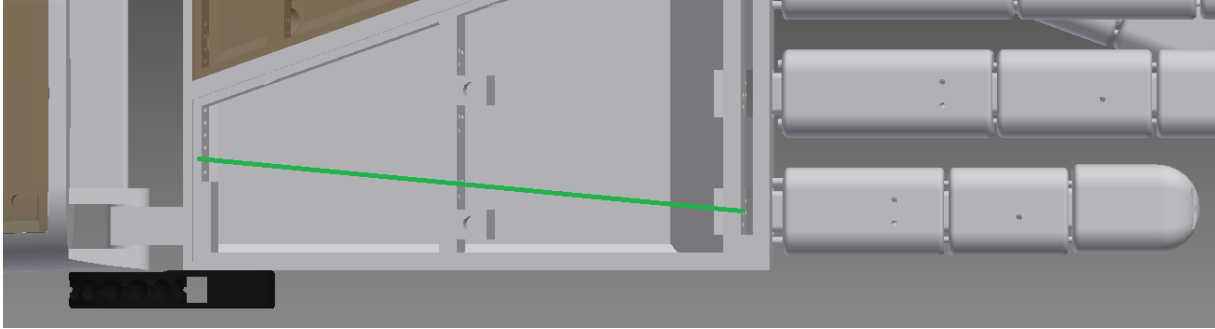


Figure 60: Path through the palm of the hand

Then the cable must cross the wrist joint. As a human wrist joint, our wrist joint has a rotation angle of 100° of which the angle of 90° is the vertical position. To ensure a minimum cable extension and reduction, an extra bar will be printed (Figure 61). The end of the bar will be provided with a fillet to guide the cables properly. Close calculations in the 3D-model have turned out that the extension and reduction is approximately 0.5 mm which can be tolerated due to the structure's backlash in reality.

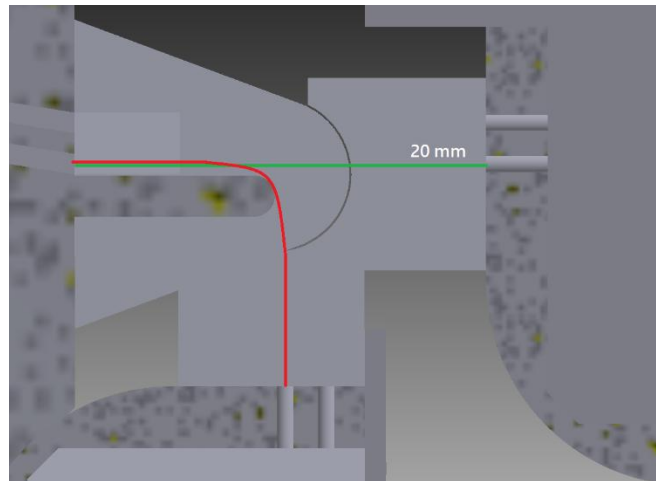


Figure 61: Extra bar wrist joint

A disadvantage is more friction in the joint. To keep the friction as less as possible both cables are separated and instead of holes there is a sleeve provided in the arm. Practice has turned out that the amount of friction in the wrist joint is tolerable. The finger movements can be executed even with a wrist angle of 90° .

When the cables crossed the wrist joint, they enter the arm. From here they only need to reach the actuators. It requires precision to place all RC servo motors nicely arranged in the arm to make the connection as smooth as possible. There are additional guidance provided to ensure exactly the same extension and reduction for each RC servo motor. The green line represents the cables from actuator to corresponding guidance in Figure 62.

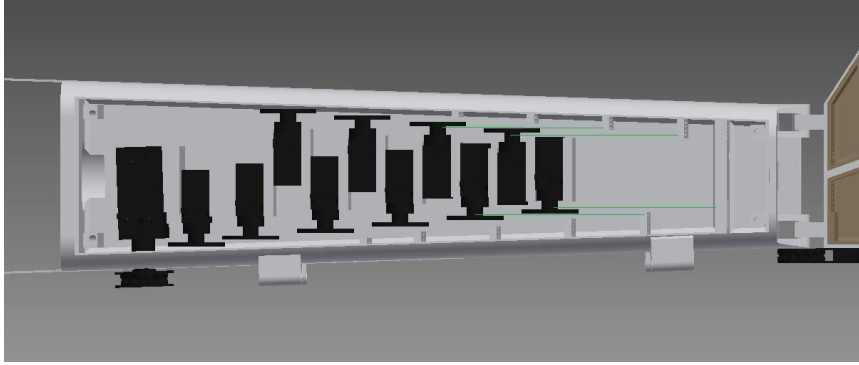


Figure 62: Location actuators in the arm

As can be seen in Figure 64 A is the distance from guidance to center of the RC servo disc, S is the length of the cable at a certain angle α , inner radius r and outer radius R of the RC servo disc. A standard RC servo motor disc will be used, because this is a standard disc and must not be custom made. This method will be used to calculate the location of the actuators and minimum, maximum extension and reduction. Within this method the influence of the distance A will be also determined related to the angle α for an outer radius of 10 mm and an inner radius of 3.45 mm and the length of the cable. From the model can be concluded that the maximum distance from the center of the RC servo motor disc to the guidance is 70 mm. The maximum extension and reduction will be 20 mm, because the cables are tied to the discs. As previously mentioned it is vital the keep the cables strained! Therefore the right knots must be used. Several knots are tested and the "eight" knot gave the best results because this knot is a self-straining knot (Figure 63). Even when the knot is self-straining it is still very difficult to strain the cables correctly. This is because when one of the two cables is a bit overstrained it could result in relaxation in the other cable and a malfunction in the finger movements. For this reason it might be useful the search another straining system the strain the cables very accurately.



Figure 63: "Eight knot"

When the distance A is determined, the link between the extension in the cable and the angle of the RC servo motor is made. Details and results can be found in Annex 12.

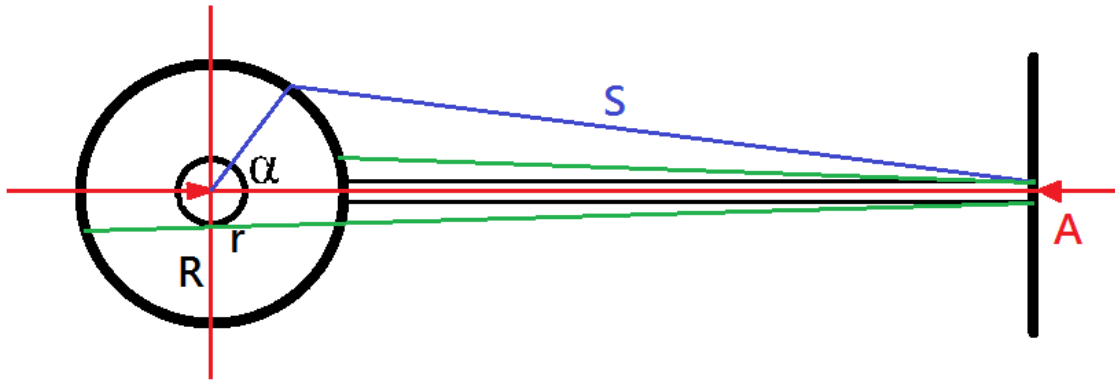


Figure 64: Situation method equal extension and reduction

In order to check the calculations an approach will be made (Figure 65). The approach is based on the cosines rule for random chosen triangles. The difference between the exact calculation and the approach is the vertical distance of 1 mm shown in Figure 64. To determine the difference in accuracy between the exact calculation and the approach a comparison is made and can be found in Annex 13. From these results can be concluded that the difference is minimum and gets less when the distance A is increased, so the distance A must be maximized.

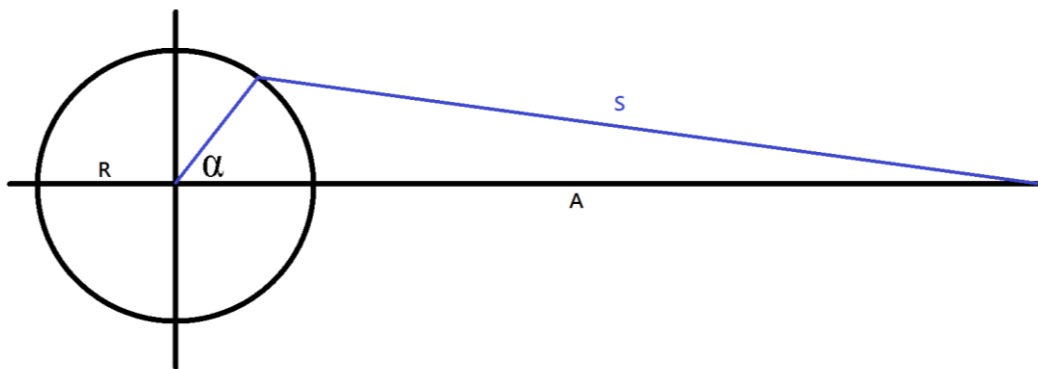


Figure 65: Approach of the exact calculation

5.8.6 Conclusion

The conclusion of this chapter is easy. It is very difficult to adjust the cable system to have the correct finger movements, because this is the most crucial part of the project. It is also the part which requires the most accuracy and precision.

When read this chapter several bottlenecks occurred. The MCP joint of the pointer finger, the TMC joint of the thumb and straining the cables in the arm. These three problems must be further examined. Few possibilities are given through this chapter, but due to a lack of time they could not be examined now.

6. Communication and position feedback

6.1 INTRODUCTION

Guy Fierens - A humanoid robot has a lot of degrees of freedom. These degrees of freedom do not only have to be actuated but there are also sensors necessary to monitor the position, movement and surroundings of the robot.

To process all this data, there needs to be a sophisticated controller capable of reading a lot of sensors and writing to a lot of outputs while making the necessary calculations. Currently, there doesn't exist a controller capable of doing all these tasks by itself. Therefore we need to use multiple devices capable of communicating with each other.

The following paragraphs will discuss the I²C-bus protocol, which is the most frequently used and implemented communication protocol in devices, and the processing of the large number of analog inputs necessary.

6.2 I²C- BUS COMMUNICATION

Created by Philips Semiconductor in 1979, (known today as NXP semiconductor) the inter-integrated circuit bus or I²C-bus provides a low-cost, high speed communication protocol. The applications of I²C-bus include chip-to-chip communications in our everyday products like computers, radios or televisions. In addition to chip-to-chip communication between chips on the same circuit board, I²C is also frequently used as a communication protocol between separate devices with a cable.

The main features of the bus protocol include:

- low-cost system because only two bus lines are necessary (SCL and SDA lines)¹²,
- adjustable baud rate,
- master/slave communication (Figure 66) as well as master/master communication (Figure 67),
- half-duplex communication,
- every connected device has its own address, programmable using software or selectable with jumpers on the circuit board,
- low current consumption.

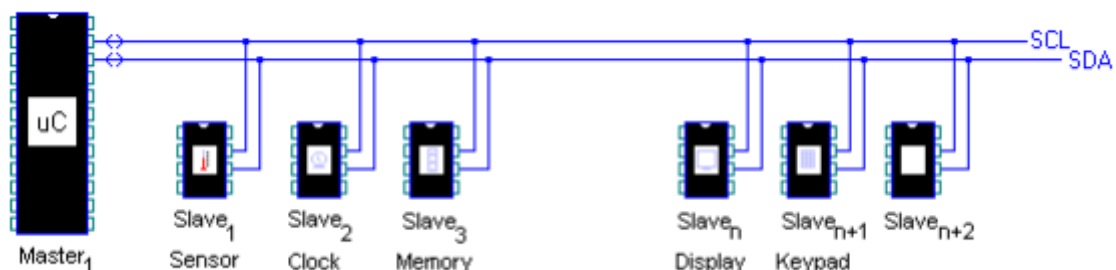


Figure 66: One I²C master with multiple slaves [Philips Semiconductors I²C handbook]

¹² A reference voltage and ground are also necessary in order to reference the received signal as a logical 0 or 1.

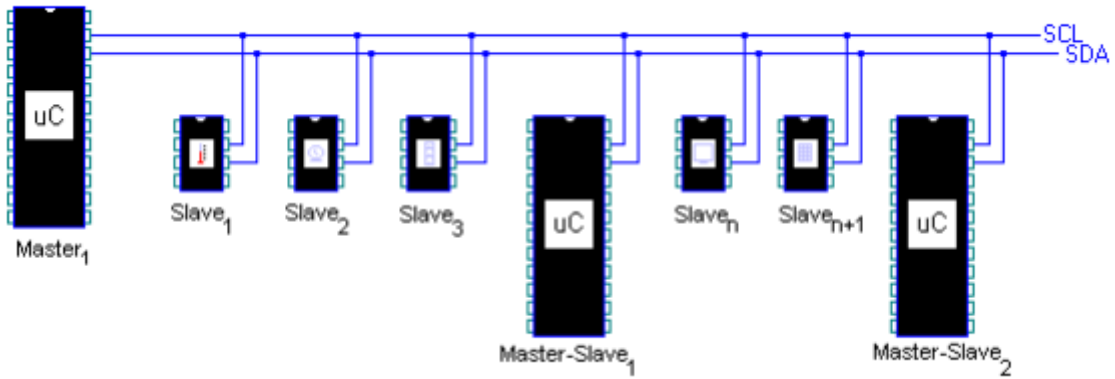


Figure 67: Master/Master communication [Philips Semiconductors I²C handbook]

In our application, a system with only one master will be used. Therefore the master/master I²C communication will be neglected in the following paragraphs. In case the reader is interested in networks with multiple masters, I refer him to [30]. Using a single-master I²C network, the communication protocol stays quite simple. We do not have to take arbitration or collision detection into account because the network will only be used when the master wants to read or write information to its slaves.

As mentioned before, the I²C-bus only needs two wires to function properly: a clock line (SCL) which synchronizes the sender and the receiver and a data line (SDA) to transfer the data. [31] Each one of these bus lines needs to have a pull-up resistor connecting the line to a positive supply voltage. These resistor are frequently integrated into I²C-devices and can be enabled or disabled using jumpers. When the bus is not in use, both lines will have a positive voltage or a logical one across it. To create a logical zero the I²C device will have to connect the bus line to the connected ground. As a reference for the logical one and zero, two wires are added: a reference voltage V_{ref} and a GND.

An I²C-message has a certain structure. A start condition is followed by the slave destination address and a read/write condition. After the start condition, slave address and read/write condition an undefined number of data bytes can be sent each followed with an acknowledge. When all data has been sent or received the master ends the message with the stop condition. A master can: write data to a slave (Figure 68), read data from a slave (Figure 69) or read/write data to multiple slaves in one message (Figure 70).

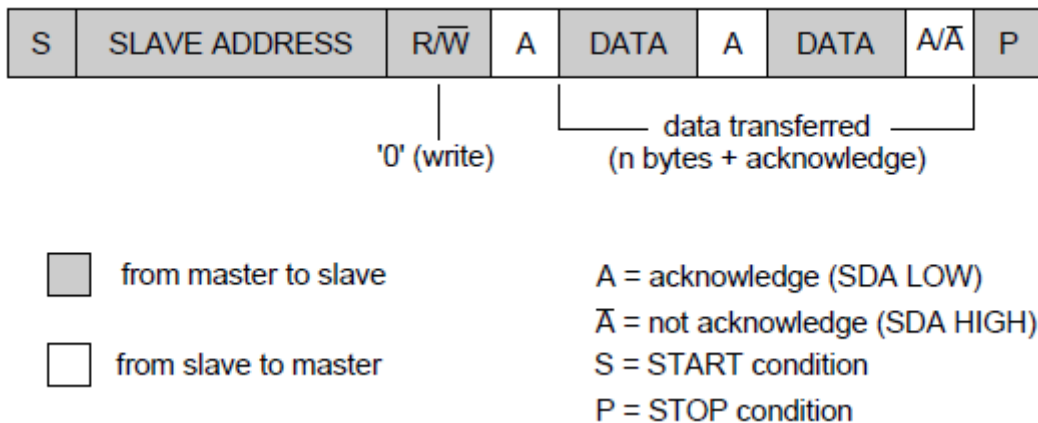


Figure 68: A master writes data to a single slave [30]

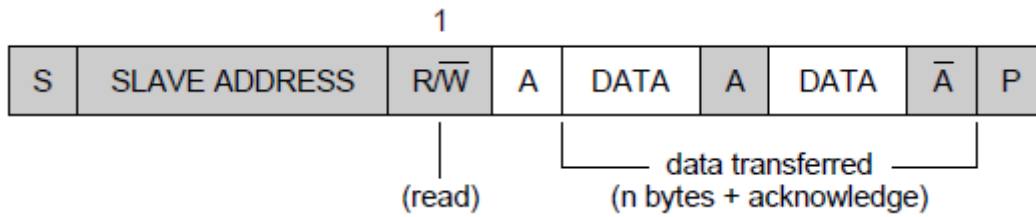


Figure 69: Master reads data from a slave [30]

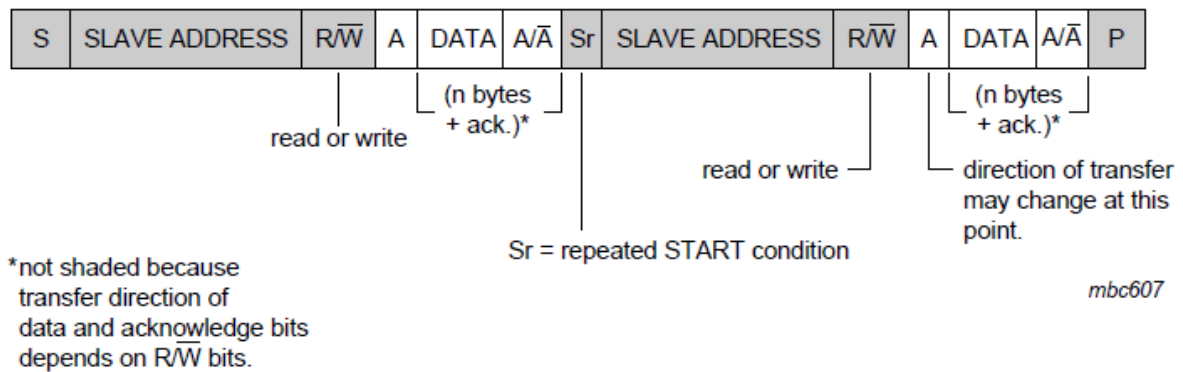


Figure 70: Master reads or writes data to multiple slaves [30]

6.3 POSITION FEEDBACK

Getting position feedback from the servo motors used in the robot is essential for a decent control and safety of the device. Without feedback, knowing the position of the different joints is impossible as well as checking for movement errors. The situation where the robot wants to reach a certain position but is obstructed, has to be monitored in order to avoid damage to the robot as well as his environment.

To obtain this information, we can use the same mechanism the servo uses as an input for its comparator, as seen in Figure 71. This input can either be a potentiometer or a decoder. Since every servo used in the Aslan robot uses potentiometer feedback, where the potentiometer is mounted on the output axis, we can simply use the same signal the servo uses to determine the position of the joint (Figure 71). Although this leaves us with a problem: many microcontrollers do not have enough analog inputs to monitor each joint position separately. The Arduino Due, used in our application, only has 12, while we need at least 16 inputs to monitor every joint.

To solve this problem and expand the number of analog¹³ inputs we have 4 options:

1. Use another Arduino as an I2C slave
2. Use an IO expansion card
3. Expand the number of inputs with a multiplexer chip
4. Use the servo control cable to get real-time feedback from the servo.

¹³ Using shift registers is another way to expand the IO-range but is not available for expanding the analog IO range. [33]

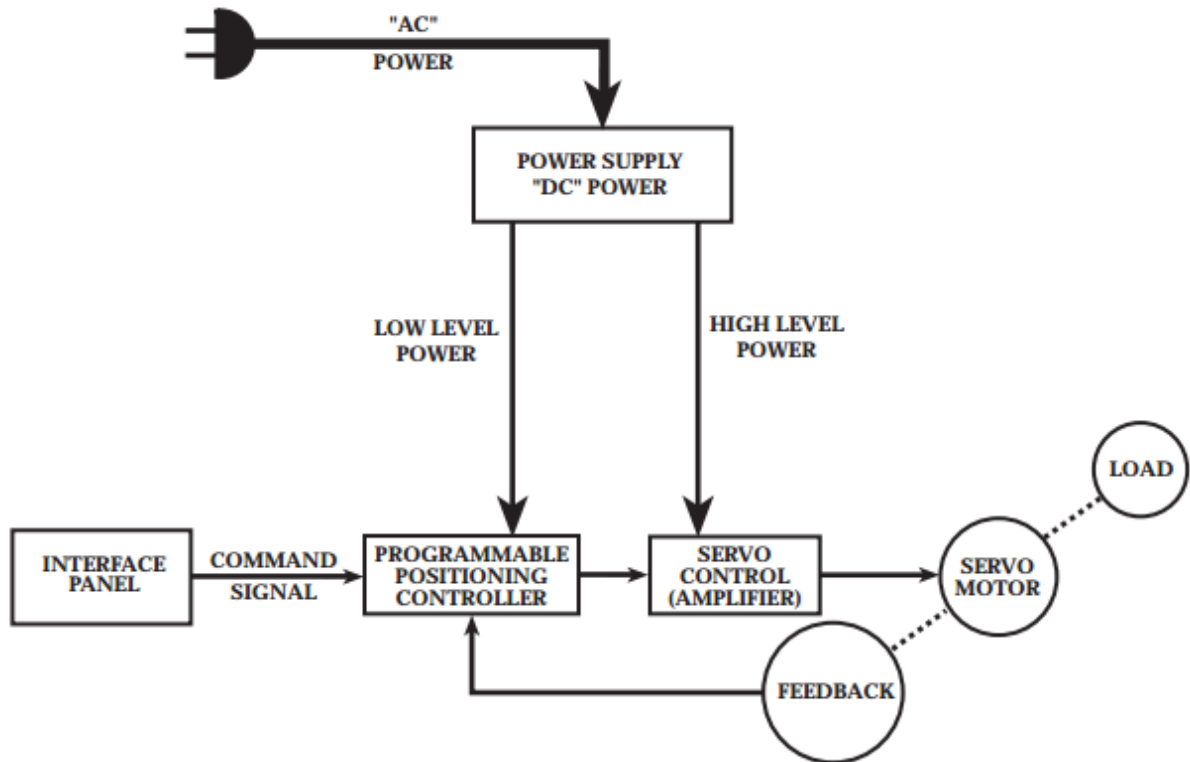


Figure 71: Servo mechanism [32]

6.3.1 Defining every option

6.3.1.1 Arduino microcontroller as an I²C slave

If we want to use an extra Arduino microcontroller as an I²C slave, we have to choose an Arduino board with an I²C communication availability and a high number of analog inputs regarding its price.

Only 5 Arduino boards come with an I²C interface: the Uno (€23.9, 6 inputs), Ethernet (€47.99, 6 inputs), Mega2560 (€51.99, 16 inputs), Due (€44.99, 12 inputs) and Leonardo (€25, 12 inputs). Comparing the boards regarding the cost per extra input, we can see the Leonardo board becomes the most interesting option with €2,10/input, the next best option is the Mega with €3,25/input followed by the Uno with €3,98/input. In the comparison below we will use the Leonardo as reference.

The downsides of using an extra Arduino is the decreasing usability of the end-product. The extra controller has to be programmed as well as connected to the I²C network. Other controllers like the Parallax Propeller board could also be used, but these controllers work with another software platform or programming language enlarging the downsides mentioned before.

6.3.1.2 IO expansion card

An IO expansion card is a fairly straightforward solution to our problem. Designers created IO expansion shields, compatible with Arduino, as well as I²C expansion boards.

The major downside to this solution however is the availability of these boards. Most of these boards are only available in the United States. This means that an order has to be shipped across the ocean, leading to longer delivery times and an unnecessary amount of environmental waste.

6.3.1.3 Expanding the number of inputs with a multiplexer chip

The number of analog inputs can also be expanded using a multiplexer chip or multiplexer. These chips enable us to guide input traffic from multiple sensors to a single analog input on the Arduino. Multiplexer chips are available in 8-channel or 16-channel versions. [33]

Using 3 or 4 digital output pins we are able to set a 3 or 4-bit binary address (8 or 16-channel multiplexer). This way, we can choose one of eight different inputs to read at the time. Figure 72 illustrates this principle.

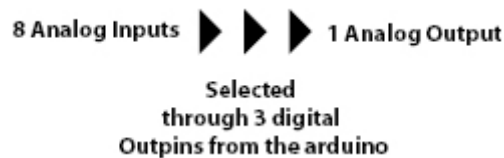


Figure 72: Multiplexer principle [Arduino.cc]

Frequently used multiplexers are: CD74HC4067 (16-channel), CD74HCT4047 (16-channel) and the CD74HCT4051E (8-channel) from Texas Instruments. These IC's are available in almost every web shop or DIY electronics store, either as the chip itself or mounted on a breakout board, simplifying the assembling process.

Comparing the 16-Channel and 8-Channel multiplexer regarding its price we can see a significant difference. A CD74HCT4067 IC costs around €0.9 while a CD74HCT4051 IC costs only around €0.70 for the IC only (i.e. not mounted on a breakout board). Adding the costs of a PCB, mounting pins and solder to this we can calculate a price of around €6 for a 16-channel and €5.7 for an 8-channel multiplexer. Neglecting the fact that multiple multiplexers could be mounted on a single PCB. Breakout boards are less available.

The major downside of the 16-channel multiplexer, and the reason we will be using an 8-channel multiplexer, is the fact that the 16-channel chips are only available in a SOIC-version (Small Outline Integrated Circuit, for surface mounting). This makes it almost impossible for the common man to solder such a chip to a PCB. The 8-channel multiplexer is available in a PDIP-version (Dual in-line package, for through hole mounting), making it easier to assemble. See Figure 73 for the difference between these two versions. The extra upside of the PDIP 8-channel multiplexer is the possibility of quick replacement when using an IC-socket.

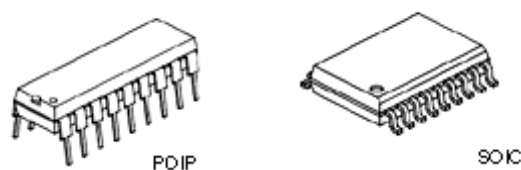


Figure 73: PDIP and SOIC chip version

6.3.1.4 Real-time servo feedback using the inverter-fed power lines

Real-time servo feedback with this technique is only possible when using encoder-based servo systems. The servo-motors used in our setup use potentiometers as an internal feedback mechanism, making this method unusable for these motors.

6.3.2 Conclusion: Choosing the best option

The best option for our application is the option which:

- has a high input/€-coefficient,
- sufficiently available,
- easy in use,
- easily expendable.

In order to choose the best option we will compare the four options regarding these requirements. In annex 13 we used 'Analytic hierarchy process' in combination with Saaty's scale of relative importance to determine the best option.

Table 19: Decision table

	Weights	Arduino I ² C slave		IO expansion card		Multiplexer		Real-time servo feedback	
Low cost	0,04	0,06	0,00	0,15	0,01	0,27	0,01	0,52	0,02
Expandability	0,33	0,06	0,02	0,15	0,05	0,27	0,09	0,52	0,17
Usability	0,10	0,31	0,03	0,40	0,04	0,52	0,05	0,25	0,02
Availability	0,33	0,40	0,13	0,33	0,11	0,52	0,17	0,25	0,08
Implementation	0,21	0,31	0,07	0,40	0,08	0,52	0,11	0,25	0,05
Score:			0,25		0,28		0,43		0,35

Concluding from the data collected in Table 19, the best available option is using a multiplexer. Besides a good availability, it is the cheapest and most expendable option. Therefore we will use the CD74HCT4051E 8-channel multiplexer from Texas Instruments to expand our analog IO range.

7. Prototyping and rapid modeling

7.1 INTRODUCTION

Stijn Huys - A humanoid arm, with the purpose to translate every word into an actual sign, needs to have a smooth and clear design so that the audience has no problems to recognize the words and letters that are presented by it. It should however also be dimensioned correctly to make a tight fit for every motor and part that should be assembled. A clever design, where only as much material is used as needed, can greatly decrease the motor loads for actuating every movement the arm is supposed to make.

The design should also be optimized for manufacturing tasks. There are a few options when it comes to producing (complicated) designs. In the next chapters we will discuss two frequently used contemporary methods: milling machines for the subtractive fabrication and 3D-printers for the additive fabrication. We will also compare them, supported by their pros and cons.

7.2 MILLING

Being a rather traditional method of manufacturing, these machines are almost at the top of their development. They are fast (for example: EMCO Linearmill 600 [34] has rapid motion speeds of up to 60 m/min), precise and they are able to work with a wide selection of materials. This method of prototyping has a big shortcoming: the fact that some operations and shapes are impossible to accomplish. This will become a crucial point for a decent design of our robotic arm. A list of pros and cons can be found in Table 20.

Table 20: Pros and cons of using milling machines

Pro	Contra
Manufacturing itself is fast	Huge amount of material goes to waste
Mature technology	Very hard/Impossible to make complicated structures
Wide knowledge	Complex software preparation (CAM)
Available at our university	
Possibility to make big parts in one piece (arm)	
Precise	

7.3 3D-PRINTING

7.3.1 Introduction

In the last two decades, 3D-printing was one of the fastest growing technologies. In 20 years it evolved from an idea and a project at MIT to a technology that can be found in modern households more frequently. Nevertheless there is a lot of space for improvement in this additive prototyping technology.

In the field of 3D-printing we can define four big sections:

- Stereolithography (SLA)
- Polyjet
- Selective Laser Sintering (SLS)
- Fused Deposition Modeling (FDM)

These sections will be explained in the next paragraph.

This technology gives us the opportunity to easily design and manufacture complex shapes but it can also be quite useless considering the fact that the available printable materials are limited and the printable dimensions are rather small.

It starts with the design of a CAD-model of the object you want to print. This file must be converted into an STL-file (Standard Tessellation Language) afterwards. This type of file only represents the geometry of the part divided in separate layers and does not contain any information about colors or specific textures.

Most of the following information was provided by Toon Roels¹⁴, who is Research & Development Manager at Materialise. We met him after a lecture about 3D-printing the 19th of November 2014, where he agreed to provide us with up-to-date information about 3D-printing.

In the upcoming chapters we are going to encounter some terms that need some explanation:

- Build material: This is the material used for creating the actual part. The properties of the used material will become the properties of the finished product. The product properties also depend on for example: extruding temperature, wall thickness and percentage of infill.
- Support material: This material's main purpose is to support the build material in places with overhang. Some printers can print overhanging structures without support material but they can suffer from collapsing structures, unevenness, variant forms and worst case scenario: total failure of the final product. The support material can be the same type of material as your build material or it can be a different type. Some support materials are water solvable and can easily be removed by adding water, while other materials need some more post-processing after the printing is done (pliers, sandpaper, acetone, ...). If it is a different material, you will need a second extruder to be able to alternate between the support and build material where needed.

¹⁴ Toon.Roels@materialise.be

7.3.2 Types of additive manufacturing

As described in the introduction, we have four big groups which can be divided as seen in Figure 74.

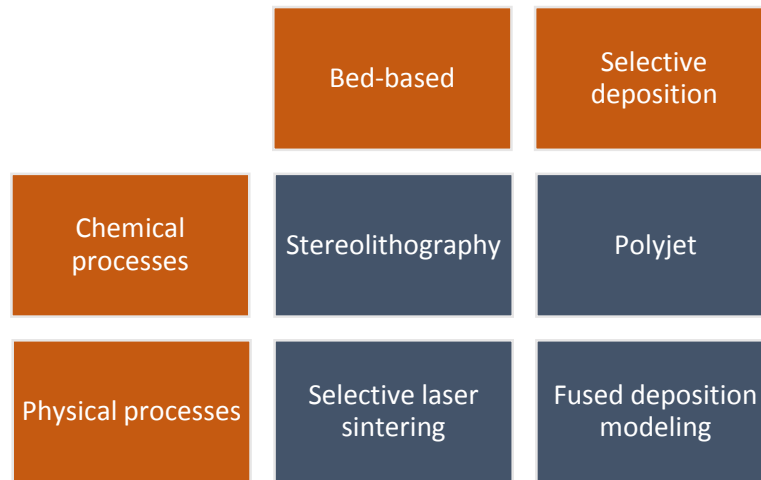


Figure 74: General representation of additive manufacturing types

Explanation of used terms:

- Bed-based: The printing will happen in a bath filled with the working material. This material can be a powder or a liquid, depending on the process.
- Selective deposition: A print head will deposit material on the ground level (first layer) or the previously printed layer.
- Chemical processes: This process turns a liquid into a solid polymer part.
- Physical processes: This process transforms polymer material (powder or solid filament) into a solid polymer part.

These technologies all have their strengths and weaknesses. For example: these days, Fused Deposition Modeling is most frequently practiced with ABS (Acrylonitrile Butadiene Styrene) or PLA (PolyLactic Acid). On top of that there is a huge difference concerning mechanical strength, porosity, surface quality, etc.

7.3.3 Stereolithography

Stereolithography (photopolymerization), also referred to as SL or SLA, is a technique where a UV laser, or another type of energy source, turns a photo-reactive resin into a polymer part, layer by layer.

An STL-file of the desired object is loaded into the Stereolithographic device where a computer-controlled laser or light cures the surface of the resin of your choice. This turns a first layer of resin, that has a thickness which can be defined according to the possibilities of the used machine, into a first solid structure which is currently attached to the platform. Once this first layer is finished, the platform will lower as much as the thickness value and the built level is refilled with resin. This layer will also be treated by the computer-controlled laser beam or light before lowering again. The depth of the light curing is a bit bigger than the step of the platform because the new layer needs to be adhesive to the previous level. This process repeats itself until the part is completely finished. A visualization is shown in Figure 75.

There are quite a few printable materials in this printing technique. In Annex 14 you can find a datasheet of the properties of some Stereolithography-printable materials available at Materialise [35].

Positive aspects of Stereolithography:

- high level of accuracy ($\pm 0.2\%$ accurate, Annex 14)
- high surface quality
- wide range of part dimensions (from switch components to car dashboards in one piece)
- wide range of materials (Annex 14)
- wide range of finishing options

Negative aspects of Stereolithography:

- expensive
- available on the market but to a lesser extent than Fused Deposition Modeling

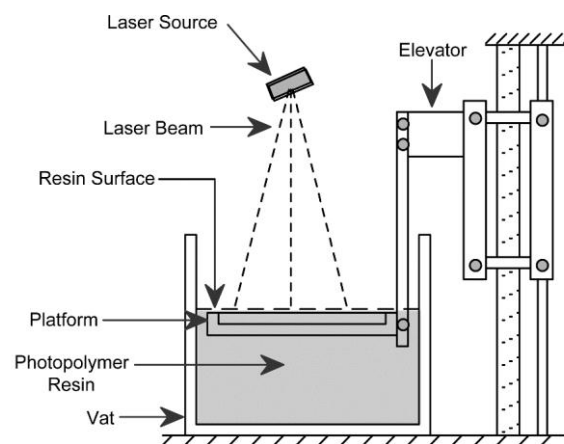


Figure 75: Basic set-up of a Stereolithography-based printer [36]

7.3.4 Polyjet

Using the same chemical process of transforming a liquid into a solid polymer part, the rapid prototyping technology named Polyjet shows a lot of similarities with the already explained Stereolithography.

The big difference between Stereolithography and Polyjet is the addition of minimum one print head and the removal of the liquid bath around the piece. The print heads will extrude support or build material, depending on which one is needed. Immediately after the extrusion of the liquid, an energetic light source will transform the liquid into a solid part. When a layer is finished, the platform will lower and the leveling blade removes excess material and imperfections. A visualization is shown in Figure 76.

The build and support material are fed to the print heads from external reservoirs.

There are quite a few printable materials in this printing technique. In Annex 15 you can find a datasheet of the properties of some Polyjet-printable materials available at Materialise [37].

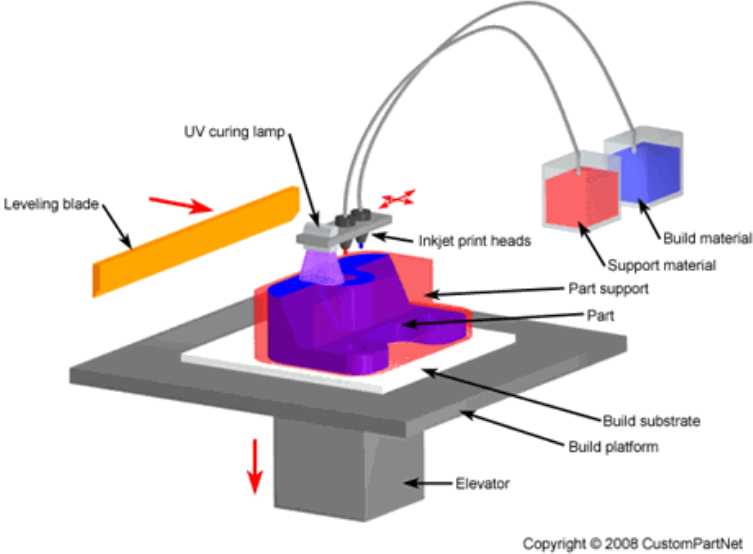


Figure 76: Basic set-up of a Polyjet printer [38]

7.3.5 Selective Laser Sintering

This type of additive manufacturing method uses a powdered form of the chosen building material to create the desired part. This process has a few other names: granular material binding, selective laser melting or electron beam melting.

Before each new layer, a roller delivers powder from the powder reservoir to the printing space with a thickness of one layer. Once this step is finished, a laser starts to cure the layer of powder where needed. When the layer is finished, the printing bed is lowered and the roller starts adding new powder so the process can start all over again. A visualization is shown in Figure 77.

The powder that has not been cured has the additional function of supporting the workpiece. This powder can be reused but manufacturers recommend to cast away the excess powder because it has been kept at a temperature right below its melting point. This will cause some particles to fuse together and this will have an influence on the precision of the next part. So there is quite a bit of waste of material after each print.

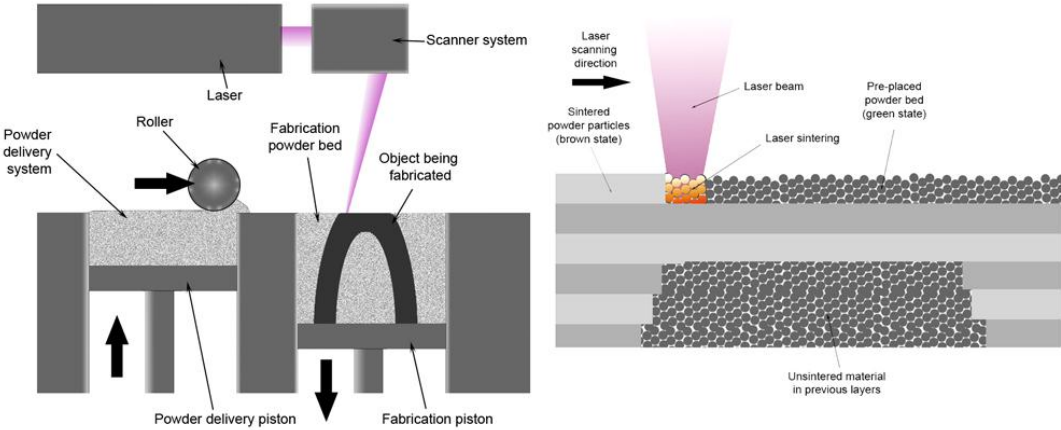


Figure 77: Basic set-up of Selective Laser Sintering [39]

7.3.6 Fused Deposition Modeling

7.3.6.1 General

Being the most commercialized and cheapest type of additive modeling, this method will be described a bit more extensively.

Fused Deposition Modeling (FDM) is also referred to as Fused Filament Fabrication (FFF) or Molten Polymer Deposition (MPD).

A feeder transports filament from a spool with the material of choice to a heated extruder. This printing head tries to keep its temperature as stable as possible near the set temperature. This temperature depends on the type of material and other additional factors (glow in the dark filament, manufacturer dependent, ...). The extruder melts the filament and deposits the liquid polymer onto the print bed (first layer) or the previously printed layer. A visualization is shown in Figure 78.

As stated before, this type of 3D-printers is getting more and more commercialized and this causes manufacturers to make new models different than others, bringing a lot of innovations to these printers. Some examples are: multiple extruder heads, heated beds, closed rooms and different positioning systems. These innovations will now be explained.

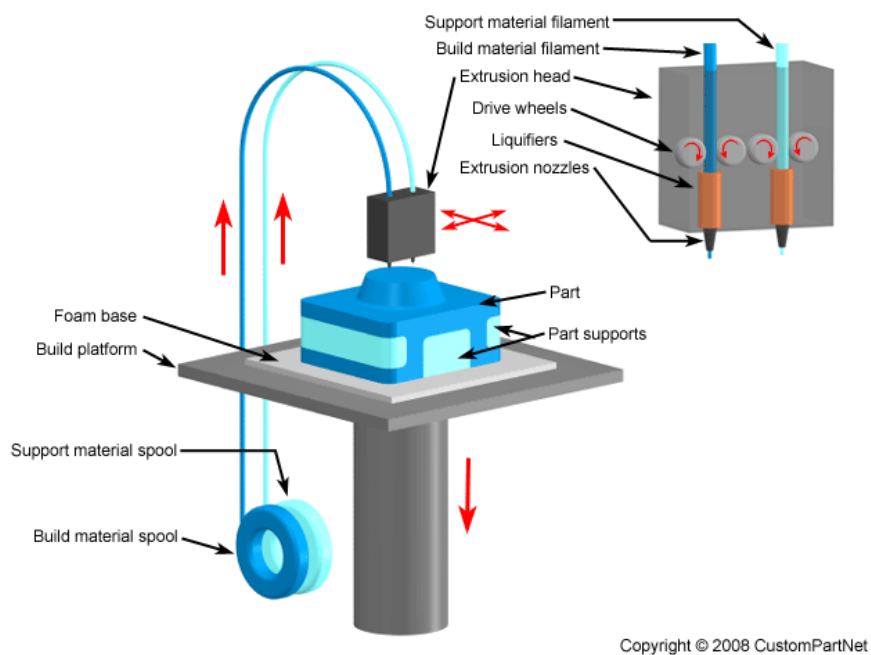


Figure 78: Basic set-up of Fused Deposition Modeling [40]

7.3.6.2 Multiple extruder heads

Nowadays FDM printers are often built with two extruder heads instead of only one. This has two possible applications: one for a specific color and the second one for another color, or one for build material and the other one for support material.

While the support extrusion is useful to print the supporting structure in water soluble material like PVA (polyvinyl alcohol), it is not essential for a decent print. You can print without support, but with risk of imperfections or structure collapse, or you can print the support structure in your building material, but some post-processing will be necessary or desired.

A second extruder for a second color of build material is only preferable if it is really needed for a visual purpose.

7.3.6.3 Materials

Fused Deposition Modeling generally uses 3 types of material: ABS, PLA and PVA.

ABS:

Acrylonitrile Butadiene Styrene is a frequently used filament because of various reasons:

- great impact resistance and toughness
- easy to sand for post-processing
- after being treated with acetone, two parts can be glued together for a bigger result
- after being treated with acetone, the part gets a very smooth surface

ABS also has a few negative points:

- recommended to use a heated bed to prevent warping of your workpiece
- causes health problems if you melt it in a closed room without proper ventilation
- requires higher temperatures than other frequently used FDM materials, which causes the printer to wear off faster

More properties of ABS can be found in Table 21 and Annex 16.

Table 21: Main properties of ABS

Density (10^3 kg/m^3)	1,01 – 1,21
Average extrusion temperature ($^{\circ}\text{C}$)	215 - 250
Young's modulus (GPa)	1,1 – 2,9
Tensile strength (MPa)	27,6 – 55,2
Solubility in water (Yes/No)	No

PLA:

PolyLactic Acid or polylactide is a frequently used filament because of various reasons:

- biodegradable
- extrusion at a lower temperature requires less effort for printing
- heated bed is not required
- stiffer than ABS

PLA also has one major negative point:

- can warp during cooling

More properties of PLA can be found in Table 22 and Annex 16.

Table 22: Main properties of PLA

Density (10^3 kg/m^3)	1,21 – 1,43
Average extrusion temperature ($^{\circ}\text{C}$)	160 - 220
Young's modulus (GPa)	3,45 – 3,83
Tensile strength (MPa)	48 – 60
Solubility in water (Yes/No)	No

PVA:

PolyVinyl Alcohol is a frequently used support filament because of the following reason:

- When printing complex 3D-parts where post-processing by hand with tools is impossible, PVA can be used to print the support structure. Placing the part with PVA support structure in water afterwards causes the PVA to dissolve.

PVA also has a negative point:

- PVA absorbs water, making printing difficult in high-humidity environments

More properties of PLA can be found in Table 23.

Table 23: Main properties of PVA

Density (10^3 kg/m^3)	1,19 – 1,31
Average extrusion temperature ($^{\circ}\text{C}$)	190
Solubility in water (Yes/No)	Yes

Others:

There are other options to use but these are used less frequently or are inapplicable for the project. Two examples: chocolate and clay.

7.3.6.4 Heated bed and closed room

Keeping the unfinished print at a certain temperature has a big, positive influence on the build quality both visually and structurally.

There are two common methods to do this: using a heated bed and a closed room.

The print bed is the surface on which the part is printed. Typical advised print bed temperatures are:

- ABS: 90 – 103 °C
- PLA: ambient – 60 °C
- PVA: 50 °C

A closed room is advised for the same reasons: this way the printed part stays at a stable temperature for a longer time and the part will not start to warp.

7.3.6.5 Position

FDM printers often come with one of the following positioning systems: moving extruder, moving bed and deltabot:

- Moving extruder: The extruder moves in a planar motion (X- and Y-axis) while the bed moves along the Z-axis. An example of this system, the Ultimaker 2 [41], is shown in Figure 79.
- Moving bed: The bed moves in a planar way (for example X- and Z-axis) while the extruder moves along the remaining axis. An example of this system, the BEETHEFIRST [42], is shown in Figure 80.
- Deltabot: Like a delta robot (which is an example of a parallel robot), this 3D-printer uses three kinematic structures that are connected to the extruder (universal joint). Thanks to the construction method of the three arms, the extruder will always keep the same orientation while printing. An example of this system, the Deltabot 3D-print manufactured by Biohazard [43], is shown in Figure 81.

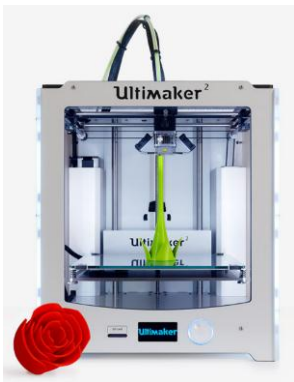


Figure 79: Ultimaker 2 (Moving extruder) [41]



Figure 80: BEETHEFIRST (Moving bed) [42]

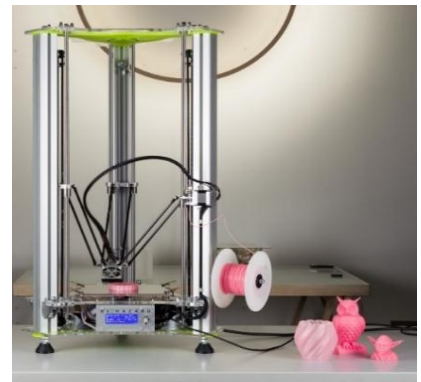


Figure 81: Biohazard Deltabot [43]

7.3.6.6 Settings

Standard drawings, like .ipt-files designed in Inventor, cannot be loaded into 3D-printing software. These files have to be converted and exported to an STL-file first. One should make sure to choose the next settings when converting your file:

- Format: Binary.
- Units: The same units used while creating the drawing. In our designing phase, we will use millimeters.
- Resolution: High.

Loading that STL-file into a 3D-printer will not give any extra information to the printer but the movement path of the extruder. In a separate program (often Cura or Slic3r) the user must fill in some parameters. The most important settings are:

- Layer height: This setting determines the thickness of each layer and thus the overall quality of your print. The smaller this value, the higher the quality.
- Fill-in density: 100% fill-in will result in the strongest part but also results in a waste of material and an addition of weight. If the fill-in is lower than 100%, the empty space is strengthened by a quadrangular structure, proportional to the chosen percentage.
- Wall thickness (shell, bottom and top): When the fill-in percentage is lower than 100%, the wall thickness will also have an important role for the strength of the part. Most programs have the possibility to choose a separate side and top/bottom thickness.
- Scaling: This factor comes in handy when a smaller prototype of a part must be printed.
- Orientation: Sometimes it is desirable to rotate a part. There can be different reasons to do this, for example: less support material required, vertical printing in one direction must be avoided (Z-axis forces will have a bigger chance to tear the layer apart), ...
- Print speed: This is the speed at which the printhead can move while extruding material. A faster print will result in a lower print resolution and a print of lower visual and structural quality.
- Travel speed: This is the speed at which the printhead can move without extruding any material, like engaging or moving from one place to another without having to print anything.
- Platform adhesion type: This option can prevent corners from lifting due to warping. There are three different options:
 - None: No special layer is added.
 - Brim: One single layer is added under the object.
 - Raft: Respectively a thick raster and a thin interface are added between the print bed and the part.

This setting may not be confused with a skirt. A skirt is an outline surrounding your part. That skirt has the purpose to help with priming your extruder and establishing a smooth flow of filament. Moreover, this line can indicate a print bed that is leveled incorrectly.

Once these settings are chosen, everything will be saved into a G-code that can be loaded into every kind of 3D-printer. This code will contain all the information needed to start printing except a few parameters that need to be changed in the printer settings:

- Used filament: Most printers have predetermined settings for PLA and ABS. These can still be changed afterwards.
- Extruder temperature: The temperature at which the print head will extrude the filament. This factor depends on the type of filament, the manufacturer, room temperature, ...
- Printing bed temperature: More information can be found in paragraph 7.14.

7.3.7 Conclusion

While all technologies are applicable for the Aslan project, there is only one affordable way of additive manufacturing: Fused Deposition Modeling.

The same argument can be used for the amount of extruders: two extruders will give a better result (thanks to the solubility of the support material PVA in water), but is not necessary. Thus in order to reduce the total cost of our project, one extruder will suffice. A closed room and heated bed are both desirable but also not necessary: only one of the two will have a big impact on the final product.

Considering material choice, tests should point out which one (ABS or PLA) is best for our application.

The positioning system is a choice of preference, but there are two remarks in favor of choosing the moving extruder:

- It requires less energy to only move the extruder than move the entire bed and workpiece.
- This way of positioning is the most commonly used and is therefore also more frequently available on the market.

7.4 FINAL CONCLUSION OF THE RESEARCH

Considering the fact that our project requires lots of little complex pieces and only little time is available, we prefer to go with 3D-printing. More precisely: Fused Deposition Modeling. Having a printer in our workshop is a huge advantage thanks to the possibility of adapting and printing small parts in a very short period of time when needed. If we would use milling however, the process would be more difficult, it would require more time and we would need to follow a strict schedule of when to use the milling machine.

7.5 CHOICE OF ADDITIVE FABRICATION AND DEVICE

Looking at the types of 3D-printers, it is quite clear which option we have to take. Stereolithography, Polyjet and Selective Laser Sintering are still too expensive for our available budget which was limited around €4000. The only method that would be suitable is Fused Deposition Modeling.

After reading a lot of reviews, descriptions and forums, three big contenders were taken into consideration: Ultimaker 2 [41], Cubify CubeX [44] and MakerBot Replicator 5th Generation [45].

With the help of a decision matrix (Annex 21.1) and some criteria, our printer for the project was chosen.

These were the criteria:

- Price: The sponsor, Sint-Augustinus NKO, gave us a nice budget to start the project (paragraph 11.3). The 3D-printer would be the greatest cost but we were told to keep the price as low as possible.
- Printing dimensions: The bigger the printing platform, the better. But a bigger buildplate will lead to a decrease of printing resolution and an increase of the price. Looking at printers on the market right now, a print volume around 250mm x 250mm x 250mm had to be the target value.
- Resolution: For our application, the resolution should be as high as possible (low value) to be able to print the functional surfaces. On top of that, our sponsor asked to choose a printer which can also be used by them for printing very precise parts like little bones inside the ear. Making an estimated guess concerning the printing resolution, 100 microns would be a decent value but the application of our sponsor could always use a better resolution. The better the resolution, the more the prints will resemble real human parts.
- Price of the filament: As mentioned before, the cost of everything should be as low as possible.
- Delivery Time: Because the budget was only available in February, there was not very much time left to finish the project so every extra day was important.

The best 3D-printer considering these criteria was the Ultimaker 2, which can be seen in Figure 82.



Figure 82: Ultimaker 2

7.6 ATTENDING RAPIDPRO: 3D-PRINTING CONVENTION

The 4th of March 2015 we attended the 3D-printing convention RapidPro in Veldhoven, The Netherlands. Here we received a lot of information and knowledge about 3D-printing in both the home professional and industrial sector. A lot of suppliers and companies were present, which gave us the opportunity to ask different distributors about their opinion on the Ultimaker 2. They all gave positive reviews and moreover the Ultimaker 2 was the most represented printer, not only at stands of resellers but also at stands of hobbyists and 3D-artists. This confirmed our choice.

7.7 PROPERTIES CHOSEN PRINTER

The chosen 3D-printer, with the properties that resemble the requirements in most ways, is the Ultimaker 2. It is a printer designed for hobbyists who make small prints at home. The price fluctuates around a price of €1900 (around €2300 with Belgian VAT included). Our printer was bought at Trideus¹⁵ where we received €100 of filament for free.

It is a Fused Filament Fabrication (FFF-based), also known as a Fused Deposition Modeling (FDM) printer with a capacity of printing volumes with maximum dimensions 230 x 225 x 205 mm. This will cause problems considering the fact that forearms are most likely larger than these dimensions. This must be taken into account when designing the bigger part of the project.

Next to the few big parts that have to be printed, there are a lot of smaller part that need quite some precision. While the diameter of filament has a standard size of 2.85 mm, the nozzle that extrudes the heated material only has a diameter of 0.4 mm. The Z-resolution is more important to the print quality. This particular printer has a layer resolution of up to 20 micron which is considered very good for a 3D-printer for use at home.

Another important factor is the print speed and precision of the printer. Considering the little amount of time, in which we have to complete the project, we must be able to get the prints rather fast, but still of good quality. The print and travel speeds go from 30 mm/s to 300 mm/s. But if the extruder head would print faster, the print quality would drop. The Ultimaker 2 has a movement precision of 12.5 microns in X- and Y-direction while the Z-direction can move with a precision rate of 5 microns.

The Ultimaker 2 also offers a wide range of obtainable temperatures. The nozzle can heat up from 180 up to 260 degrees Celsius. The heated bed can vary from 50 to 100 degrees Celsius but it can also be turned off so its temperature approaches room temperature (around 20 degrees Celsius). In order to get the optimal result, the manufacturers recommend a room temperature between 15 and 32 degrees Celsius.

In operational mode, the Ultimaker 2 causes average noise of 49dBA. According to the ARAB [46] (Algemeen Reglement voor de ArbeidsBescherming, general regulations for labor protection in Belgium), measures must be taken to protect the employees when exceeding 85 dBA. The Ultimaker 2 doesn't approach this limit so no safety equipment needs to be provided.

The entire datasheet of the Ultimaker 2 can be found in Annex 22.5.

¹⁵ www.trideus.be

7.8 CURA SOFTWARE

Cura is the standard supplied software by Ultimaker. Once the STL-file is loaded into the program, settings like orientation, scaling and printing quality properties can be adjusted as desired.

Although Cura is a program developed and maintained by Ultimaker, it is still possible to load different printers, even printers from other companies. This option loads all the basic settings into the program to be able to get a clear view of the possibilities of the used printer. These basic settings contain build volume, build plate shape, printer head size, ...

Once these properties are known, they will be used to design the lay-out of the printer. This way, Cura can calculate the maximum volume of the chosen part and it can also calculate whether or not the axes will interfere with previously printed parts on the same print bed. If this is the case, Cura will write a G-code such that the printer will print a layer at the same height for both part A and B before starting the next layer. This way, the printing time will be longer because of the increased distance the printhead has to travel. This is called 'Print all at once' and is shown in Figure 83.

If the parts are small enough, Cura will adjust its G-code by first giving the command to print part A before starting to print part B. This last method is called 'Print one at a time' and it is shown in Figure 84.

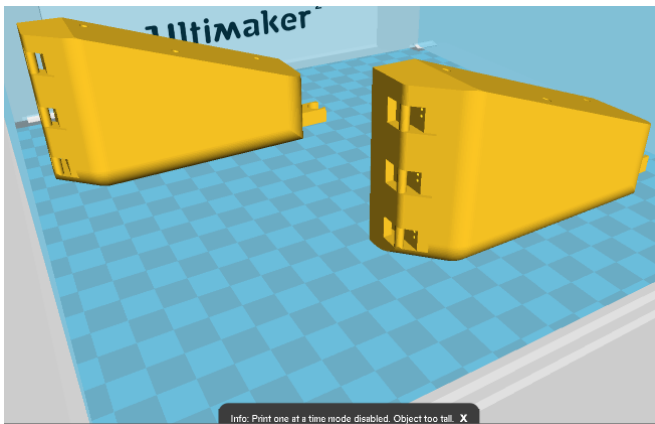


Figure 83: 'Print all at once'-function

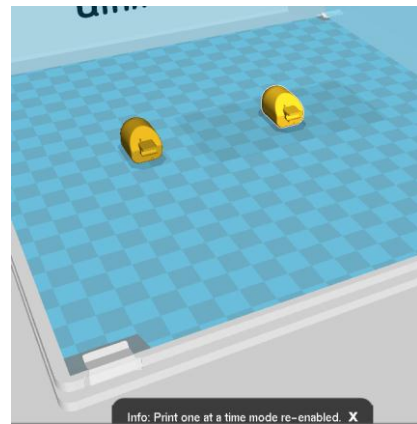


Figure 84: 'Print one at a time'-function

Once every setting is chosen as desired, the file can easily be saved as a G-code on the sd-card which is needed to load the printing task into the Ultimaker 2.

7.9 DEVELOPMENT OF THE SETTINGS

After the arrival of our Ultimaker 2, we have tested several settings for creating the optimal set-up for the project. The quality was not allowed to suffer because of the limited amount of time on our hands, but choosing settings with the slowest printer speeds and a 100% fill-in would take a huge amount of time. Also, a 100% fill-in would make the parts a lot heavier which is disadvantageous for dimensioning the strength of the servo-motors and it would require a lot more material and money.

Cura offers the option to choose between a quick print or a full expert mode. The quick print mode is a way to give hobbyists an easy choice when it comes to printer settings. This mode contains four choices: fast print, normal print, high quality and uli-quality. The order in which we tried the settings was: normal print, uli-quality, high quality and afterwards the personal settings for project Aslan were created. The most important values for all settings are listed in Table 24.

While the normal print gave us a rather fast print, the quality was not good enough if we look at the functional axes of the finger joints. This is a problem caused by the layer height of 0.1 mm.

The high and uli-quality gave a better quality print because they offer a layer height of 0.06 and 0.04 mm respectively. This would however lead to a very long printing time. Moreover, the thickness of the shell is set to 0.8 mm and the bottom and top thickness is set to 0.6 mm which will lead to a rather weak part.

Because of the fact that the orientation of the parts is in function of the functional parts and not in function of the appearance, the bottom, top and shell thickness should be the same. Moreover, the shell thickness must be a plurality of the nozzle size. The standard nozzle that comes with the Ultimaker 2 has a nozzle size of 0.4 mm. This leaves values as: 0.4, 0.8, 1.2, 1.6, 2, ... mm. Most of the walls in the design of the robotic arm have a thickness of 3 mm. This led to the choice of 1.2 mm as thickness for the shell, top and bottom.

We also printed a small cone with every setting to compare the visual results, which can be seen in Figure 85. The best results were achieved using the high quality settings and our own settings, while the uli-settings, which should give us the best quality, ruined the top of the cone.

Table 24: Most important values of various printing settings

	Fast	Normal	High	Uli	Personal settings
Layer height (mm)	0.15	0.1	0.06	0.04	0.08
Shell thickness (mm)	0.8	0.8	0.8	0.8	1.2
Bottom/Top thickness (mm)	0.6	0.6	0.6	0.6	1.2
Printing time (Distal phalanx index) (minutes)	12	28	47	71	55
Amount of material (meters of filament)	0.28	0.28	0.28	0.28	0.40



Figure 85: Visual comparison of every setting. From left to right: Fast print, normal print, high quality, ultra-quality and our custom settings

7.10 DESIGN RULES FOR 3D-PRINTING

Putting some thoughts into 3D-printing can save a lot of precious time. Choosing correct settings and orientation will decrease the print time drastically, while thinking about some frequently made mistakes can save a lot of failed prints.

One of the biggest factors that should be taken into consideration when starting to 3D-print is overhang. Overhang is a problem that occurs when a structure has to be printed above an empty space. This means that a new layer has to be printed onto the previous layer but that layer is not there because it is not present or needed in the drawing of the part that needs to be printed.

To solve this problem, Cura can create a support structure. This is a temporary structure, which can easily be removed after the print is finished. Some tools like pliers and knives can be used to ease the removal of the support. There are three options available in Cura: 'none', 'touching build plate' and 'everywhere':

- 'None' will add no extra material, but overhanging structures will most likely collapse and ruin the print unless no overhanging structure is present in the part. Looking at Figure 86, neither the red or green structure will be printed for this letter "A".
- 'Touching build plate' will only add support material where there is an empty space between the build plate and an overhanging structure. If there is overhang above a previously printed surface, Cura will not provide any support. This will avoid remaining spots of the support material but the probability of the overhanging part collapsing will still be present. Looking at Figure 86, only the green structure will be printed for this letter "A".
- 'Everywhere' will add support material where needed. This contains both overhang above the build plate and overhang above previously printed surfaces. It will avoid collapsing of the overhanging structures. Looking at Figure 86, both the red and green structure will be printed for this letter "A".

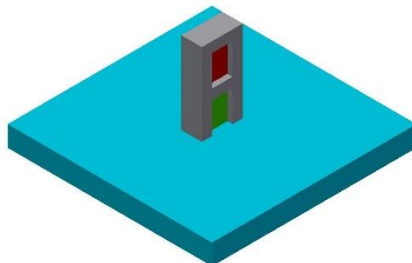


Figure 86: Example for support settings

The downside of this last option will always be that the clean-up of the printed part will take a while. The rough parts of the support are easily removed by using pliers but the remaining adhesive spots need some extra attention with a sharp knife, especially when the overhanging structures are functional surfaces like finger joints.

The support material added by Cura are vertical planes which are connected by stringy structures (visible in Figure 87). These are fixed to the part using little spots as a connection. These spots are the weakest places and this is where the material will break. The spots will leave little dots that will need to be removed afterwards, especially on the functional surfaces.

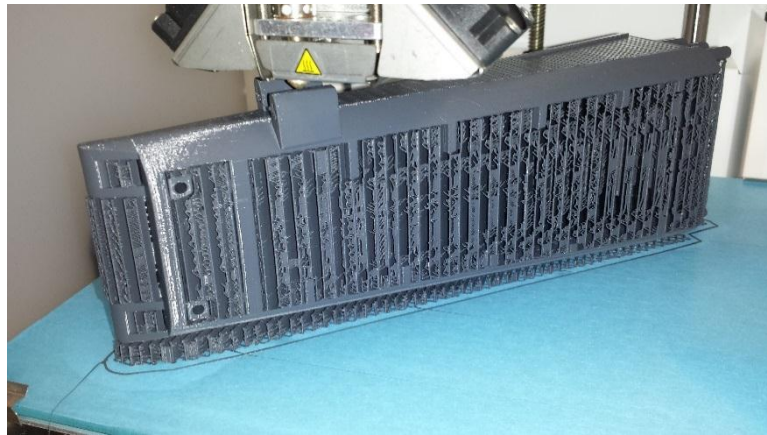


Figure 87: Forearm with a lot of support material

The overhanging structures contain impurities, even when they are printed with support material all around. This is disadvantageous for functional surfaces where a correct fitting is needed.

The decision was made to focus on avoiding overhang and support material at the functional surfaces because this will cause more friction and resistance while rotating the joints. This is caused by the first layers that are printed on top of the support material. These layers will lower a bit between the vertical planes of the support material because of the gravitational force, causing the axis to be a little bit bigger than designed, which leads to the extra friction. Moreover, avoiding support material on these surfaces leads to less clean-up afterwards and it will guarantee a better print quality of those important surfaces.

Looking at the joints between the phalanx bones, it would be better to rotate the parts 90 degrees around the longitudinal axis. This way the axis and C-shape will stand up, giving us a clean printing result without any big irregularities. This orientation is shown in Figure 88 and Figure 89. The outlook can be less smooth this way, but the function of the joint is more important than the exterior of the finger. This last one may contain some irregularities that can still be deleted with some post-processing.

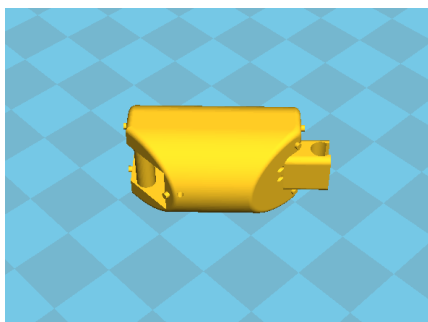


Figure 88: Orientation for good functional surfaces

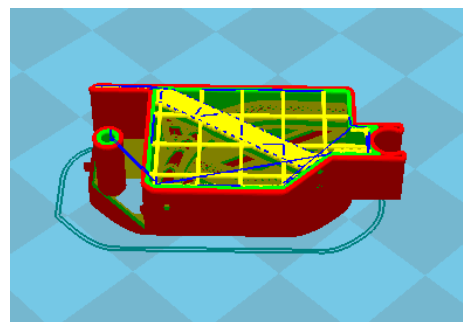


Figure 89: Sliced view of a 3D-print structure

The same logic can be applied to the wrist and every phalanx bone except those who belong to the index finger. Because the index finger has to be able to abduct and adduct, a special joint has been designed to make both abduction/adduction and flexion/extension possible. This is visible in Figure 90 and is explained more extensively in paragraph 8.5.

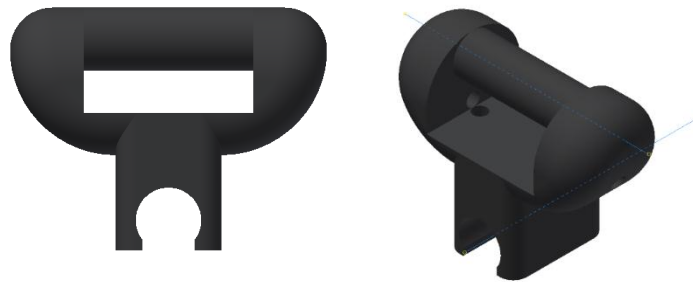


Figure 90: Abduction and adduction joint of the index finger

This joint has two functional surfaces with both axes perpendicular, so only one surface could be printed without any disfiguration. Because the index finger should flex/extend more than it should abduct/adduct, the axis describing the flex/extend rotation, should have the best quality. This is the cylinder. The C-shape shall be a bit more rough, even after clean-up, but that does not really matter because the unevenness will prevent the index finger from tilting, but it will not hinder the abduction/adduction enough to prevent that motion.

Because of this index finger joint, i.e. for the added abduction/adduction motion, one axis located at the palm shall have another orientation than the other three. To ensure a good rotation around each joint, the palm has been split into two parts: a part for the middle finger, ring finger and little finger and another part for the index finger and the thumb. Looking at Figure 91, it is clear that all functional axes, except one joint for the wrist (which can be cleaned more easily because of its bigger size), are pointing upwards.

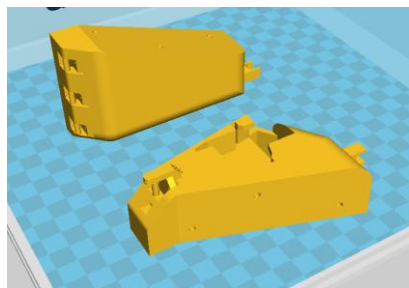


Figure 91: Orientation of functional axes

7.11 PRINTING TIMES

Once the printing settings and the printing positions were determined, the printing times could have been computed. The printing position is an important factor of the printing time because with a high layer resolution there will be more layers and the bigger the distance is between the print bed and the top of the part, the more layers the print will need. These layers extend the printing time enormously. Printing the whole assembly of the robotic arm will take 138 hours and 54 minutes.

A brief list of the printing times, with correct orientation and settings, can be found in Table 25.

A complete list of the printing times, with correct orientation and settings, can be found in Annex 17.

Table 25: Brief list of printing times

Name	Time	Material (meter)
Middle finger Distal	48 min	0,35
Middle finger Intermedial	1h21	0,55
Middle finger Proximal	1h40	0,69
Palm 2 fingers	12h43	6,11
Palm 3 fingers	15h59	7,57
Wrist side hand	1h2	0,4
Wrist side motor	1h3	0,39
Ring finger Distal	48 min	0,35
Ring finger Intermedial	1h10	0,47
Ring finger Proximal	1h31	0,63
Abduction/Adduction joint of the index finger	15 min	0,08
Forearm back	37h53	21,49
Forearm front	53h	27,01

7.12 MATERIAL

The standard filaments delivered by Ultimaker are PLA and ABS, additionally, one spool of PLA was included with the printer itself. When the decision was made to use Fused Deposition Modeling, we also decided to do some testing both with PLA and ABS. Due to the budget being available rather late, we had to consider our choice very well, very quickly and most importantly without the time for testing both of them.

The criteria that made us go for PLA are:

- Stiffness: PLA is stiffer than ABS. This is useful for our project because the motors inside the forearm will be clamped inside a tight fit and any tolerance caused by elastic deformation should be avoided as much as possible.
- Poisonous gasses: Our workspace is a rather small room in a cellar with mediocre ventilation so poisonous and irritating gasses should be avoided. ABS would thus be a bad choice.
- Load on the printer: The printer should be able to last with the project and the sponsor for a few years. When printing with a higher extrusion temperature, the extruder will wear off faster. While ABS is printed at temperatures around an average of 230 degrees Celsius, PLA only requires a temperature around 190 degrees Celsius.
- Early testing: While working with the spool of PLA that was given to us together with the printer, we achieved good results. After tweaking some of the settings, we analyzed the prints and concluded that the realized quality would certainly suffice for our project.

7.13 FILAMENT

PLA being the material of our choice, we ordered filament to start our project. One reel of silver PLA was included with the printer. Besides that, we ordered three more reels of PLA: orange, dark gray and pearl white.

The orange, silver and pearl white filament were all of the brand Ultimaker, while the dark gray filament was manufactured by ICE filaments. All these filaments are pictured in Figure 92.

Tests showed that the filaments delivered by Ultimaker printed better at a temperature of 210 degrees Celsius while the ICE filament printed best at a temperature of 205 degrees Celsius. We will mostly print the pearl white filament at a temperature of 210 degrees Celsius.

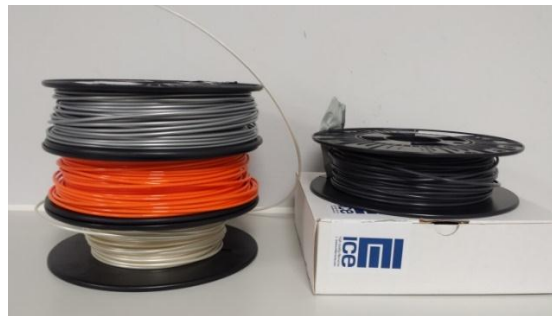


Figure 92: Used spools of filament

7.14 PRINT BED

The first prints were all printed on a heated bed of fifty degrees Celsius with a layer of glue, as recommended by the manufacturer. This gave us good printing results but sometimes it was rather hard to separate the part from the build plate without the part being damaged. Even when the part got loose, there would still be glue stuck on the part which was hard to remove. On top of that, after three prints, the print bed had to be cleaned because of the previous layers of glue which created an uneven layer that could have an unfavorable influence on the printing.

The distributor who sold us the Ultimaker 2 also mentioned using painter's tape, without heating the print bed, to keep the part from warping and moving. After some research we bought Tesa Masking Tape (Figure 93). This tape gave perfect prints which came loose easily when removing the finished print and it only has to be changed once every ten prints.



Figure 93: Used painter's tape

7.15 PROBLEMS

Using the Ultimaker 2, we encountered a few problems. Most of the time these problems were caused by bad settings or by the filament.

The reel of ICE filament caused the biggest printer problem of the project. The filament was not wrapped around the reel very well, which led to the filament tightening itself onto the reel (Figure 94). This caused the material feeder on the printer to scrape through the same spot on the filament (Figure 95).



Figure 94: Badly wrapped spool of filament



Figure 95: Scraped filament

This happened two times in a row, so we changed the ICE filament to a reel of Ultimaker filament. Because the filament got stuck, the material inside the print head got clogged a bit without us noticing. Adding the new filament only made it worse, causing the print head to clog entirely. After two hours of cleaning with a needle and an extruder head at 260 degrees Celsius to make the material as liquid as possible, we managed to unclog the printer and to start printing again.

Unfortunately, after the next small print, the nozzle got clogged again and the difficult decision was made to disassemble the entire printer. Both the printhead and the feeder were opened up to clean and remove all the PLA that was left behind.

When opening up the feeder (Figure 96), we found a lot of powdered PLA that got left behind when the cable got scraped. It got stuck behind the bearing and the moving parts. After blowing every piece of contamination away, the problems in the feeder were solved.



Figure 96: Disassembled and assembled feeder

While disassembling the printhead (left and middle picture of Figure 97), we had to remove the temperature sensor and the heating element. The heating element came loose very easily but the temperature sensor, to keep the printing nozzle at a stable temperature, was stuck. While pulling it out, the cable snapped and the sensor broke off (right picture of Figure 97). After calling the distributor of the Ultimaker 2, we learned that this was a common problem and we received a new sensor in warranty.

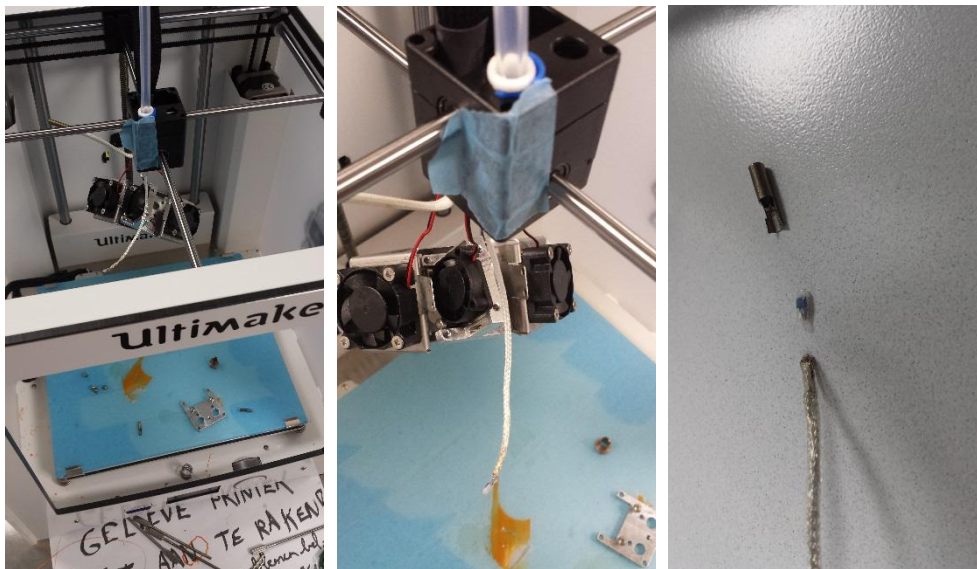


Figure 97: Disassembled Ultimaker 2 and broken sensor

Disassembling the printhead completely revealed the biggest problems: the nozzle was clogged entirely and the Teflon tube had a small deformation and burning marks (Figure 98). This was probably caused by the filament that could not go anywhere and thus always got a heat treatment going from room temperature to 260 degrees Celsius (when trying to extrude the clogged material).

The deformation in the Teflon tube can cause friction between the inside of the tube and the filament and this friction will make it even harder to extrude the material through the nozzle. The right picture of Figure 98 shows the new tube we received in warranty (left side), the old tube with the deformation (right side) and the nozzle made out of brass (top of the picture). We unclogged this nozzle by placing it into acetone for the night and cleaning it with a needle the next day.



Figure 98: The new Teflon tube and the old one.

To replace the broken sensor, we had to open the electronics compartment at the bottom of the printer to disconnect the old cable and connect the new one.

While it was a big inconvenience causing us to lose a lot of precious time, we still learned a lot about the working principles of the Ultimaker 2.

7.16 MESHMIXER

Meshmixer is freeware delivered by Autodesk. It is mostly used to clean up STL-files (after scanning an object) or meshing two STL-files together into one part. But the feature that seemed most interesting was the overhang analysis.

Meshmixer [47] detects all overhanging surfaces starting from an angle of your own choice. Afterwards it creates a special form of support structure that saves as much filament as possible. It uses a special algorithm to create a tree-like structure (Figure 99). This would be interesting for our project because of the limited budget, but it was not applicable to our drawings because the parts are too small to create this special structure effectively.

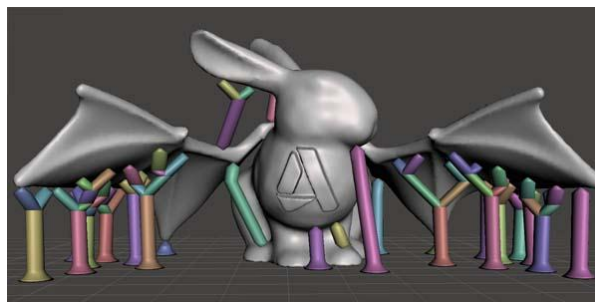


Figure 99: Tree-like support structure created by Meshmixer [47]

7.17 FINAL CONCLUSION

Besides the problems we had with our 3D-printer, caused by the ICE-filament, we still think this method of manufacturing was very fitting. The results were good and the overall printing times were short. All of this was achieved thanks to the Ultimaker 2 that gave us those high quality prints.

After tweaking some of the printing preferences and analyzing previous prints, we were able to get the most fitting setting for our project.

Even though the research told us to opt for a heated bed or a closed room, we obtained cleaner results while using painter's tape on a print bed that is not heated rather than applying a single layer of glue on a print bed that is at least 50 degrees Celsius.

PLA, being the choice of building and support material, gave us good looking, strong and stiff results. Opting an overall wall thickness of 1.2 millimeters, layer resolution of 0.08 millimeters and a part infill rate of 20% resulted in a very strong part that kept everything in place and that could take a lot of hits or drops without breaking. That is an important property considering the arm should be able to be transported quite a lot.

So overall, the only remark that should be kept in mind is: rather pay more to buy genuine Ultimaker filament instead of filament manufactured by ICE. It can save a lot of problems and time.

In Figure 100, our Ultimaker 2 can be seen while printing one of the parts of the forearm.

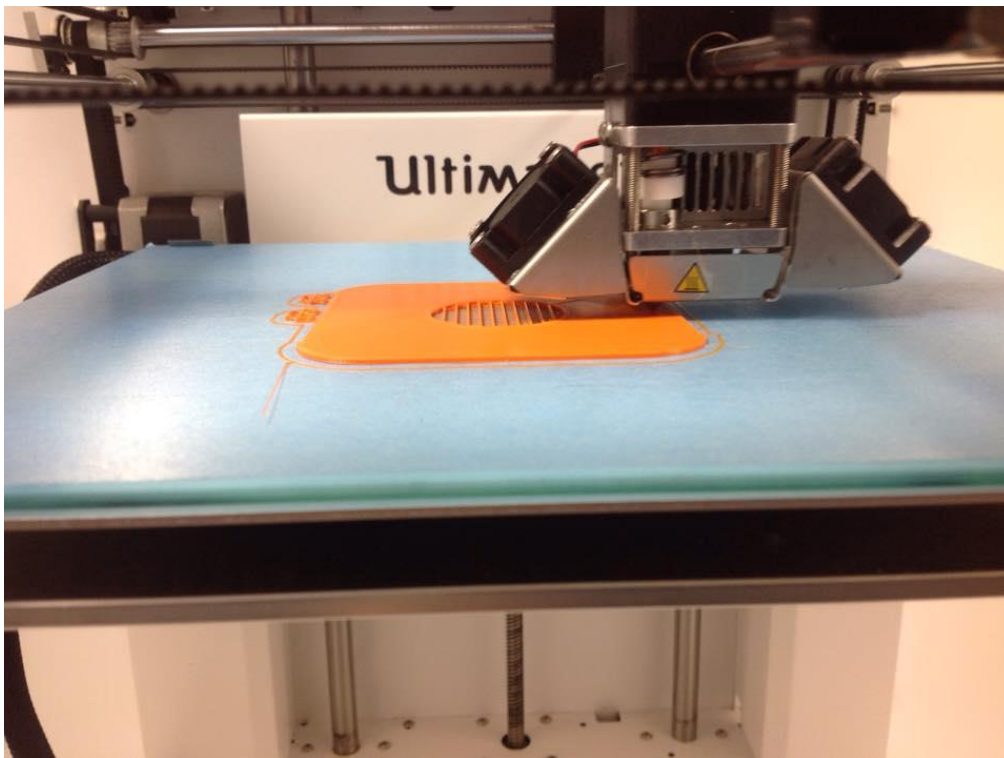


Figure 100: Our Ultimaker 2 while printing

8. Mechanical design

8.1 INTRODUCTION

Stijn Huys – In this chapter, the complete mechanical design process of the Aslan robot will be described. Starting from researching existing robotic arms and the adaptation of existing technologies and progressing to dimensioning our own robotic arm. When designing every single component, our goals like easy-to-assemble and a human-like design, will be applied as much as possible to create a working prototype.

8.2 EXISTING HUMANOID ARMS

8.2.1 Introduction

Building a humanoid arm is a very hard task if you have to start from scratch. Getting inspiration from other robotic technologies can give an enormous boost in time and efficiency.

In the upcoming chapter, we will talk about a few existing robotic hands and arms. Only the most important properties and technologies will be mentioned, using some illustrations to support my task as mechanical designer of our project.

A big problem we will encounter is the confidentiality of other robotic projects: only few information can be found so most of the gathered information will come from reading brief papers and observing several pictures.

8.2.2 Anthromorphic 20-DOF Robotic Hand

Being a 3D-printed hand, this robotic hand [48] (Figure 101 and Figure 102) resembled our own project the most. There are three types of joints in this model (thumb excluded): DIP, PIP and MCP. The DIP and PIP joint both got one degree of freedom while the MCP joint has two degrees of freedom.

The fingers are being assembled with snap-on joints (Figure 103). The engineers working on this robotic hand were inspired by LEGO mechanics. This type of joints makes it easier to (dis)assemble and replace broken pieces.

The different parts of each finger are created in a way such that they block the path for specific movements. This way they created a mechanical safety for their robot.

The rest of this interesting paper does not provide us any more useful information because it focusses on the tactile sensing and the force behaviors of the robotic hand.

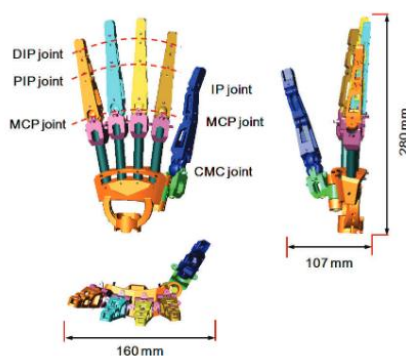


Figure 101: Assembled anthropomorphic 20-DOF robotic hand with visible joints [48]



Figure 102: Final product of the anthropomorphic 20-DOF robotic hand [48]

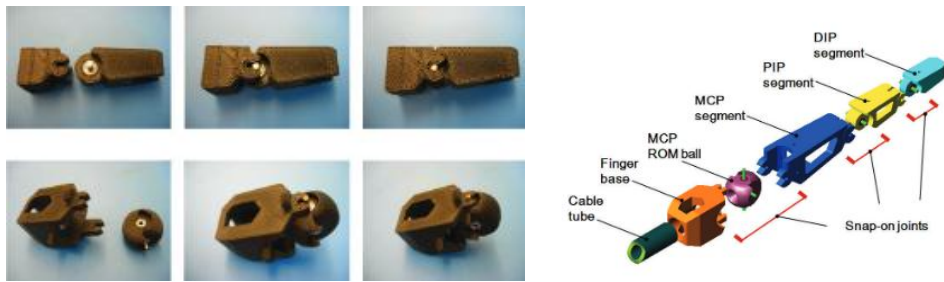


Figure 103: Snap-on joints of the anthropomorphic 20-DOF robotic hand [48]

8.2.3 TBM-Hand

This is a robotic hand [49] (Figure 106) created in 2001 by the university of Toronto. The most important technology to remember is the spring used in the thumb to force it back to the default position. They use rigid-link transmissions to make the grabbing motions possible. The thumb (Figure 105) has four links, the other four fingers (Figure 104) have six links per finger.

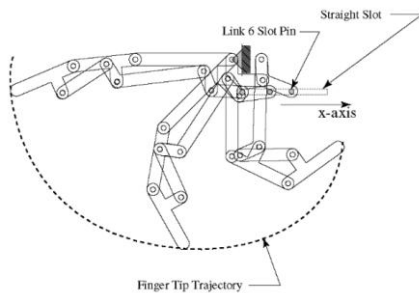


Figure 104: Composition of one finger of the TBM-hand [49]

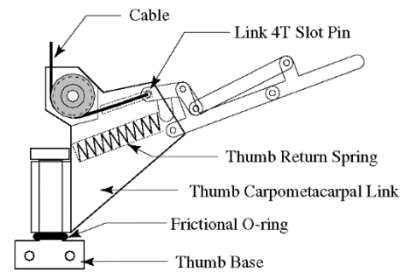


Figure 105: Composition of the thumb of the TBM-hand [49]

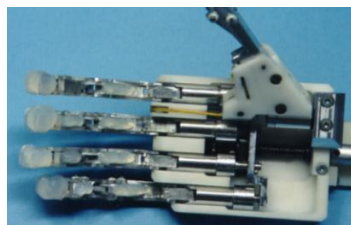


Figure 106: Final product of the TBM-hand [49]

8.2.4 DLR Arm Hand System

The DLR Arm Hand System [50] (Figure 107), designed by DLR robotics and mechatronics, comes very close to what project Aslan should become, being a set-up from hand to shoulder with a torso included. This gives us the opportunity to compare their properties with ours.

Their main properties are:

- 27 degrees of freedom
- 50 motors
- 108 position sensors
- Weight: 13.5 kg



Figure 107: The DLR Arm Hand System [50]

8.2.5 Tuat/Karlsruhe hand

The Tuat/Karlsruhe hand [51] (Figure 108) is especially designed to grasp and hold objects. They focused on the flexion/extension of the fingers while a big force was applied on the hand. The clean and easy design of the index finger (Figure 109) makes it worth mentioning this project.

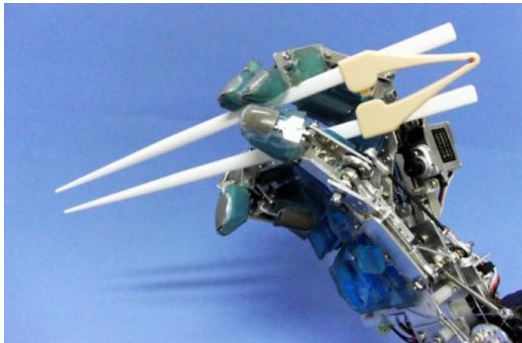


Figure 108: The Tuat/Karlsruhe hand [51]

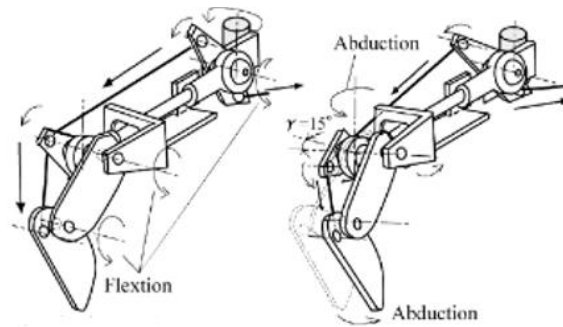


Figure 109: Design of a finger of the Tuat/Karlsruhe hand [51]

8.2.6 Gifu III Hand

This model [52](Figure 110) has 16 degrees of freedom in total. The thumb has four joints and four degrees of freedom while each other finger has four joints and three degrees of freedom. Looking at the design of this hand together with the sign language motions, the idea about the amount of degrees of freedom we should use in our hand, was constructed.



Figure 110: The Gifu III Hand [52]

8.2.7 IH2 Azzurra Hand

The IH2-Azzurra hand [53] (Figure 111) is designed by Prensilia (Grasping Innovation). Although there is little information, this robotic hand is worth mentioning because of its lightweight: 640 grams. This is a good target to aim for with Project Aslan. It does however only have 11 degrees of freedom in total.

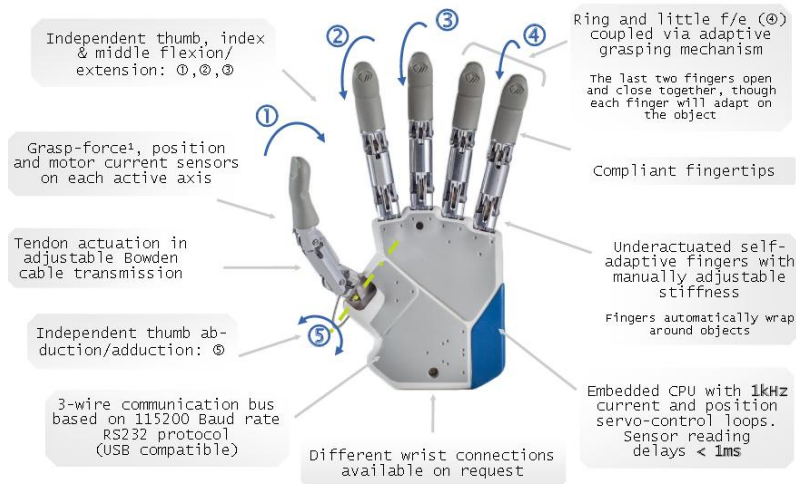


Figure 111: The IH2 Azzurra Hand [53]

8.2.8 Open Hand Project

Being an open-source project [54] (Figure 112), this one gave us quite some ideas for the design of our project. Drawings of this hand can be found on their website¹⁶ for free.

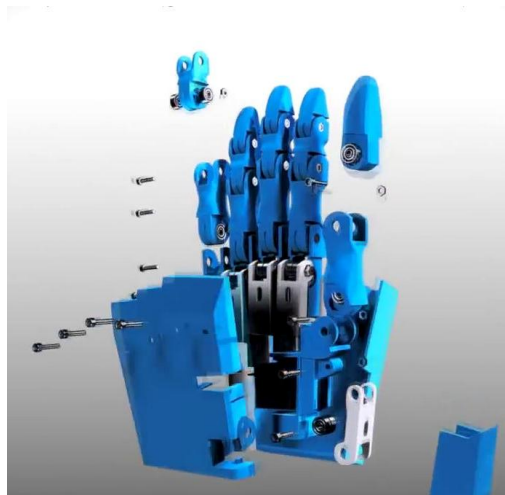


Figure 112: Exploded view of the Open Hand Project [54]

¹⁶ <http://www.openhandproject.org/>

8.2.9 Inmoov Robot

The Inmoov robot [55] (Figure 113) created by a French model maker, Gael Langevin, is an Open Source life-sized robot. The smart design of the thumb, where it rotates around an axis parallel to the palm, will make it possible to create all the needed movements of the thumb to resemble every letter of the Flemish Sign Language alphabet, if however some tweaks are made.



Figure 113: Inmoov robot [55]

8.2.10 MA-I Hand

MA-I Hand [56] (Figure 114) is mentioned for the same reasons as the Inmoov robot: the position and design of the thumb make it possible to form every letter that is needed.

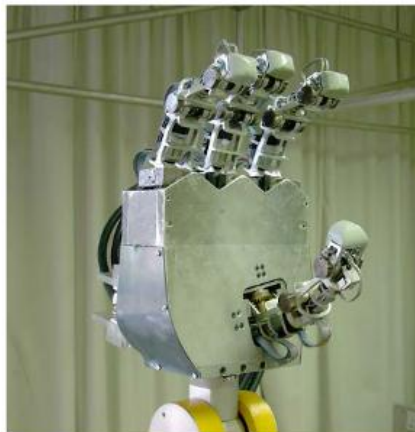


Figure 114: MA-I Hand [56]

8.2.11 Conclusion

While most of these humanoid arms and hands are made for grasping, I was still able to gather some valuable information considering our project.

Doing this research about existing robotic arms and hands, it became very clear that most of these projects are very secluded and if they release some information about their findings or techniques, it will be rather limited and vague.

8.3 ADAPTING EXISTING TECHNOLOGIES

8.3.1 Introduction

In this paragraph we will shortly consider whether it would be better to start from scratch or to modify an existing technology.

8.3.2 Adapting a prosthetic arm

Prosthetic arms, like the *Bebionic* [57] in Figure 115, are becoming more and more advanced and high-tech, but there are two major problems:

- They are only designed to grab daily things like a pencil, a can,... This means they can only do one grabbing motion. The index finger for example can't adduct or abduct, which is needed in, for example, the letter "V". Another example: the index finger and thumb got to be able to make a circle, the letter "O", but the index finger should also be able to be pressed against the palm of your hand, which is a required motion to form the letter "S".
- These arms only exist of a hand and a forearm. For some motions we need the degrees of freedom of the elbow and shoulders as well.

Fixing these problems will raise the costs of our project.



Figure 115: Bebionic [57]

8.3.3 Adapting a robotic spider

Somebody gave us the idea of modifying a robotic spider: the T8X Robotic spider from Robugtix [58] (Figure 116). This robotic device gives us all the degrees of freedom we need, but we still stumble upon two problems:

- Assuming we can convert the spider to a working humanoid hand, we will still need an arm, elbow and shoulder. The oldest model costs \$2950 and the newest one \$675. Creating the arm and shoulder would still cost a lot and the total cost will probably exceed the costs of 3D-printing the structure and designing the electronics ourselves.
- The oldest and most expensive model isn't available anymore and the newest one can only be pre-ordered with unknown delivery dates.

Some of the key features of this robotic spider are:

- Wirelessly controlled via Wi-Fi
- Powered by 26 advanced Robugtix servo motors with PID control and customization features
- Built-in battery charging system
- Rechargeable battery pack and power adapter included



Figure 116: T8X Robotic spider [58]

8.3.4 Conclusion

The modification of existing technologies will probably cost more than making it ourselves. On top of that we will need to solve difficult problems with limited funds.

8.4 DIMENSIONS OF THE HUMAN ARM

8.4.1 Introduction

One of the goals of the project is to build a humanoid hand that resembles the reality of sign language as close as possible. This requires a life-sized hand with average dimensions.

8.4.2 General

Georgia Tech Research Institute gathered data [59] of these dimensions from British adults ages 19 to 65. The resulting averages are listed in Table 26.

Table 26: Average hand dimensions gathered from British adults

Dimensions	Gender	Millimeters
Hand length	Male	178-189
	Female	167-174
Palm Length	Male	107
	Female	97
Thumb Length	Male	51
	Female	47
Thumb Breadth	Male	23
	Female	20-21
Index Finger Length	Male	72
	Female	67
Hand Breadth	Male	87
	Female	76

8.4.3 Conclusion

After comparing these dimensions for the male sex with the corresponding dimensions of our team members, we concluded that we came very close to these average results. Therefore we will be using dimensions derived from our own limbs to design our humanoid arm.

8.5 MECHANICAL DESIGN OF PROJECT ASLAN

8.5.1 Introduction

In the early stages of the project, the team chose a few objectives to guide the process in the right direction. Designing everything to create parts that can easily be assembled by an adult while still keeping the human outlook, was one of those big objectives. Since Project Aslan is a new project and we only had one year to build something, our main goal this year was to create a robotic hand that is able to produce every letter in the Flemish Sign Language alphabet. These goals should lead to a working prototype that can be optimized over the next years.

8.5.2 Dimensions of the parts

The outlook of the humanoid arm and hand should resemble a real human arm and hand as much as possible, both by the exterior form and the motions. This way, every sign will be recognized more easily and the transition between a human interpreter and our robot will be less difficult.

The most important factors to keep in mind will be weight and strength. Increasing the weight of a few parts will lead to bigger motors to be able to actuate the bigger loads. When these bigger motors are located furthest from the fixed point, every motor in between those two spots will need to be stronger and thus will increase the overall weight even more. This phenomenon will continue throughout the entire arm. The other important factor is strength. The humanoid arm will be a practical device that will need to be carried around quite a lot and must be able to take a few hits without breaking immediately.

A part of these factors is already determined in paragraph 7.9, where wall thickness, bottom thickness, top thickness and infill were determined. Every thickness was chosen to be 1.2 millimeters while the infill would be 20 percent. This way the parts will be able to take quite a hit, considering the Young's modulus of PLA lying between 3.45 - 3.83 GPa (Annex 16). The infill of 20 percent will keep the part stiffer and stronger than a hollow part while still being a lightweight.

Every finger is designed to be the same shape but with a different length. The shape of every finger is based on a square of 15 millimeters by 15 millimeters with two types of fillets (Figure 117): two fillets of 4 millimeters at the dorsal side of the finger and one fillet of 7.5 millimeters to round the ventral side of the finger.

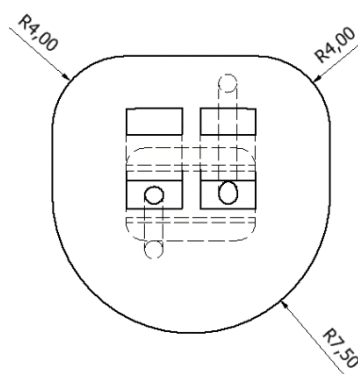


Figure 117: Top view of the distal phalanx of the ring finger

The lengths of all parts of each finger are listed in Table 27 below. While most of the people have index and ring fingers with approximately the same length, our lengths are different. These values are not the same because of the special joint created to make the adduction and abduction of the index finger possible (paragraph 7.10).

Table 27: Lengths of finger measured from axis to C-shape

	Thumb	Index Finger	Middle Finger	Ring Finger	Little Finger
Distal Phalanx	30 mm	25 mm	25 mm	25 mm	25 mm
Intermediate Phalanx	N/A	27 mm	31 mm	27 mm	21 mm
Proximal Phalanx	36.5 mm	35 mm	40 mm	36.5 mm	28 mm

The general dimensions of the palm are quite basic: the overall length is 100 millimeters and the width of the front of the palm is 80 millimeters while the widest part approaches 94 millimeters. The top view of the palm, which was split to achieve decently printed surfaces for the rotation axes, is illustrated in Figure 118.

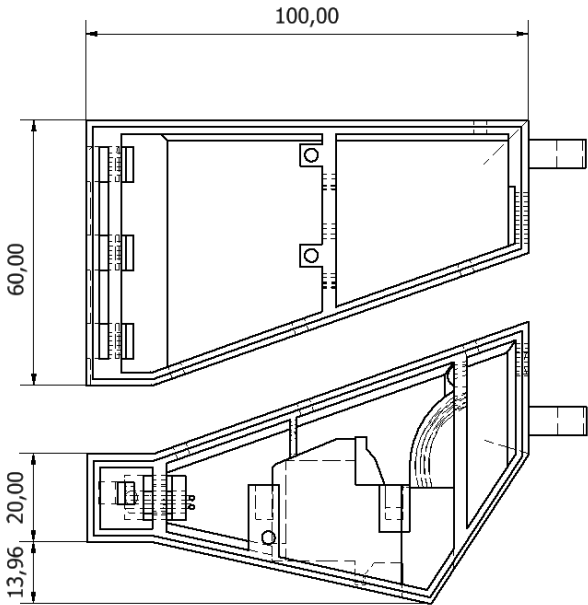


Figure 118: General dimensions of the palm

Due to the limited size of the print volume of the Ultimaker 2 (230 mm x 225 mm x 205 mm), the forearm had to be split into two smaller parts. The front, being the narrowest of the two, has a length of 190 millimeters while the back part has a length of 110 millimeters (Figure 119).

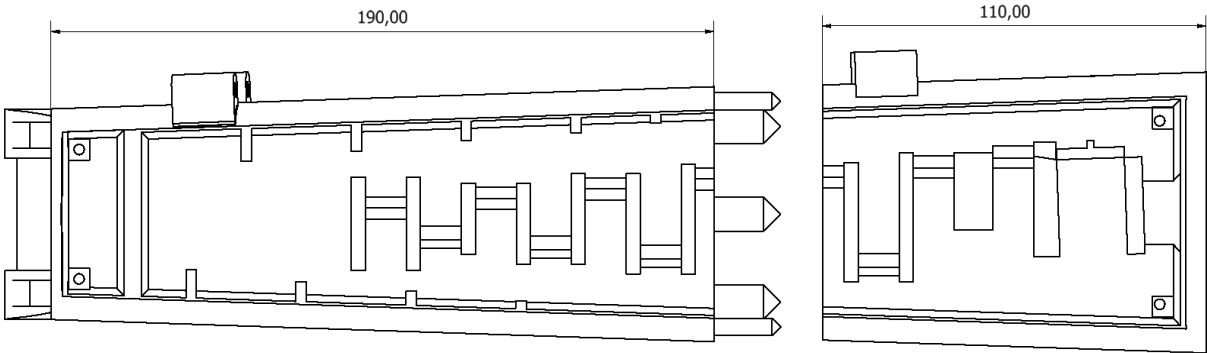


Figure 119: Dimensions of the forearm

The forearm is a transitional shape starting from a rounded rectangle with width 60 millimeters and height 30.31 millimeters and ending in a rounded square with width 80 millimeters (Figure 120).

The fillets are not approaching human-like values because this would have a negative influence on the functionality of the fabricated forearm.

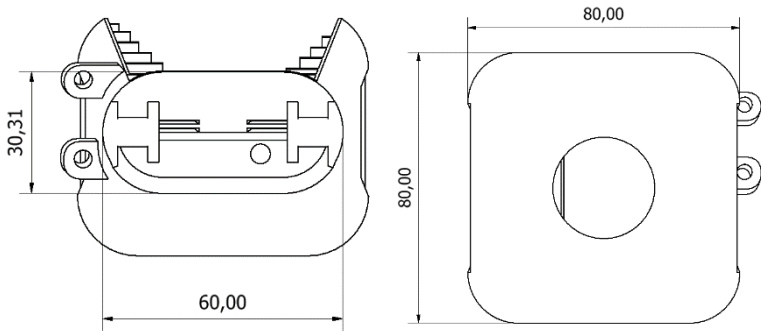


Figure 120: Shape of the forearm

8.5.3 Snap-on joints

One of the goals set at the start of the project was to create a modular robotic arm which can be rebuilt at home for everyone who downloaded the plans and drawings. Another goal was to design everything in a way that it would be easy to assembly, disassemble and replace every part in a short time. As seen in paragraph 8.2.2, a good solution for this problem is the use of snap-on joints.

To simplify every actuation, we replaced every ball joint by using two perpendicular snap-on joints. Thus for every movement one or more C-shape snap-on joints will be used.

A paper released by Ticona [60], *Design calculations for snap fit joints in plastic parts*, states for a ball and socket snap-fit (Figure 121):

$$\varepsilon = \frac{D_g - D_k}{D_k} \times 100\%$$

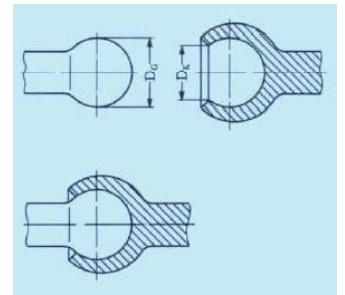


Figure 121: Ball and socket snap-fit [60]

Equation 27

With:

ε = elongation (%)

D_k = socket opening diameter (mm)

D_g = ball diameter (mm)

PLA has an average elongation of six percent. With a ball diameter of, for example, 3 millimeters, this will give us a socket opening of approximately 2.8 millimeters using Equation 27.

These values were not entirely in line with our findings. This was caused by the 3D-printing imperfections and the transformation from a ball to a cylinder. The final values have been chosen as follows:

- The snap-on joints of the fingers:
 - The radius of the axis: 3 millimeters
 - The radius of the C-shape: 3.1 millimeters
 - The opening of the C-shape: 2.5 millimeters

- The snap-on joints of the wrist:
 - The radius of the axis: 7.3 millimeters
 - The radius of the C-shape: 7.5 millimeters
 - The opening of the C-shape: 6 millimeters

A simple C-shape without any reinforcements is not able to hold on to the axis tight enough because of the imperfections caused by the overhang of the 3D-printing and the lack of stiffness. This problem is shown in Figure 122.

Reinforcing the sides of the C-shape and extending the end a bit solved this problem completely and gave us the final design of the snap-on joint which can be seen in Figure 123.

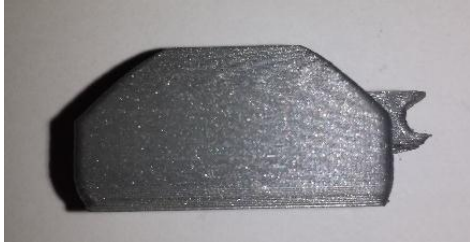


Figure 122: Unreinforced C-shape



Figure 123: Reinforced C-shape

8.5.4 Design of the thumb

The thumb is a very complex digit with a lot of possible positions it can be in. If we would replicate the real human thumb it would make the design and actuation unnecessary difficult. For our application we simplified it to three degrees of freedom instead of the five degrees of freedom a real human thumb has.

The TMC of the thumb has been reduced to one degree of freedom, as seen by Inmoov Robot (paragraph 8.2.9). It has a rotation around an axis parallel to the side of the palm of the hand and the four other fingers. This axis will become the axis of the motor. When adding a special attached piece that keeps the thumb itself at an angle of 45 degrees relative to that axis of the motor, we will be able to reach every needed position for each letter.

In Figure 124, the assembly of the thumb is shown. The metacarpal I (light grey part) is the piece that keeps the proximal and distal phalanx I (dark grey part) rotated 45 degrees relative to the axis of the motor that is represented by the blue line.

In Figure 125, the most extreme positions of the thumb are shown by our own finished product.

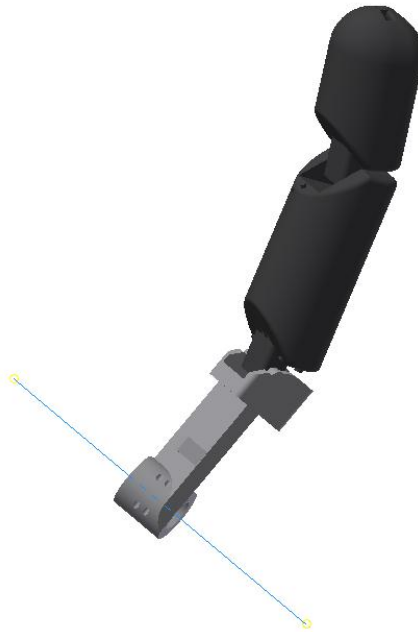


Figure 124: Assembly of the thumb



Figure 125: The most extreme positions of the thumb

8.5.5 Design of the adduction and abduction of the index finger

As mentioned before, in paragraph 7.10, the index finger was going to be the only finger in our robotic hand that had to be able to perform an adduction and abduction. This is where we introduced a special joint that has two perpendicular rotational axes (Figure 126).

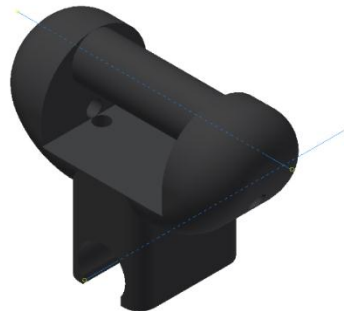


Figure 126: Joint for adduction/abduction of the index finger

The design of the joint itself is already covered in paragraph 7.10, but the implementation of this new piece had some influences on the design of the palm. First of all, the axis where the index finger and the joint would snap on needed to be rotated 90 degrees to get a correct orientation of the finger. But another important factor was that with most people, the index and ring finger approximately have the same length. This led to lowering the axis by the distance between the two perpendicular axes of the joint because we wanted to keep the same height of axes for extending and flexing the fingers. To be able to move the index finger in front of the middle finger, for example to form the letter “R” (Figure 127), the axis on the palm also had to get an offset closer to the palm of the hand to avoid collision between the index and middle finger.

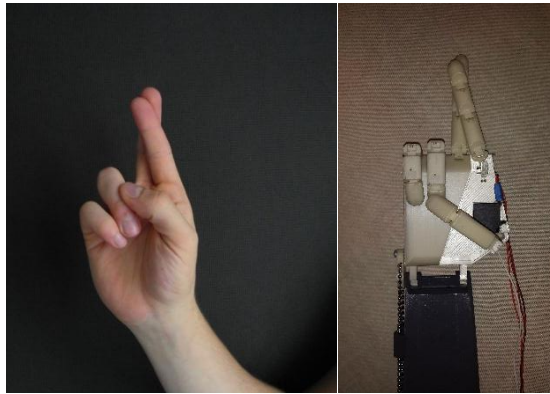


Figure 127: The letter R formed by a human hand (left) and by our robotic hand (right)

The actuation of the abduction/adduction is controlled by a motor in the palm. On the axis of that motor, a small, custom wheel is attached to be able to connect the cables to the actuation.

8.5.6 Design of the wrist

When starting the project, we decided to reduce the amount of degrees of freedom because it would lower the complexity of the robotic arm. For the wrist, this led to keeping the extension and flexion but dropping the ulnar and radial deviation.

We kept the design as simple as possible. The connection between the forearm and the palm is realized by placing two C-shaped snap-on joints on the palm and two axes on the forearm, as mentioned in paragraph 8.5.3.

For realizing the extension and flexion of the wrist, we determined to take a 1:1 transmission between the palm and the motor located in the back of the forearm. The motor is located here because it is the heaviest one and it would minimize the forces on the motors of the elbow.

The different parts of the total design are:

- Ball chain: We chose a ball chain because it would be a cheap, strong, flexible and adaptable way of driving the palm. The chosen chain has a diameter of 3.6 millimeters and as stated in DIN 5280 [61] (Figure 128), the maximum length between the center points of two adjacent balls is 4.5 millimeters. Once these numbers were known, the attachments were designed.

d	t
2,0	2,6
2,2	2,8
2,5	3,2
2,8	3,4
3,2	4,0
3,6	4,5
4,0	5,0
4,5	5,5

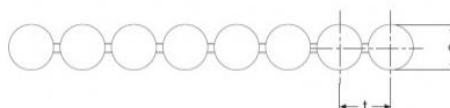


Figure 128: Ball chains: DIN 5280 [61]

- Fixed attachment on the palm (Figure 129): This attachment is fixed to the palm using two bolts. It is designed in a way that the center axis of the wheel is coincident with the axis of the rotation of the joint. The area where the ball chain is located is an extrusion of the ball chain, positioned deep enough so that the chain cannot escape or slip.



Figure 129: Fixed attachment on the palm for wrist extension and flexion

- Gear on the motor (Figure 130): This is the same principle as the attachment of the palm but it is designed with an axis that can be mounted on the axis of the motor and be bolted together.



Figure 130: Gear on the motor for wrist extension and flexion

- Tension mechanism (Figure 131): Because the chain has to be strained, we needed a design that would make it possible to position the cable correctly and to strain it afterwards. We designed a small beam with two holes for bolts and a special hole where the ball chain could clinch into. When both pieces are mounted onto each end of the chain, that is cut to the length of the outline of the mechanism minus two balls, it can be bolted together as tight as needed to put the strain onto the cable.



Figure 131: Tension mechanism used for the ball chain

- Guidance holes: These are introduced to guide the cable more safely. This is also visible on the left side of Figure 130.

8.5.7 Open design with lids

Both the arm and forearm have an open design to be able to connect and manage every motor and cable. We opted for a lid made out of clear polystyrene with a thickness of 2.5 millimeters to keep the weight low (a total mass of 66 grams) and to be able to spot problems inside the arm like cables that are fraying out or on the point of breaking. Obviously, it is also possible to print those lids in colored or clear PLA yourself instead of cutting out the shapes. The lids are held in place by bolts (M3, length of 10mm) that are screwed into holes of 3 millimeters.

8.5.8 Assembling the arm

As mentioned before, the assembly of all fingers and the palm of the hand does not require tools because they simply snap on each other. On the other hand, the two pieces of the palm are held together by three bolts (M3, length of 10 mm) and 3 nuts.

The two parts of the forearm, that had to be split because of the limited printing area, are held together by 9 pins by a tight fit and are extra secured by the aluminum frame that will connect the arm to the motors of the elbow, once this delivery will arrive.

The clear lids to close the arm and palm are also bolted together in the same way as the two parts of the palm are held together.

The motors are easily placed: the bottom part of the motor fits right into an extrusion of the forearm, while the sides of the motor are clamped between two walls. This way, the movement of the motors is prevented and they are still easily replaceable.

The fully assembled arm, without cable management, is pictured in Figure 132 (Inventor) and Figure 133 (finished product).

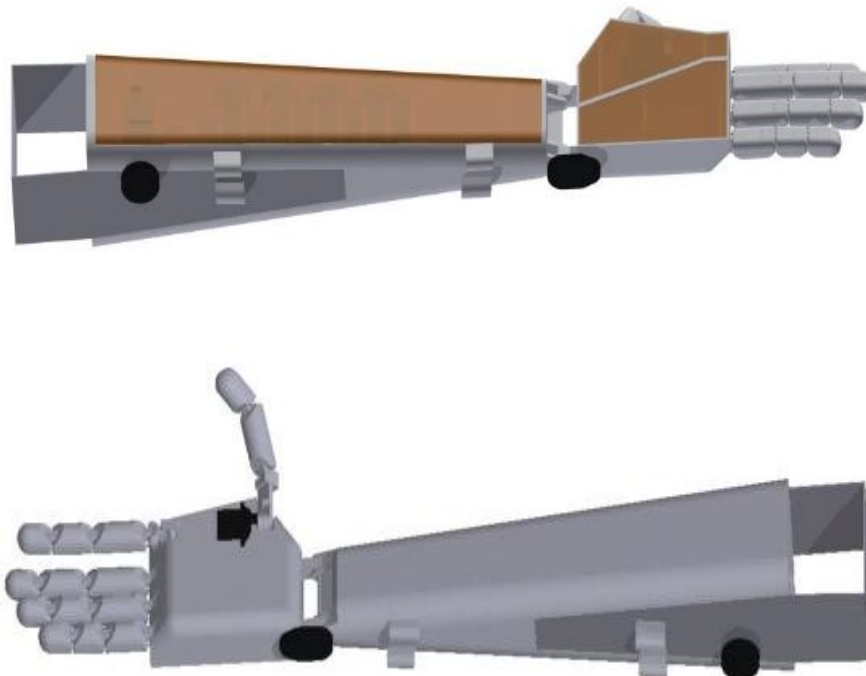


Figure 132: Fully assembled arm (Inventor rendering)

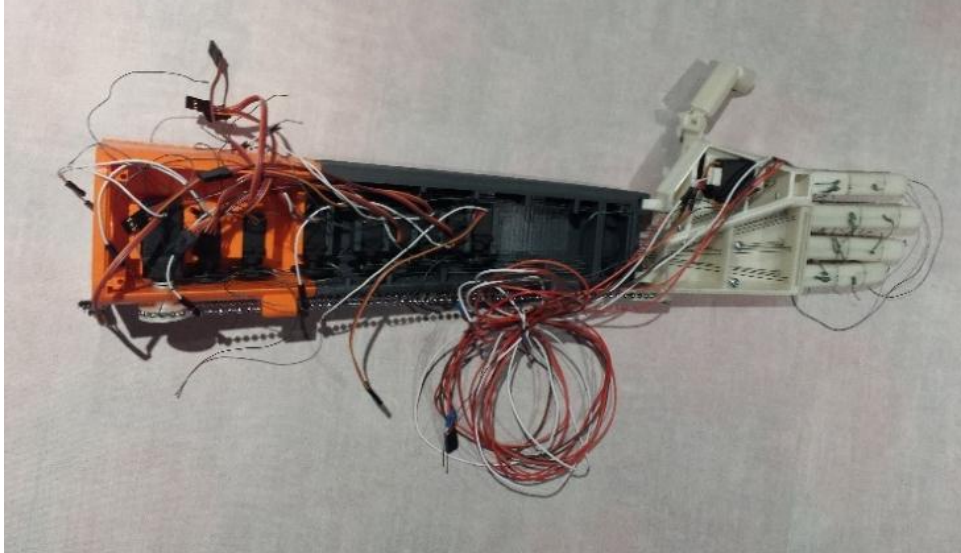


Figure 133: Fully assembled arm (Finished product)

8.6 SIMULATIONS

At the start of this academic year, while writing our thesis description, the plan was made to do a small strength analysis using Siemens NX to simulate deformations and stress.

While doing some research, it became more and more clear that this was not as straight forward as expected. 3D-printed parts (can) contain a special quadrangular infill structure, wall thickness, deformations, inaccuracies and a layered structure. This causes problems when importing Inventor-files or STEP-files into NX. It is possible to simulate and analyze everything but it will not resemble the reality. Drawings can be adapted by drawing the part again with correct wall thickness and the same quadrangular infill but it would take a lot of time.

If there is an adapted part with correct thickness and infill, the results will come closer to the real situation but the biggest problem (the layered structure) is still present. If a force is placed perpendicular onto all layers, the weakest link will be the connection between two layers, where it would break when the force is great enough. This weak spot is hard to simulate because it is influenced by a lot of factors like printing temperature, cooling time and fan speed. On top of that, from experience we know that 3D-printing will never be 100 percent accurate and misprints can easily decrease the strength of the part.

The 21th of April 2015, an external expert of CAE in Siemens NX, Christophe Vandeveld, came to the university to give a lecture about computer aided engineering. After the lecture, I discussed my problem with him and he confirmed the impossibility to analyze a 3D-printed part correctly but he was able to tell me that they are working on plugins to approach the stress analysis results of 3D-printed parts in Siemens NX.

8.7 CONCLUSION

While adapting some existing ideas and adding our own innovations, we were able to create a good looking and working robotic arm. We are very pleased with the outcome of the drawings: all of the goals that were set at the beginning of the project are completed and we were able to deliver a strong product that however can be optimized over the next years.

The robotic hand is able to form all the gestures of the Flemish Sign Language alphabet, is quite easy to assemble and is lightweight. So the main goals of the design are achieved.

9 System architecture and programming

9.1 INTRODUCTION

Guy Fierens - When designing a robotic system, which can become quite complex, it is important to maintain a certain structure or architecture. In this context architecture can be defined as: “The division of a system into subsystems and the interactions between these subsystems”. [10] The main advantages of designing a robotic system with a certain, well-conceived structure are: an increased understandability, facilitates the testing of the different subsystems and an increased reusability of functions called on different moments in the program.

The following chapter will discuss the design and choice of the different subsystems in the Aslan robot. In a first part, the general construction of the system and the division into subsystems will be handled. Then the VGT (Flemish Sign Language) will be analyzed in terms of movement timing and in terms to reduce the number of different movements.

9.2 GENERAL SYSTEM ARCHITECTURE

Figure 134 shows the general setup of our system. As we can see the system can be divided into three main parts: an input part, a processing part and a controlling part. The diagram only shows the complete flow for the thumb in order to keep the diagram clean. It is clear that for the other joints, the diagram follows the same steps.

The input part will consist of keyboard-input in an initial part of the project. In the future this way of obtaining input can be changed into e.g. speech recognition or visual analysis to interact more with the other communication partner (i.e. a person who communicates with the robot using sign language). The inputs will then be processed in order for further use in the program. Initially, the letters from the keyboard will be used to select the right gesture.

Selecting the right gesture will happen in the processing part of the system. Each symbol the user enters with the keyboard will be forwarded to the processing part. Here, the letter or number entered will be translated into a set of commands to move the joints to the right position. The commands used in the processing parts will be a set of functions written to move specific joints (e.g. a function specifically written to move the thumb). Using these functions, we are able to easily identify which joints need to be moved to show a certain gesture. By then adding an extra variable to the finger-movement function, it becomes possible to move all four fingers using only one function. On their turn, these functions will consist of a number of possible joint positions. (Figure 135)

A disadvantage of programming every movement in these functions is that the physical movement of the robot becomes sequential. Every movement function will start an average of 100 ms later than the last. The global movement of the robot therefore becomes less natural. An alternative of programming with functions would be programming every gesture separately, creating the advantage of a more natural movement because the command to move the servo motors will be sent simultaneously. This however will make the program much longer and less surveyable.

Finally the controlling part will monitor two important variables: on the one hand the size of the movement error ϵ , which is the difference of the desired joint angle Θ and the measured joint angle Θ_s . And on the other hand the time it takes to reach a certain position. If one of these two factors exceed a certain predefined value, the robot will go into a stop mode triggering an alarm. The measured joint angle Θ_s is obtained converting position feedback data to joint angles.

This conversion happens on the basis of a calibration of the joint angles in relation to the position feedback during the first usage of the robot. When off course both variables do not exceed the predefined value, the program will start to execute the next gesture after a hold-time t_h wherein the robot keeps the current gesture position.

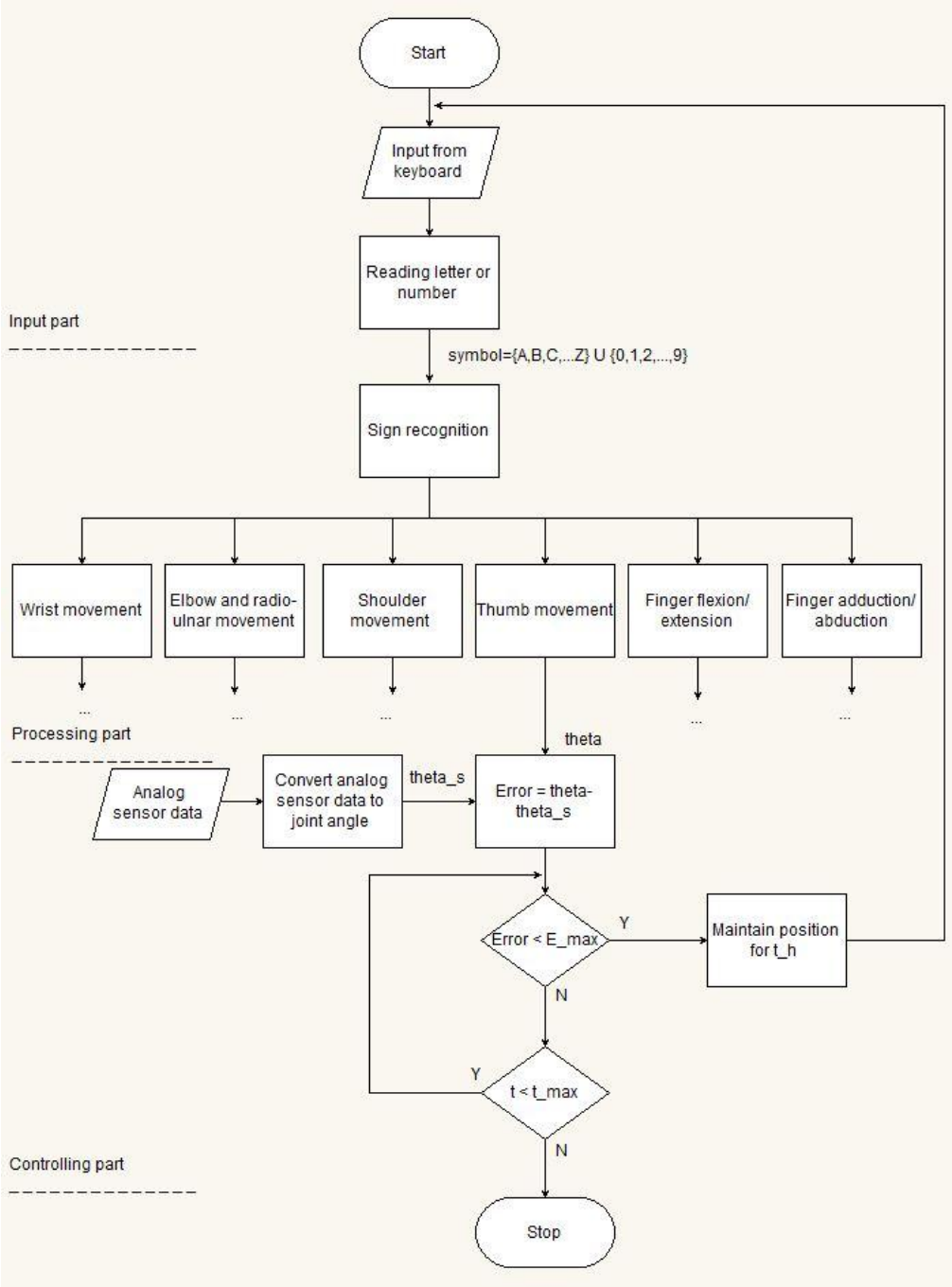


Figure 134: General system architecture

```

#define index 1;    // Assign each finger to an integer value
#define pointer 2; ...
void setup() {
    // put your setup code here, to run once:
}
void loop() {
    // put your main code here, to run repeatedly:
    char symbol = readSymbol();    // Read a character from the keyboard.

    switch (symbol){
        case 'A':                // Double switch command, to eliminate case sensitivity
        case 'a':
            wrist(1);            // Move the wrist to position 1
            thumb(4);            // Move the thumb to position 4
            finger(index, 3);    // Move the index finger to position 3 (flexion or extension)
            finger(little, 1);   // Move the little finger to position 1
            indexAa(2);          // Abduct or adduct the index finger to position 2
            break;               // Terminate the switch command
        case 'B':
        case 'b':
            ...
    }
}

char readSymbol(){
    // Read a character from the keyboard.
    ...
}

void finger(int finger, int jointPosition){
    if(finger==1){ //If the index needs to be moved
        switch(jointPosition){
            case 1:
                servo_angle(servo_pin, angle); //Move every servo actuating the index in the necessary angle
                ...
                break;
            case 2:
                ...
        }
    }
    else if(finger==2) { // If the pointer needs to be moved
        switch(jointPosition){
            case 1:
                ...
        }
    }
    ...
}

```

Figure 135: Program example

9.3 FLEMISH SIGN LANGUAGE

As we've learned from Chapter 3 that the Flemish sign language (VGT) has a quite complex structure. In order to translate the different gestures into the simplest possible program, the following paragraph will analyze the VGT regarding two subjects: movement timing and the decomposition of the gestures in a small number of sub-movements.

9.3.1 Movement timing

With the movement timing, we mean the amount of time it takes to complete the following sequence:

- Move each joint to a certain position in a maximum time of t_m
- Keep the joints in this position during a time t_h

The total time it takes to execute and show a certain gesture is therefore $t_m + t_h$. However in reality, this time can differ. Some people prefer spelling words fast while others rather take their time to clearly transmit their message. [62]

Because of this timing subjectivity, we made a well-considered choice to fix both times t_h and t_m at one second. This way, we create enough time to move to a certain position and give the receptor (person watching the gestures) enough time to analyze and determine the gesture.

9.3.2 Gesture decomposition

In Annex 18, each letter as well as each number is converted into joint angles for each joint of the upper extremity. Joint angles that can be chosen freely are left open.

In order to analyze these three tables properly, we have to make a few assumptions:

- The finger movements will be split up into two general functions: a function for flexion and extension of the fingers, and a function for the adduction and abduction of the index finger. The function for flexion/extension will carry two variables, while the function for adduction/abduction only needs one. The first variable of the flexion/extension function, and the only variable of the abduction/adduction function, will be the position the finger needs to move to. The second variable in the flexion/extension function will describe which finger needs to move. (Figure 135)
- The movement of the thumb, wrist, shoulder and elbow will each have its own function. This means that for the elbow the elbow joint and the radio-ulnar joint will be combined into a single function.

As we can conclude we can decompose every symbol into the number of positions shown in Table 28. These joint angles are ranked in their respective tables in Annex 19.

Table 28: Number of positions for each function

Function	Number of positions	Marked in
Finger flexion/extension	12	Yellow
Finger adduction/abduction	4	Green
Thumb	14	Blue
Wrist	3	Red
Elbow	7	Purple
Shoulder	4	Grey

9.4 SOFTWARE SAFETY

As we mentioned before, the software safety of the robot will consist of two major parts working together: a part that checks the amplitude of the movement error ϵ and a part that checks the time necessary to reach a certain position. When either the maximum error ϵ_{max} or the maximum time t_m is exceeded, the robot will go into a stop mode, triggering an alarm. A manual or software reset will put the robot back in its normal functioning mode.

The two parts will work together in order to provide a maximum safety. When the movement starts, the timer as well as the movement error function will start monitoring. Only if the robot reaches its desired position in a reasonable time, the next gesture can be executed. If however only the maximum time is reached before reaching the desired position, the robot will stop the current process. (Figure 134)

As we can see in Figure 134, every function we have defined, has its own timer and position monitoring. Each of these safety systems individually can trigger the stop mode. For structural reasons, the mentioned functions will be called in the respective movement functions.

9.5 PROGRAMMING

9.5.1 List of used symbols

...control	Suffix of integer value used to write variables to the servo motors control register. Prefix of the variable is one of the before mentioned joint indices.
...position	Suffix of integer value used to write variables to the servo motors position register. Prefix of the variable is one of the before mentioned joint indices.
abduction(int pos) address	Function for the abduction of the index finger Integer value to describe which servo driver needs to be accessed
elbow(int pos)	Function for the two DOF movement of the elbow
finger	Integer value describing which finger needs to be moved.
finger(int finger, int pos)	Finger movement function, first variable describing the finger that needs to be moved while the second variable defines the position.
l	Integer length of spell.
pos	Integer value describing the position.
Register	Register value to write variables to a servo Driver
shoulder(int pos)	Function for the simplified shoulder movement
spell	String variable entered with the keyboard.
symbol[l]	Spell converted to an array of characters.
thumb(int pos)	Movement function for the thumb.
Value	Value used to send to the servo driver
wrist(int pos)	Movement function for the thumb.
WriteRegister(int address, byte Register, byte Value)	Function to write variables to the different servo drivers.

9.5.2 Programming log

For the programming of the robot, a lot of different versions of software have been used and tested. All these different versions and their respective contents have been logged in Annex 20. The reader is referred to Annex 20 in order to review the software development progress.

9.5.3 Programming with the Designer Systems DS-DSX18.S servo driver

Initial testing of the code in combination with the physical setup showed a couple of problems regarding the control and movability of the servo motors. The Batan S1123 micro servo motors not only seem to have a limited movability of 150° instead of 180°, but also do not always react and move as desired.

In order to resolve these issues, a number of experiments have been conducted, which can be found in Annex 24 and Annex 25.

As a result of these experiments, a new thesis topic has been defined. To resolve not only the limited movability of the chosen micro servo motors, but also to simplify the robot's controls, the feedback potentiometers can be mounted directly on the driven joint. This way, the effect of the movement of proximal joints referenced to a specific joint becomes negligible. In the current design e.g. the movement of the wrist joint will also move the tendons responsible for finger movement. By mounting the feedback potentiometer directly on the joint, the servo motor will keep moving until the desired joint angle is reached. This however might imply the need of removing the mechanical constraint responsible for the limited movement range of 180°.

9.6 CONCLUSION

As we learned in this chapter, the software of the Aslan robot will become quite complex. A lot of different functions need to be combined with the different servo drivers. An additional difficulty is the calibration of each servo individually, making each servo motor in the system unique and disabling the possibility of simply replacing motors by other motors.

10 Electrical design

10.1 INTRODUCTION

Guy Fierens - The hardware design of the robot is at least as important as the software design. The selection of the right components in combination with their correct placement in the system is key to making the robot work.

This chapter will discuss the design of the electrical hardware of the robot. All the key parts will be selected and the electrical schematics will be discussed regarding the fuses, connectors and heat dissipation of the components.

10.2 COMPONENTS

10.2.1 Microcontroller

The main processing part of the robot will be the microcontroller. This component is responsible for analyzing and processing the data. Every input, either coming from the user or the sensors inside the robot, will be processed by this component.

In the last few years, a lot of new companies and open source projects have been started all over the world. A few examples are the Raspberry Pi foundation¹⁷, Arduino¹⁸, Udoo¹⁹, and the Galileo projects from Intel²⁰. These companies all offer their own microcontroller platform to control different kind of projects.

The requirements the microcontroller needs in our application are a large available number of analog inputs, I²C communication available, a large available memory and a good usability/availability. Ten different microcontroller models from different manufacturers have been compared in order to choose the most compatible controller for our application.

In Annex 21.2 each of these models have been compared using 'Analytic hierarchy process' in combination with Saaty's scale of relative importance to determine the best option. As a result of this analysis, the Arduino Due has been selected. Although this model has only a small advantage of 2.6% compared to the second best model (Arduino Mega 2560), we will choose the Due.

Since the Arduino does not offer a technical data sheet, a brief summary of all relevant specifications is listed in Table 29. [63]

¹⁷ <http://www.raspberrypi.org/>

¹⁸ <http://arduino.cc/>

¹⁹ <https://www.udoo.org/>

²⁰ <http://www.intel.com/content/www/us/en/do-it-yourself/galileo-maker-quark-board.html>

Table 29: Arduino Due specifications

Specification	Value
Operating voltage	3.3VDC
Recommended input voltage	7-12VDC
Digital input/output pins	54, of which 12 provide PWM output
Analog input pins	12
Total DC output current on all I/O lines	130mA
DC Current for 3.3V/5V pin	800mA
Flash memory	512kB
SRAM	96kB
Power supply connection	2.1mm center-positive plug
Programming connection	Micro USB

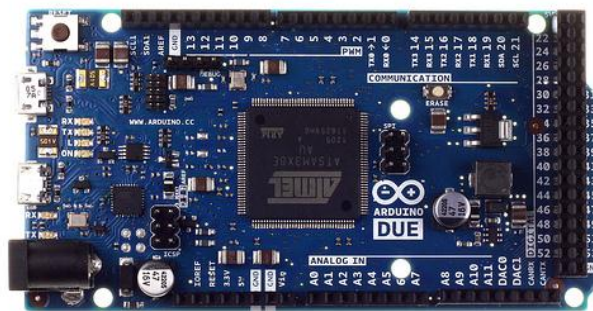


Figure 136: Arduino Due [63]

10.2.2 Servo controller

Using the same decision analysis as used to define the best option for the microcontroller, a servo controller to control the 5V RC servos has been chosen. Four different models have been compared on the following requirements:

- 5V Supply voltage,
- I²C available,
- compatibility with Arduino,
- good availability and usability,
- large number of servo motors per device.

The analysis showed the best option for these demands was the DS-SCX18.S servo controller from Designer systems (performed as in Annex 21.2). This model has an advantage of 32.8% compared to the closest following model. A datasheet of this component can be found in Annex 22.1



Figure 137: Designer Systems DS-SCX18.5 [designersystems.co.uk]

10.2.3 Stabilized power supply

To power the two components mentioned before we need a stabilized 5V power supply. The only requirements this power supply needs, are:

- Input voltage: 230VAC,
- output voltage: 5VDC,
- maximum output current sufficient to power the robot in the current version, as well as with expansions in the future.

Because of these limited amount of requirements needed to choose a power supply, a decision analysis has not been performed. A power supply from TDK Lambda, type LS100-5 has been selected to power the robot. This model can deliver a maximum output current of 16A, has a good availability and is low cost compared to other models.

The technical datasheet of the TDK Lambda LS100-5 can be found in Annex 22.2



Figure 138: TDK Lambda LS 100-5 [us.tdk-lambda.com]

10.2.4 Servo motors and position feedback

Since the position feedback has already been discussed in paragraph 6.3, we do not have to discuss this component in this chapter. For completeness however, we also mention this component in this part of this work.

The technical datasheet of the 8-channel multiplexer chip CD74HCT4015E from Texas Instruments can be found in Annex 22.3.

10.3 PRACTICAL REALISATION OF THE I²C NETWORK

Building on the theoretical background given in paragraph 6.2, a practical realization of an I²C network with one master and three slaves needs to be made. This implies the correct wiring of the component and the addressing of each slave separately.

The wiring of the I²C-network is limited to connecting the four wires SDA, SCL, V_{ref} and GND according to Figure 66. Every component needs to be connected parallel relative to the other components, meaning that every component's SDA-wire needs to be connected to each other, as well as the SCL, V_{ref} and GND wires of the components need to be connected to the other components respective wires.

The I²C-addresses of the different servo drivers are set using the two address jumpers on the respective boards. The I²C addresses of the different servo drivers are set to:

- 0x74 for the first Designer Systems DS-SCX18.S
- 0x75 for the second Designer Systems DS-SCX18.S
- 0x76 for the third Designer Systems DS-SCX18.S

Regarding the heat dissipation of the servo drivers, three servo drivers needed to be purchased, as mentioned in paragraph 10.4.2

To provide the source current necessary for I²C-communication, only one of the four network devices needs to provide pull-up resistors. The pull-up resistors of the third servo driver are enabled using the two jumpers on the board.

10.4 ELECTRICAL DESIGN

10.4.1 Fuses

The fuse ratings used in the electrical design are derived from the datasheets of the respective components. Table 30 shows the fuse ratings for the different components.

Table 30: Fuse ratings

Component	Fuse
Power Supply TDK Lambda LS 100-5	F4A, 250V
Arduino Due	T0.8A, 250V
Servo controller DS-SCX18.S	F4A, 250V
Sunon cooling fan	T0.2A,250V

Since Annex 22 only contains the relevant component data, the datasheet for the power supply is a brief selection of the product catalog of TDK-Lambda. Since the selected pages did not cover the external fuse rating, Figure 139 shows the part of the catalog regarding fuse ratings.

Refer to the following fuse rating when selecting the external input fuse. Surge current flows when input turns on. Fuse rating is specified by Inrush Current value at input turn on. Do not select the fuse according to input current (rms) values under the actual load condition.

LS25	:	F1.6A , 250V
LS35, LS50	:	T2A , 250V
LS75	:	T2.5A, 250V
LS100	:	F4A, 250V
LS150	:	F5A, 250V

Figure 139: Power supply external fuse rating [64]

10.4.2 Heat dissipation

According to the component datasheets in Annex 22, the following operating temperatures can be found:

Table 31: Component operating temperatures

Component	Operating temperature
TDK-Lambda LS 100-5 Power Supply	-25 to 70°C
Designer Systems DS-SCX18.S Servo Driver	0 to 70°C
Arduino Due	Not available
Texas Instruments CD74HCT4051E	-55 to 125°C

As we can conclude from Table 31, the absolute maximum temperature as well as the absolute minimum temperature is determined by the servo driver from Designer Systems. A relative maximum temperature can also be defined. The datasheet of the LS 100-5 power supply states in the output derating curve that a maximum temperature of 45°C should be maintained.

Initial testing of the robot prototype showed that the servo driver is sensitive to overheating. To relieve the driver, two other drivers will be purchased in order to distribute the load. This will lead to less heat dissipation. In cooperation with two cooling fans, the problem of overheating should be solved.

To create the necessary airflow, two two-wire cooling fans with a supply voltage of 5VDC can be used. Since the amplitude of airflow is not a key feature in the cooling process, two standard fans have been selected. The Sunon fans selected, deliver an airflow of approximately 11.89 m³/h at a power consumption of only 0.9W. An extraction of the datasheet, describing the relevant specifications can be found in Annex 22.

10.4.3 Connectors

In order to easily transport the robot, the casing (or torso of the robot) and the robot arm are designed to be taken apart. To be able to do this without too much effort from the user, the torso will be designed including a couple of connectors.

Essentially, the robot only needs to have only 3 connectors: one to connect the electrical system to the grid, one to connect the microcontroller to a computer and one to connect the arm to the torso. This last one will need to have a lot of contacts in order to connect every motor and sensor in the arm to the torso.

The first connector, connecting the robot to the grid with a 3G1.5 electrical wire needs to have 3 contacts. The standard IEC 60320 describes the connectors for connecting power supply wires to a grid up to 250VAC. The standard states that for a maximum current of 10A, a C13/C14 or C15/C16 connector can be used. Where the lowest number of the two is the female or the appliance part while the higher, even number is the male, plug part. Since C13/C14 and C15/C16 are compatible with each other, a combination of the two is possible (Figure 140). The robot will feature a C16 male plug connector and a C13 female appliance connector. The connector will also feature an on/off-switch in combination with a 10A fuse. Keeping in mind the maximum ratings of the connector, a 10A fuse is necessary. At the moment this is a too large fuse rating, but it could become necessary in the future. Since the fuse mounting is already implemented in the switch, the fuse holder will house the 4A fuse for the 5VDC power supply.

Mating Appliance Coupler IEC60320-1					Appliance Inlets														
					Gender Male														
					Symbol														
					Type	C6	C8	C8p	C10	C14	C16	C16A	C18	C20	C22	C24			
					Current [A]	2.5	2.5	2.5	6	10	10	10	10	16	16	16			
					Temperature [°C]	70	70	70	70	70	120	155	70	70	155	70			
					Protection classe	1	2	2	2	1	1	1	2	1	1	2			
IEC60320 Connectors	Gender Female	Symbol	Type	Current [A]	Temperature [°C]	Protection classe													
			C5	2.5	70	1	•												
			C7	2.5	70	2		•											
			C7p	2.5	70	2			•										
			C9	6	70	2				•									
			C13	10	70	1					•			□					
			C15	10	120	1					□	•		□					
			C15A	10	155	1					□	□	•	□					
			C17	10	70	2									•				
			C19	16	70	1										•			□
			C21	16	155	1											•	•	•
			C23	16	70	2													•

Figure 140: IEC60320 mating [Schurter.com]

The key requirement of the second connector is the large amount of contacts needed. For the 16 motors used in the hand and wrist we need at least $16 \times 3 = 48$ contacts in the connector. When we add $16 + 1 = 17$ cables for the position feedback this leads to a total of 65 contacts necessary. The closest amount of contacts on available industrial connectors however are 44 or 70 contacts. This creates 3 options:

1. One connector of 44 contacts and one connector of at least 20 contacts
2. two connectors of 44 contacts,
3. one connector with 70 contacts.

With the purpose of expanding the robot with extra sensors and motors, a connector with 70 contacts has been chosen. By using a single connector, we minimize the chance the user connects the robot arm incorrectly and in the same time decrease the assembly time.

The third connector is the micro USB port to program the Arduino microcontroller. Since the dimensions of this connector are according to the USB standard, any micro USB connector will suffice.

10.5 CASING DESIGN

Every previously defined component has to be integrated in a ready-to-go system. The components have to be connected in a rigid casing. The casing can be connected to the grid or the robot arm using the connectors defined in paragraph 10.4.3.

As mentioned above, the casing has to be easy-to-go, but since the robot is a prototype, it has to be easy to dismount and well structured. This has to simplify the modification of the system.

In the physical realization of the electrical schematics in Annex 23, the components have to be arranged in a way that the connections between the components are logical and do not contain unnecessary long cables. Keeping in mind the following extra, often component related, requirements:

- The LS 100-5 power supply is best mounted horizontally, with the PCB on the downside, enabling heat to dissipate through the holes in the topside.
- A minimum distance of 15mm should be kept between the power supply and the peripheral parts.
- The grid connector should be in a direct line with the power supply, this way the power wires do not have to cross any other components.
- The servo drivers should be in a direct line to the connector with 70 contacts. The maximum of 70 wires connecting these two components should be easy accessible and not cover any other component.
- The servo drivers should not be mounted on top of the Arduino Due. Although this is a possibility, the servo driver should be mounted separately in order to easily implement other servo drivers when the robot is expanded.
- The analog inputs of the Arduino Due should be direct in line with the 70 contacts connector and the multiplexer.
- A central “I²C-hub” needs to be installed. Since every component on the I²C-network needs to be connected parallel regarding the other components, a combination of four connection rails needs to be installed.

As a casing, an installation housing will be used. This offers a clean and solid casing with mounting points for the components. The components themselves will be mounted on a mounting plate. By mounting the components on a plate, the mounting can be done outside the housing. When all of the components are in place, and partially wired, the plate itself can be mounted inside the housing for further wiring.

To make the connections with the servo driver, female header pins can be used. These female headers can be simply plugged onto the right contact. This simplifies modifications of the dismounting of the installation. By adding wire tags, the wires can easily be identified.

Figure 141 illustrates the practical organization of the components inside the casing. Numbered from zero to eight:

- (0) Arduino Due
- (1) Designer Systems DS-SCX18.S Servo driver
- (2) Designer Systems DS-SCX18.S Servo driver
- (3) Designer Systems DS-SCX18.S Servo driver
- (4) TDK Lambda 5VDC Power Supply
- (5) I²C-hub
- (6) On/off-switch
- (7) Cooling fan
- (8) 70p-connector

To obtain a clear overview of the installation, the 70p-connector has been dismantled.

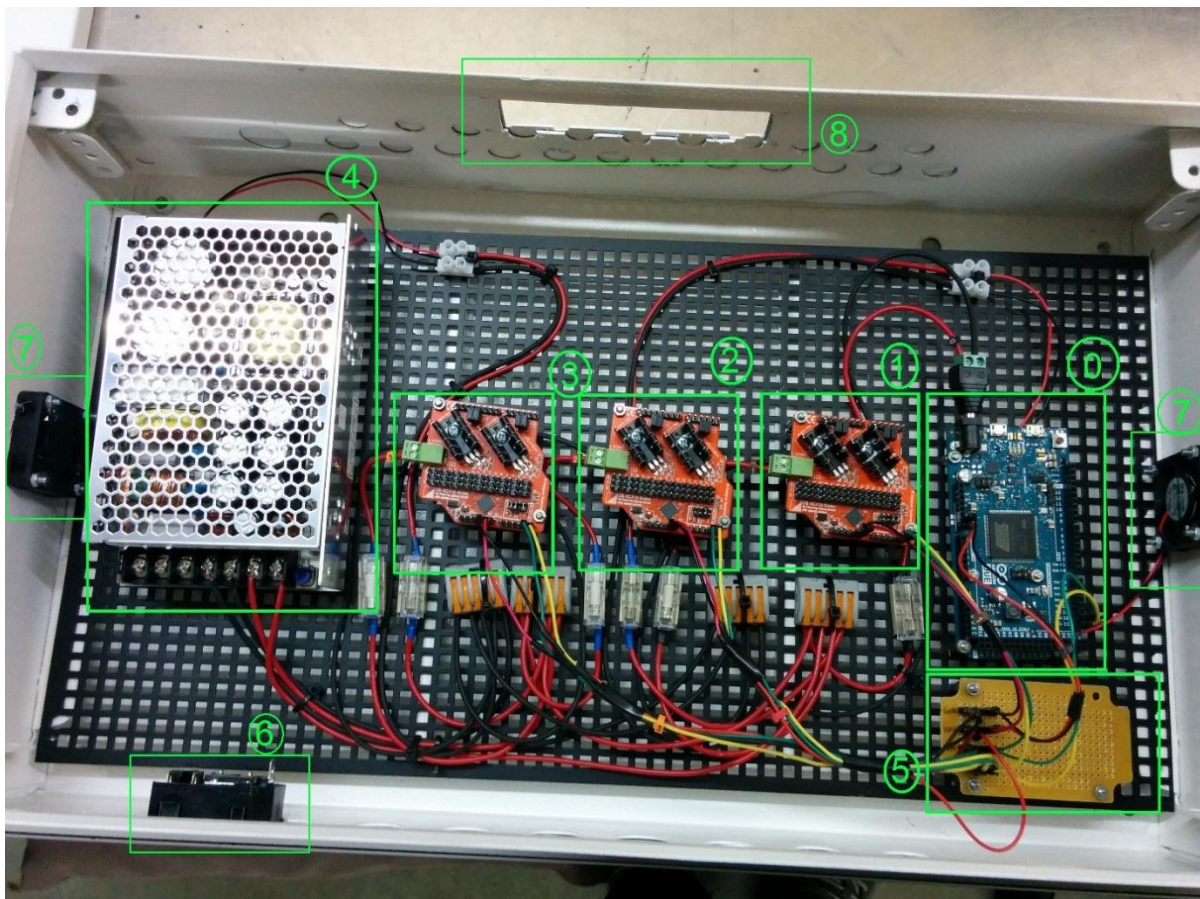


Figure 141: Organization of the components

10.6 SERVO MOTOR DISTRIBUTION

To distribute the load, the 16 different servo motors need to be divided among the three different drivers. This to minimize the heat dissipation in the voltage regulators of the drivers, as mentioned in paragraph 10.4.2.

Table 32 describes all relevant data for the mounting and use of the servo motors. The order of the servo drivers is described in Figure 141, the registers are as stated in the DS-SCX18.S datasheet in Annex 22.1. The cable number is mentioned to clarify the wire tags in the practical installation.

Table 32: Servo motor distribution

Servo motor for the movement of:	Mounted on driver number:	Registers used:	Cable number:
Little finger MCP	1	R1 and R2	1
Little finger PIP	1	R3 and R4	2
Ring finger MCP	1	R5 and R6	3
Ring finger PIP	1	R7 and R8	4
Middle finger MCP	1	R9 and R10	5
Middle finger PIP	1	R11 and R12	6
Index finger MCP flexion and extension	1	R13 and R14	7
Index finger PIP	1	R15 and R16	8
Index finger MCP abduction and adduction	2	R1 and R2	9
Thumb TMC abduction and adduction	2	R3 and R4	10
Thumb MCP flexion and extension	2	R5 and R6	11
Thumb IP	2	R7 and R8	12
Wrist flexion and extension	2	R9 and R10	13
Radio ulnar joint	3	R1 and R2	14
Elbow flexion and extension	3	R3 and R4	15
Shoulder abduction and adduction (moved to the elbow)	3	R5 and R6	16

10.7 CONCLUSION

By analyzing and discussing every single component used in the Aslan robot and the interaction between the different components an installation has been designed optimal for prototyping as well as using the robot.

11 Organization of the project

11.1 INTRODUCTION

Since this is a completely new project for the University of Antwerp, a lot of arrangements had to be made in order to make the physical realization of the robot a possibility. The organization of the project has been a time-consuming part of the project, and is therefore definitely worth mentioning in this paper.

The following chapter will discuss every aspect of the organization. This includes the search for sponsorship, the determination of the necessary budget, naming the project, PR,... Every member of the team has done his part in making this project work, and in order to distinguish which member was responsible for which part each paragraph will mention the respective team member(s).

11.2 NAMING THE PROJECT

11.2.1 Naming the project

Guy Fierens, Stijn Huys, Jasper Slaets – The name of this project needed to be short and sweet. A short, meaningful name that is easy to remember for anyone who hears it. To pick the perfect name for the robot, a lot of options have been compared.

The name we eventually have chosen is Aslan, which is an abbreviation for “Antwerp Sign Language Actuator Node”. The full name of the robot explains its purpose, we have developed a robot or actuator which can perform Flemish sign language as a part of the regular communication between sender (speaking person) and receiver (deaf person). The name Aslan is not only chosen in function of its abbreviation, but more importantly because of its two other meanings.

The first, and most important one is that Aslan is Turkish for ‘lion’ and therefore a symbol of strength and wisdom. Secondly, this is amplified by the movie series Narnia from Waldon Media, where the lion Aslan is one of the main characters. Since these movies are known by a lot of people, Aslan will be a name that will be easier remembered because of these associations people can make.

11.2.2 Designing a logo

Stijn Huys - The logo of Project Aslan (Figure 142) is designed using Adobe Photoshop and is based on three basic elements: A lion, the name of the project and a gear. The lion is chosen because Aslan means lion in Turkish and the gear resembles our studies in engineering.



Figure 142: The logo of Project Aslan

11.3 DETERMINATION OF THE BUDGET

Guy Fierens – Setting up a new project, one of the most important things to do is making a budget estimation. With this estimation, a search for funding can be started. The estimation however needs to be as accurate as possible, since a wrong estimation can either lead to an insufficient amount of money or a lack of interest of possible sponsors when the estimation is too high.

The result of the budget estimation is €4.000,- with the purchase of a €2.300,- 3D-printer included, necessary to build the Aslan robot.

11.4 SPONSORSHIP

11.4.1 Finding a sponsor

Guy Fierens, Stijn Huys – To obtain the funding necessary for designing and building the Aslan robot, a number of options were available of which crowdfunding and sponsorship were the two most important ones. Because sponsorship also brings a lot of immaterial benefits for both the sponsor and the project, we opted for a sponsorship.

After a long search and after contacting a lot of firms active in a relative sector, we met Joost Van Dinther. A surgeon at the otorhinolaryngology department of the Sint-Augustinus hospital in Antwerp with a lot of faith in the project and in the message we bring. After a presentation for dr. Van Dinther and his colleagues at the hospital, a cooperation was born between us (the university) and the ‘European Institute for Otorhinolaryngology – Head & Neck surgery’ of which dr. Van Dinther is a part.

11.4.2 About our sponsor

“The department of ENT at the Sint-Augustinus hospital, founded by the late professor Jean Marquet MD as a university department, has been renamed in 2012 to the European Institute for Otorhinolaryngology - Head & Neck Surgery. This modification was partly carried out to make the name align more with the reality, which is a centre for Otorhinolaryngology – Neck and face surgery with four major European colored pillars:

- Clinical care,
- scientific research,
- training,
- home of the European Secretariat of the World Federation of NKO (IFOS) and the European Academy of Otolology & Neurotology (EAONO).

“ – NKO Sint-Augustinus Antwerp²¹



Figure 143: European Institute for Otorhinolaryngology - Head & Neck Surgery logo

²¹ http://www.neus-keel-oor.be/nl/onze_dienst/historie/nieuwe_naam/

11.4.3 Sponsorship and contracts

Guy Fierens – Trying to define this newly born cooperation, contracts had to be made between the University and the sponsor. Unfortunately, a sponsorship template for student-founded projects is not yet available at the University. Therefore, a custom made contract had to be made in collaboration with the university's legal department.

As this is a very time consuming and complex procedure, another solution had to be provided in order to start the physical realization of the robot in time. By applying for an internship at the 'European Institute for Otorhinolaryngology – Head & Neck surgery' with a standard internship contract, a solution was found in time to start the production.

11.4.4 Planning of our time in the Skillslab

Guy Fierens – In the Skillslab²², the research facility of the sponsor we are able to design and produce the robot in a quiet and peaceful setting. Working together in the lab proved to be a useful tool in designing the robot. Instead of working separately and comparing results, each team member designed his part in a close cooperation with his colleagues, leading to a more qualitative global design.

The time spent in the Skillslab however, had to be planned carefully, taking into account the students course schedules and the planned activities in the Skillslab. Merging these two together lead to a schedule which enables us to plan and reserve our time in the Skillslab.

11.4.5 Sponsoring by Trideus

Stijn Huys - When buying our 3D-printer at Trideus, we explained the purpose of the printer and the project. Being very interested, the boss of the company, Jesse Buteneers, offered us 100 euros of filament to fund our project.

11.5 PUBLIC RELATIONS

11.5.1 Website

Guy Fierens – To make the project public, a website is designed containing information about the progress, the sponsor and the team members. People with interests in the project are able to get a clear view of the project, with the possibility of leaving a message if they have a question about something.

To address a broader public, the website is written in a Dutch, as well as an English version.

The website can be accessed via the following URL: www.projectaslan.be

11.5.1.1 Webhosting

A webhosting package with domain name has been provided by PC Grafix.²³

11.5.1.2 Website design

As mentioned before, the website is available in two languages. A user-friendly website design has been created in two steps. A first version of the website has been designed by Guy Fierens. The second version is designed in cooperation with Felix Rijkers from Twinlabs. The first version of the website can be found in the digital portfolio, the second version can be viewed online.

²² <http://www.skillslab-antwerpen.be/>

²³ www.pcgrafix.be

11.5.1.3 Email addresses

Using the domain name 'projectaslan.be', four email addresses have been made. One email address for each team member forwarding the emails received to their respective email addresses of the University of Antwerp. This email address can be used in email signatures, leading to a more professional and independent image of the project.

The fourth email address is info@projectaslan.be, an email address visitors of the website can use to ask questions. The mails sent to this email address are forwarded to the email address of Guy Fierens.

11.5.2 Demo model at the open house

Guy Fierens, Stijn Huys, Jasper Slaets – When the university asked us to deliver a demo of our project to show during the open houses, we designed a set-up where one finger was actuated for constantly extending and flexing. This was exposed together with a Powerpoint presentation giving some more information about the project and our sponsor.

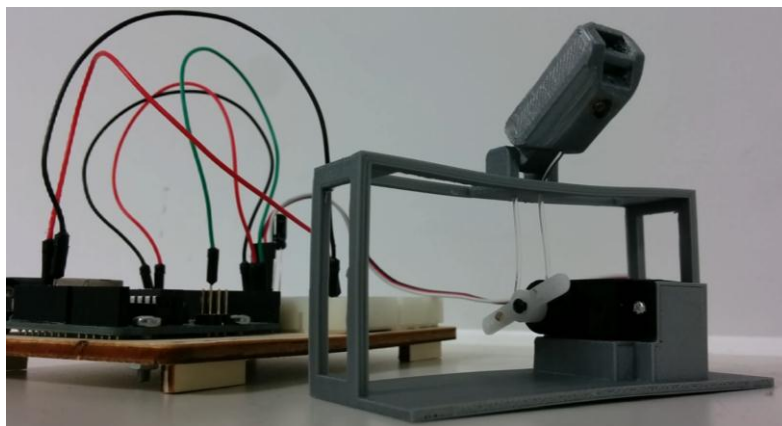


Figure 144: Demo set-up shown at the open house

11.6 PLACING/TRACKING ORDERS AND FINANCIAL MATTERS

Guy Fierens – To simplify the communication between the sponsor and the team, only one of the team members received the responsibility controlling the financial matters of the project.

The financial aspect of the project consists of placing orders, updating and controlling the budget, problem solving regarding orders and paying orders in advance in case a payment term is not possible.

11.7 CONCLUSION

As shown in this chapter, the organization and set up of a new project can be a very time consuming activity. A lot of aspects and actions have to be taken into account in order to make the physical realization of the robot a possibility. To distribute the workload, each team member has done his part in the organization of the project.

Conclusion

Evaluating the Aslan Project in its current state and regarding the preset goals of creating a robot that is easy-to-assemble, affordable, easy-to-use and is able to spell the Flemish sign language alphabet in a natural way, we can conclude the following.

The preset goals were achieved. We were able to create an entire , humanoid robotic arm for less than 900 euros (Bill Of Materials can be found in Annex 26), 3D-printer not included. The 3D-printed arm, that can be printed within 140 hours using only one spool of filament, can be assembled within five minutes. The humanoid arm is able to perform all the required gestures with its custom built electronics and remote tendon actuation system.

The overall design can however be optimized regarding different topics. First of all, a more specific study regarding the tendons in the upper extremities will lead to a better understanding of the remote actuation of the human hand. This in order to create a more human-like design. Like the tendons in the hand, elastic fibers can be used. This implies however that additional position sensors, like the nerves in our hands are required since the movement will become non-linear.

The specific study of the tendons will lead to a better design considering the guidance of the cables of the thumb and index finger.

While the assembly of the 3D-printed parts is fairly easy, the connection and the calibration of the cables is not, which makes the product less accessible for the broad public.

As mentioned in Annex 24 and Annex 25, the Batan S1123 micro servo motors are not capable to deliver the required functions for our application. Combined with the sequentially programmed code, the robot's movements are less natural and smooth. With the planned expansion and adaptations of the current arm, the performed gestures will become more human-like due the newly written software.

To summarize, the current design can be optimized in a number of aspects.

In the last year, we were able to found a promising project thanks to teamwork and perseverance. Overall, we are satisfied with the progress we made considering the setback we had due to the long search for sponsorship.

Bibliography

- [1] A. Waugh, "Anatomie en fysiologie in gezondheid en ziekte," Edinburgh, Churchill-Livingstone Elsevier, 2006, pp. 383-425.
- [2] F. Waschke, Atlas van de menselijke anatomie, München: Elsevier GmbH, 2011.
- [3] M. Ferre, First prototype of hand model sufficient for mimicking realistic hand motions, Immersence, 2007.
- [4] W. Platzer, Atlas van de anatomie: bewegingsapparaat, Schoten: Uitgeverij Westland nv., 1988.
- [5] C. Welman, "Inverse kinematics and geometric constraints for articulated figure manipulation," British Columbia, Canada, Simon Fraser University, 1993, pp. 17-25.
- [6] R. Penne, "Projectieve meetkunde en mechanische toepassingen in het vlak," Antwerpen, Universiteit Antwerpen, 2013, pp. 2-12.
- [7] L. Barinka, Inverse kinematics - Basic methods, Praag: Czech Technical University.
- [8] S. Buss, "Introduction to inverse kinematics with jacobian transpose, pseudoinverse and damped least square methods," San Diego, University of California, 2009, pp. 3-6.
- [9] Caltech University, "The Moore-Penrose Pseudo Inverse," Caltech University, p. 3.
- [10] K. E. Siciliano, in *Springer handbook of robotics*, Berlin, Springer-Verlag, 2008, pp. 187-204.
- [11] K. J. De Laurentis and C. Mavroidis, "Mechanical design of a shape memory alloy actuated prosthetic hand".
- [12] K. J. Kim and S. Tadokoro, "Electroactive polymers for robotic applications," pp. 49-90, 2007.
- [13] F. Ficuciello, "Modelling and control for soft finger manipulation and human-robot interaction," November 2010.
- [14] W. Storr, "Basic Electronics Tutorials," 14 April 2015. [Online]. Available: http://www.electronics-tutorials.ws/io/io_7.html. [Accessed 16 April 2015].
- [15] R. Catthoor, Stepermotors, Hoboken: Universiteit Antwerpen, 2014.
- [16] T. Engdahl, "ePanorama.net," 2009. [Online]. Available: <http://www.epanorama.net/links/motorcontrol.html#related>.
- [17] D. W. Jones, "Control of Stepping Motors," 1998. [Online]. Available: <http://homepage.cs.uiowa.edu/~jones/step/>.
- [18] A. De Winter, Direct current machines, Hoboken: University of Antwerp, 2013.
- [19] P. Cools, Direct current motor, Hoboken: University of Antwerp, 2014.

- [20] Futaba, Digital FET servos, Futaba.
- [21] Adafruit, "RC servo motors," [Online]. Available: www.adafruit.com.
- [22] R. C. Hibbeler, Statica 12th edition, United States: Pearson Education, 2010.
- [23] J. Smet, Chemics and materials: Sythetic materials, Hoboken: Karel de Grote-Hogeschool, 2012.
- [24] W. Six, Research visco-elastic properties, Oostende, 2011.
- [25] Goodfellow, "Stainless steel," [Online]. Available: <http://www.goodfellow.com/E/Stainless-Steel-AISI-316.html>.
- [26] Goodfellow, "Nylon 6," [Online]. Available: <http://www.goodfellow.com/E/Polyamide-Nylon-6.html>.
- [27] Pelicanrope, "Dyneema," [Online]. Available: http://www.pelicanrope.com/pdfs2010/DYNEEMA_factsheet_UHMWPE.pdf.
- [28] R. C. Hibbeler, Mechanics of Materials, 8th edition, United States: Pearson Education, 2011.
- [29] C. S. Sava, "Mechanical cable construction," 2006. [Online]. Available: http://www.savacable.com/pages/wire_rope_construction.html.
- [30] NXP Semiconductors, I²C-bus specification and user manual, NXP Semiconductors N.V., 2014.
- [31] Philips Semiconductor, Philips Semiconductors I²C handbook, 2004.
- [32] Baldor Motors and Drives, Servo control facts, Arkansas, USA: Baldor Electric Company.
- [33] STMicroelectronics, AN2591 Microcontroller input/output expander, Switzerland: STMicroelectronics, 2007.
- [34] EMCO group, EMCO, [Online]. Available: <http://www.emco-world.com/en/products/industry/milling/cat/25/pr/linearmill-600.html>.
- [35] Materialise, "Stereolithography materials & datasheets," [Online]. Available: <http://manufacturing.materialise.com/stereolithography-materials-datasheets>. [Accessed 17 03 2015].
- [36] Solidsmack. [Online]. Available: <http://www.solidsmack.com/fabrication/stereolithography-110-micron-old-world-laboratories-nano-3d-printer/>.
- [37] Materialise, "Polyjet materials & datasheets," [Online]. Available: <http://manufacturing.materialise.com/materials-datasheets-polyjet>. [Accessed 17 03 2015].
- [38] CustomPartNet. [Online]. Available: <http://www.custompartnet.com/wu/jetted-photopolymer>.
- [39] LiveScience. [Online]. Available: <http://www.livescience.com/38862-selective-laser-sintering.html>.

- [40] CustomPartNet. [Online]. Available: <http://www.custompartnet.com/wu/fused-deposition-modeling>.
- [41] Ultimaker. [Online]. Available: <https://ultimaker.com/en/products/ultimaker-2-family/ultimaker-2>.
- [42] B. BEECREATIVE. [Online]. Available: <https://beeverycreative.com/beethefirst/>.
- [43] Biohazard Deltabot, [Online]. Available: <http://3dtiskanje.si/>.
- [44] Cubify. [Online]. Available: <http://cubify.com/cube>.
- [45] Makerbot. [Online]. Available: <https://www.makerbot.com/replicator>.
- [46] A. e. S. O. Federale Overheidsdienst Werkgelegenheid. [Online]. Available: <http://www.werk.belgie.be/defaultTab.aspx?id=609#AutoAncher0>.
- [47] A. Meshmixer. [Online]. Available: <http://www.meshmixer.com>.
- [48] V. K. a. E. T. Zhe Xu, "A Low-cost and Modular, 20-DOF Anthropomorphic Robotic Hand: Design, Actuation and Modeling," <http://homes.cs.washington.edu/~vikash/Projects/Finger/AnthromorphicRoboticHand%28humanoids13%29.pdf>.
- [49] W. C. S. N. N. Dechev, "Toronto Bloorview Macmillan (TBM) Hand (Multi-Fingered, Adaptive Grasp Prosthetic Hand: Better Function and Cosmesis)," <http://www.engr.uvic.ca/~mech350/Core-Files/SAMPLE-Presentation-%28TBM-Hand%29.pdf>.
- [50] DLR: Robotics and Mechatronics Center, [Online]. Available: http://www.dlr.de/rm/en/desktopdefault.aspx/tabid-5486/8995_read-16713/.
- [51] T. A. R. D. a. S. T. Naoki Fukaya, "Development of a Five-Finger Dexterous Hand without Feedback control: the TUAT/Karlsruhe Humanoid Hand," <http://h2t.anthropomatik.kit.edu/pdf/Fukaya2013.pdf>.
- [52] H. K. K. Y. J. T. a. S. I. Tetsuya Mouri, "Anthropomorphic Robot Hand: Gifu Hand III," http://mindtrans.narod.ru/pdfs/Gifu_Hand_III.pdf.
- [53] Prensilia s.r.l.: Grasping Innovation, [Online]. Available: <http://www.prensilia.com/index.php?q=en/node/40>.
- [54] Open Hand Project, [Online]. Available: <http://www.openhandproject.org/>.
- [55] Inmoov, [Online]. Available: <http://www.inmoov.fr/>.
- [56] Raúl Suárez and Patrick Grosch, "DEXTEROUS ROBOTIC HAND MA-I," <https://iocnet.upc.edu/usuaris/raulsuarez/papers/img04-sg.pdf>.
- [57] Bebionic, [Online]. Available: <http://bebionic.com/>.
- [58] Robugtix, "T8X Robotic Spider," [Online]. Available: <http://www.robugtix.com/t8x/>.

- [59] Georgia Tech Research Institute, [Online]. Available: http://usability.gtri.gatech.edu/eou_info/hand_anthro.php.
- [60] Ticona, "Design calculations for snap fit joints in plastic parts," [Online]. Available: http://files.engineering.com/download.aspx?folder=7fd183bb-7ac8-4891-9378-a8badd6a102d&file=Design_for_Snapfit_revi-10.pdf.
- [61] Kettenfabrik Unna, "Ball Chains DIN 5280," [Online]. Available: <http://www.kettenfabrik-unna.de/kugelketten-din-5280-p-442.html>. [Accessed 07 04 2015].
- [62] S. V. D. Donck, Interviewee, *VGT Sign Language Translator*. [Interview]. August 2014.
- [63] Arduino, "<http://arduino.cc/en/Main/arduinoBoardDue>," Arduino, [Online]. Available: <http://arduino.cc/en/Main/arduinoBoardDue>. [Accessed 24 03 2015].
- [64] TDK Lambda, "www.tdk-lambda.com," TDK-Lambda, [Online]. Available: <http://www.tdk-lambda.com/products/sps/catalog/eng/ls.pdf>. [Accessed 29 03 2015].
- [65] F. D. Smedt, *Hydraulica*, Brussel: Vrije Universiteit Brussel, 2010.
- [66] J.-P. Smet, *Granta CES Material Selector*.
- [67] D. Sawicz, *Hobby Servo Fundamentals*, Princeton : Princeton University.
- [68] A. Colomé, *Redundant inverse kinematics: experimental comparative review and two enhancements*, Barcelona: Institut de Robotica i Informàtica Industrial.
- [69] J. Burdick, *The Moore-Penrose Pseudoinverse*, Pasadena, CA: Caltech Institute of technology, 2010.



Annexes: Humanoid robot for sign language

Candidates: Guy Fierens, Stijn Huys, Jasper Slaets

Thesis supervisors

Internal	Ing. Erwin Smet
External	Dr. Joost Van Dinther

2014-2015

Masterproef tot het behalen van het diploma

Master of Science in de industriële wetenschappen: Elektromechanica

Annexes: Humanoid robot for sign language

Candidates: Guy Fierens, Stijn Huys, Jasper Slaets

Thesis supervisors

Internal	Ing. Erwin Smet
External	Dr. Joost Van Dinther

2014-2015

Masterproef tot het behalen van het diploma

Master of Science in de industriële wetenschappen: Elektromechanica

Annexes

ANNEX 1: MUSCLES IN THE UPPER EXTREMITIES.

Muscles responsible for shoulder movement.

Table 33: Muscles responsible for shoulder movement

Muscle	Function	Proximal attachment point	Distal attachment point
Deltoideus – Anterior part	Anteversion, adduction and endorotation	Clavicula	Humerus
Deltoideus – medial part	Abduction and exorotation	Scapula	Humerus
Deltoideus – posterior part	Retroversion, adduction and exorotation	Scapula	Humerus
Pectoralis Major	Anteversion and adduction	Chest	Humerus
Coracobrachialis	Adduction	Scapula	Humerus
Biceps Brachii and triceps	Stability of the arm		

Muscles responsible for elbow movement

Table 34: Muscles responsible for elbow movement

Muscle	Function	Proximal attachment point	Distal attachment point
Biceps brachii	Flexion and supination	Humerus	Radius
Brachialis	Flexion	Humerus	Ulna
Triceps	Extension	Scapula (1x), Humerus (2x)	Radius
Musculus anoneus	Extension	Humerus	Ulna
Brachioradialis	Flexion	Humerus	Radius
Extensor carpi radialis longus and brevis	Limited flexion	Humerus	Os metacarpi
Extensor digitorum	Extension	Humerus	Os metacarpi
Pronator teres	Flexion and rotation of the radio-ulnar joint	Humerus and ulna	Radius
Flexor digitorum superficialis	Flexion	Humerus and ulna	Metacarpal

Muscles responsible for wrist movement

Table 35: Muscles responsible for wrist movement

Muscle	Function	Proximal attachment point	Distal attachment point
Pronator quadratus	Pronation of the hand	Radius and ulna	
Pronator teres	Rotation of the radio-ulnar joint (pronation hand)	Humerus and ulna	Radius
Supinator	Supination by rotating radio-ulnar joint		
Flexor carpi radialis	Flexion and adduction	Humerus	Os metacarpi
Flexor carpi ulnaris	Flexion and adduction	Humerus	Os metacarpi
Extensores carpi radialis longus and brevis	Dorsiflexion and abduction	Humerus	Os metacarpi
Extensor carpi ulnaris	Dorsiflexion and abduction	Humerus	Os metacarpi
Extensor digitorum	Limited extension	Humerus	Os metacarpi
Flexor digitorum superficialis	Flexion	Humerus and ulna	Metacarpals

Muscles responsible for hand movement

The muscles that control the movement of the fingers are located mainly in the forearm. These muscles give the hand and fingers their strength, but may not be able to carry out fine and precise movements. There are smaller muscles responsible for precise movements who are attached to the ossa carpi and ossa metacarpi. The muscles in the forearm providing extension or stretching of the fingers are located at the top of the forearm (anterior) while the muscles providing flexion or bending the fingers are located posterior on the forearm when the hand is in writing mode.

Extensors of the fingers:

- **Metacarpophalangeal and proximal interphalangeal joints:** extensor digitorum, extensor digiti minimi and extensor indicis.
- **Distal interphalangeal joints of the fingers:** lubricales and interossei palmares and dorsales.
- **Metacarpophalangeal joint of the thumb:** extensor pollicis brevis.
- **Interphalangeal joint of the thumb:** extensor pollicis longus.

Flexors of the fingers:

- **Metacarpophalangeal joints:** interossei palmares and dorsales (and lubricales).
- **Proximal interphalangeal joints:** flexor digitorum superficialis.
- **Distal interphalangeal joints:** flexor digitorum profundus.

Muscles responsible for abduction and adduction of the fingers:

- **Adduction:** Interossei palmares
- **Abduction:** Interossei dorsales

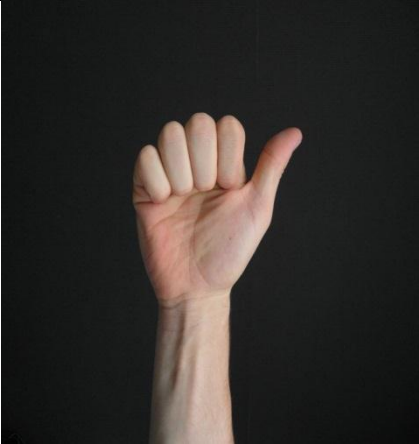


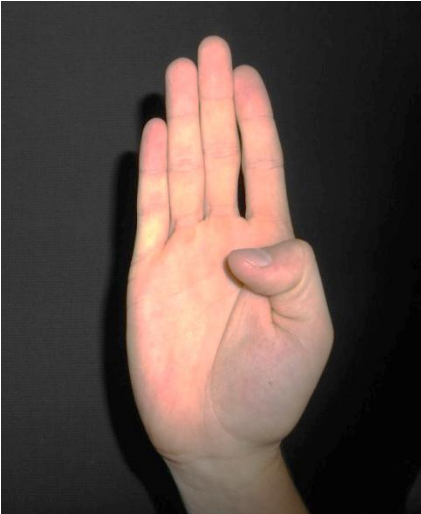
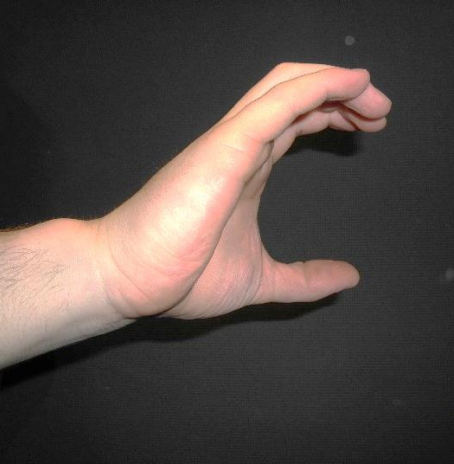
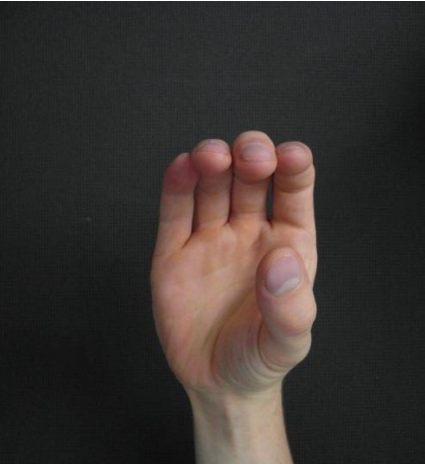
ANNEX 2: FLEMISH SIGN LANGUAGE ALPHABET.

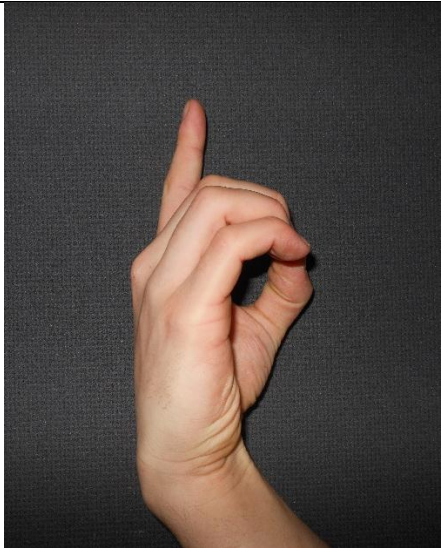
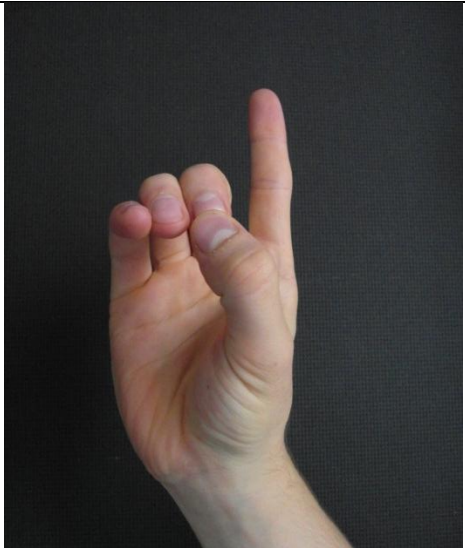

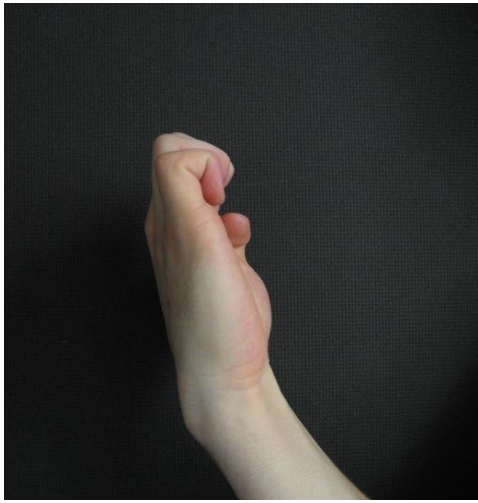
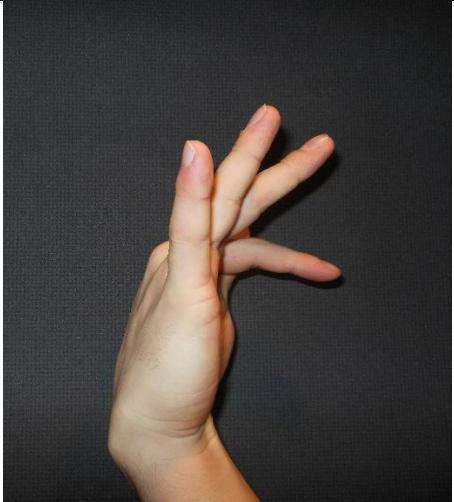
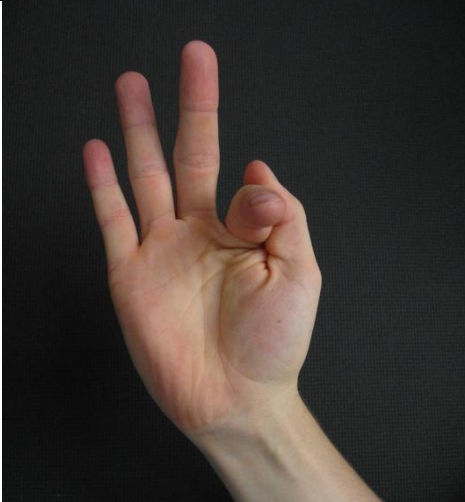
Table 36: List of descriptions

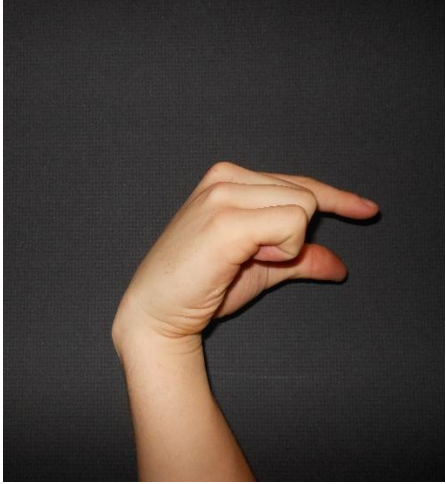


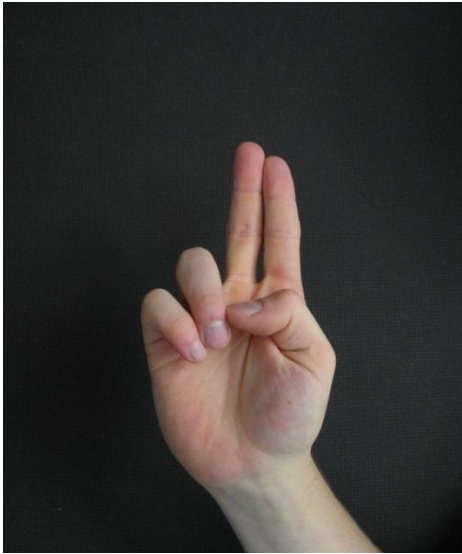
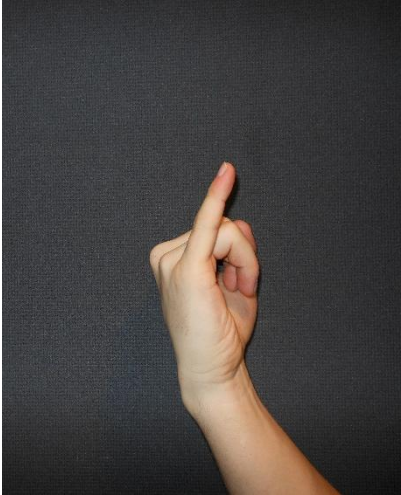
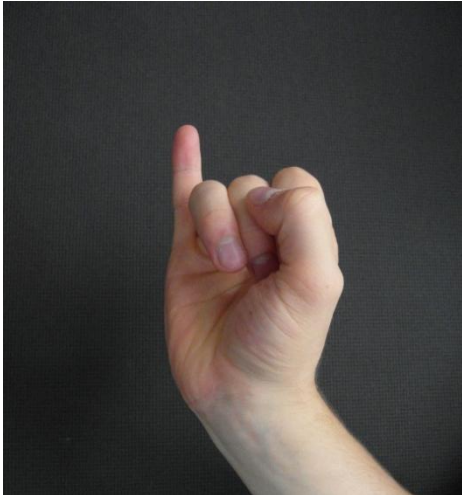
Char	Description	Figure
"A"	The "A" looks like a fist, all fingers are flexed but the thumb is extended.	See Table 17: Figures of characters, "A"
"B"	All fingers are extended but the thumb is flexed in front of the palm of the hand.	See Table 17: Figures of characters, "B"
"C"	Make a "C", all fingers and the thumb are all half extended, half flexed. The thumb is rotated perpendicular to the palm of the hand.	See Table 17: Figures of characters, "C"
"D"	The pointer finger is extended, the thumb reaches the middle finger and the other fingers are half flexed.	See Table 17: Figures of characters, "D"
"E"	The thumb is flexed in front of the palm of the hand, the MCP of all the fingers are extended and the PIP and DIP of all the fingers are flexed.	See Table 17: Figures of characters, "E"
"F"	All the fingers are extended, but the pointer finger does a palmar flexion of 90° while the thumb touches the pointer finger from aside.	See Table 17: Figures of characters, "F"
"G"	The little, ring and middle finger are flexed, the pointer finger and thumb are parallel extended and the palm does a palmar flexion of 90°.	See Table 17: Figures of characters, "G"
"H"	The little and ring finger are flexed, the middle finger and pointer finger are extended and the thumb is flexed in front of the palm of the hand.	See Table 17: Figures of characters, "H"
"I"	The little finger is extended and the other fingers and thumb are flexed, but the thumb is in front of the fingers.	See Table 17: Figures of characters, "I"
"J"	Same configuration as "I", but the hand makes a "J" motion in the air.	See Table 17: Figures of characters, "J"
"K"	The little and ring finger are flexed, the middle finger and pointer finger are extended, but away from each other and the thumb is flexed between the middle finger and pointer finger.	See Table 17: Figures of characters, "K"
"L"	You make an "L" with the hand: little, ring and middle finger are flexed, while the pointer finger and thumb are extended.	See Table 17: Figures of characters, "L"
"M"	Same configuration as "B", but the palm of the hand does a palmar flexion of 90° and the fingers are pointing down.	See Table 17: Figures of characters, "M"
"N"	Same configuration as "H", but the palm of the hand does a palmar flexion of 90° and the fingers are pointing down.	See Table 17: Figures of characters, "N"
"O"	Make an "O" with your hand: all 5 fingers half flexed, and the thumb touches the pointer finger.	See Table 17: Figures of characters, "O"

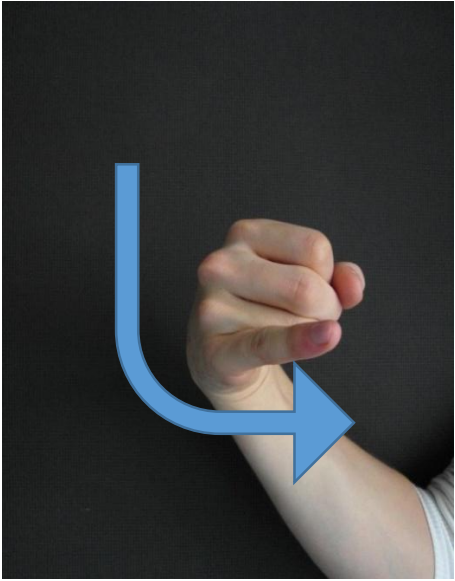
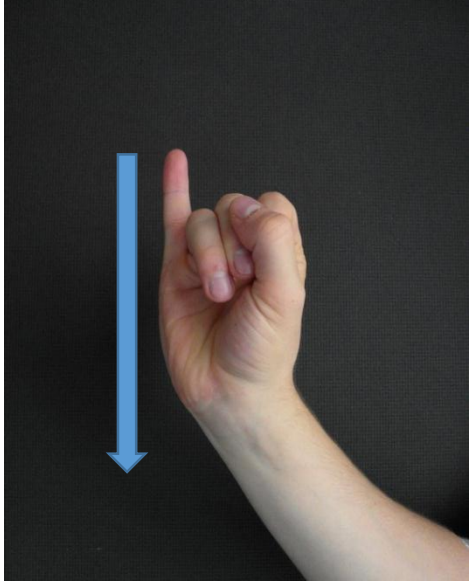
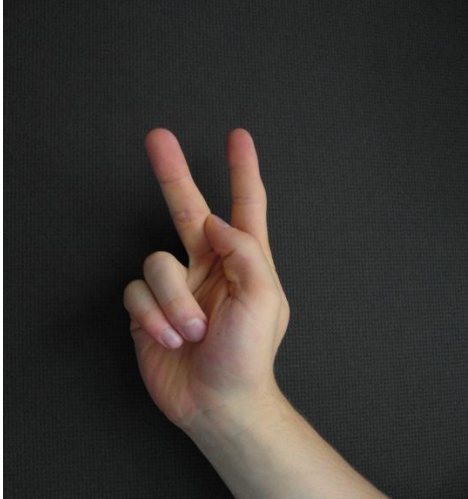
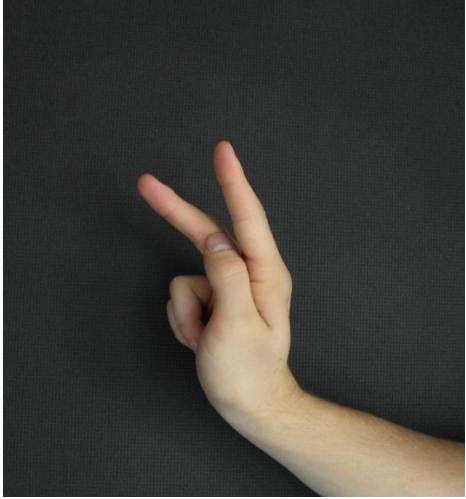

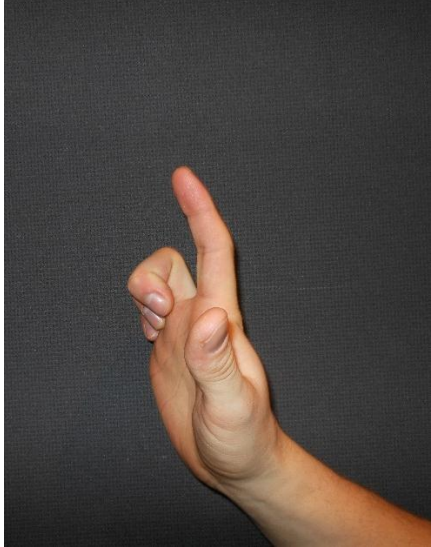
“Q”	Same configuration as “G”, but the palm of the hand does a palmar flexion of 90° and the fingers are pointing down.	See Table 17: Figures of characters, “Q”
“R”	The little and ring finger are flexed, the middle finger and pointer finger are extended, but crossed and the thumb is flexed towards the ring finger.	See Table 17: Figures of characters, “R”
“S”	Make a fist, but the thumb is flexed in front of the fingers.	See Table 17: Figures of characters, “S”
“T”	The little, ring, and middle finger are flexed, the thumb is flexed towards the middle finger and the pointer finger is flexed over the thumb.	See Table 17: Figures of characters, “T”
“U”	Same configuration as “H”, but the palm of the hand is facing the people.	See Table 17: Figures of characters, “U”
“V”	Same configuration as “U”, but the middle finger and pointer finger are extended away from each other.	See Table 17: Figures of characters, “V”
“W”	The little and ring finger are flexed and the other fingers and thumb are extended away from each other.	See Table 17: Figures of characters, “W”
“X”	Make a hook with the pointer finger and move the hand towards yourself.	See Table 17: Figures of characters, “X”
“Y”	The little finger and the thumb are extended and the other fingers are flexed.	See Table 17: Figures of characters, “Y”
“Z”	Same configuration as “D”, but the pointer finger is pointing forwards and make a “Z” motion with the hand in the air.	See Table 17: Figures of characters, “Z”

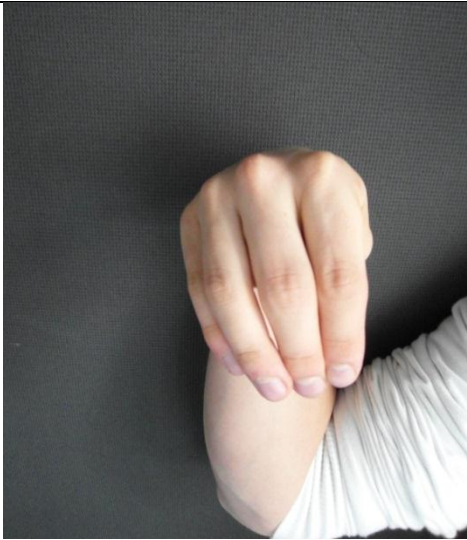
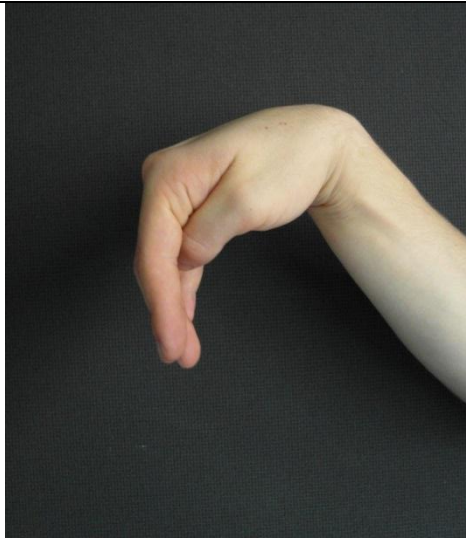

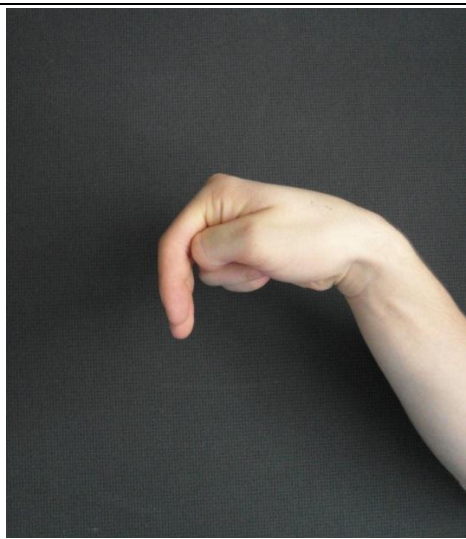
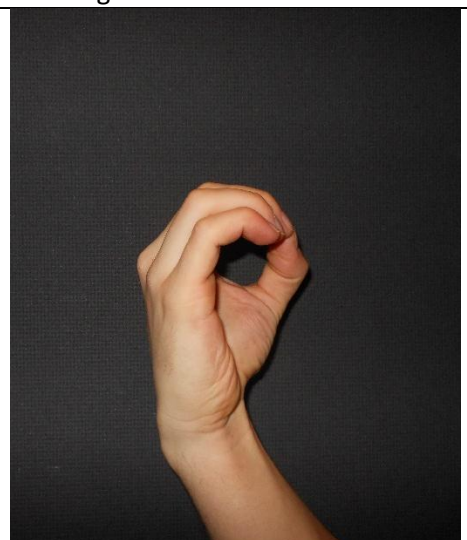

Table 37: List of images

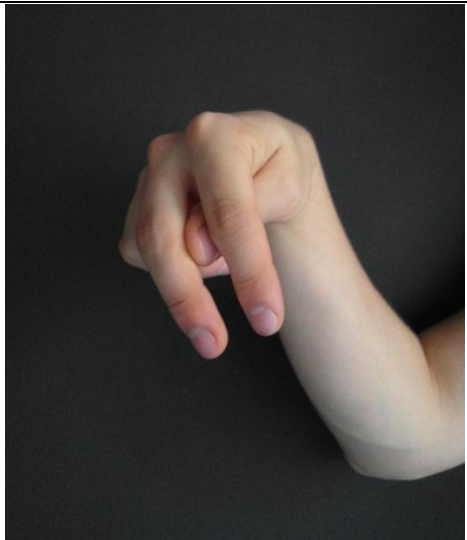
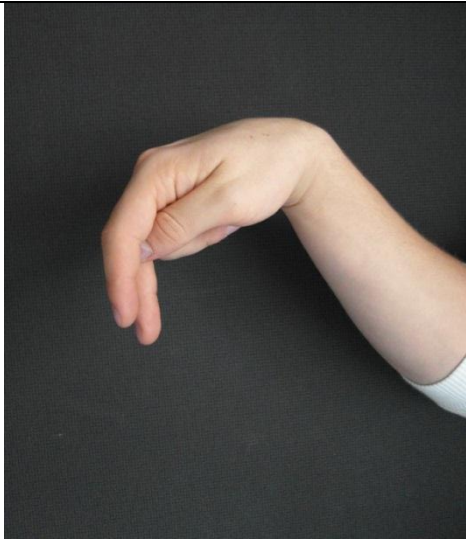
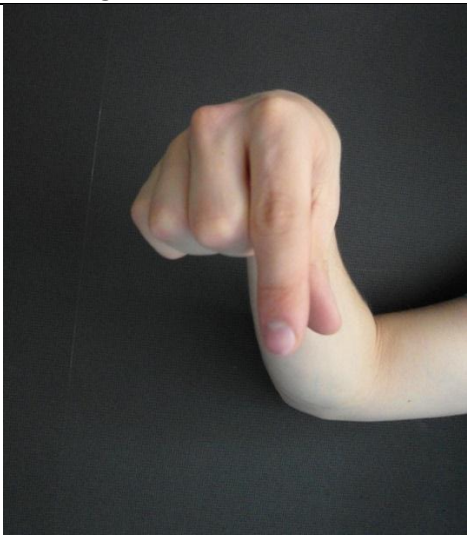
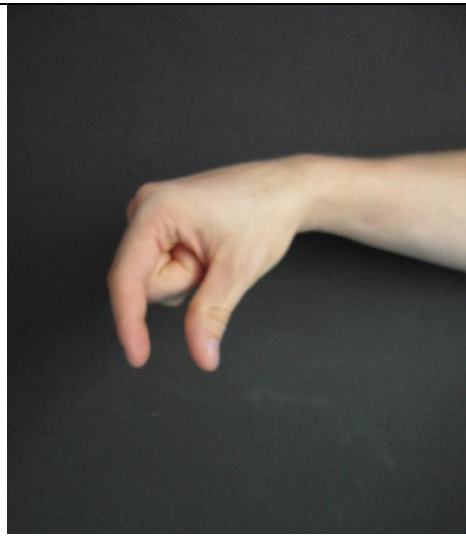
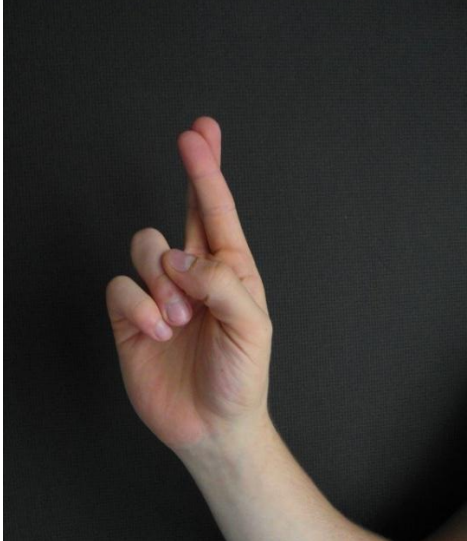
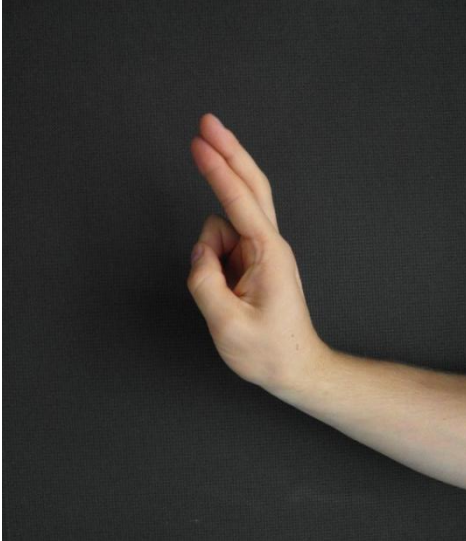
Char	Front view	Side view
"A"	 <p data-bbox="443 732 761 763">Figure 145: Front view "A"</p>	 <p data-bbox="975 732 1329 763">Figure 146: Left side view "A"</p>
"B"	 <p data-bbox="443 1283 761 1314">Figure 147: Front view "B"</p>	 <p data-bbox="975 1283 1329 1314">Figure 148: Left side view "B"</p>
"C"	 <p data-bbox="443 1787 761 1818">Figure 149: Front view "C"</p>	 <p data-bbox="975 1787 1329 1818">Figure 150: Left side view "C"</p>

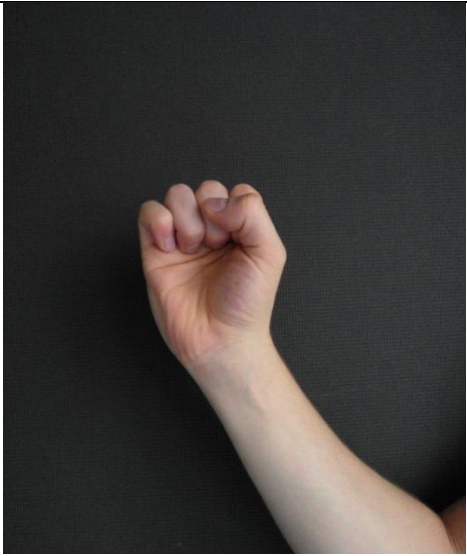
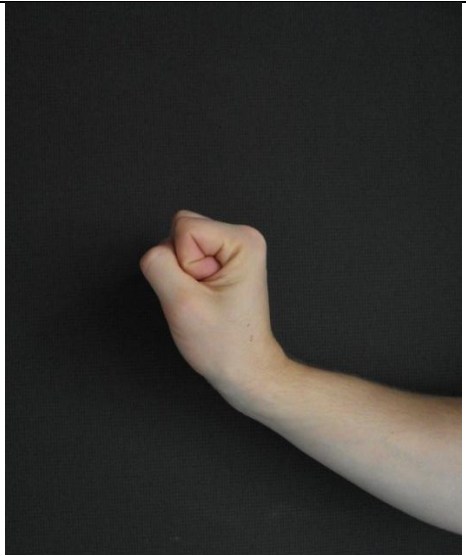

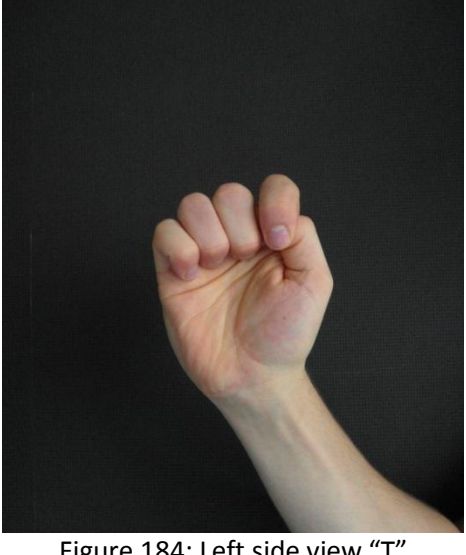
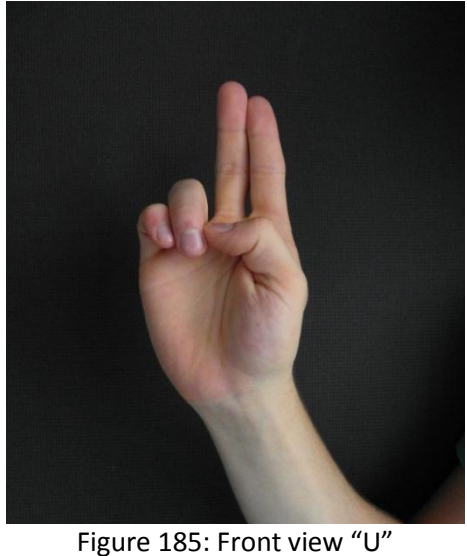
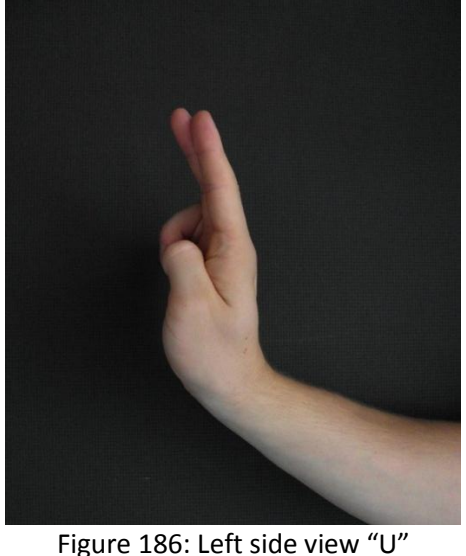
<p>"D"</p>	 <p>Figure 151: Front view "D"</p>	 <p>Figure 152: Left side view "D"</p>
<p>"E"</p>	 <p>Figure 153: Front view "E"</p>	 <p>Figure 154: Left side view "E"</p>
<p>"F"</p>	 <p>Figure 155: Front view "F"</p>	 <p>Figure 156: Left side view "F"</p>


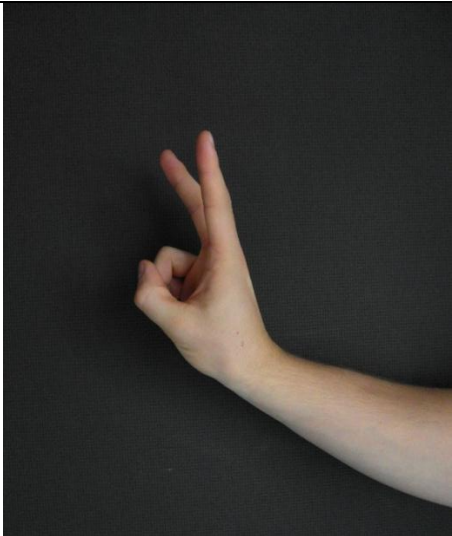
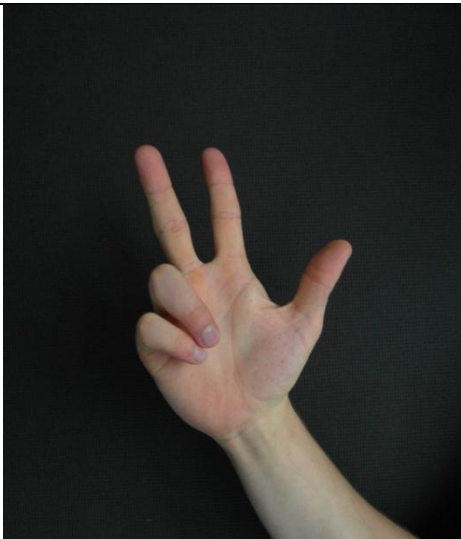
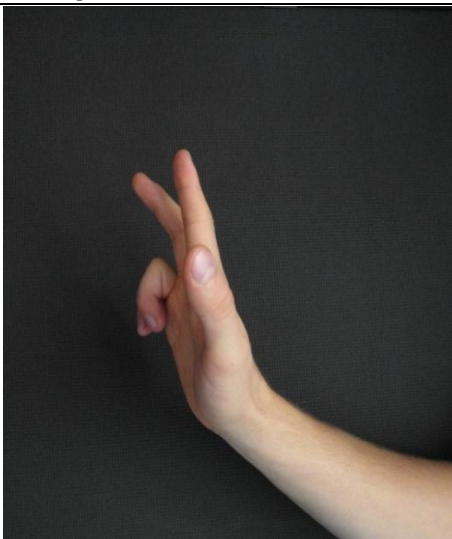

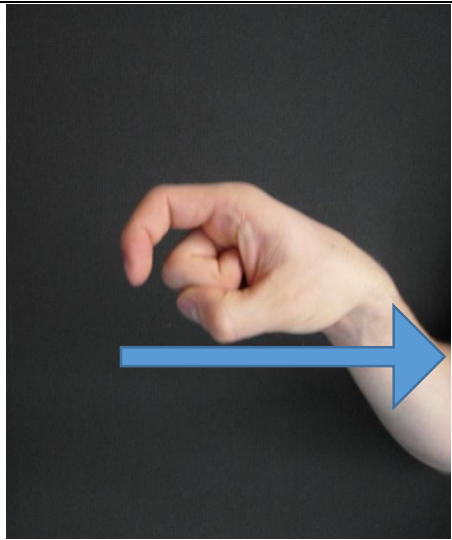
<p>"G"</p>	 <p>Figure 157: Front view "G"</p>	 <p>Figure 158: Left side view "G"</p>
<p>"H"</p>	 <p>Figure 159: Front view "H"</p>	 <p>Figure 160: Left side view "H"</p>
<p>"I"</p>	 <p>Figure 161: Front view "I"</p>	 <p>Figure 162: Left side view "I"</p>

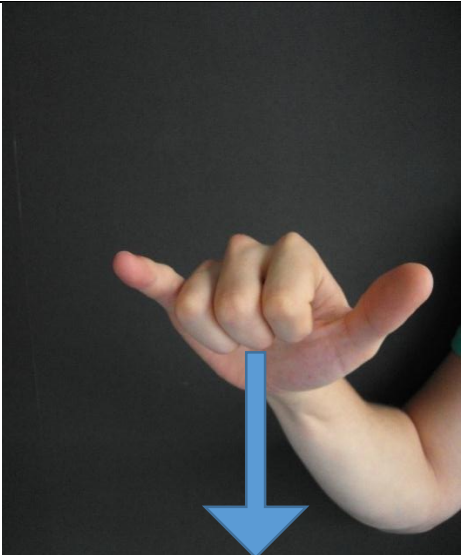
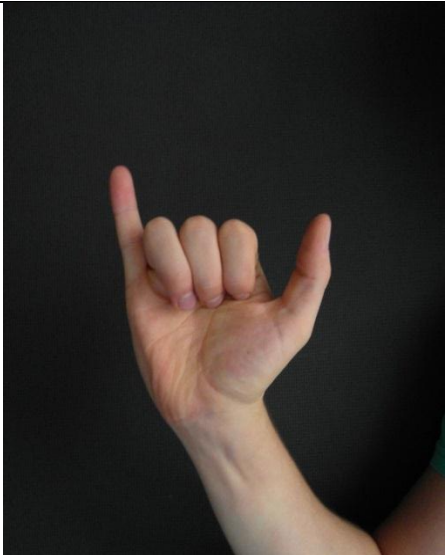
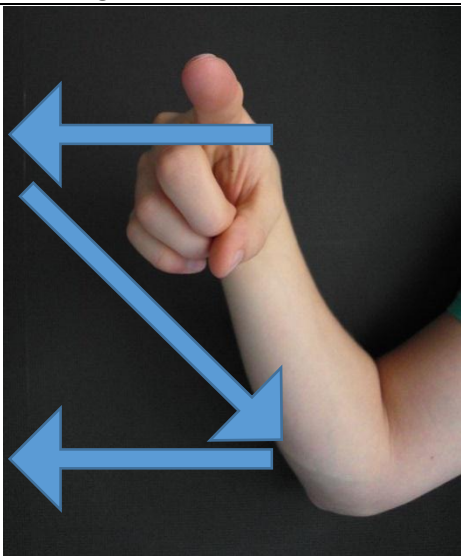
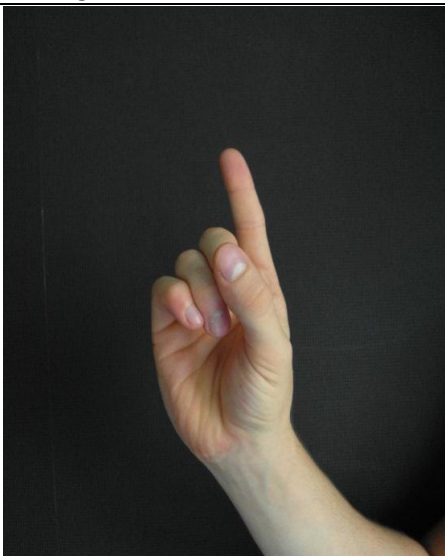
<p>“J”</p>	 <p>Figure 163: Front view “J”</p>	 <p>Figure 164: Left side view “J”</p>
<p>“K”</p>	 <p>Figure 165: Front view “K”</p>	 <p>Figure 166: Left side view “K”</p>
<p>“L”</p>	 <p>Figure 167: Front view “L”</p>	 <p>Figure 168: Left side view “L”</p>

<p>"M"</p>	 <p>Figure 169: Front view "M"</p>	 <p>Figure 170: Left side view "M"</p>
<p>"N"</p>	 <p>Figure 171: Front view "N"</p>	 <p>Figure 172: Left side view "N"</p>
<p>"O"</p>	 <p>Figure 173: Front view "O"</p>	 <p>Figure 174: Left side view "O"</p>

<p>"P"</p>	 <p>Figure 175: Front view "P"</p>	 <p>Figure 176: Left side view "P"</p>
<p>"Q"</p>	 <p>Figure 177: Front view "Q"</p>	 <p>Figure 178: Left side view "Q"</p>
<p>"R"</p>	 <p>Figure 179: Front view "R"</p>	 <p>Figure 180: Left side view "R"</p>

<p>“S”</p>	 <p>Figure 181: Front view “S”</p>	 <p>Figure 182: Left side view “S”</p>
<p>“T”</p>	 <p>Figure 183: Front view “T”</p>	 <p>Figure 184: Left side view “T”</p>
<p>“U”</p>	 <p>Figure 185: Front view “U”</p>	 <p>Figure 186: Left side view “U”</p>

<p>"V"</p>	 <p>Figure 187: Front view "V"</p>	 <p>Figure 188: Left side view "V"</p>
<p>"W"</p>	 <p>Figure 189: Front view "W"</p>	 <p>Figure 190: Left side view "W"</p>
<p>"X"</p>	 <p>Figure 191: Front view "X"</p>	 <p>Figure 192: Left side view "X"</p>

<p>"Y"</p>	 <p>Figure 193: Front view "Y"</p>	 <p>Figure 194: Bottom view "Y"</p>
<p>"Z"</p>	 <p>Figure 195: Front view "Z"</p>	 <p>Figure 196: Bottom view "Z"</p>

ANNEX 3: VOLUME EXPERIMENT

Which materials are needed to do this experiment? A measuring cup, water and a scale. How will procedure be? Take the measuring cup and fill it for three-quarters. When done put the measuring cup on the scale. Push the tare button to set a zero value. When all is done, our experiment can be started.

Next, only the distal part of the pointer finger is put in the water. The scale shows 5g. How is it possible to convert this to volume? Well Archimedes said: *“The upward force experienced by a body in a fluid or gas is equal to the weight of the displaced fluid or gas.”*

When this information is converted to a formula, it would look like this (Figure 197):

$$F = \rho_{fl} * g * V_{fl}$$

Equation 28: Archimedes

and

$$F = m_{scale} * g$$

Equation 29: Weight

With F = buoyancy, ρ_{fl} = 1000 kg/m³ (density water), g = gravity force, V_{fl} = volume displaced fluid (volume finger) and m_{scale} = buoyancy measured on scale.

When Equation 28 and Equation 29 are combined, the result is:

$$m_{scale} * g = \rho_{fl} * g * V_{fl}$$

Equation 30: combined

$$V_{fl} = \frac{m_{scale}}{\rho_{fl}}$$

Equation 31: Volume finger

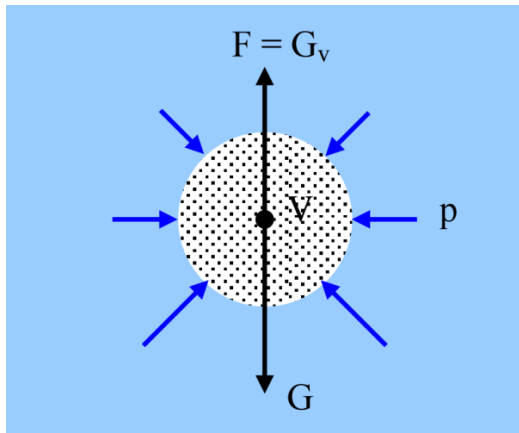


Figure 197: Archimedes [65]

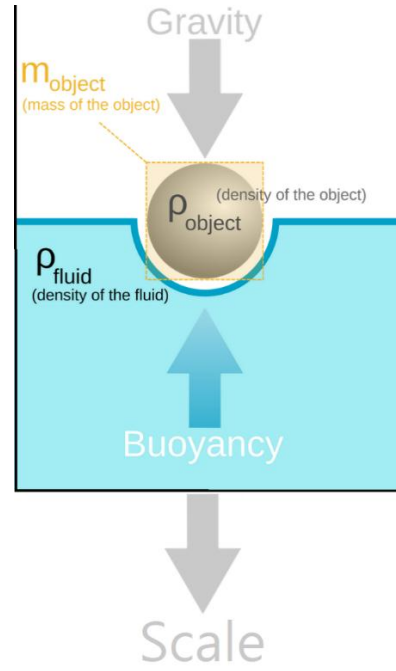


Figure 198: Experiment

With previous information can be said that, if the scale shows: 5g then the estimated volume will be 5cm³. Next the pointer finger is put in the water up to the medial part. Now the scale shows: 10g (≈ 10cm³), for the distal and the medial part! When previous volume is deducted, the resulted volume of only the medial part is: (≈ 10cm³ - ≈ 5cm³ = ≈ 5cm³).

This method can be repeated for each other part of the hand.

Table 38: Estimated volumes

Volumes								
	Pointer finger	Distal	5	cm ³	Middle finger	Distal	4	cm ³
		Medial	5	cm ³		Medial	9	cm ³
		Proximal	10	cm ³		Proximal	11	cm ³
	Ring finger	Distal	5	cm ³	thumb	Distal	8	cm ³
		Medial	5	cm ³		Proximal	8	cm ³
		Proximal	6	cm ³		TMC	50	cm ³
	Little finger	Distal	3	cm ³	Palm of the hand		373	cm ³
		Medial	3	cm ³	Lower arm		580	cm ³
		Proximal	4	cm ³	Upper arm		843	cm ³

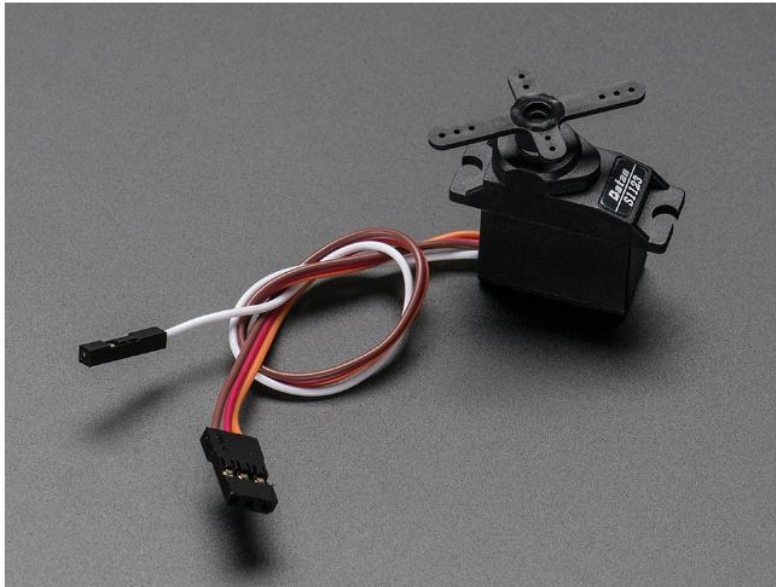
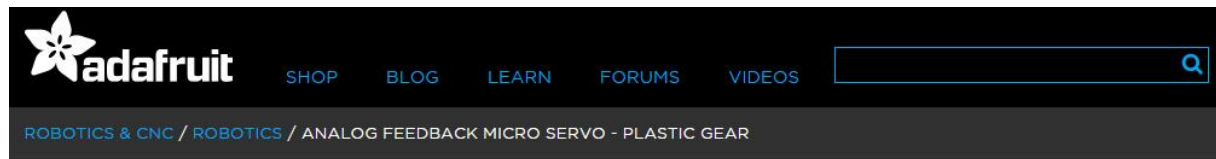
ANNEX 4: TORQUE ESTIMATION

Table 39: Estimated torque

Torque	PLA 80% Steel 20%										
Pointer finger	DIP	0.00077	Nm	0.007890194	kgcm	Middle finger	DIP	0.00063	Nm	0.0063879	kgcm
	PIP	0.00387	Nm	0.039450972	kgcm		PIP	0.00505	Nm	0.0515198	kgcm
	MCP	0.01151	Nm	0.117406093	kgcm		MCP	0.01509	Nm	0.1539156	kgcm
Ring finger	DIP	0.00079	Nm	0.008047998	kgcm	Thumb	IP	0.00141	Nm	0.0143412	kgcm
	PIP	0.00405	Nm	0.041313058	kgcm		MCP	0.00636	Nm	0.0648385	kgcm
	MCP	0.00954	Nm	0.097257692	kgcm		TMC		Nm		kgcm
Little finger	DIP	0.00043	Nm	0.004431133	kgcm						
	PIP	0.00217	Nm	0.022155666	kgcm						
	MCP	0.00505	Nm	0.051507189	kgcm						
Wrist		0.366522603	Nm	3.737490409	kgcm						
Elbow		2.92138765	Nm	29.78986351	kgcm						

Torque	ABS 80% Steel 20%										
Pointer finger	DIP	0.00074	Nm	0.007590092	kgcm	Middle finger	DIP	0.00060	Nm	0.0061449	kgcm
	PIP	0.00372	Nm	0.03795046	kgcm		PIP	0.00486	Nm	0.0495603	kgcm
	MCP	0.01108	Nm	0.112940568	kgcm		MCP	0.01452	Nm	0.1480614	kgcm
Ring finger	DIP	0.00076	Nm	0.007741894	kgcm	Thumb	IP	0.00135	Nm	0.0137958	kgcm
	PIP	0.00390	Nm	0.039741721	kgcm		MCP	0.00612	Nm	0.0623723	kgcm
	MCP	0.00917	Nm	0.093558509	kgcm		TMC		Nm		kgcm
Little finger	DIP	0.00042	Nm	0.004262596	kgcm						
	PIP	0.00209	Nm	0.021312978	kgcm						
	MCP	0.00486	Nm	0.04954812	kgcm						
Wrist		0.305571037	Nm	3.115957403	kgcm						
Elbow		2.44294315	Nm	24.91108737	kgcm						

ANNEX 5: RC SERVO MOTORS



Analog Feedback Micro Servo - Plastic Gear

PRODUCT ID: 1449

\$9.95
IN STOCK

1 [ADD TO CART](#)

QTY	DISCOUNT
1-9	\$9.95
10-99	\$8.96
100+	\$7.96

[ADD TO WISHLIST](#)

[DESCRIPTION](#)

[TECHNICAL DETAILS](#)

[LEARN](#)



DESCRIPTION

It looks like a micro servo, it acts like a micro servo, but it's more than just a micro servo! We got a factory to custom-make these classic 'micro' sized hobby servos with a twist - the feedback (potentiometer wiper) line is brought out to a fourth white wire. You can read this wire with an analog input such as those on an Arduino, to get the servo's position. That information can be used in robotics to improve stability or even allow 'recording' of servo motion.

TECHNICAL DETAILS



- Dimensions: 11.57mm / 0.45" x 22.75mm / 0.89" x 29.45mm / 1.15"
- Max Dimensions: 11.57mm / 0.45" x 32.71mm / 1.28" x 31.76mm / 1.25"
- Wire length (at least): 131.67mm / 5.18" long
- Torque: 22.24 oz*in / 1.6 kg*cm @ 6V
- Speed: 0.1 sec/60° @ 6V
- Weight: 13.82 grams
- Dual ball bearing
- Plastic gearbox



Analog Feedback Servo

PRODUCT ID: 1404

\$14.95

IN STOCK

ADD TO CART

QTY DISCOUNT

1-9 \$14.95

10-99 \$13.46

100+ \$11.96

ADD TO WISHLIST

[DESCRIPTION](#)

[TECHNICAL DETAILS](#)

[LEARN](#)

DESCRIPTION

It looks like a servo, it acts like a servo, but it's more than just a servo! We got a factory to custom-make these classic 'standard' sized hobby servos with a twist - the feedback (potentiometer wiper) line is brought out to a fourth white wire. You can read this wire with an analog input such as those on an Arduino, to get the servo's position. That information can be used in robotics to improve stability or even allow 'recording' of servo motion.

TECHNICAL DETAILS



- Dimensions: 39.55mm / 1.5" x 39.55mm / 1.5" x 19.5mm / 0.7"
- Max Dimensions: 55.36mm / 2.1" x 43.34mm / 1.7" x 19.5mm / 0.7"
- Wire length (at least): 13cm / 5.1" long
- Torque: 90.26 oz*in / 6.5 kg*cm
- Speed: 0.21 sec/60°
- Weight: 46 grams
- Dual ball bearing
- Plastic gearbox

ANNEX 6: ESTIMATED MINIMUM DISTANCES

Table 40: Estimated minimum distances

Min Distance	PLA 80%	Steel 20%						
	Pointer finger	Distal	0.049297	mm	Middle finger	Distal	0.039911	mm
		Medial	0.246484	mm		Medial	0.321889	mm
		Proximal	0.733538	mm		Proximal	0.961644	mm
	Ring finger	Distal	0.050283	mm	Thumb	Distal	0.089602	mm
		Medial	0.258118	mm		Proximal	0.405102	mm
		Proximal	0.607653	mm		TMC		mm
	Little finger	Distal	0.027685	mm				
		Medial	0.138426	mm				
		Proximal	0.321810	mm				

Min Distance	PLA 80%	Steel 20%						
	Pointer finger	Distal	0.047422	mm	Middle finger	Distal	0.038393	mm
		Medial	0.237109	mm		Medial	0.309646	mm
		Proximal	0.705638	mm		Proximal	0.925068	mm
	Ring finger	Distal	0.048370	mm	Thumb	Distal	0.086194	mm
		Medial	0.248301	mm		Proximal	0.389694	mm
		Proximal	0.584541	mm		TMC		mm
	Little finger	Distal	0.026632	mm				
		Medial	0.133161	mm				
		Proximal	0.309570	mm				

ANNEX 7: PROPERTIES DYNEEMA, NYLON AND STAINLESS STEEL

Dyneema



Fatigue resistance.

Dyneema® fiber applications have a higher resistance to repeated axial loading than other fiber types. The fibers combine high strength with high fatigue resistance, even if the loading is partly in compression as in repeated bending of rope applications. Despite its high modulus, the fibers are flexible and have a long flexural fatigue life. Because of the low friction coefficient and good abrasion resistance, internal abrasion of ropes is usually negligible.

FATIGUE RESISTANCE		
Abrasion resistance (yam-on-yarn)	ASTM D6611	Excellent*
Abrasion resistance (covered rope)		Excellent*
Cutting resistance (covered rope)		Excellent
Flexural fatigue (fiber)		Excellent
Bending fatigue (rope)		Excellent
Tension fatigue (rope)		Excellent*

Environmental properties.

Dyneema® fiber is used in various outdoor applications under harsh weather conditions. In air the fiber is stable for many years. No special precautions are necessary during processing or storage. Only strong oxidizing media are able to attack the mechanical properties. Compared to other high tenacity fibers, long term exposure to UV shows the lowest decrease in strength and elongation at break.

* Detailed information per fiber type, as Product Data Sheet, Product Specification Sheet, Material Safety Data Sheet and Fact Sheet, is available on request.

www.dyneema.com

Dyneema® and Dyneema®, the world's strongest fiber™ are trademark(s) (application) owned by Royal DSM N.V.

All information supplied by or on behalf of DSM Dyneema LLC and/or DSM Dyneema BV ("DSM") in relation to its products, whether in the nature of data, recommendations or otherwise, is supported by research and/or experience and believed reliable, but DSM gives no warranties of any kind, expressed or implied, including, but not limited to, those of correctness, completeness, merchantability or fitness for a particular purpose and DSM assumes no liability whatsoever in respect of application, processing, use of, or reliance on, the aforementioned information or products, or any consequence thereof, including but not limited to any infringement of the rights owned or controlled by a third party in intellectual, industrial or other property. Any information provided by DSM does not release the user from the obligation to verify such information and to perform its own testing and analysis to determine the suitability of the products for the intended process, use or specific application. The user accepts all liability in respect of or resulting from the application, processing, use of, or reliance on, the aforementioned information or products or any consequences thereof.

Issued: 01-01-2008
Page: 4/4
Ref.: CIS YA100

ENVIRONMENTAL PROPERTIES		
Visible light exposure		Excellent*
UV-exposure	ISO 4892	Very good*
Weathering	ISO 12224	Excellent
Oxidation (28 days, 80°C, 50 bar)	ISO 13438	Passed

Fungal resistance.

Dyneema® fiber has excellent biological resistance. The fiber neither stimulates undesired growth nor is sensitive to any attack by micro-organisms.

FUNGAL RESISTANCE		
Aspergillus niger	RTCA DO160	Excellent
Aspergillus flavus	RTCA DO160	Excellent
Aspergillus versicolor	RTCA DO160	Excellent
Penicillium funiculosum	RTCA DO160	Excellent
Chaetomium globosum	RTCA DO160	Excellent

Toxicity.

Polyethylene is regarded as biologically inert. The Dyneema® fibers are IARC classified 3 (not classifiable carcinogenic to human) based upon its length weighted geometric mean diameter. This diameter is too large to produce respirable fibers, meaning they will never reach the deeper part of the respiratory tract and fibrogenic or carcinogenic effects on the lung will not occur.

Dyneema® high-strength, high-modulus polyethylene fiber

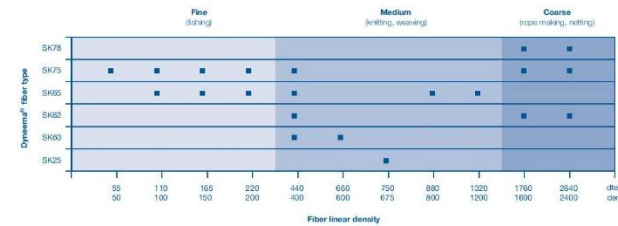
Dyneema® fiber combines excellent mechanical properties with low density, resulting in high performance-on-weight basis.

The Dyneema® fiber is a gel-spun, multi-filament fiber produced from ultra high molecular weight polyethylene (UHMW-PE), with main characteristics: high strength, low density, low elongation at break, and resistance to most chemicals. To stimulate developments, this sheet provides an overview of properties measured on Dyneema® fibers. The disclosed data is not valid for any other source of high-modulus polyethylene fibers.

Fiber range.

Dyneema® fibers are produced in three strength ranges and several linear densities with a characteristic very low filament diameter. Especially for medical applications Dyneema Purity® is produced in low linear densities. The tensile properties are correlated with the fiber linear density. Detailed information per fiber type is available on request, as Product Data Sheets, Product Specification Sheets, Material Safety Data Sheets and Fact Sheets.

Fiber type	Tensile strength			Tensile modulus			Elongation to break %
	N/tex	g/den	GPa	N/tex	g/den	GPa	
Dyneema® SK78 Dyneema® SK75	3.4 – 4.0	38 – 45	3.3 – 3.9	112 – 137	1267 – 1552	109 – 132	3-4
Dyneema® SK65 Dyneema® SK62 Dyneema® SK60	2.5 – 3.4	28 – 38	2.4 – 3.3	67 – 102	759 – 1158	65 – 100	
Dyneema® SK25	2.2	25	2.2	54	608	52	



Issued: 01-01-2008
Page: 1/4
Ref.: CIS YA100



Mechanical properties.

Dyneema® fibers have a high strength and a high modulus (resistance against deformation) in the fiber direction. In combination with the low density this results in an extremely high strength on weight basis, making it one of the strongest man-made fibers. The elongation at break is relatively low, but owing to the high strength, the energy to break is high. In contrast to other synthetic fibers, the mechanical properties are not influenced by the presence of water.

Due to the anisotropic structure of high modulus polyethylene fibers, the modulus and strength in transverse direction are lower than in fiber direction.

Subjecting HMPE fiber to long-term static loads leads to a permanent elongation called creep. The Dyneema® fiber types have a higher creep resistance than other HMPE fibers enabling their use in various static loading conditions.

MECHANICAL		
Free breaking length	378	km
Axial tensile strength	3.6*	GPa
Axial tensile modulus	116*	GPa
Axial compressive strength	0.1	GPa
Axial compressive modulus	116	GPa
Transverse tensile strength	0.03	GPa
Transverse modulus	3	GPa
Transverse compressive strength	0.1	GPa
Elongation at break	3 – 4 %	
Work to break	45 – 70	MJ/m ³
Creep at 30°C, 300 MPa (Dyneema® SK75)	0.02*	%/day
Creep at 30°C, 300 MPa (Dyneema® SK78)	0.006*	%/day

Thermal properties.

Like other synthetic fibers, the mechanical properties of HMPE fibers are influenced by temperature. The strength and modulus increase at sub-ambient temperatures and decrease at higher temperatures. For long duration exposure Dyneema® fibers can be used from cryogenic conditions up to a temperature of 70°C.

Relative to 23°C	-60°C	+23°C	+60°C	+100°C
Tensile strength	110%	100%	80%	55%
Tensile modulus	110%	100%	85%	60%
Elongation at break	90%	100%	100%	105%

Issued: 01-01-2008
Page: 2/4
Ref.: CIS YA100

THERMAL		
Melting range	144 – 152	°C
Decomposition temperature	> 300	°C
Advised lowest temperature	No limit	
Advised long duration temperature limit	70	°C
Advised short duration temperature limit (non-constrained fiber)	130	°C
Advised short duration temperature limit (constrained fiber)	145	°C
Coefficient of linear thermal expansion	-12 x 10 ⁻⁴	1/K
Specific heat capacity	1850	J/kg.K
Thermal conductivity (axial)	20	W/m.K
Thermal conductivity (transverse)	0.2	W/m.K

Chemical resistance.

Dyneema® fiber is very resistant against chemicals. Because it is produced from ultra high molecular weight polyethylene, it does not contain any aromatic rings or any amide, hydroxylic or other chemical groups that are susceptible to attack by aggressive agents.

CHEMICAL RESISTANCE		
Resistance to acids		Excellent*
Resistance to alkali		Excellent*
Resistance to most chemicals		Excellent*
Resistance to water		Excellent*
Aviation Jet A fuel (ISO 1817 test liquid F)	RTCA DO160	Excellent
Hydraulic fluid (ISO 1817 test liquid 103)	RTCA DO160	Excellent
Lubricating oil (ISO 1817 test liquid 101)	RTCA DO160	Excellent
Solvents and cleaning fluid (Isopropyl alcohol)	RTCA DO160	Excellent
De-icing fluid (Ethylene glycol)	RTCA DO160	Excellent
Insecticide (Pyrethroid pesticide)	RTCA DO160	Excellent
Fire extinguishant (Protein, Fluoroprotein)	RTCA DO160	Excellent

Physical properties.

Dyneema® fibers feel smooth due to their low friction coefficient. Its low density enables it to float on water. The water absorption in the fiber is negligible.

PHYSICAL		
Natural color	Opaque white	
Density	970 – 980	kg/m ³
Crystallinity	< 85 %	
Filament linear density	1 – 3	dpt
Filament diameter	12 – 21	µm
Filament cross section (other types)	Round	
Filament cross section (Dyneema® SK60, Dyneema® SK65)	Bone shape	
Equilibrium moisture regain	None	
Water pick-up (soaked)	None	
Boiling water shrinkage	< 1 %	
Hysteresis loss factor (23°C, 5 Hz)	0.02	
Friction coefficient (yarn-on-yarn)	0.05 – 0.07	

Electrical properties.

Polyethylene is an insulator and has no groups with dipole character. After scouring, the Dyneema® fiber is characterized by a high electrical resistance, low dielectric constant and a very low dielectric loss factor.

ELECTRICAL		
Resistance	>10 ¹⁴	Ohm
Dielectric strength	900	kV/cm
Dielectric constant (22 °C, 10 GHz)	2.25	
Dielectric loss factor	0.0002	

Acoustic properties.

Dyneema® fiber has a high sonic velocity. In the fiber direction, the sonic velocity is higher than in the transverse direction.

The acoustic impedance, the product of density and transverse sonic velocity, is near that of water.

ACOUSTIC		
Sonic velocity (axial)	10000 - 12000	m/s
Sonic velocity (transverse)	2000	m/s

Optical properties.

Dyneema® fibers are visually opaque. The fiber is invisible to an UV-light source due to the low UV absorption coefficient in combination with no fluorescence or phosphorescence. It is also invisible for thermal imaging devices because of its low IR absorption coefficient and high thermal conductivity. The low reflectivity of radar waves results in a high transparency for radar sources. The refractive index axial to the fiber axis differs from the transverse direction making the fiber perform birefringence.

OPTICAL	
Ultraviolet visibility (UV)	Transparent
Eye visibility (MS)	Translucent
Near Infrared visibility (NIR)	Highly transparent
Infrared visibility (IR)	Highly transparent
Radar visibility	Highly transparent
Refractive Index (axial)	1.59
Refractive Index (transverse)	1.53
Birefringence	0.06

Flammability.

Fabrics and panels produced from Dyneema® fibers have passed various standards on flammability. Like any other synthetic fiber, it will burn slowly if ignited in atmospheric conditions and is qualified as being self-extinguishing upon removal of the flame.

FLAMMABILITY		
Limited oxygen index	< 20%	
Fabric, horizontal	FMVSS 302	Passed
Fabric, vertical	FAR 25.853b	Passed
Ballistic panel, vertical	DIN 4102	Passed

Issued: 01-01-2008
Page: 3/4
Ref.: CIS YA100

Nylon 6

19-5-2015

Polyamide - Nylon 6 - online catalogue source - supplier of research materials in small quantities - Goodfellow

Buy Polyamide - Nylon 6 on-line

We stock and supply the following standard forms:



Film



Granule



Monofilament



Powder



Rod



Sheet



Tube

Choose a form to search our on-line catalogue

Common Brand Names:

Akulon K and F, Capron, Maranyl B, Nylacast, Orgamid, Ultramid B

General Description:

See also General Information under Nylon 6,6.

General Description : A semi-crystalline, white engineering thermoplastic very similar to nylon 6,6 with which it is in many respects interchangeable. Its melt viscosity is not quite as low as 6,6 so it is generally slightly easier to process and often preferred for moulding. Relative to 6,6 it has somewhat higher impact strength but somewhat lower strength and stiffness and higher water absorption (the highest of all nylons).

It can be monomer cast, commonly called just cast - ie. polymerised in a mould direct to a semi-fabricated shape. This allows the production of thick sections without voiding and gives a product with a slightly different balance of properties - a little stronger and stiffer, slightly reduced extensibility and impact strength.

Its applications are similar to those of nylon 6,6.

Chemical Resistance

Acids - concentrated	Poor
Acids - dilute	Poor
Alcohols	Good
Alkalis	Good-Fair
Aromatic hydrocarbons	Good
Greases and Oils	Good
Halogenated Hydrocarbons	Good-Poor
Halogens	Poor
Ketones	Good

Electrical Properties

Dielectric constant @1MHz	3.6
Dielectric strength (kV m m ⁻¹)	25
Dissipation factor @ 1kHz	0.2
Surface resistivity (Ohm/sq)	5x10 ¹⁰
Volume resistivity (Ohm cm)	5x10 ¹²

Mechanical Properties

Abrasive resistance - ASTM D1044 (mg/1000 cycles)	5
---	---

data:text/html;charset=utf-8,%3C%20style%3D%22margin%3A%20px%20px%20.2em%3B%20padding%3A%20px%3B%20font-weight%3A%20bold%... 1/3

19-5-2015

Polyamide - Nylon 6 - online catalogue source - supplier of research materials in small quantities - Goodfellow

Coefficient of friction	0.2-0.3
Hardness - Rockwell	M82
Izod impact strength (J m ⁻¹)	30-250
Poisson's ratio	0.39
Tensile modulus (GPa)	2.6-3.0
Tensile strength (MPa)	78

Physical Properties

Density (g cm ⁻³)	1.13
Flammability	HB
Limiting oxygen index (%)	25
Radiation resistance	Fair
Refractive index	1.53
Resistance to Ultra-violet	Poor
Water absorption - equilibrium (%)	>8
Water absorption - over 24 hours (%)	2.7

Thermal Properties

Coefficient of thermal expansion (x10 ⁻⁶ K ⁻¹)	95
Heat-deflection temperature - 0.45MPa (C)	200
Heat-deflection temperature - 1.8MPa (C)	80
Lower working temperature (C)	-40
Specific heat (J K ⁻¹ kg ⁻¹)	1700
Thermal conductivity @23C (W m ⁻¹ K ⁻¹)	0.24-0.28
Upper working temperature (C)	80-160

Properties for Polyamide - Nylon 6 Film

Property		Value
Dielectric Constant @ 1MHz		2.7
Dielectric Strength @25µm thick	kV mm ⁻¹	56
Dissipation Factor @1MHz		0.025
Elongation at Break	%	250-550
Extension to break - Longitudinal	%	375-500 - crystalline, 60-70 - monax.
Extension to break - Transverse	%	375-500 - crystalline, 400-450 - monax.
Heat-sealing Temperature	C	193-232
Permeability to Carbon Dioxide @25C	x10 ⁻¹³ cm ³ . cm cm ⁻² s ⁻¹ Pa ⁻¹	0.06
Permeability to Nitrogen @25C	x10 ⁻¹³ cm ³ . cm cm ⁻² s ⁻¹ Pa ⁻¹	0.007

data:text/html;charset=utf-8,%3C%3D%22margin%3A%20px%20px%20.2em%3B%20padding%3A%20px%3B%20font-weight%3A%20bold%... 2/3

19-5-2015

Polyamide - Nylon 6 - online catalogue source - supplier of research materials in small quantities - Goodfellow

Permeability to Oxygen @25C	$\times 10^{-13} \text{ cm}^3 \cdot \text{cm cm}^{-2} \text{ s}^{-1} \text{ Pa}^{-1}$	0.03
Permeability to Water @38C	$\times 10^{-13} \text{ cm}^3 \cdot \text{cm cm}^{-2} \text{ s}^{-1} \text{ Pa}^{-1}$	700
Shrinkage	%	<3 @ 150C - cryst , 8-15/1-2 @ 200C - monax.
Tensile strength - Longitudinal	MPa	70-110 - crystalline, 290-320 - monax.
Tensile strength - Transverse	MPa	70-110 - crystalline, 90-110 - monax.

Stainless steel

19-5-2015

Stainless Steel - AISI 316 - online catalogue source - supplier of research materials in small quantities - Goodfellow

Buy [Stainless Steel - AISI 316 on-line](#)

We stock and supply the following standard forms:



Foam



Foil



Insulated Wire Mesh



Powder



Rod



Sphere



Tube



Wire

Choose a form to search our on-line catalogue

General Description:

Stainless steels are iron based alloys containing at least 10.5% Chromium. They achieve their stainless characteristics through the formation of an invisible and adherent Chromium rich oxide film. Alloy 316 is a general purpose austenitic stainless steel with a face centered cubic structure. It is essentially non-magnetic in the annealed condition and can only be hardened by cold working.

Molybdenum has been added to increase corrosion resistance particularly in chloride containing environments, and the lower Carbon content of alloy 316L gives even better corrosion resistance in welded structures.

Electrical Properties

Electrical resistivity ($\mu\text{Ohm cm}$)	70-78
Temperature coefficient (K^{-1})	-

Mechanical Properties

Elongation at break (%)	<60
Hardness - Brinell	160-190
Izod impact strength (J m^{-1})	20-136
Modulus of elasticity (GPa)	190-210
Tensile strength (MPa)	460-860

Physical Properties

Density (g cm^{-3})	7.96
Melting point (C)	1370-1400

Thermal Properties

Coefficient of thermal expansion @20-100C ($\times 10^{-6} \text{K}^{-1}$)	16-18
Specific heat @23C ($\text{J K}^{-1} \text{kg}^{-1}$)	502
Thermal conductivity @23C ($\text{W m}^{-1} \text{K}^{-1}$)	16.3

data:text/html;charset=utf-8,%3C h1%20style%3D%22margin%3A%200px%20px%200.2em%3B%20padding%3A%200px%3B%20font-weight%3A%20bold%20... 1/1

ANNEX 8: DETAILS MEASUREMENTS PIP JOINT LITTLE FINGER

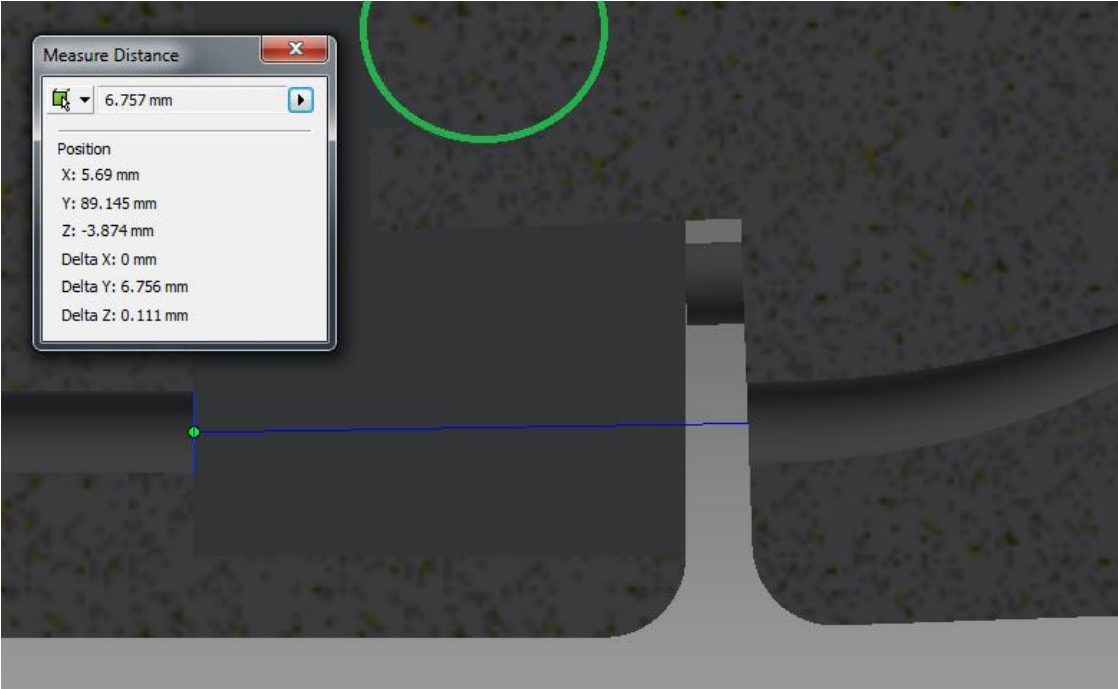


Figure 199: Details lower cable maximum position

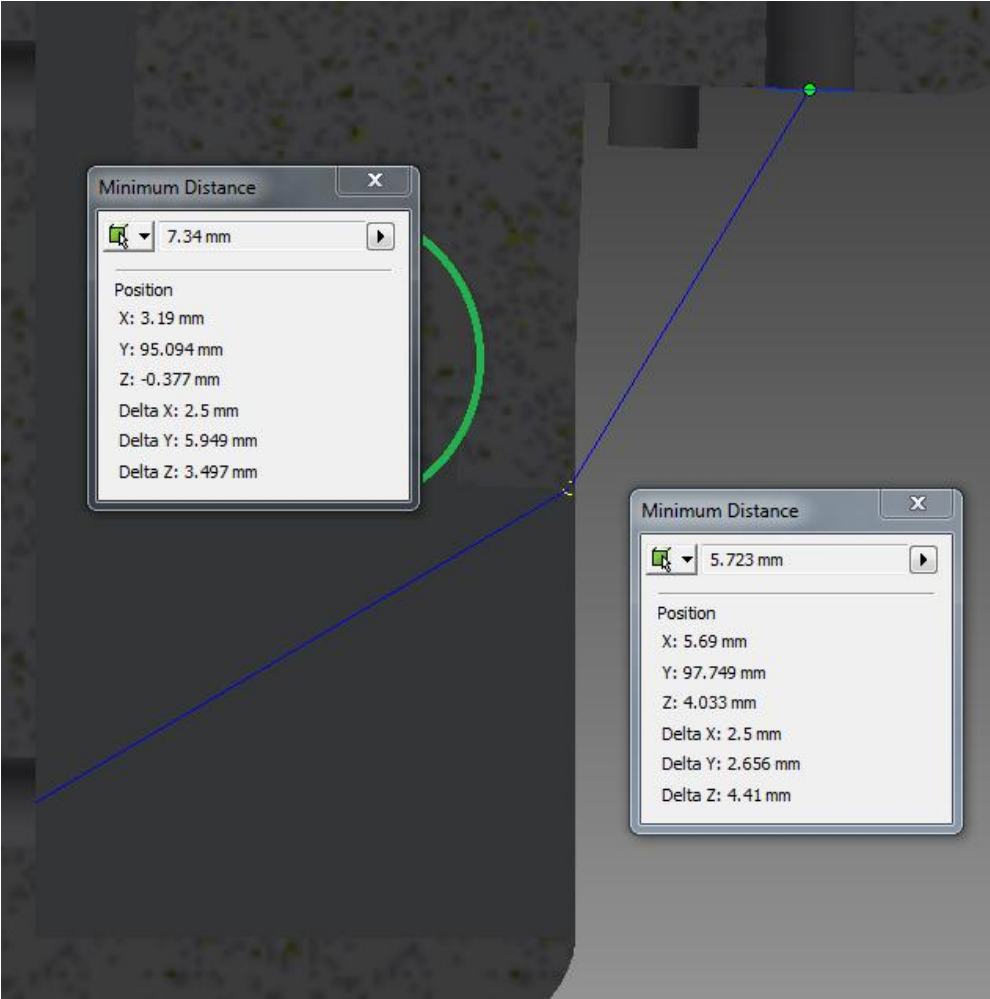


Figure 200: Details lower cable minimum position

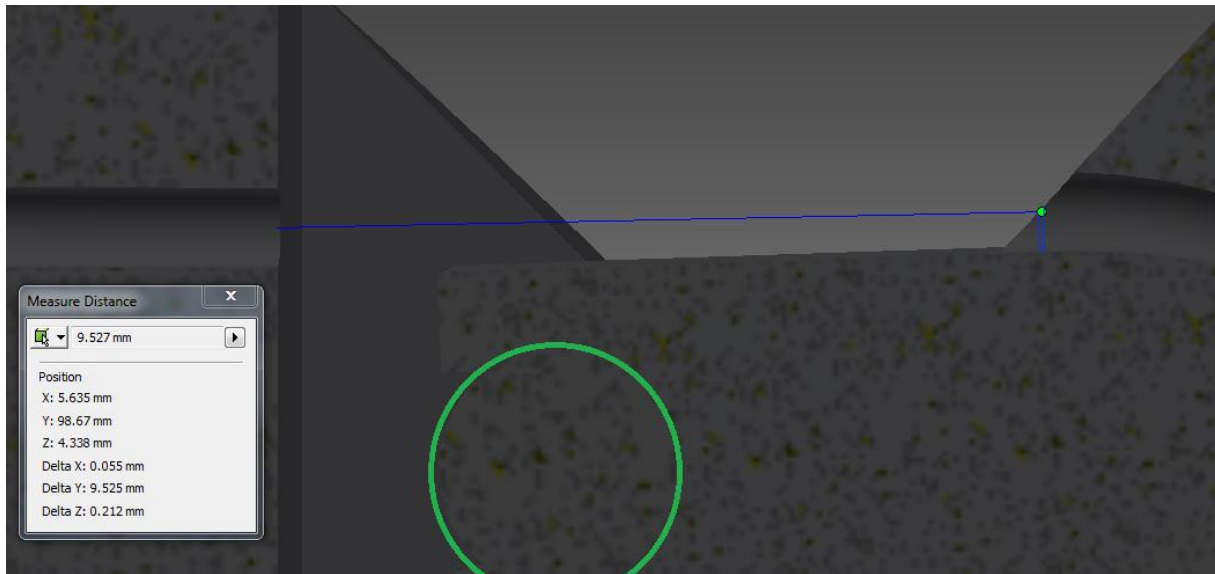


Figure 201: Details upper cable maximum position

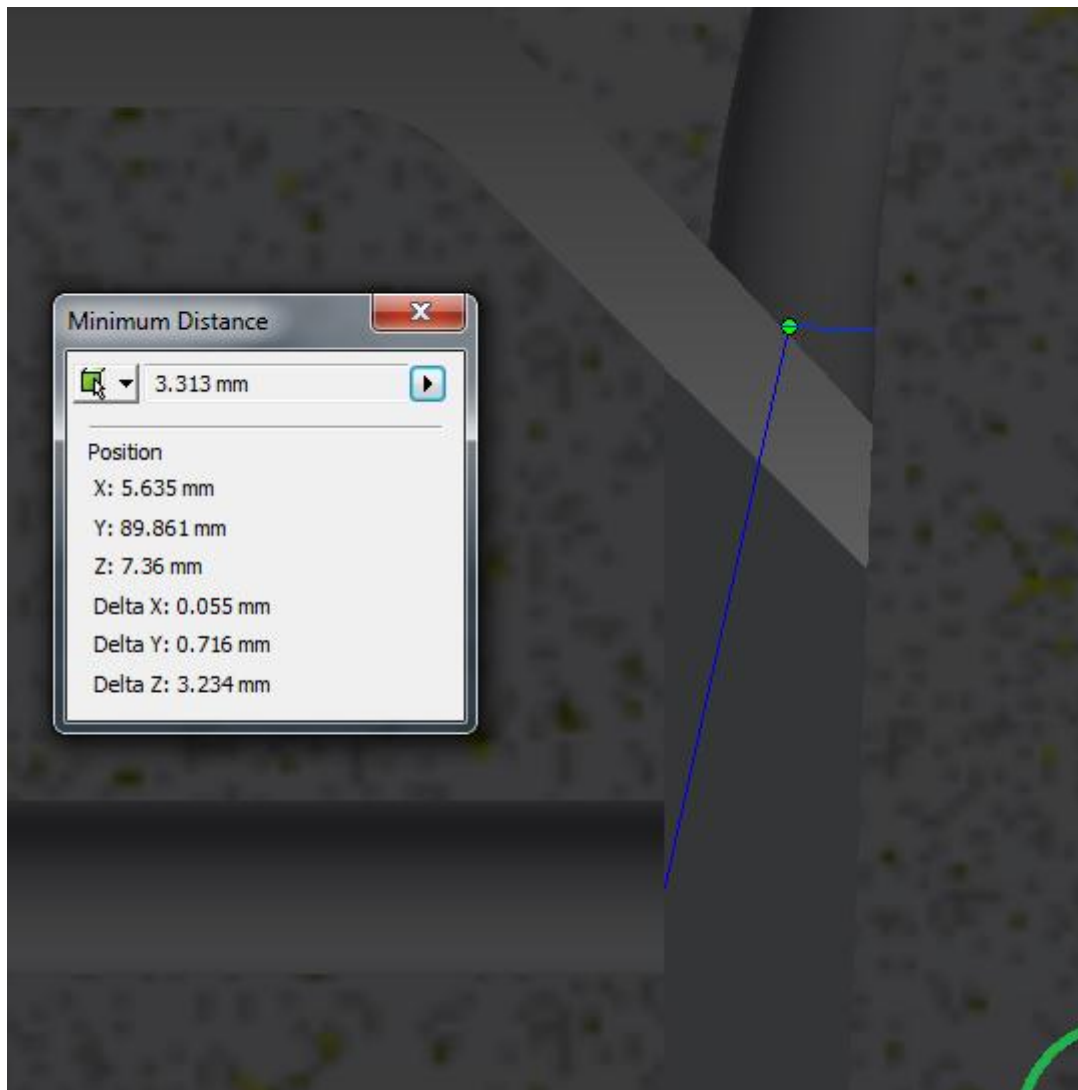


Figure 202: Details upper cable minimum position

ANNEX 9: DETAILS MEASUREMENT MCP JOINT POINTER FINGER

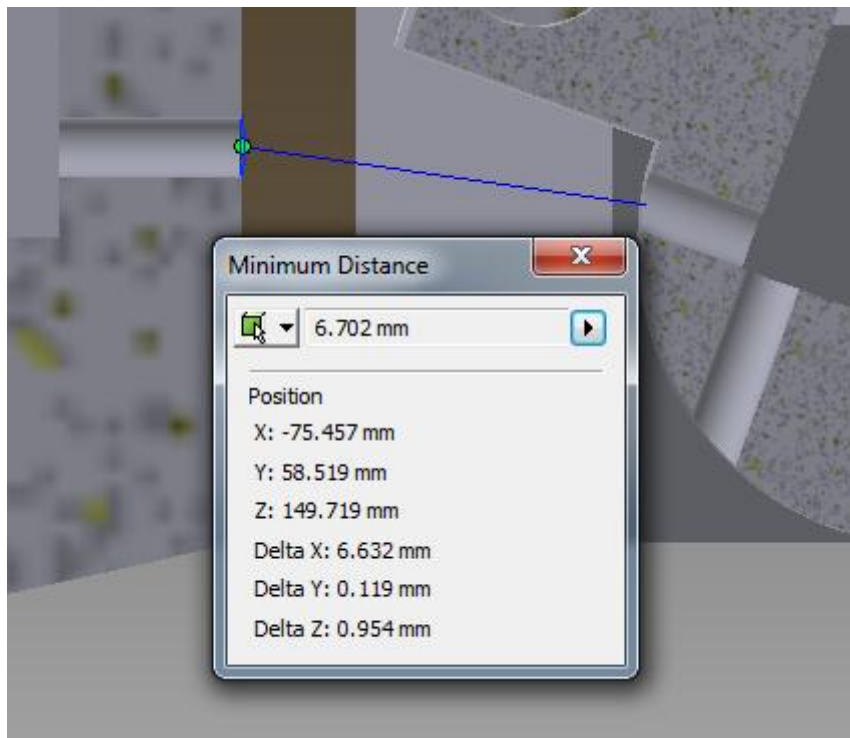


Figure 203: Details lower cable adduction minimum position

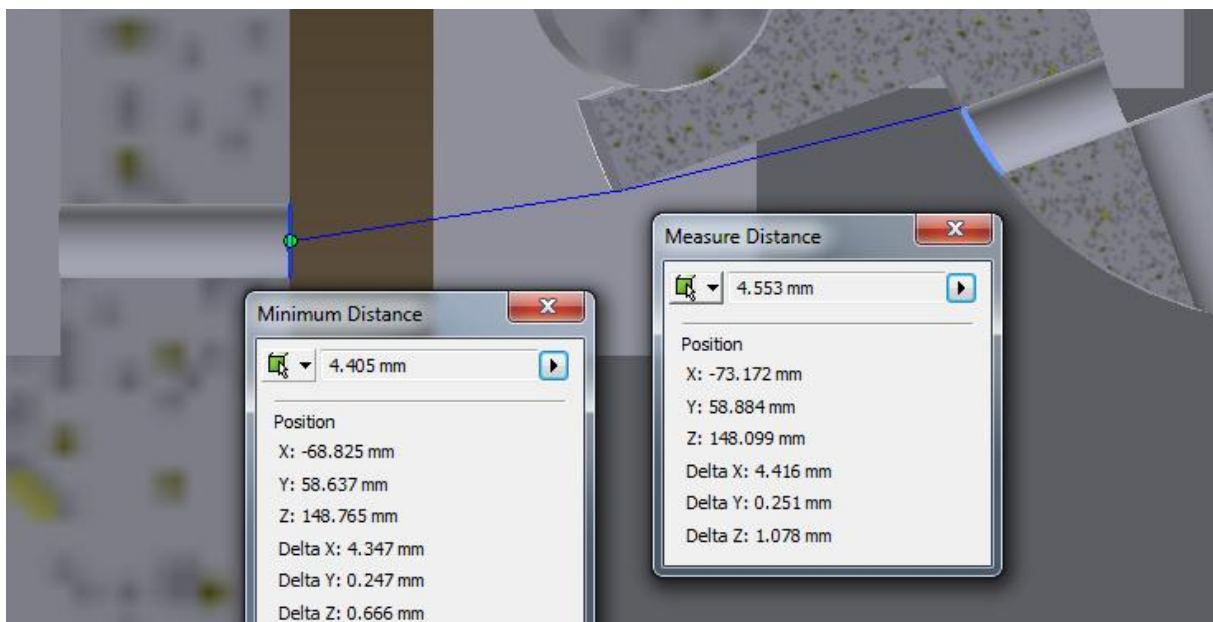


Figure 204: Details lower cable abduction maximum position

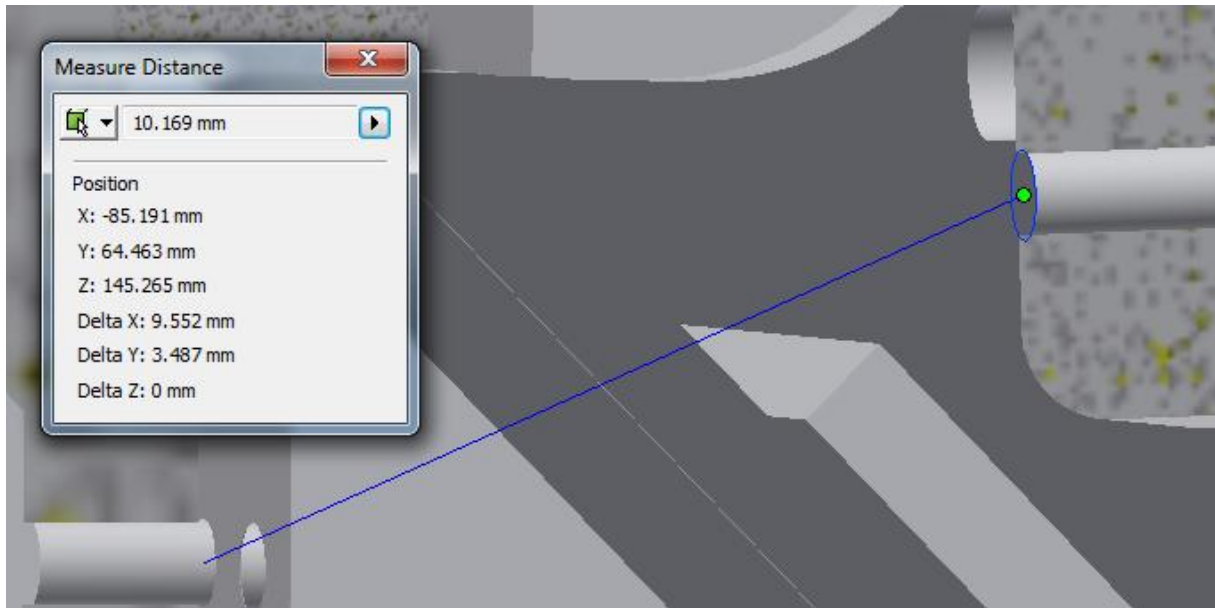


Figure 205: Details lower cable MCP minimum position

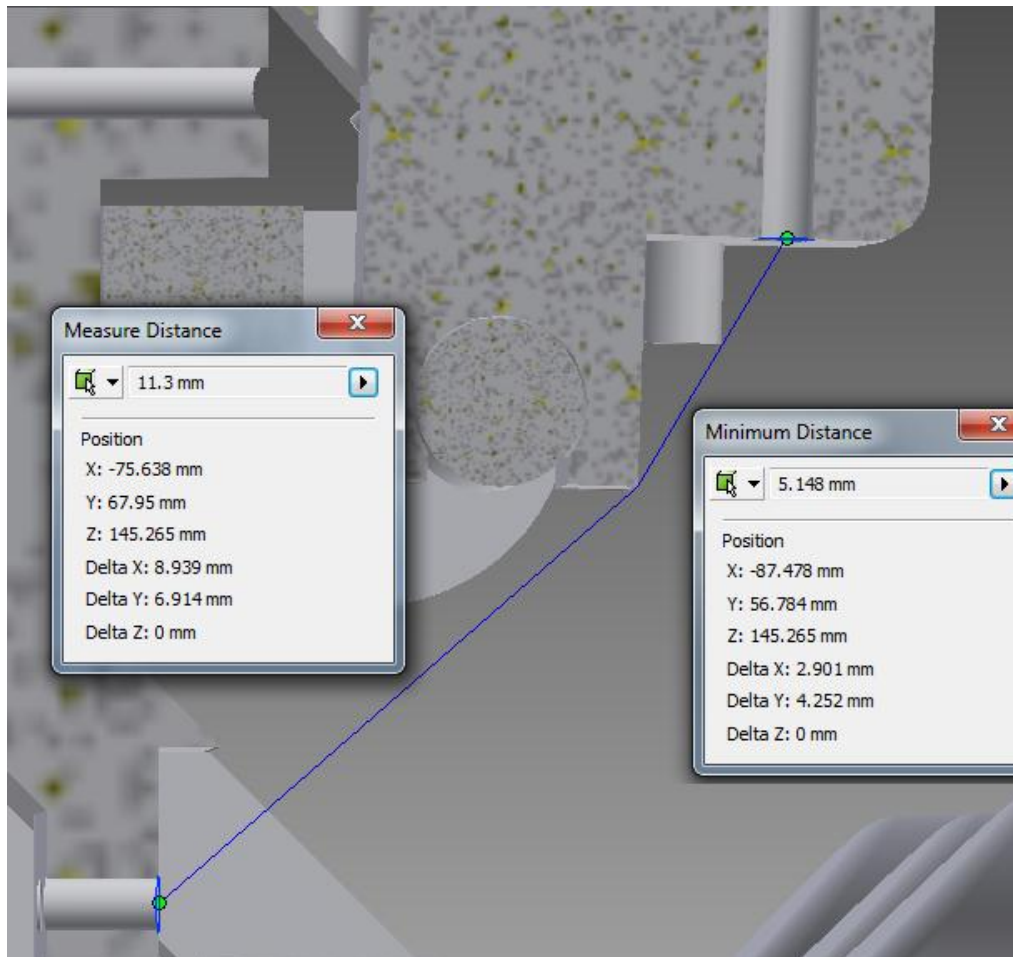


Figure 206: Details lower cable MCP maximum position

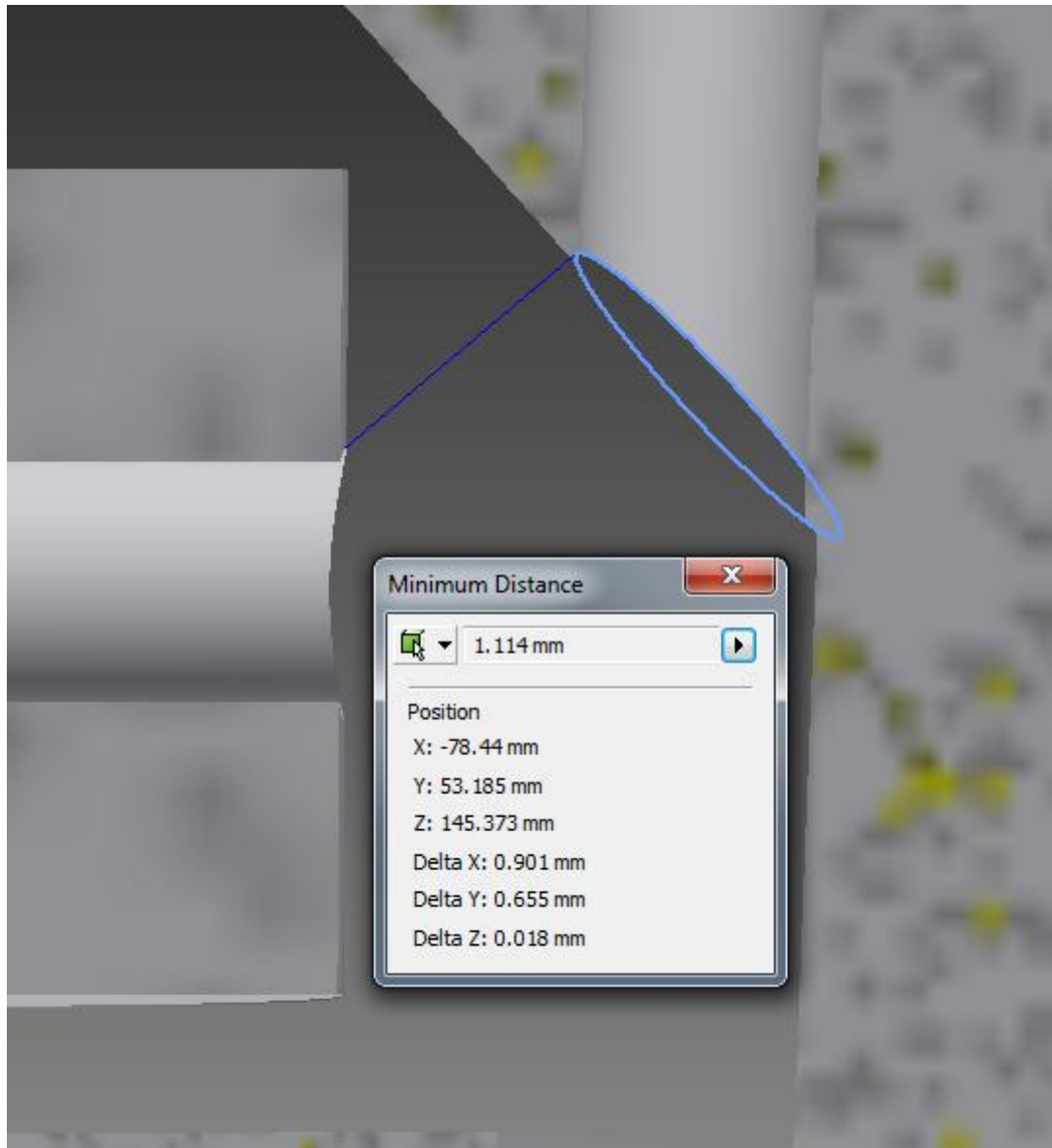


Figure 207: Details upper cable MCP minimum position

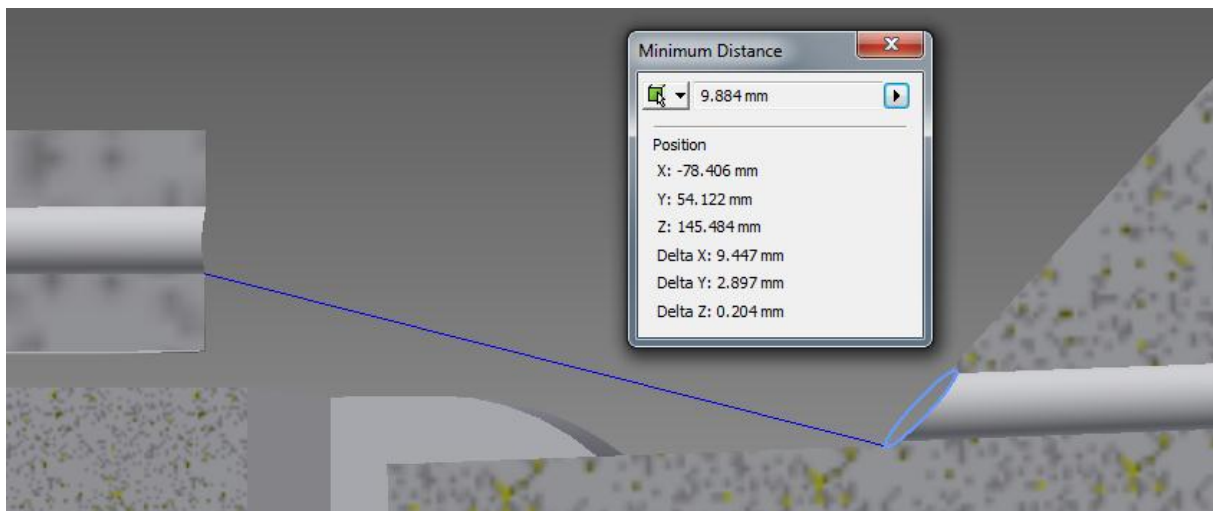


Figure 208: Details upper cable MCP maximum position

ANNEX 10: DETAIL MEASUREMENTS TMC JOINT THUMB

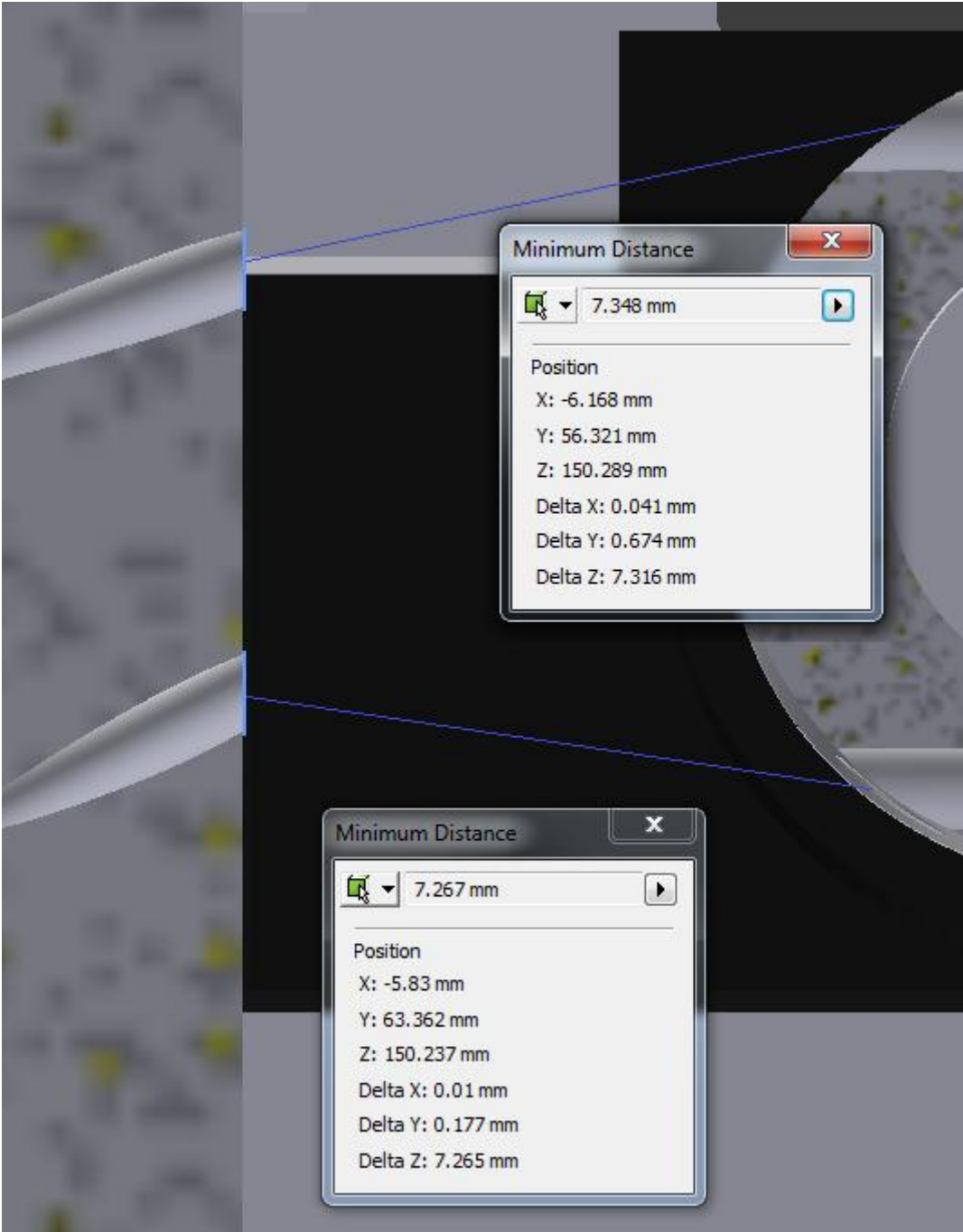


Figure 209: Details minimum distance TMC

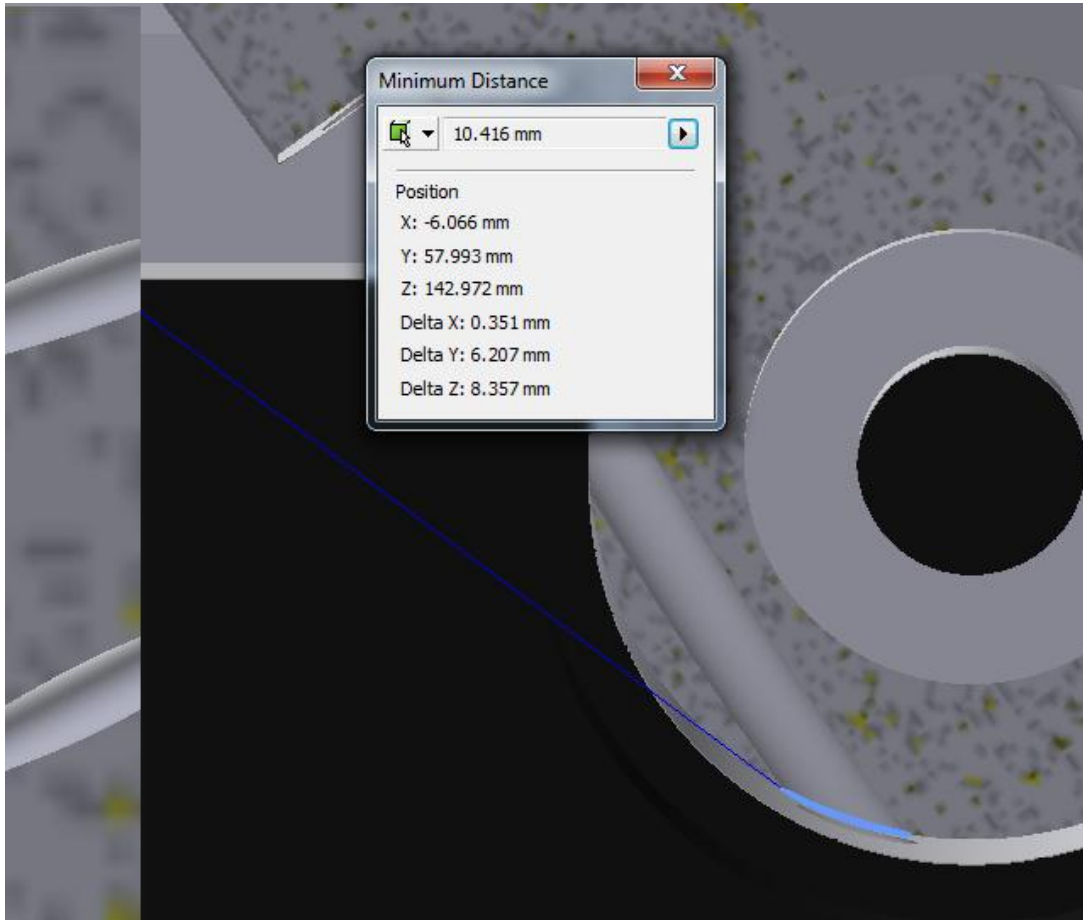


Figure 210: Details measurement upper cable TMC maximum position

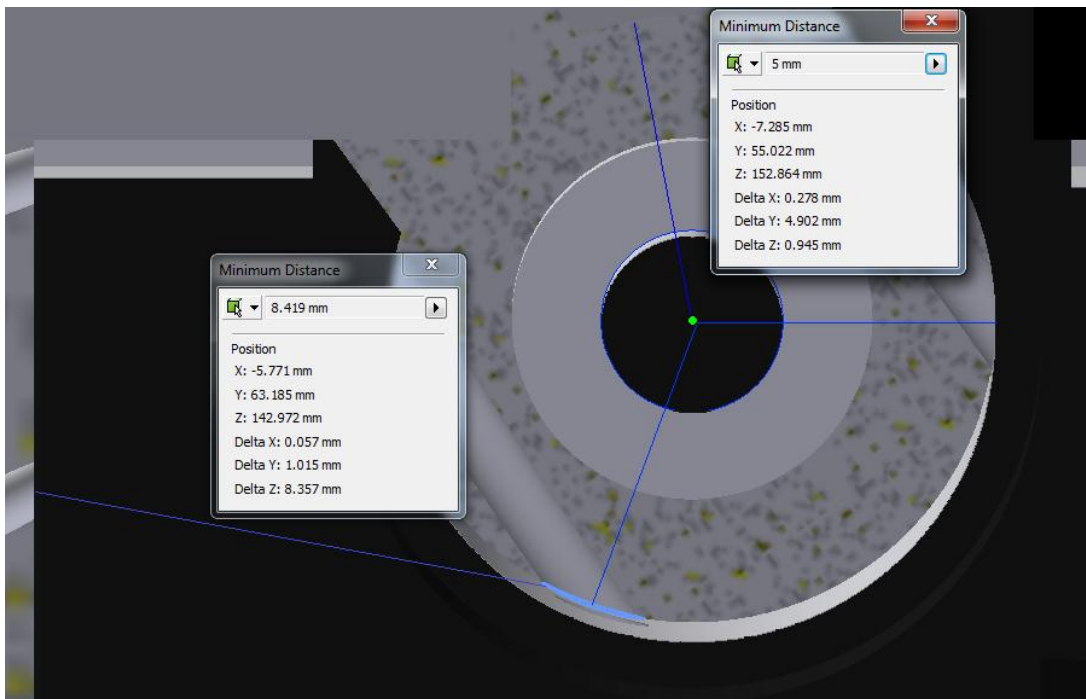


Figure 211: Details lower cable TMC maximum position

ANNEX 11: LOCATION ACTUATORS

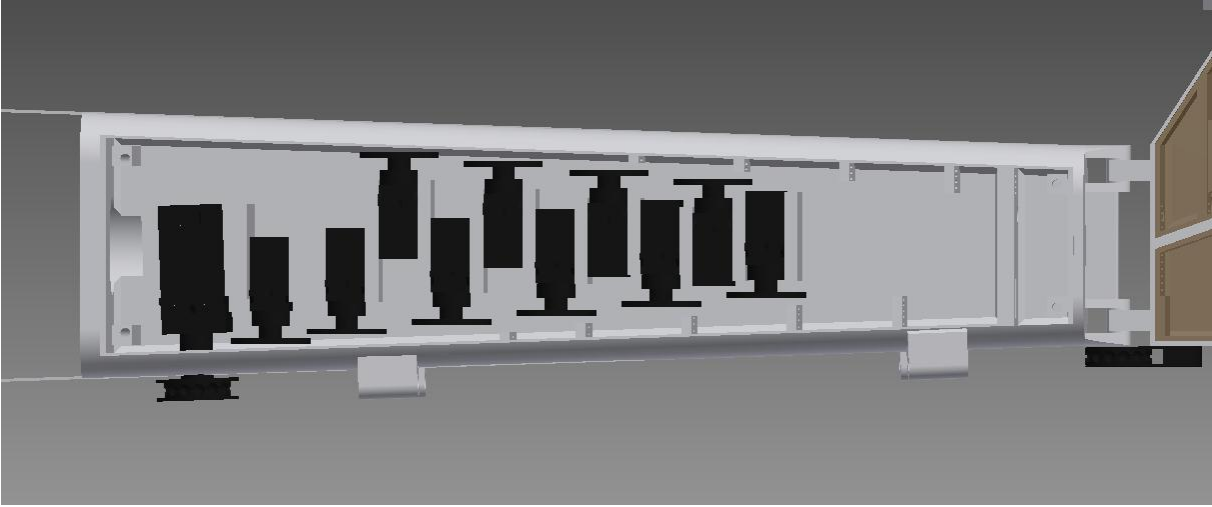


Figure 212: Location actuator in arm

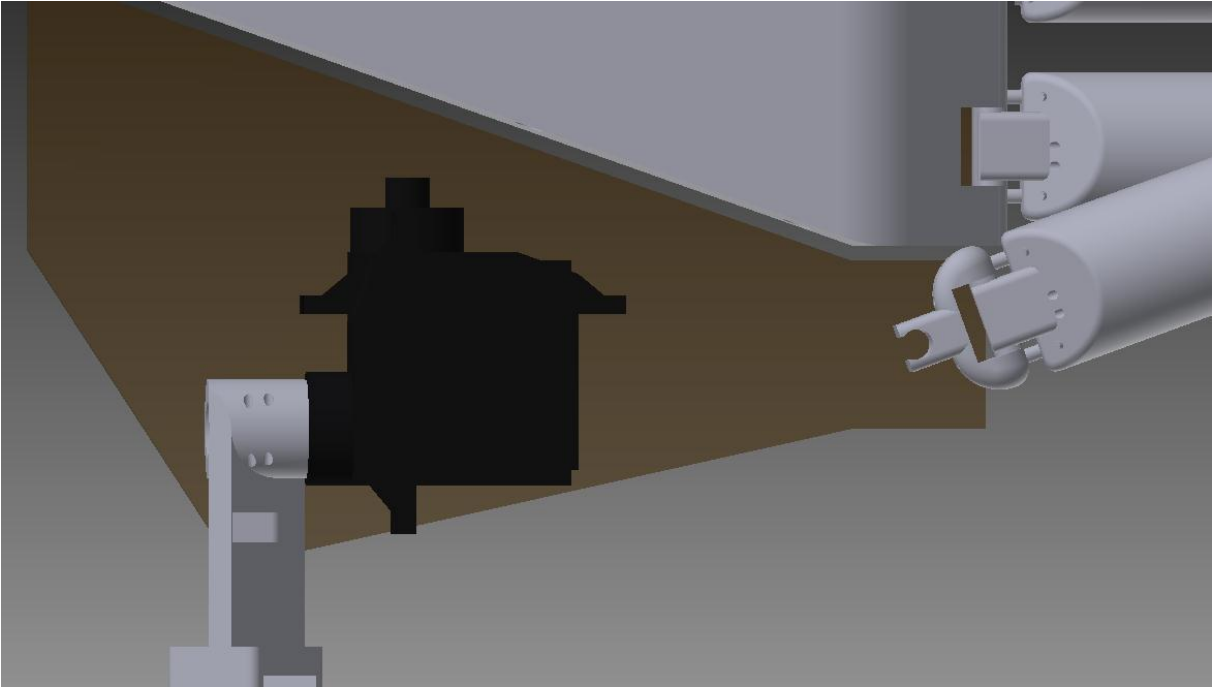


Figure 213: Location actuators in the palm of the hand

ANNEX 12: DESIGN CABLE SYSTEM IN ARM

Table 41: Exact calculations depending in distance until guidance

R =	10	mm								
		A (mm) =	30	40	50	60	70	80	90	100
Extension =		S =	20	30	40	50	60	70	80	90
	1		21	31	41	51	61	71	81	91
	2		22	32	42	52	62	72	82	92
	3		23	33	43	53	63	73	83	93
	4		24	34	44	54	64	74	84	94
	5		25	35	45	55	65	75	85	95
	6		26	36	46	56	66	76	86	96
	7		27	37	47	57	67	77	87	97
	8		28	38	48	58	68	78	88	98
	9		29	39	49	59	69	79	89	99
	10		30	40	50	60	70	80	90	100
	11		31	41	51	61	71	81	91	101
	12		32	42	52	62	72	82	92	102
	13		33	43	53	63	73	83	93	103
	14		34	44	54	64	74	84	94	104
	15		35	45	55	65	75	85	95	105
	16		36	46	56	66	76	86	96	106
	17		37	47	57	67	77	87	97	107
	18		38	48	58	68	78	88	98	108
	19		39	49	59	69	79	89	99	109
	20		40	50	60	70	80	90	100	110

Table 42: Solution left part of the equation

$$\frac{-S^2 + A^2 + R^2 + 1}{2R} = \sin \alpha + A \sin \alpha$$

		A (mm) =	30	40	50	60	70	80	90	100
Extension (mm) =		Solution left part =	30.05	40.05	50.05	60.05	70.05	80.05	90.05	100.05
	1		28	37	46	55	64	73	82	91
	2		25.85	33.85	41.85	49.85	57.85	65.85	73.85	81.85
	3		23.6	30.6	37.6	44.6	51.6	58.6	65.6	72.6
	4		21.25	27.25	33.25	39.25	45.25	51.25	57.25	63.25
	5		18.8	23.8	28.8	33.8	38.8	43.8	48.8	53.8
	6		16.25	20.25	24.25	28.25	32.25	36.25	40.25	44.25
	7		13.6	16.6	19.6	22.6	25.6	28.6	31.6	34.6
	8		10.85	12.85	14.85	16.85	18.85	20.85	22.85	24.85
	9		8	9	10	11	12	13	14	15
	10		5.05	5.05	5.05	5.05	5.05	5.05	5.05	5.05
	11		2	1	0	-1	-2	-3	-4	-5
	12		-1.15	-3.15	-5.15	-7.15	-9.15	-11.15	-13.15	-15.15
	13		-4.4	-7.4	-10.4	-13.4	-16.4	-19.4	-22.4	-25.4
	14		-7.75	-11.75	-15.75	-19.75	-23.75	-27.75	-31.75	-35.75
	15		-11.2	-16.2	-21.2	-26.2	-31.2	-36.2	-41.2	-46.2
	16		-14.75	-20.75	-26.75	-32.75	-38.75	-44.75	-50.75	-56.75

	17		-18.4	-25.4	-32.4	-39.4	-46.4	-53.4	-60.4	-67.4
	18		-22.15	-30.15	-38.15	-46.15	-54.15	-62.15	-70.15	-78.15
	19		-26	-35	-44	-53	-62	-71	-80	-89
	20		-29.95	-39.95	-49.95	-59.95	-69.95	-79.95	-89.95	-99.95

Table 43: Solution right part of the equation

		A (mm) =	50	60	70	80	90	100
Degrees	Radials							
		Solution right part =						
1	0.017453		50.01	60.01	70.01	80.01	90.00	100.00
2	0.034907		50.00	60.00	69.99	79.99	89.98	99.97
3	0.05236		49.98	59.97	69.96	79.94	89.93	99.92
4	0.069813		49.95	59.92	69.90	79.87	89.85	99.83
5	0.087266		49.90	59.86	69.82	79.78	89.74	99.71
6	0.10472		49.83	59.78	69.72	79.67	89.61	99.56
7	0.122173		49.75	59.67	69.60	79.53	89.45	99.38
8	0.139626		49.65	59.56	69.46	79.36	89.26	99.17
9	0.15708		49.54	59.42	69.29	79.17	89.05	98.93
10	0.174533		49.41	59.26	69.11	78.96	88.81	98.65
11	0.191986		49.27	59.09	68.90	78.72	88.54	98.35
12	0.20944		49.12	58.90	68.68	78.46	88.24	98.02
13	0.226893		48.94	58.69	68.43	78.17	87.92	97.66
14	0.244346		48.76	58.46	68.16	77.87	87.57	97.27
15	0.261799		48.56	58.21	67.87	77.53	87.19	96.85
16	0.279253		48.34	57.95	67.56	77.18	86.79	96.40
17	0.296706		48.11	57.67	67.23	76.80	86.36	95.92
18	0.314159		47.86	57.37	66.88	76.39	85.90	95.41
19	0.331613		47.60	57.06	66.51	75.97	85.42	94.88
20	0.349066		47.33	56.72	66.12	75.52	84.91	94.31
21	0.366519		47.04	56.37	65.71	75.04	84.38	93.72
22	0.383972		46.73	56.01	65.28	74.55	83.82	93.09
23	0.401426		46.42	55.62	64.83	74.03	83.24	92.44
24	0.418879		46.08	55.22	64.35	73.49	82.63	91.76
25	0.436332		45.74	54.80	63.86	72.93	81.99	91.05
26	0.453786		45.38	54.37	63.35	72.34	81.33	90.32
27	0.471239		45.00	53.91	62.82	71.73	80.64	89.55
28	0.488692		44.62	53.45	62.28	71.11	79.93	88.76

29	0.506145		44.22	52.96	61.71	70.45	79.20	87.95
30	0.523599		43.80	52.46	61.12	69.78	78.44	87.10
31	0.541052		43.37	51.95	60.52	69.09	77.66	86.23
32	0.558505		42.93	51.41	59.89	68.37	76.85	85.33
33	0.575959		42.48	50.86	59.25	67.64	76.02	84.41
34	0.593412		42.01	50.30	58.59	66.88	75.17	83.46
35	0.610865		41.53	49.72	57.91	66.11	74.30	82.49
36	0.628319		41.04	49.13	57.22	65.31	73.40	81.49
37	0.645772		40.53	48.52	56.51	64.49	72.48	80.47
38	0.663225		40.02	47.90	55.78	63.66	71.54	79.42
39	0.680678		39.49	47.26	55.03	62.80	70.57	78.34
40	0.698132		38.95	46.61	54.27	61.93	69.59	77.25
41	0.715585		38.39	45.94	53.49	61.03	68.58	76.13
42	0.733038		37.83	45.26	52.69	60.12	67.55	74.98
43	0.750492		37.25	44.56	51.88	59.19	66.50	73.82
44	0.767945		36.66	43.86	51.05	58.24	65.44	72.63
45	0.785398		36.06	43.13	50.20	57.28	64.35	71.42
46	0.802851		35.45	42.40	49.35	56.29	63.24	70.19
47	0.820305		34.83	41.65	48.47	55.29	62.11	68.93
48	0.837758		34.20	40.89	47.58	54.27	60.96	67.66
49	0.855211		33.56	40.12	46.68	53.24	59.80	66.36
50	0.872665		32.91	39.33	45.76	52.19	58.62	65.04
51	0.890118		32.24	38.54	44.83	51.12	57.42	63.71
52	0.907571		31.57	37.73	43.88	50.04	56.20	62.35
53	0.925025		30.89	36.91	42.93	48.94	54.96	60.98
54	0.942478		30.20	36.08	41.95	47.83	53.71	59.59
55	0.959931		29.50	35.23	40.97	46.71	52.44	58.18
56	0.977384		28.79	34.38	39.97	45.56	51.16	56.75
57	0.994838		28.07	33.52	38.96	44.41	49.86	55.30
58	1.012291		27.34	32.64	37.94	43.24	48.54	53.84
59	1.029744		26.61	31.76	36.91	42.06	47.21	52.36

60	1.047198		25.87	30.87	35.87	40.87	45.87	50.87
61	1.064651		25.12	29.96	34.81	39.66	44.51	49.36
62	1.082104		24.36	29.05	33.75	38.44	43.14	47.83
63	1.099557		23.59	28.13	32.67	37.21	41.75	46.29
64	1.117011		22.82	27.20	31.58	35.97	40.35	44.74
65	1.134464		22.04	26.26	30.49	34.72	38.94	43.17
66	1.151917		21.25	25.32	29.39	33.45	37.52	41.59
67	1.169371		20.46	24.36	28.27	32.18	36.09	39.99
68	1.186824		19.66	23.40	27.15	30.90	34.64	38.39
69	1.204277		18.85	22.44	26.02	29.60	33.19	36.77
70	1.22173		18.04	21.46	24.88	28.30	31.72	35.14
71	1.239184		17.22	20.48	23.74	26.99	30.25	33.50
72	1.256637		16.40	19.49	22.58	25.67	28.76	31.85
73	1.27409		15.57	18.50	21.42	24.35	27.27	30.19
74	1.291544		14.74	17.50	20.26	23.01	25.77	28.52
75	1.308997		13.91	16.50	19.08	21.67	24.26	26.85
76	1.32645		13.07	15.49	17.90	20.32	22.74	25.16
77	1.343904		12.22	14.47	16.72	18.97	21.22	23.47
78	1.361357		11.37	13.45	15.53	17.61	19.69	21.77
79	1.37881		10.52	12.43	14.34	16.25	18.15	20.06
80	1.396263		9.67	11.40	13.14	14.88	16.61	18.35
81	1.413717		8.81	10.37	11.94	13.50	15.07	16.63
82	1.43117		7.95	9.34	10.73	12.12	13.52	14.91
83	1.448623		7.09	8.30	9.52	10.74	11.96	13.18
84	1.466077		6.22	7.27	8.31	9.36	10.40	11.45
85	1.48353		5.35	6.23	7.10	7.97	8.84	9.71
86	1.500983		4.49	5.18	5.88	6.58	7.28	7.97
87	1.518436		3.62	4.14	4.66	5.19	5.71	6.23
88	1.53589		2.74	3.09	3.44	3.79	4.14	4.49
89	1.553343		1.87	2.05	2.22	2.40	2.57	2.75
90	1.570796		1.00	1.00	1.00	1.00	1.00	1.00

91	1.58825		0.13	-0.05	-0.22	-0.40	-0.57	-0.75
92	1.605703		-0.75	-1.09	-1.44	-1.79	-2.14	-2.49
93	1.623156		-1.62	-2.14	-2.66	-3.19	-3.71	-4.23
94	1.640609		-2.49	-3.19	-3.89	-4.58	-5.28	-5.98
95	1.658063		-3.36	-4.23	-5.10	-5.98	-6.85	-7.72
96	1.675516		-4.23	-5.28	-6.32	-7.37	-8.41	-9.46
97	1.692969		-5.10	-6.32	-7.54	-8.76	-9.98	-11.19
98	1.710423		-5.97	-7.36	-8.75	-10.14	-11.54	-12.93
99	1.727876		-6.83	-8.40	-9.96	-11.53	-13.09	-14.66
100	1.745329		-7.70	-9.43	-11.17	-12.91	-14.64	-16.38
101	1.762783		-8.56	-10.47	-12.38	-14.28	-16.19	-18.10
102	1.780236		-9.42	-11.50	-13.58	-15.65	-17.73	-19.81
103	1.797689		-10.27	-12.52	-14.77	-17.02	-19.27	-21.52
104	1.815142		-11.13	-13.55	-15.96	-18.38	-20.80	-23.22
105	1.832596		-11.98	-14.56	-17.15	-19.74	-22.33	-24.92
106	1.850049		-12.82	-15.58	-18.33	-21.09	-23.85	-26.60
107	1.867502		-13.66	-16.59	-19.51	-22.43	-25.36	-28.28
108	1.884956		-14.50	-17.59	-20.68	-23.77	-26.86	-29.95
109	1.902409		-15.33	-18.59	-21.84	-25.10	-28.36	-31.61
110	1.919862		-16.16	-19.58	-23.00	-26.42	-29.84	-33.26
111	1.937315		-16.98	-20.57	-24.15	-27.74	-31.32	-34.90
112	1.954769		-17.80	-21.55	-25.30	-29.04	-32.79	-36.53
113	1.972222		-18.62	-22.52	-26.43	-30.34	-34.25	-38.15
114	1.989675		-19.42	-23.49	-27.56	-31.63	-35.69	-39.76
115	2.007129		-20.22	-24.45	-28.68	-32.90	-37.13	-41.36
116	2.024582		-21.02	-25.40	-29.79	-34.17	-38.55	-42.94
117	2.042035		-21.81	-26.35	-30.89	-35.43	-39.97	-44.51
118	2.059489		-22.59	-27.29	-31.98	-36.67	-41.37	-46.06
119	2.076942		-23.37	-28.21	-33.06	-37.91	-42.76	-47.61
120	2.094395		-24.13	-29.13	-34.13	-39.13	-44.13	-49.13
121	2.111848		-24.89	-30.05	-35.20	-40.35	-45.50	-50.65

122	2.129302		-25.65	-30.95	-36.25	-41.55	-46.84	-52.14
123	2.146755		-26.39	-31.84	-37.29	-42.73	-48.18	-53.63
124	2.164208		-27.13	-32.72	-38.31	-43.91	-49.50	-55.09
125	2.181662		-27.86	-33.60	-39.33	-45.07	-50.80	-56.54
126	2.199115		-28.58	-34.46	-40.34	-46.21	-52.09	-57.97
127	2.216568		-29.29	-35.31	-41.33	-47.35	-53.36	-59.38
128	2.234021		-30.00	-36.15	-42.31	-48.46	-54.62	-60.78
129	2.251475		-30.69	-36.98	-43.28	-49.57	-55.86	-62.15
130	2.268928		-31.37	-37.80	-44.23	-50.66	-57.08	-63.51
131	2.286381		-32.05	-38.61	-45.17	-51.73	-58.29	-64.85
132	2.303835		-32.71	-39.40	-46.10	-52.79	-59.48	-66.17
133	2.321288		-33.37	-40.19	-47.01	-53.83	-60.65	-67.47
134	2.338741		-34.01	-40.96	-47.91	-54.85	-61.80	-68.75
135	2.356194		-34.65	-41.72	-48.79	-55.86	-62.93	-70.00
136	2.373648		-35.27	-42.47	-49.66	-56.85	-64.05	-71.24
137	2.391101		-35.89	-43.20	-50.51	-57.83	-65.14	-72.45
138	2.408554		-36.49	-43.92	-51.35	-58.78	-66.21	-73.65
139	2.426008		-37.08	-44.63	-52.17	-59.72	-67.27	-74.81
140	2.443461		-37.66	-45.32	-52.98	-60.64	-68.30	-75.96
141	2.460914		-38.23	-46.00	-53.77	-61.54	-69.31	-77.09
142	2.478368		-38.78	-46.66	-54.55	-62.43	-70.31	-78.19
143	2.495821		-39.33	-47.32	-55.30	-63.29	-71.28	-79.26
144	2.513274		-39.86	-47.95	-56.04	-64.13	-72.22	-80.31
145	2.530727		-40.38	-48.58	-56.77	-64.96	-73.15	-81.34
146	2.548181		-40.89	-49.18	-57.47	-65.76	-74.05	-82.34
147	2.565634		-41.39	-49.78	-58.16	-66.55	-74.94	-83.32
148	2.583087		-41.87	-50.35	-58.83	-67.31	-75.79	-84.27
149	2.600541		-42.34	-50.91	-59.49	-68.06	-76.63	-85.20
150	2.617994		-42.80	-51.46	-60.12	-68.78	-77.44	-86.10
151	2.635447		-43.25	-51.99	-60.74	-69.48	-78.23	-86.98
152	2.6529		-43.68	-52.51	-61.34	-70.17	-79.00	-87.83

153	2.670354		-44.10	-53.01	-61.92	-70.83	-79.74	-88.65
154	2.687807		-44.50	-53.49	-62.48	-71.47	-80.45	-89.44
155	2.70526		-44.89	-53.96	-63.02	-72.08	-81.15	-90.21
156	2.722714		-45.27	-54.41	-63.54	-72.68	-81.81	-90.95
157	2.740167		-45.63	-54.84	-64.04	-73.25	-82.45	-91.66
158	2.75762		-45.98	-55.26	-64.53	-73.80	-83.07	-92.34
159	2.775074		-46.32	-55.66	-64.99	-74.33	-83.66	-93.00
160	2.792527		-46.64	-56.04	-65.44	-74.83	-84.23	-93.63
161	2.80998		-46.95	-56.41	-65.86	-75.32	-84.77	-94.23
162	2.827433		-47.24	-56.75	-66.26	-75.78	-85.29	-94.80
163	2.844887		-47.52	-57.09	-66.65	-76.21	-85.78	-95.34
164	2.86234		-47.79	-57.40	-67.01	-76.63	-86.24	-95.85
165	2.879793		-48.04	-57.70	-67.36	-77.02	-86.67	-96.33
166	2.897247		-48.27	-57.98	-67.68	-77.38	-87.08	-96.79
167	2.9147		-48.49	-58.24	-67.98	-77.72	-87.47	-97.21
168	2.932153		-48.70	-58.48	-68.26	-78.04	-87.83	-97.61
169	2.949606		-48.89	-58.71	-68.52	-78.34	-88.16	-97.97
170	2.96706		-49.07	-58.91	-68.76	-78.61	-88.46	-98.31
171	2.984513		-49.23	-59.10	-68.98	-78.86	-88.74	-98.61
172	3.001966		-49.37	-59.28	-69.18	-79.08	-88.98	-98.89
173	3.01942		-49.51	-59.43	-69.36	-79.28	-89.21	-99.13
174	3.036873		-49.62	-59.57	-69.51	-79.46	-89.40	-99.35
175	3.054326		-49.72	-59.68	-69.65	-79.61	-89.57	-99.53
176	3.071779		-49.81	-59.78	-69.76	-79.74	-89.71	-99.69
177	3.089233		-49.88	-59.87	-69.85	-79.84	-89.82	-99.81
178	3.106686		-49.93	-59.93	-69.92	-79.92	-89.91	-99.90
179	3.124139		-49.97	-59.97	-69.97	-79.97	-89.97	-99.97
180	3.141593		-50.00	-60.00	-70.00	-80.00	-90.00	-100.00

Table 44: Maximum and minimum angel depending on the shape of the disc

$$\alpha = \sin^{-1} \frac{3.45 \text{ mm}}{R} * \frac{180}{PI} [^\circ]$$

Maximum angle within a radius of is 3.45 mm

α =	20.1818								
Additional length due to the difference of the holes at the guidance to the center of the disc									In both directions!!
A (mm) =	30	40	50	60	70	80	90	100	
Y add =	0.813957	0.611354	0.489413	0.407993	0.349786	0.306106	0.2721214	0.244927	
Y total =	4.263957	4.061354	3.939413	3.857993	3.799786	3.756106	3.7221214	3.694927	
Max α =	25.23904	23.9623	23.19996	22.69337	22.33236	22.06206	21.852111	21.68433	

The situation of the exact calculation is given in Figure 214.

The red part of Table 43 is the part that cannot be used due to 1 mm difference of the cable at the guidance to the center of the RC servo motor disc and the inner radius of the RC servo motor disc. The green and yellow part of the table are solutions of the left part of the equation related to the angle of the disk at different distances to the guidance. Now each mm extension can be translated to a certain angle of the RC servo motor disc.

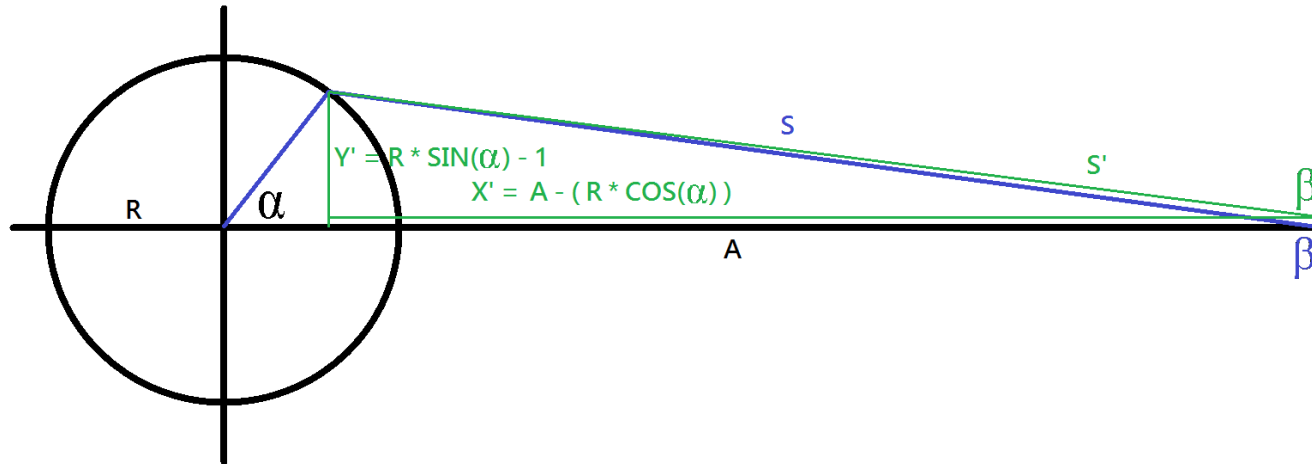


Figure 214: Situation exact calculation

Next equations can be concluded from Figure 214:

$$S'^2 = Y'^2 + X'^2$$

Equation 32: Pythagoras

$$Y' = (R * \sin \alpha) - 1$$

Equation 33: Y' component

$$X' = A - (R * \cos \alpha)$$

Equation 34: X' component

When Equation 33 and Equation 34 are substituted in Equation 32 the result will be:

$$\frac{-S^2 + A^2 + R^2 + 1}{2R} = \sin \alpha + A \sin \alpha$$

Equation 35: Formula exact calculation

ANNEX 13: CONTROL BY APPROACH

All the distances are in mm and angles are in degrees. The calculations are based on the situation given in Figure 214.

Table 45: Approach angles alpha and beta

	A =	30	40	50	60	70	80	90	100		30	40	50	60	70	80	90	100
Extension =	$\alpha =$	0.00	0.00	0.00	0.00	0.00	0.00	0.00	0.00	$\beta =$	6.96	5.49	4.52	3.84	3.33	2.94	2.63	2.38
1		21.30	22.52	23.22	23.68	24.00	24.23	24.42	24.56		9.79	7.68	6.30	5.33	4.62	4.08	3.65	3.30
2		30.68	32.33	33.28	33.90	34.34	34.66	34.92	35.11		11.92	9.29	7.59	6.41	5.55	4.89	4.37	3.95
3		38.28	40.20	41.32	42.06	42.57	42.96	43.25	43.49		13.64	10.56	8.60	7.25	6.26	5.51	4.92	4.44
4		45.04	47.16	48.39	49.21	49.78	50.21	50.54	50.80		15.08	11.60	9.42	7.92	6.83	6.01	5.36	4.84
5		51.32	53.58	54.90	55.77	56.39	56.85	57.20	57.49		16.29	12.46	10.08	8.46	7.29	6.40	5.71	5.15
6		57.32	59.67	61.05	61.97	62.61	63.10	63.47	63.77		17.30	13.16	10.61	8.88	7.64	6.71	5.97	5.38
7		63.15	65.56	66.98	67.92	68.59	69.09	69.48	69.79		18.12	13.70	11.01	9.21	7.91	6.93	6.17	5.56
8		68.90	71.34	72.78	73.74	74.42	74.93	75.33	75.64		18.75	14.10	11.30	9.43	8.09	7.09	6.30	5.67
9		74.63	77.07	78.52	79.48	80.17	80.68	81.08	81.40		19.19	14.36	11.48	9.56	8.19	7.17	6.37	5.73
10		80.41	82.82	84.26	85.22	85.90	86.42	86.82	87.13		19.43	14.47	11.54	9.59	8.21	7.18	6.37	5.73
11		86.27	88.64	90.06	91.00	91.68	92.18	92.58	92.89		19.46	14.43	11.47	9.52	8.14	7.11	6.31	5.67
12		92.29	94.59	95.97	96.89	97.55	98.05	98.43	98.74		19.25	14.22	11.28	9.35	7.98	6.96	6.18	5.55
13		98.53	100.73	102.06	102.95	103.59	104.07	104.44	104.74		18.78	13.82	10.94	9.05	7.72	6.73	5.97	5.36

14		105.07	107.16	108.42	109.27	109.88	110.33	110.69	110.98		18.00	13.21	10.43	8.62	7.34	6.40	5.67	5.09
15		112.02	113.97	115.15	115.94	116.51	116.94	117.28	117.55		16.85	12.33	9.72	8.02	6.83	5.94	5.26	4.72
16		119.56	121.33	122.41	123.14	123.66	124.06	124.36	124.61		15.24	11.12	8.75	7.21	6.14	5.34	4.72	4.23
17		127.95	129.51	130.47	131.11	131.57	131.92	132.20	132.42		12.96	9.44	7.41	6.10	5.19	4.51	3.99	3.57
18		137.73	139.03	139.82	140.35	140.74	141.03	141.26	141.44		9.52	6.92	5.43	4.47	3.79	3.29	2.91	2.61
19		150.27	151.19	151.76	152.15	152.43	152.64	152.80	152.94		0.00	0.00	0.00	0.00	0.00	0.00	0.00	0.00
20		180.00	180.00	180.00	180.00	180.00	180.00	180.00	180.00		0.00	0.00	0.00	0.00	0.00	0.00	0.00	0.00

$$\alpha = \cos^{-1}\left(\frac{R^2 + A^2 - S^2}{2AR}\right) * \frac{180}{PI} [^\circ]$$

$$\beta = \sin^{-1}\left(\frac{R \sin \alpha}{A}\right) * \frac{180}{PI} [^\circ]$$

Table 46: Approach Y' and beta'

	A =	30	40	50	60	70	80	90	100		30	40	50	60	70	80	90	100
Extension =	Y' =	-1.00	-1.00	-1.00	-1.00	-1.00	-1.00	-1.00	-1.00	β' =	-2.86	-1.91	-1.43	-1.15	-0.95	-0.82	-0.72	-0.64
1		2.63	2.83	2.94	3.02	3.07	3.10	3.13	3.16		7.26	5.26	4.12	3.39	2.88	2.51	2.22	1.99
2		4.10	4.35	4.49	4.58	4.64	4.69	4.72	4.75		10.85	7.85	6.15	5.06	4.30	3.74	3.30	2.96
3		5.19	5.46	5.60	5.70	5.77	5.81	5.85	5.88		13.20	9.57	7.51	6.19	5.26	4.57	4.05	3.63
4		6.08	6.33	6.48	6.57	6.64	6.68	6.72	6.75		14.84	10.80	8.50	7.01	5.96	5.19	4.59	4.12
5		6.81	7.05	7.18	7.27	7.33	7.37	7.41	7.43		15.99	11.69	9.22	7.61	6.49	5.65	5.00	4.49
6		7.42	7.63	7.75	7.83	7.88	7.92	7.95	7.97		16.78	12.32	9.74	8.06	6.87	5.99	5.31	4.77
7		7.92	8.10	8.20	8.27	8.31	8.34	8.37	8.38		17.27	12.73	10.09	8.36	7.14	6.23	5.52	4.96
8		8.33	8.47	8.55	8.60	8.63	8.66	8.67	8.69		17.51	12.97	10.30	8.55	7.31	6.38	5.66	5.09
9		8.64	8.75	8.80	8.83	8.85	8.87	8.88	8.89		17.54	13.04	10.39	8.63	7.39	6.46	5.73	5.16
10		8.86	8.92	8.95	8.97	8.97	8.98	8.98	8.99		17.37	12.97	10.35	8.62	7.38	6.45	5.74	5.16
11		8.98	9.00	9.00	9.00	9.00	8.99	8.99	8.99		17.01	12.75	10.20	8.50	7.29	6.38	5.68	5.11
12		8.99	8.97	8.95	8.93	8.91	8.90	8.89	8.88		16.48	12.40	9.94	8.30	7.12	6.24	5.55	5.00
13		8.89	8.83	8.78	8.75	8.72	8.70	8.68	8.67		15.77	11.90	9.57	8.00	6.87	6.02	5.36	4.83
14		8.66	8.55	8.49	8.44	8.40	8.38	8.35	8.34		14.87	11.26	9.07	7.59	6.53	5.73	5.10	4.60
15		8.27	8.14	8.05	7.99	7.95	7.91	7.89	7.87		13.77	10.46	8.44	7.08	6.09	5.35	4.77	4.30
16		7.70	7.54	7.44	7.37	7.32	7.28	7.25	7.23		12.43	9.47	7.66	6.43	5.54	4.86	4.34	3.91

17		6.89	6.71	6.61	6.53	6.48	6.44	6.41	6.38		10.78	8.24	6.67	5.61	4.83	4.25	3.79	3.42
18		5.73	5.56	5.45	5.38	5.33	5.29	5.26	5.23		8.70	6.67	5.40	4.54	3.92	3.45	3.08	2.78
19		3.96	3.82	3.73	3.67	3.63	3.60	3.57	3.55		5.84	4.48	3.63	3.05	2.63	2.32	2.07	1.87
20		-1.00	-1.00	-1.00	-1.00	-1.00	-1.00	-1.00	-1.00		-1.43	-1.15	-0.95	-0.82	-0.72	-0.64	-0.57	-0.52

$$Y' = (R \sin a) - 1$$

$$\beta' = \tan^{-1} \frac{Y'}{X'} * \frac{180}{PI} [^\circ]$$

Table 47: Approach X' and S'

	A =	30	40	50	60	70	80	90	100		30	40	50	60	70	80	90	100
Extension =	X' =	20.00	30.00	40.00	50.00	60.00	70.00	80.00	90.00	S' =	20.02	30.02	40.01	50.01	60.01	70.01	80.01	90.01
1		20.68	30.76	40.81	50.84	60.86	70.88	80.89	90.91		20.85	30.89	40.92	50.93	60.94	70.95	80.96	90.96
2		21.40	31.55	41.64	51.70	61.74	71.78	81.80	91.82		21.79	31.85	41.88	51.90	61.92	71.93	81.94	91.94
3		22.15	32.36	42.49	52.58	62.64	72.68	82.72	92.75		22.75	32.82	42.86	52.88	62.90	72.91	82.92	92.93
4		22.93	33.20	43.36	53.47	63.54	73.60	83.64	93.68		23.72	33.80	43.84	53.87	63.89	73.90	83.91	93.92
5		23.75	34.06	44.25	54.38	64.46	74.53	84.58	94.63		24.71	34.78	44.83	54.86	64.88	74.89	84.91	94.92
6		24.60	34.95	45.16	55.30	65.40	75.48	85.53	95.58		25.69	35.77	45.82	55.85	65.87	75.89	85.90	95.91
7		25.48	35.86	46.09	56.24	66.35	76.43	86.49	96.55		26.69	36.77	46.81	56.85	66.87	76.89	86.90	96.91
8		26.40	36.80	47.04	57.20	67.31	77.40	87.47	97.52		27.68	37.76	47.81	57.84	67.87	77.88	87.90	97.91
9		27.35	37.76	48.01	58.18	68.29	78.38	88.45	98.51		28.68	38.76	48.81	58.84	68.86	78.88	88.89	98.91
10		28.33	38.75	49.00	59.17	69.29	79.38	89.44	99.50		29.69	39.76	49.81	59.84	69.86	79.88	89.89	99.91
11		29.35	39.76	50.01	60.18	70.29	80.38	90.45	100.51		30.69	40.77	50.81	60.84	70.87	80.88	90.90	100.91
12		30.40	40.80	51.04	61.20	71.31	81.40	91.47	101.52		31.70	41.77	51.82	61.85	71.87	81.89	91.90	101.91
13		31.48	41.86	52.09	62.24	72.35	82.43	92.49	102.55		32.71	42.78	52.82	62.85	72.87	82.89	92.90	102.91
14		32.60	42.95	53.16	63.30	73.40	83.48	93.53	103.58		33.73	43.79	53.83	63.86	73.88	83.89	93.91	103.91
15		33.75	44.06	54.25	64.38	74.46	84.53	94.58	104.63		34.75	44.81	54.84	64.87	74.89	84.90	94.91	104.92
16		34.93	45.20	55.36	65.47	75.54	85.60	95.64	105.68		35.77	45.82	55.86	65.88	75.90	85.91	95.92	105.93

17		36.15	46.36	56.49	66.58	76.64	86.68	96.72	106.75		36.80	46.85	56.88	66.89	76.91	86.92	96.93	106.94
18		37.40	47.55	57.64	67.70	77.74	87.78	97.80	107.82		37.84	47.87	57.90	67.91	77.93	87.93	97.94	107.95
19		38.68	48.76	58.81	68.84	78.86	88.88	98.89	108.91		38.89	48.91	58.93	68.94	78.95	88.95	98.96	108.96
20		40.00	50.00	60.00	70.00	80.00	90.00	100.00	110.00		40.01	50.01	60.01	70.01	80.01	90.01	100.00	110.00

$$X' = A - (R * \cos a)$$

$$S' = \sqrt{Y'^2 + X'^2}$$

Table 48: Deviation from exact calculation

A =	30.00	40.00	50.00	60.00	70.00	80.00	90.00	100.00		A =	30.00	40.00	50.00	60.00	70.00	80.00	90.00	100.00
$\Delta b =$	9.82	7.40	5.95	4.98	4.29	3.76	3.35	3.02		$\Delta S =$	-0.02	-0.02	-0.01	-0.01	-0.01	-0.01	-0.01	-0.01
	2.54	2.43	2.18	1.94	1.74	1.57	1.43	1.31			0.15	0.11	0.08	0.07	0.06	0.05	0.04	0.04
	1.06	1.44	1.44	1.35	1.25	1.15	1.06	0.98			0.21	0.15	0.12	0.10	0.08	0.07	0.06	0.06
	0.44	0.99	1.09	1.06	1.00	0.94	0.87	0.82			0.25	0.18	0.14	0.12	0.10	0.09	0.08	0.07
	0.24	0.81	0.92	0.91	0.87	0.82	0.77	0.72			0.28	0.20	0.16	0.13	0.11	0.10	0.09	0.08
	0.30	0.77	0.86	0.85	0.80	0.75	0.70	0.66			0.29	0.22	0.17	0.14	0.12	0.11	0.09	0.08
	0.52	0.84	0.87	0.83	0.77	0.72	0.66	0.62			0.31	0.23	0.18	0.15	0.13	0.11	0.10	0.09
	0.85	0.97	0.92	0.84	0.77	0.70	0.65	0.60			0.31	0.23	0.19	0.15	0.13	0.11	0.10	0.09
	1.24	1.13	1.00	0.88	0.78	0.70	0.64	0.58			0.32	0.24	0.19	0.16	0.13	0.12	0.10	0.09
	1.65	1.32	1.09	0.93	0.81	0.71	0.64	0.58			0.32	0.24	0.19	0.16	0.14	0.12	0.11	0.09
	2.06	1.51	1.19	0.98	0.83	0.72	0.64	0.57			0.31	0.24	0.19	0.16	0.14	0.12	0.11	0.09
	2.44	1.68	1.27	1.02	0.85	0.73	0.63	0.56			0.31	0.23	0.19	0.16	0.13	0.12	0.10	0.09
	2.77	1.82	1.34	1.05	0.86	0.72	0.62	0.55			0.30	0.23	0.18	0.15	0.13	0.11	0.10	0.09
	3.01	1.92	1.37	1.05	0.85	0.71	0.60	0.52			0.29	0.22	0.18	0.15	0.13	0.11	0.10	0.09
	3.13	1.94	1.36	1.02	0.81	0.67	0.56	0.48			0.27	0.21	0.17	0.14	0.12	0.11	0.09	0.09
	3.09	1.87	1.28	0.95	0.74	0.60	0.50	0.42			0.25	0.19	0.16	0.13	0.11	0.10	0.09	0.08
	2.81	1.65	1.10	0.79	0.60	0.47	0.38	0.32			0.23	0.18	0.14	0.12	0.10	0.09	0.08	0.07

	2.17	1.19	0.74	0.50	0.35	0.26	0.20	0.15			0.20	0.15	0.12	0.11	0.09	0.08	0.07	0.06
	0.81	0.25	0.03	-0.08	-0.13	-0.15	-0.17	-0.17			0.16	0.13	0.10	0.09	0.07	0.07	0.06	0.05
	-5.84	-4.48	-3.63	-3.05	-2.63	-2.32	-2.07	-1.87			0.11	0.09	0.07	0.06	0.05	0.05	0.04	0.04
	1.43	1.15	0.95	0.82	0.72	0.64	0.57	0.52			-0.01	-0.01	-0.01	-0.01	-0.01	-0.01	0.00	0.00
MAX $\Delta b =$	3.13	2.43	2.18	1.94	1.74	1.57	1.43	1.31		MAX $\Delta S =$	0.32	0.24	0.19	0.16	0.14	0.12	0.11	0.09

$$\Delta b = b - b'$$

$$\Delta S = S - S'$$

From the result shown in Table 48 it can be seen that the deviation between exact calculation and the approach is minimum and the deviation gets less by increasing the distance from the center of the RC servo motor disc to the additional guidance. Therefore it is necessary to maximize the distance between RC servo motor and guidance.

ANNEX 14: STEREO LITHOGRAPHY: PROPERTIES AND MATERIALS



Details Stereolithography

Standard lead time:	From 2 days, depending on the size of the parts and the number of components.
Standard accuracy:	Standard stereolithography $\pm 0.2\%$ (min ± 0.2 mm). Sensitive to UV-light (e.g. direct sunlight).
Surface finish:	Without post-finishing, dependent upon the orientation of the layers. Different finishes from high gloss to a rough texture are obtained by post-finishing.
Maximum part dimensions:	2100x700x800 mm
Capacity:	Materialise has over 30 stereolithography machines: 4 Next Day machines; 13 Mammoth machines; 8 SLA250 machines; 3 SLA3500 machines; 1 SLA5000 machine and 4 SLA7000 machines.
Materials:	Tusk Somos® SolidGrey3000 TuskXC2700T / Tusk2700W Poly1500 Xtreme PerFORM Protogen White WaterClear

Details Next Day Stereolithography

Lead time:	Parts ordered before 12am are shipped the same day.
Standard accuracy:	$\pm 0.2\%$ (min ± 0.2 mm)
Surface finish:	Basic finishing
Maximum part dimensions:	650x650x480 mm (x, y, z)
Capacity:	The overall Next Day capacity is sufficient to produce supported parts that fit in an envelope of 650x650x480 mm (x, y, z). Our stereolithography machine park houses 4 Next Day machines.
Materials:	Poly1500 Tusk2700W Protogen White

Details Mammoth Stereolithography

Lead time:	From 2 days, depending on the size of the parts and the number of components
Accuracy:	$\pm 0.2\%$ (min ± 0.2 mm)
Surface finish:	Different finishes from smooth finish up to high gloss can be obtained by post-finishing
Maximum part dimensions:	2100x700x800 mm
Capacity:	13 Mammoth machines

1 The information and values included in these datasheets, although based on Materialise's knowledge and experience and thus presented in good faith and believed to be accurate, is provided for your guidance only. This information does not release a third party from conducting his own procedures and tests to determine suitability. All guarantees with respect to the information contained herein are explicitly denied.

Last update: July 2014

Datasheet			
Tusk Somos® SolidGrey3000			
	Units	ASTM#	Range
Density	g/cm ³		1.18 – 1.2
Tensile Modulus	MPa	D638M	2970 – 3285
Tensile Strength at yield	MPa	D638M	60 – 66
Elongation at Yield	%	D638M	3.0
Elongation at Break	%	D638M	4.6 – 7.2
Flexural Modulus	MPa	D790M	1843 – 2017
Hardness	ShoreD	D2240	84
Notched Izod Impact	J/m	D256A	30 – 35
Water Absorption	%	D570-98	0.36 – 0.40
Tg	°C	E1545-05a	40–48
Heat Deflection Temp (0.46MPa)	°C	D648 - 07B	53 – 57
Heat Deflection Temp (1.82MPa)	°C	D648 - 07B	49 – 57
Appearance	Opaque Gray		
Actual values may vary with build conditions			



- ✓ Stiff
- ✓ Impact resistant
- ✓ Water resistant
- ✓ Durable

- ✓ Automotive body parts
- ✓ Machine covers
- ✓ Functional prototypes
- ✓ Durable concept models
- ✓ Robust scale models

Datasheet			
TuskXC2700T / Tusk2700W			
	Units	ASTM#	Range
Density	g/cm ³		1.18 – 1.2
Tensile Modulus	MPa	D638M	2650 – 2880
Tensile Strength	MPa	D638M	47.1 – 53.6
Elongation at Break	%	D638M	11 – 20
Flexural Modulus	MPa	D790M	2040 – 2370
Flexural Strength	MPa	D790M	63.1 – 74.16
Notched Izod Impact	J/m	D256A	20 – 30
Hardness	Shore D	D2240	81
Heat Deflection Temp	°C	D648 - 98c	at 0.46 MPa: 45.9 – 54.5 at 1.81 MPa: 49.0 – 49.7
Colour	Transparent or white		
Actual values may vary with build conditions			

- ✓ Transparent (TuskXC2700T)
- ✓ Strong
- ✓ Water resistant
- ✓ Durable

- ✓ Functional prototypes
- ✓ Wind tunnel testing
- ✓ Water flow analysis
- ✓ High-end finished models
- ✓ ABS-like parts

2 The information and values included in these datasheets, although based on Materialise's knowledge and experience and thus presented in good faith and believed to be accurate, is provided for your guidance only. This information does not release a third party from conducting his own procedures and tests to determine suitability. All guarantees with respect to the information contained herein are explicitly denied.

Last update: July 2014

Datasheet			
Protogen White			
	Units	ASTM#	Range
Density	g/cm ³		1.18 – 1.2
Tensile Modulus	MPa	D638M	2310
Tensile Strength	MPa	D638M	43.8
Elongation at Break	%	D638M	16
Flexural Modulus	MPa	D790M	2130
Flexural Strength	MPa	D790M	70.5
Notched Izod Impact	J/m	D256A	22
Hardness	Shore D	D2240	88
Water Absorption	%	D570-98	0.68%
Tg	°C	E1545-00	57 - 59
Heat Deflection Temp	°C	D648 - 98c	at 0.46 MPa: 56 at 1.82 MPa: 47
Colour	White		
Actual values may vary with build conditions			

- ✓ Flexible
- ✓ Impact resistant
- ✓ Tough
- ✓ Durable
- ✓ Automotive components
- ✓ Electronic housings
- ✓ Snap-fit assemblies
- ✓ PP-like parts

Datasheet			
Poly1500			
	Units	ASTM#	Range
Density	g/cm ³		1.18 – 1.2
Tensile Modulus	MPa	D638M	1227 – 1462
Tensile Strength	MPa	D638M	30 – 32
Elongation at Break	%	D638M	15 – 25
Flexural Modulus	MPa	D790M	1310 – 1455
Flexural Strength	MPa	D790M	41 – 46
Notched Izod Impact	J/m	D256A	48 – 53
Hardness	Shore D	D2240	80 – 82
Heat Deflection Temp at 0,46 MPa	°C	D648	52 – 61
Colour	Translucent		
Actual values may vary with build conditions			

- ✓ Tough
- ✓ Good surface quality
- ✓ Good thermal properties
- ✓ Durable
- ✓ Impellers
- ✓ Duct work and connectors
- ✓ Automotive housings
- ✓ Dashboard assemblies
- ✓ High-end finished models

3 The information and values included in these datasheets, although based on Materialise's knowledge and experience and thus presented in good faith and believed to be accurate, is provided for your guidance only. This information does not release a third party from conducting his own procedures and tests to determine suitability. All guarantees with respect to the information contained herein are explicitly denied.

Last update: July 2014

Datasheet			
PerFORM			
	Units	ASTM#	Range
Density	g/cm ³		1,61 @ 25°C
Tensile Modulus	MPa	D638M	10500
Tensile Strength	MPa	D638M	61.7 – 78
Elongation at Break	%	D638M	1,1
Flexural Modulus	MPa	D790M	10000
Flexural Strength	MPa	D790M	120
Notched Izod Impact	J/m	D256A	17
Water Absorption	%	D570-98	0,2
Heat Deflection Temp	°C	D648-98c	at 0.46 MPa: 225 at 1.82 MPa: 85 – 90
Colour	Off white		
Actual values may vary with build conditions			

- ✓ Stiff
- ✓ High temperature resistance
- ✓ Superior sidewall quality
- ✓ Brittle

- ✓ High temperature applications
- ✓ Automotive
- ✓ Aerospace

Datasheet			
Xtreme			
	Units	ASTM#	Range
Density	g/cm ³		1,18 – 1,2
Tensile Modulus	MPa	D638M	1790 – 1980
Tensile Strength	MPa	D638M	38 – 44
Elongation at Break	%	D638M	14 – 22
Flexural Modulus	MPa	D790M	1520 – 2070
Notched Izod Impact	J/m	D256A	35 – 52
Heat Deflection Temp	°C	D648-98c	at 0.45 MPa: 62 at 1.82 MPa: 54
Colour	Grey		
Actual values may vary with build conditions			

- ✓ Tough
- ✓ Impact resistant
- ✓ High elongation at break
- ✓ Excellent surface quality

- ✓ Tough enclosures
- ✓ Snap-fit assemblies
- ✓ Replacing CNC machined parts
- ✓ High-end finished models

4 The information and values included in these datasheets, although based on Materialise's knowledge and experience and thus presented in good faith and believed to be accurate, is provided for your guidance only. This information does not release a third party from conducting his own procedures and tests to determine suitability. All guarantees with respect to the information contained herein are explicitly denied.

Last update: July 2014

Datasheet			
WaterClear			
	Units	ASTM#	Range
Density	g/cm ³		1.18 – 1.2
Tensile Modulus	MPa	D638M	2860 – 2900
Tensile Strength at Break	MPa	D638M	55 – 56
Elongation at Break	%	D638M	6 – 9
Flexural Modulus	MPa	D790M	2410 – 2570
Flexural Strength	MPa	D790M	82 – 85
Notched Izod Impact	J/m	D256A	24 – 26
Water Absorption	%	D570-98	1.1
Tg	°C	E1545-00	42 – 46
Heat Deflection Temp	°C		At 0.46 Mpa: 46 – 47 At 1.82 MPa: 42 – 43
Colour	Transparant		
Actual values may vary with build conditions			

- ✓ Optically clear
- ✓ Lower mechanical properties than TuskXC2700T
- ✓ Prototype parts that require fully neutral transparency

5 The information and values included in these datasheets, although based on Materialise's knowledge and experience and thus presented in good faith and believed to be accurate, is provided for your guidance only. This information does not release a third party from conducting his own procedures and tests to determine suitability. All guarantees with respect to the information contained herein are explicitly denied.

Last update: July 2014

Name	Impact strength	Stiffness	Humidity resistance	Heat resistance	Durability	Appearance	Mould	Details	Description	Applications
Tusk Somos® SolidGrey3000	Excellent	Excellent	Excellent	Good	Good	Grey	Good	Good	Stiff Impact resistant Water resistant Durable	Automotive body parts Machine covers Functional prototypes Durable concept models Robust scale models
TuskXC2700T Tusk2700W	Good	Good	Excellent	Sensitive	Good	Optical clear with a light blue tinge or White	Excellent	Moderate	Tough Impact resistant High elongation at break Excellent surface quality	Functional prototypes Wind tunnel testing Water flow analysis High-end finished models ABS-like parts
Protogen White	Good	Good	Good	Good	Good	White	Excellent	Good	Tough Good surface quality Good thermal properties Durable	Impellers Duct work and connectors Automotive housings Dashboard assemblies High-end finished models
Poly1500	Good	Moderate	Moderate	Moderate	Good	Translucent	Moderate	Good	Flexible Impact resistant Tough Durable	Automotive components Electronic housings Snap-fit assemblies PP-like parts
Xtreme	Excellent	Good	Good	Good	Good	Grey	Good	Excellent	Tough Impact resistant High elongation at break Excellent surface quality	Tough enclosures Snap-fit assemblies Replacing CNC machined parts High-end finished models
PerFORM	Sensitive	Excellent	Excellent	Excellent	Excellent	Off white	Moderate	Excellent	Stiff High temperature resistance Superior sidewall quality Brittle	High temperature applications Automotive Aerospace
WaterClear	Good	Good	Moderate	Sensitive	Good	Optical clear with neutral tinge	Excellent	Moderate	Optically clear Lower mechanical properties than TuskXC2700T	Prototype parts that require fully neutral transparency

6 The information and values included in these datasheets, although based on Materialise's knowledge and experience and thus presented in good faith and believed to be accurate, is provided for your guidance only. This information does not release a third party from conducting his own procedures and tests to determine suitability. All guarantees with respect to the information contained herein are explicitly denied.

Last update: July 2014

ANNEX 15: POLYJET: PROPERTIES AND MATERIALS



Details PolyJet Digital Materials

- Standard lead time:** 2 – 4 working days
- Standard accuracy:** 0.1 – 0.3 mm
(accuracy varies according to geometry, part orientation and print size)
- Surface finish:** Basic finish
From high gloss to a rough texture are obtained by post-finishing
- Maximum part dimensions:** 500x400x200 mm (x,y,z)
- Capacity:** 1 Objet Connex machine
- Primary Materials:** Objet VeroWhitePlus is a general-purpose resin and has a white colour offering enhanced mechanical properties and the ability to withstand bending. Objet TangoBlackPlus is a flexible rubber-like resin, offering exceptional elongation at break, making it suitable for prototypes of rubber components like seals, non-slip surfaces, etc.
- Digital Materials:** Composite materials with preset combinations of mechanical properties. Shore A40 – Shore A50 – Shore A60 – Shore A70 – Shore A85 – Shore A95
- Multi-Material Models:** To combine materials with different properties in one model. Separate STL files are needed.

Datasheet				
PolyJet				
	Units	ASTM#	Objet VeroWhitePlus	Objet TangoBlackPlus
Tensile Strength	MPa	D-638	49.8	1.5
Elongation at Break	%	D-638	15% – 25%	218
Modulus of Elasticity	MPa	D-638	2495	
Flexural Strength	MPa	D790	74.6	
Flexural Modulus	MPa	D790	2137	
Notched Izod Impact	J/m	D256	37.5	
Hardness	Shore	Scale	83D	27A
Rockwell	Scale M	Scale M	81.0	
Heat Deflection Temp	°C	D648 @ 0.45MPa D648 @ 1.82MPa	47.6 43.6	
Tg	°C	DMA, E"	58.0	-10
Ash Content			<0.40%	
Tensile Tear resistance	Kg/cm	D-324		3
Colour			White	Black
Actual values may vary with build conditions				

Datasheet						
PolyJet Digital Materials						
Primary material: VeroWhitePlus Secondary material: TangoBlackPlus	DM_9840/ Shore A40	DM_9850/ Shore A50	DM_9860/ Shore A60	DM_9870/ Shore A70	DM_9885/ Shore A85	DM_9895 Shore A95
Tensile Strength (MPa)	0.5 – 1.5	0.5 – 1.5	2 – 4	2 – 4	4 – 8	15 – 25
Elongation at Break (%)	150 – 170	130 – 150	80 – 100	50 – 70	50 – 60	25 – 35
SHORE (Scale A)	35 – 45	45 – 55	55 – 65	65 – 75	80 – 90	90 – 100
Colour	Black	Black	Black	Black	Black	Black
Actual values may vary with build conditions						

7 The information and values included in these datasheets, although based on Materialise's knowledge and experience and thus presented in good faith and believed to be accurate, is provided for your guidance only. This information does not release a third party from conducting his own procedures and tests to determine suitability. All guarantees with respect to the information contained herein are explicitly denied.

Last update: 24/10/2013

ANNEX 16: ABS AND PLA PROPERTIES [66]

Acrylonitrile butadiene styrene (ABS)

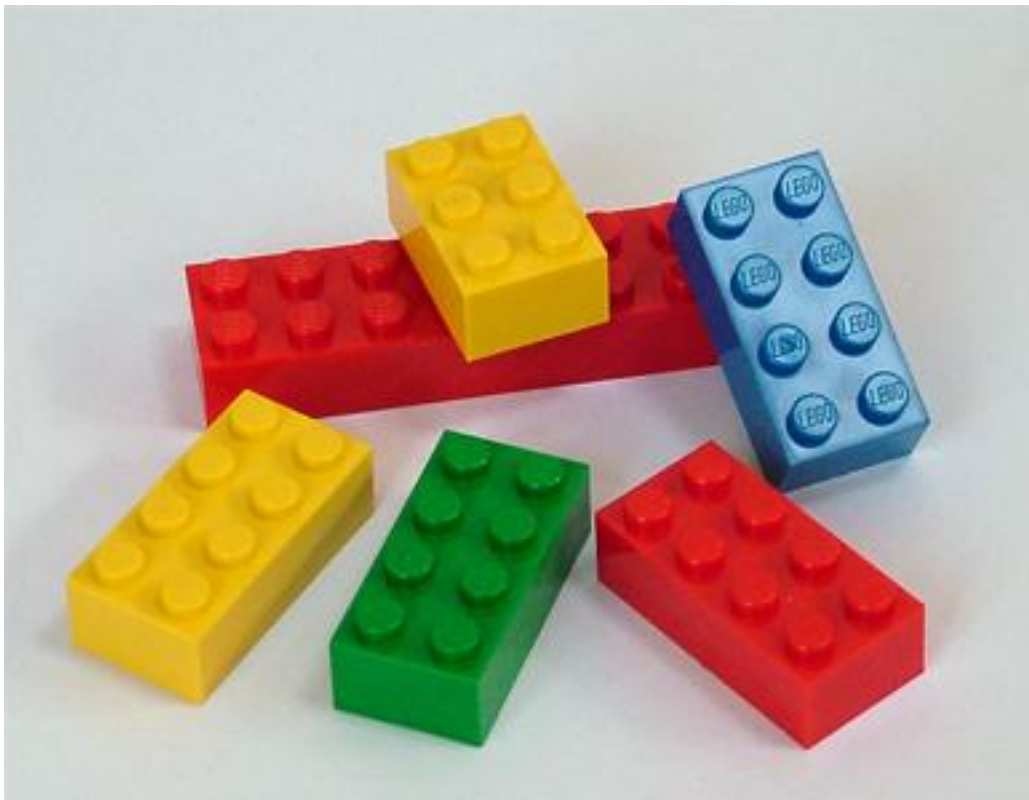
Description

The material

ABS (Acrylonitrile-butadiene-styrene) is tough, resilient, and easily molded. It is usually opaque, although some grades can now be transparent, and it can be given vivid colors. ABS-PVC alloys are tougher than standard ABS and, in self-extinguishing grades, are used for the casings of power tools.

Composition (summary)

Block terpolymer of acrylonitrile (15-35%), butadiene (5-30%), and styrene (40-60%).



Caption

The picture says a lot: ABS allows detailed moldings, accepts color well, and is non-toxic and tough enough to survive the worst that children can do to it.

General properties

Density	1.01e3	-	1.21e3	kg/m ³
Price	* 2.26	-	2.49	EUR/kg
Date first used	1937			

Mechanical properties

Young's modulus	1.1	-	2.9	GPa
Shear modulus	0.319	-	1.03	GPa
Bulk modulus	3.8	-	4	GPa
Poisson's ratio	0.391	-	0.422	
Yield strength (elastic limit)	18.5	-	51	MPa
Tensile strength	27.6	-	55.2	MPa
Compressive strength	31	-	86.2	MPa
Elongation	1.5	-	100	% strain

Hardness - Vickers	5.6	-	15.3	HV
Fatigue strength at 10 ⁷ cycles	11	-	22.1	MPa
Fracture toughness	1.19	-	4.29	MPa.m ^{0.5}
Mechanical loss coefficient (tan delta)	0.0138	-	0.0446	

Thermal properties

Glass temperature	87.9	-	128	°C
Maximum service temperature	61.9	-	76.9	°C
Minimum service temperature	-123	-	-73.2	°C
Thermal conductor or insulator?	Good insulator			
Thermal conductivity	0.188	-	0.335	W/m.°C
Specific heat capacity	1.39e3	-	1.92e3	J/kg.°C
Thermal expansion coefficient	84.6	-	234	µstrain/°C

Electrical properties

Electrical conductor or insulator?	Good insulator			
Electrical resistivity	3.3e21	-	3e22	µohm.cm
Dielectric constant (relative permittivity)	2.8	-	3.2	
Dissipation factor (dielectric loss tangent)	0.003	-	0.007	
Dielectric strength (dielectric breakdown)	13.8	-	21.7	100000 V/m

Optical properties

Transparency	Opaque			
Refractive index	1.53	-	1.54	

Processability

Castability	1	-	2	
Moldability	4	-	5	
Machinability	3	-	4	
Weldability	5			

Eco properties

Embodied energy, primary production	* 90.3	-	99.9	MJ/kg
CO2 footprint, primary production	* 3.64	-	4.03	kg/kg

Supporting information

Design guidelines

ABS has the highest impact resistance of all polymers. It takes color well. Integral metallics are possible (as in GE Plastics' Magix.) ABS is UV resistant for outdoor application if stabilizers are added. It is hygroscopic (may need to be oven dried before thermoforming) and can be damaged by petroleum-based machining oils. ASA (acrylic-styrene-acrylonitrile) has very high gloss; its natural color is off-white but others are available. It has good chemical and temperature resistance and high impact resistance at low temperatures. UL-approved grades are available. SAN (styrene-acrylonitrile) has the good processing attributes of polystyrene but greater strength, stiffness, toughness, and chemical and heat resistance. By adding glass fiber the rigidity can be increased dramatically. It is transparent (over 90% in the visible range but less for UV light) and has good color, depending on the amount of acrylonitrile that is added this can vary from water white to pale yellow, but without a protective coating, sunlight causes yellowing and loss of strength, slowed by UV stabilizers. All three can be extruded, compression molded or formed to sheet that is then vacuum thermo-formed. They can be joined by ultrasonic or hot-plate welding, or bonded with polyester, epoxy, isocyanate or nitrile-phenolic adhesives.

Technical notes

ABS is a terpolymer - one made by copolymerizing 3 monomers: acrylonitrile, butadiene and styrene. The acrylonitrile gives thermal and chemical resistance, rubber-like butadiene gives ductility and strength, the styrene gives a glossy surface, ease of machining and a lower cost. In ASA, the butadiene component (which gives poor UV resistance) is replaced by an acrylic ester. Without the addition of

butyl, ABS becomes, SAN - a similar material with lower impact resistance or toughness. It is the stiffest of the thermoplastics and has excellent resistance to acids, alkalis, salts and many solvents.

Typical uses

Safety helmets; camper tops; automotive instrument panels and other interior components; pipe fittings; home-security devices and housings for small appliances; communications equipment; business machines; plumbing hardware; automobile grilles; wheel covers; mirror housings; refrigerator liners; luggage shells; tote trays; mower shrouds; boat hulls; large components for recreational vehicles; weather seals; glass beading; refrigerator breaker strips; conduit; pipe for drain-waste-vent (DWV) systems.

Tradenames

Claradex, Comalloy, Cycogel, Cicolac, Hanalac, Lastilac, Lupos, Lustran ABS, Magnum, Multibase, Novodur, Polyfabs, Polylac, Porene, Ronfalin, Sinkral, Terluran, Toyolac, Tufrex, Ultrastyr

Poly lactide (PLA)

Description

The material

Poly lactide, PLA, is a biodegradable thermoplastic derived from natural lactic acid from corn, maize or milk. It resembles clear polystyrene, provides good aesthetics (gloss and clarity), but it is stiff and brittle and needs modification using plasticizers for most practical applications. It can be processed like most thermoplastics into fibers, films, thermoformed or injection molded.



Caption

Cargill Dow poly lactide food packaging

General properties

Density	1.21e3	-	1.25e3	kg/m ³
Price	* 1.75	-	2.11	EUR/kg
Date first used	1993			

Mechanical properties

Young's modulus	3.45	-	3.83	GPa
Shear modulus	* 1.23	-	1.37	GPa
Bulk modulus	* 5.7	-	6.3	GPa
Poisson's ratio	* 0.38	-	0.4	
Yield strength (elastic limit)	48	-	60	MPa
Tensile strength	48	-	60	MPa
Compressive strength	48	-	60	MPa
Elongation	5	-	7	% strain
Hardness - Vickers	* 14	-	18	HV
Fatigue strength at 10 ⁷ cycles	* 14	-	18	MPa
Fracture toughness	* 0.7	-	1.1	MPa.m ^{0.5}
Mechanical loss coefficient (tan delta)	0.02	-	0.1	

Thermal properties

Melting point	160	-	177	°C
Glass temperature	56	-	58	°C
Maximum service temperature	70	-	80	°C
Minimum service temperature	-12	-	-10	°C
Thermal conductor or insulator?	Good insulator			
Thermal conductivity	0.12	-	0.13	W/m.°C
Specific heat capacity	1.18e3	-	1.21e3	J/kg.°C
Thermal expansion coefficient	* 126	-	145	µstrain/°C

Electrical properties

Electrical conductor or insulator?	Good insulator		
Electrical resistivity	* 1e17	-	1e19 μohm.cm
Dielectric constant (relative permittivity)	* 3.5	-	5
Dissipation factor (dielectric loss tangent)	* 0.02	-	0.07
Dielectric strength (dielectric breakdown)	* 12	-	16 1000000 V/m

Optical properties

Transparency	Transparent		
Refractive index	* 1.4	-	1.48

Processability

Moldability	4	-	5
Formability	* 4	-	5
Machinability	* 4	-	5
Weldability	* 3	-	4

Eco properties

Embodied energy, primary production	* 49	-	54.2 MJ/kg
CO2 footprint, primary production	* 3.43	-	3.79 kg/kg

Supporting information

Design guidelines

PLA is a biopolymer that can be molded, thermoformed and extruded, much like any other thermoplastic. It is transparent and has FDA approval for food packaging. PLA film and sheet can be printed and laminated. Biopolymers are, however, expensive, costing 2 to 6 times as much as commodity plastics like polypropylene.

Technical notes

PLA is a thermoplastic derived primarily from annually renewable resources (maize, corn or milk). It is available in a number of grades, designed for ease of processing. In-line drying may be needed to reduce water content for extrusion and molding. The recommended molding temperature is 165 - 170 C.

Typical uses

Food packaging, plastic bags, plant pots, diapers, bottles, cold drink cups, sheet and film.

Tradenames

NatureWorks PLA, BOPLA

ANNEX 17: SPECIFIC PRINTING TIMES

Name	Time	Material (meter)	Amount Needed	Total time	Total amount of material
Abduction/Adduction attachment motor	4 min	0,03	1	4 min	0,03
Thumb Distal	59 min	0,43	1	59 min	0,43
Thumb Proximal	1h29	0,64	1	1h29	0,64
Chain connection	4 min	0,03	2	8 min	0,06
Middlefinger Distal	48 min	0,35	1	48 min	0,35
Middlefinger Intermedial	1h21	0,55	1	1h21	0,55
Middlefinger Proximal	1h40	0,69	1	1h40	0,69
Thumb TMC	38 min	0,29	1	38 min	0,29
Palm 2 fingers	12h43	6,11	1	12h43	6,11
Palm 3 fingers	15h59	7,57	1	15h59	7,57
Little finger Distal	48 min	0,35	1	48 min	0,35
Little finger Intermedial	54 min	0,36	1	54 min	0,36
Little finger Proximal	1h12	0,49	1	1h12	0,49
Wrist side hand	1h2	0,4	1	1h2	0,4
Wrist side motor	1h3	0,39	1	1h3	0,39
Ring finger Distal	48 min	0,35	1	48 min	0,35
Ring finger Intermedial	1h10	0,47	1	1h10	0,47
Ring finger Proximal	1h31	0,63	1	1h31	0,63
Abduction/Adduction joint of the index finger	15 min	0,08	1	15 min	0,08
Forearm back	37h53	21,49	1	37h53	21,49
Forearm front	53h	27,01	1	53h	27,01
Index finger Distal	48 min	0,35	1	48 min	0,35
Index finger Intermedial	1h11	0,48	1	1h11	0,48
Index finger Proximal	1h30	0,62	1	1h30	0,62

138h54min

Annex 18: Joint angles **Fout! Ongeldige koppeling.**

Letter		A	B	C	D	E	F	G	H	I	J	K	L	M
Little finger	DIP	90	0	45	45	90	0	90	90	0	0	90	90	0
	PIP	90	0	45	45	90	0	90	90	0	0	90	90	0
	MCP F/E	90	0	45	45	0	0	90	90	0	0	90	90	45
Ring finger	DIP	90	0	45	45	90	0	90	90	90	90	90	90	0
	PIP	90	0	45	45	90	0	90	90	90	90	90	90	0
	MCP F/E	90	0	45	45	0	30	90	90	90	90	90	90	45
Middle finger	DIP	90	0	45	45	90	0	90	0	90	90	0	90	0
	PIP	90	0	45	45	90	0	90	0	90	90	0	90	0
	MCP F/E	90	0	45	45	0	60	90	0	90	90	45	90	45
Index finger	DIP	90	0	45	0	90	0	45	0	90	90	0	0	0
	PIP	90	0	45	0	90	0	45	0	90	90	0	0	0
	MCP F/E	90	0	45	0	0	90	0	0	90	90	0	0	45
	MCP Abd/Add	0	0	0	0	0	0	0	0	0	0	0	0	0
Thumb	IP	0	90	45	45	90	0	45	90	90	90	0	0	90
	MCP	0	10	0	20	10	0	0	10	10	10	0	0	0
	TMC Abd/Add	0	0	90	90	0	0	90	0	90	90	90	0	0
Wrist	Flexion/extension	0	0	0	0	0	0	0	0	0	0	0	0	90
Elbow	Flexion/extension													
	Pron/sup	0	90	90	90	0	90	90	90	90	90...180	0	0	0
Shoulder	Adduction/abduction										45			45

Fout! Ongeldige koppeling.Fout! Ongeldige koppeling.

ANNEX 19: RANKED POSITIONS

Table 49: Ranked positions for finger movement

Position	MCP (°)	PIP (°)	DIP (passively) (°)
1	0	0	0
2	0	45	45
3	0	90	90
4	-10	0	0
5	30	0	0
6	45	0	0
7	45	45	45
8	60	0	0
9	60	45	45
10	60	90	90
11	90	0	0
12	90	90	90
13	0...90	0...90	0...90

Table 50: Ranked positions for thumb movement

Position	TMC	MCP	IP
1	0	0	0
2	0	0	90
3	0	10	90
4	0	30	90
5	90	0	0
6	90	0	45
7	90	0	90
8	90	10	0
9	90	10	45
10	90	10	90
11	90	20	45
12	90	30	0
13	90	30	90
14	90	45	90

Table 51: Ranked positions for wrist movement

Position	Flexion/Extension	Abduction/Adduction
1	0	0
2	0...90	0
3	90	0

Table 52: Ranked positions for elbow movement

Position	Flexion/Extension	Pronation/Supination
1	Free to choose ²⁴	0
2	Free to choose	45
3	Free to choose	90
4	Free to choose	90...180
5	Free to choose	0...90...0...90
6	Free to choose	180
7	45...90	0

Table 53: Ranked positions for shoulder movement

Position	Abduction/Adduction
1	Free to choose
2	45
3	0...45...0...45
4	90

²⁴ The position values that are free to choose will be calibrated upon first use of the robot.

ANNEX 20: PROGRAMMING LOG

Software safety

Version 0.0: Experimenting with the timer library with the intent of calling the right timer functions. Date: 24-02-2015

Version 0.1: A timer can be set and a stop function can be triggered. The stop-mode can be reset using a button. Date: 24-02-2015

Version 0.2: Integration of a RGB led for signaling an error. During start-up, the led blinks green at a frequency of 0.5Hz. During normal operation the LED burns green. When an error is detected, the LED blinks at 0.5Hz for 3s before lighting up continuously. Date: 24-02-2015

Aslan

Version 0.0: Setting up the general architecture for the program. The Serial library is implemented and used to prompt the user for input. Date: 23-02-2015

Version 0.1: A string of characters can be entered with the keyboard. Date: 25-02-2015

Version 0.2: The string of characters can be converted to an array of characters of a non-predefined length. This enables the user to enter strings from different lengths. The array of characters is then used in a switch command, used to select the right movements. Because of the double case states we are able to remove case sensitivity. Date: 28-02-2015

Version 0.3: The finger movement function is programmed and implemented. As a result, the memory of the Arduino Uno used became insufficient. Therefore, a switch to an Arduino Due has been made. Switching between those Arduino Microcontrollers led to the malfunctioning of the program. The function used to read the string stopped working properly. After a period of debugging this problem was solved. Date: 02-03-2015

Version 0.4: Further implementation of the finger movement function. In version 0.3 only the letters A and B had been fitted with the finger movement function. Date: 09-03-2015

Version 0.5: Implementation of the adduction/abduction movement function of the index finger. Date: 10-03-2015

Version 0.6: Implementation of the thumb movement function and implementation of wrist movement function. Date: 16-03-2015

Version 0.7: Implementation of the DS-SCX18.s servo controller for a single finger and the expansion of the I²C network to a network with 3 DS-SCX18.S servo drivers. Date: 02-04-2015

Version 0.8: Implementation of the DS-SCX18.s servo controller for the four fingers. Date: 29-04-2015

Version 0.9: Implementation of the DS-SCX18.s servo controller for the abduction of the index finger and the movement of the thumb and wrist. Date: 11-05-2015

Version 0.10: Implementation of the shoulder and elbow movement functions. Date: 12-05-2015

Motor calibration

Version 0.1: The calibration program has been written in two major parts. In the first part of the program, the entire byte is tested for an increasing binary value. This way, the interval between the motor can be addressed can be measured. The user can log this data and calculate the decimal values for 0, 30, 45, 60, 90 and 180°. The calculated values can be entered in the second part of the program, where these values can be tweaked.

Servo testing

Hypothesis 1 Limited movability

The servo testing program prompts the user for pulse width input. This way the user can visually determine the bandwidth and movability of the servo motor.

Hypothesis 2 Limited movability

Using two external potentiometer, the effect of repositioning the internal feedback servo can be simulated. Via a 10k Ω potentiometer the user can set a certain movement angle. By using the 5k Ω potentiometer, the servo can be tricked in any position.

Hypothesis 3 Limited movability

Four different servo motors are repeatedly moved to their respective minimum and maximum positions enabling the user to visually determine the actual movement range of the different servo motors.

ANNEX 21: DECISION ANALYSIS

21.1 Decision matrix Fused Deposition Modeling printer

	Price	Printing dimensions	Resolution	Price Filament	Time To Deliver
Price	x	0	0	0	0
Printing dimensions	1	x	1	0	1
Resolution	1	0	x	1	1
Price Filament	1	1	0	x	1
Time To Deliver	1	0	0	0	x
Sum	4	1	1	1	3

		Ultimaker 2	Cubify CubeX	MakerBot Replicator 5th Gen
Price (euro)	4	2300	2500	2899
Printing dimensions (mm)	1	230 x 225 x 205	275 x 240 x 265	252 x 199 x 150
Calculated (m ³)	1	10,8445	17,49	7,5222
Resolution (microns)	1	20	100	100
Price Filament (euro/kg)	1	42	110	50
Time To Deliver	3	1 day (Trideus)	9 days (Alternate)	3 days (KD85)

Wishes	W	Ultimaker 2	Ultimaker 2	Cubify CubeX	Cubify CubeX	Makerbot	Makerbot
Wishes	W	S	S*W	S	S*W	S	S*W
Price	4	9	36	8	32	6	24
Printing dimensions	1	7	7	9	9	4	4
Resolution	1	10	10	8	8	8	8
Price Filament	1	8	8	5	5	7	7
Time To Deliver	1	10	10	5	5	8	8
Total			71		59		51

21.2 Analytical Hierarchy Process with Saaty's scale of relative importance

Demands I²C communication Wishes: Low cost
 Analog inputs available Availability
 Usability
 High number of analog inputs
 Large available memory for long and complex programs

Options:	Price	I ² C	Analog inputs
Raspberry Pi 2 model B	€ 44,99	Yes	Only using expansion
Intel Galileo Gen 2	€ 74,99	Yes	6
Udoo Quad	€ 139,00	Yes	12
Arduino Uno	€ 23,90	Yes	6
Arduino Due	€ 44,99	Yes	12
Arduino Mega2560	€ 49,99	Yes	16
Arduino Mega ADK	€ 75,00	Yes	16
Arduino Micro	€ 21,99	No	12
Arduino Leonardo	€ 25	Yes	12
Arduino Ethernet	€ 47,99	Yes	6

Determining the weight

	Low cost	Availability	Usability	Memory	Number of analog inputs	Average
Low cost	1	0,2	3	0,333333333	3	1,506666667
Availability	5	1	3	0,333333333	0,333333333	1,933333333
Usability	0,333333333	0,333333333	1	3	1	1,133333333
Memory	3	3	0,333333333	1	7	2,866666667
Number of analog inputs	0,333333333	3	1	0,142857143	1	1,095238095
Sum:	9,666666667	7,533333333	8,333333333	4,80952381	12,33333333	7,44

Normailize and average

	Low cost	Availability	Usability	Memory	Number of analog inputs	Average
Low cost	0,103448276	0,026548673	0,36	0,069306931	0,243243243	0,160509424
Availability	0,517241379	0,132743363	0,36	0,069306931	0,027027027	0,22126374
Usability	0,034482759	0,044247788	0,12	0,623762376	0,081081081	0,180714801
Memory	0,310344828	0,398230088	0,04	0,207920792	0,567567568	0,304812655
Number of analog inputs	0,034482759	0,398230088	0,12	0,02970297	0,081081081	0,13269938
Sum:	1	1	1	1	1	1

Assigning a score to every option

LOW COST	Intel Galileo Gen 2	Udoo Quad	Arduino Uno	Arduino Due	Arduino Mega 2560	Arduino Mega ADK	Arduino Leonardo	Arduino Ethernet	Average:
Intel Galileo Gen 2	1	1	0	0	0	1	0	0	0,375
Udoo Quad	0	1	0	0	0	0	0	0	0,125
Arduino Uno	1	1	1	1	1	1	1	1	1
Arduino Due	1	1	0	1	0	1	0	1	0,625
Arduino Mega2560	1	1	0	0	0	1	0	0	0,375
Arduino Mega ADK	0	1	0	0	0	1	0	0	0,25
Arduino Leonardo	1	1	0	1	1	1	1	1	0,875
Arduino Ethernet	1	1	0	0	1	1	0	1	0,625
Sum:	6	8	1	3	3	7	2	4	4,25

LOW COST	Intel Galileo Gen 2	Udoo Quad	Arduino Uno	Arduino Due	Arduino Mega 2560	Arduino Mega ADK	Arduino Leonardo	Arduino Ethernet	Average:
Intel Galileo Gen 2	0,16666667	0,125	0	0	0	0,142857143	0	0	0,054315476
Udoo Quad	0	0,125	0	0	0	0	0	0	0,015625
Arduino Uno	0,16666667	0,125	1	0,333333333	0,333333333	0,142857143	0,5	0,25	0,35639881
Arduino Due	0,16666667	0,125	0	0,333333333	0	0,142857143	0	0,25	0,127232143
Arduino Mega2560	0,16666667	0,125	0	0	0	0,142857143	0	0	0,054315476
Arduino Mega ADK	0	0,125	0	0	0	0,142857143	0	0	0,033482143
Arduino Leonardo	0,16666667	0,125	0	0,333333333	0,333333333	0,142857143	0,5	0,25	0,23139881
Arduino Ethernet	0,16666667	0,125	0	0	0,333333333	0,142857143	0	0,25	0,127232143
Sum:	1	1	1	1	1	1	1	1	1

AVAILABILITY	Intel Galileo Gen 2	Udoo Quad	Arduino Uno	Arduino Due	Arduino Mega 2560	Arduino Mega ADK	Arduino Leonardo	Arduino Ethernet	Average:
Intel Galileo Gen 2	1	0	0	0	0	0	0	0	0,125
Udoo Quad	0	1	0	0	0	0	0	0	0,125
Arduino Uno	1	1	1	0	0	0	0	0	0,375
Arduino Due	1	1	0	1	0	0	0	0	0,375
Arduino Mega2560	1	1	0	0	1	0	0	0	0,375
Arduino Mega ADK	1	1	0	0	0	1	0	0	0,375
Arduino Leonardo	1	1	0	0	0	0	1	0	0,375
Arduino Ethernet	1	1	0	0	0	0	0	1	0,375
Sum:	7	7	1	1	1	1	1	1	2,5

AVAILABILITY	Intel Galileo Gen 2	Udoo Quad	Arduino Uno	Arduino Due	Arduino Mega 2560	Arduino Mega ADK	Arduino Leonardo	Arduino Ethernet	Average:
Intel Galileo Gen 2	0,142857143	0	0	0	0	0	0	0	0,017857143
Udoo Quad	0	0,142857143	0	0	0	0	0	0	0,017857143
Arduino Uno	0,142857143	0,142857143	1	0	0	0	0	0	0,160714286
Arduino Due	0,142857143	0,142857143	0	1	0	0	0	0	0,160714286
Arduino Mega2560	0,142857143	0,142857143	0	0	1	0	0	0	0,160714286
Arduino Mega ADK	0,142857143	0,142857143	0	0	0	1	0	0	0,160714286
Arduino Leonardo	0,142857143	0,142857143	0	0	0	0	1	0	0,160714286
Arduino Ethernet	0,142857143	0,142857143	0	0	0	0	0	1	0,160714286
Sum:	1	1	1	1	1	1	1	1	1

USABILITY	Intel Galileo Gen 2	Udoo Quad	Arduino Uno	Arduino Due	Arduino Mega 2560	Arduino Mega ADK	Arduino Leonardo	Arduino Ethernet	Average:
Intel Galileo Gen 2	1	1	0	0	0	0	0	0	0,25
Udoo Quad	0	1	0	0	0	0	0	0	0,125
Arduino Uno	1	1	1	0	0	0	0	0	0,375
Arduino Due	1	1	0	1	0	0	0	0	0,375
Arduino Mega2560	1	1	0	0	1	0	0	0	0,375
Arduino Mega ADK	1	1	0	0	0	1	0	0	0,375
Arduino Leonardo	1	1	0	0	0	0	1	0	0,375
Arduino Ethernet	1	1	0	0	0	0	0	1	0,375
Sum:	7	8	1	1	1	1	1	1	2,625

USABILITY	Intel Galileo Gen 2	Udoo Quad	Arduino Uno	Arduino Due	Arduino Mega 2560	Arduino Mega ADK	Arduino Leonardo	Arduino Ethernet	Average:
Intel Galileo Gen 2	0,142857143	0,125	0	0	0	0	0	0	0,033482143
Udoo Quad	0	0,125	0	0	0	0	0	0	0,015625
Arduino Uno	0,142857143	0,125	1	0	0	0	0	0	0,158482143
Arduino Due	0,142857143	0,125	0	1	0	0	0	0	0,158482143
Arduino Mega2560	0,142857143	0,125	0	0	1	0	0	0	0,158482143
Arduino Mega ADK	0,142857143	0,125	0	0	0	1	0	0	0,158482143
Arduino Leonardo	0,142857143	0,125	0	0	0	0	1	0	0,158482143
Arduino Ethernet	0,142857143	0,125	0	0	0	0	0	1	0,158482143
Sum:	1	1	1	1	1	1	1	1	1

MEMORY	Intel Galileo Gen 2	Udoo Quad	Arduino Uno	Arduino Due	Arduino Mega 2560	Arduino Mega ADK	Arduino Leonardo	Arduino Ethernet	Average:
Intel Galileo Gen 2	1	0	1	1	1	1	1	1	0,875
Udoo Quad	1	1	1	1	1	1	1	1	1
Arduino Uno	0	0	1	0	0	0	0	0	0,125
Arduino Due	0	0	1	1	1	1	1	1	0,75
Arduino Mega2560	0	0	1	0	1	0	1	1	0,5
Arduino Mega ADK	0	0	1	0	1	1	1	1	0,625
Arduino Leonardo	0	0	1	0	0	0	1	1	0,375
Arduino Ethernet	0	0	1	0	0	0	0	1	0,25
Sum:	2	1	8	3	5	4	6	7	4,5

MEMORY	Intel Galileo Gen 2	Udoo Quad	Arduino Uno	Arduino Due	Arduino Mega 2560	Arduino Mega ADK	Arduino Leonardo	Arduino Ethernet	Average:
Intel Galileo Gen 2	0,5	0	0,125	0,333333333	0,2	0,25	0,166666667	0,142857143	0,214732143
Udoo Quad	0,5	1	0,125	0,333333333	0,2	0,25	0,166666667	0,142857143	0,339732143
Arduino Uno	0	0	0,125	0	0	0	0	0	0,015625
Arduino Due	0	0	0,125	0,333333333	0,2	0,25	0,166666667	0,142857143	0,152232143
Arduino Mega2560	0	0	0,125	0	0,2	0	0,166666667	0,142857143	0,079315476
Arduino Mega ADK	0	0	0,125	0	0,2	0,25	0,166666667	0,142857143	0,110565476
Arduino Leonardo	0	0	0,125	0	0	0	0,166666667	0,142857143	0,054315476
Arduino Ethernet	0	0	0,125	0	0	0	0	0,142857143	0,033482143
Sum:	1	1	1	1	1	1	1	1	1

ANALOG INPUTS	Intel Galileo Gen 2	Udoo Quad	Arduino Uno	Arduino Due	Arduino Mega 2560	Arduino Mega ADK	Arduino Leonardo	Arduino Ethernet	Average:
Intel Galileo Gen 2	1	0	1	0	0	0	0	1	0,375
Udoo Quad	1	1	1	1	0	0	0	1	0,625
Arduino Uno	0	0	1	0	0	0	0	1	0,25
Arduino Due	1	0	1	1	0	0	1	1	0,625
Arduino Mega2560	1	1	1	1	1	1	1	1	1
Arduino Mega ADK	1	1	1	1	0	1	1	1	0,875
Arduino Leonardo	1	1	1	1	0	0	1	1	0,75
Arduino Ethernet	0	0	0	0	0	0	0	1	0,125
Sum:	6	4	7	5	1	2	4	8	4,625

ANALOG INPUTS	Intel Galileo Gen 2	Udoo Quad	Arduino Uno	Arduino Due	Arduino Mega 2560	Arduino Mega ADK	Arduino Leonardo	Arduino Ethernet	Average:
Intel Galileo Gen 2	0,16666667	0	0,142857143	0	0	0	0	0,125	0,054315476
Udoo Quad	0,16666667	0,25	0,142857143	0,2	0	0	0	0,125	0,110565476
Arduino Uno	0	0	0,142857143	0	0	0	0	0,125	0,033482143
Arduino Due	0,16666667	0	0,142857143	0,2	0	0	0,25	0,125	0,110565476
Arduino Mega2560	0,16666667	0,25	0,142857143	0,2	1	0,5	0,25	0,125	0,329315476
Arduino Mega ADK	0,16666667	0,25	0,142857143	0,2	0	0,5	0,25	0,125	0,204315476
Arduino Leonardo	0,16666667	0,25	0,142857143	0,2	0	0	0,25	0,125	0,141815476
Arduino Ethernet	0	0	0	0	0	0	0	0,125	0,015625
Sum:	1	1	1	1	1	1	1	1	1

Defining the best option

Weights	Intel Galileo Gen2	Udoo Quad	Arduino Uno	Arduino Due	Arduino Mega2560	Arduino Mega ADK	Arduino Leonardo	Arduino Ethernet									
Low cost	0,160509424	0,054315476	0,008718146	0,015625	0,00250796	0,35639881	0,057205368	0,127232143	0,020421958	0,054315	0,008718	0,033482	0,005374	0,231399	0,037142	0,127232	0,020422
Availability	0,22126374	0,125	0,027657967	0,125	0,027657967	0,375	0,082973902	0,375	0,082973902	0,375	0,082974	0,375	0,082974	0,375	0,082974	0,375	0,082974
Usability	0,180714801	0,033482143	0,006050719	0,015625	0,002823669	0,158482143	0,028640069	0,158482143	0,028640069	0,158482	0,02864	0,158482	0,02864	0,158482	0,02864	0,158482	0,02864
Memory	0,304812655	0,214732143	0,065453075	0,339732143	0,103554657	0,015625	0,004762698	0,152232143	0,046402284	0,079315	0,024176	0,110565	0,033702	0,054315	0,016556	0,033482	0,010206
Analog inputs	0,13269938	0,054315476	0,00720763	0,110565476	0,01467197	0,033482143	0,00444306	0,110565476	0,01467197	0,329315	0,0437	0,204315	0,027113	0,141815	0,018819	0,015625	0,002073
Score:		0,115087537			0,151216223		0,178025096		0,193110183		0,188208		0,177802		0,184131		0,144315



18 Channel Servo Driver Shield

for Arduino™ and Raspberry-PI™

Technical Data

DS-SCX18.S

Features

- Arduino™ UNO Shield standard form factor for simple integration into any Arduino project
- Frees up the Arduino™ IO lines normally used for servo control
- I²C interface for simple connection to Arduino or Raspberry-PI
- Dual on-board 5Volt 3Amp regulators, with heatsinking, for servo power with enable jumpers
- Sixteen (16) level speed control for each servo
- Movement complete and soft-start complete status for each servo
- Global activation control ensures all servos start moving together, important for multi-legged robots
- I²C address links allow up to four [4] shields to be used together to provide up to 72 servos
- LVD, RoHS and WEEE compliant product

Description

The Designer Systems DS-SCX18.S is an eighteen [18] channel RC servo driver with advanced servo control features. Specifically targeted at the Arduino UNO board user [all other Arduino boards supported] and the Raspberry-PI the SCX18.S features high speed I²C communication for easy project integration and smooth speed control.

Once connected each servo can be positioned (with speed control), enabled, reversed and soft-started by simply writing a value to an internal register over the connected I²C interface. The SCX18.S caters for the majority of servos by providing a wide pulse width range of 0.50mS to 2.50mS with 8uS per step accuracy and also provides global activation of new servo position, soft-start & movement complete registers for superior control.

The SCX18.S provides dual high power regulators capable of supplying 5V @ 3A to the connected servos from an external Li-Pol or



Ni-MH battery pack of 7.2 to 8.4V and features a disable link to allow the use of low voltage battery packs of 3.6 to 4.8V. The on-board I²C pull-ups are jumper configurable to allow disconnection when connecting to the Raspberry-PI, which has its own pull-ups.

Applications

The SCX18.S has applications in robotics, including quadruped, hexapod and octopod robots, process control & sensor manipulation when used in conjunction with standard RC servos.

CONTROL MODULES

Selection Guide

Description	Part Number
18 Channel Servo Driver Shield	DS-SCX18.S
HS311 Standard hobby servo	DS-HS311

Raspberry-PI, Arduino, NANO, UNO & MEGA are trademark.

Power requirements

The DS-SCX18.S takes the power necessary for operation (approx. 2-25mA) from an external battery or power adaptor or power from the Arduino or Raspberry-PI board. The SCX18 provides three PCB pads, two marked 'GND' and one marked 'Vin' in the same format as that present on the UNO board, which should be connected to negative and positive battery/power supply terminals respectively. The input voltage range is 4.75 - 16VDC with the internal circuitry being protected against power supply reversal.

The two on-board servo regulators provide a clean regulated 5V supply for the connected servos at a maximum current of 3Amps each, the left hand regulator powering servos 1 to 9 and the right hand regulator servos 10-18. The following table indicates if a regulator needs to be enabled or disabled dependant on supply voltage:

Status	Battery pack/supply voltage
Disabled	3.6V to 4.8V
Enabled	7.2V to 8.5V

The servo regulators are enabled or disabled with on-board double links just above the regulator heat-sinks which can be configured as follows:

Enabled (ON):



Disabled (OFF):



Refer to the voltage rating of the servos you wish to use before configuring the servo regulator.

Connection of the external supply - battery / mains adaptor - to the SCX18 module is through a two (2) way pluggable screw terminal block marked '3-8.5VDC @ 6A Max'.

Note: This supply is NOT reverse connection protected but is marked with a series of '+++++' signs to denote positive.

© 1997-2013 Designer Systems
INTERFACE 13.04.13 Revision 1.00

I²C connection

The I²C connections are marked 'SDA' and 'SCL' and allow connection to the Arduino UNO board 'ANALOG IN' pins 4 and 5 or the Raspberry-PI GPIO port pins 3 and 5 (see Fig. 2.0) or another I²C Master device.

The DS-SCX18.S is fitted with pull-up jumpers that can be configured to provide the source current necessary for I²C communication. The following jumpers should normally be set when using the UNO board, as long as the I²C bus does not have existing pull-up's provided by another device. **These jumpers MUST be removed when using the Raspberry-PI:**



I²C communication

Up to four DS-SCX18.S modules may be connected to the same UNO / Raspberry-PI board or I²C bus and accessed individually using their own individual address. The address is configured with the following jumpers:



The following table shows how the jumpers are placed for the different binary addresses:

Address xx	A0	A1
00 (default)	ON	ON
01	OFF	ON
10	ON	OFF
11	OFF	OFF

The binary address (xx) above is used in conjunction with the device ID 11101xxD to form the complete device address i.e. if both jumpers are left connected (default) then the device address would be 1110100D_{binary}.

The 'D' bit determines if a read or a write to the SCX18 is to be performed. If the 'D' bit is set '1' then a register read is performed or if clear '0' a register write.

To access individual registers a device write must be undertaken by the I²C Master which consists of a Start condition, device ID ('D' bit cleared), register to start write, one or more bytes of data to be written and a stop condition (see Figure 1.0 for I²C write protocol).

There are 37 individual registers that can be written within the SCX18 that control output as follows:

SCX I²C address
R3 [1 1 1 1 1 0 1 X X 0]
XX = SCX18 address

Register address
R0 [U U B B B B B B]
B, B = 0 to 37
U, U = unused on this implementation

Servo 1 position
R1 [P P P P P P P P]
P, P = Servo position 0 to 255 (0.5mS to 2.50mS)

Servo 1 control
R2 [A B C D S S S S]
A = Operate (0 - Servo disabled 1 - Servo enabled)
B = Reverse (0 - Servo normal 1 - Servo reversed)
C = Soft-start control (0 - Disabled 1 - Enabled)
D = Speed control (0 - Disabled 1 - Enabled)
S, S = Servo speed value 0 to 15 (0 = slowest)

Servo 2 position
R3 [P P P P P P P P]
P, P = Servo position 0 to 255 (0.5mS to 2.50mS)

Servo 2 control
R4 [A B C D S S S S]
A = Operate (0 - Servo disabled 1 - Servo enabled)
B = Reverse (0 - Servo normal 1 - Servo reversed)
C = Soft-start control (0 - Disabled 1 - Enabled)
D = Speed control (0 - Disabled 1 - Enabled)
S, S = Servo speed value 0 to 15 (0 = slowest)

Servo 3 position
R5 [P P P P P P P P]
P, P = Servo position 0 to 255 (0.5mS to 2.50mS)

Servo 3 control
R6 [A B C D S S S S]
A = Operate (0 - Servo disabled 1 - Servo enabled)
B = Reverse (0 - Servo normal 1 - Servo reversed)
C = Soft-start control (0 - Disabled 1 - Enabled)
D = Speed control (0 - Disabled 1 - Enabled)
S, S = Servo speed value 0 to 15 (0 = slowest)

Servo 4 position
R7 [P P P P P P P P]
P, P = Servo position 0 to 255 (0.5mS to 2.50mS)

Servo 4 control
R8 [A B C D S S S S]
A = Operate (0 - Servo disabled 1 - Servo enabled)
B = Reverse (0 - Servo normal 1 - Servo reversed)
C = Soft-start control (0 - Disabled 1 - Enabled)
D = Speed control (0 - Disabled 1 - Enabled)
S, S = Servo speed value 0 to 15 (0 = slowest)

Servo 5 position
R9 [P P P P P P P P]
P, P = Servo position 0 to 255 (0.5mS to 2.50mS)

Servo 5 control
R10 [A B C D S S S S]
A = Operate (0 - Servo disabled 1 - Servo enabled)
B = Reverse (0 - Servo normal 1 - Servo reversed)
C = Soft-start control (0 - Disabled 1 - Enabled)
D = Speed control (0 - Disabled 1 - Enabled)
S, S = Servo speed value 0 to 15 (0 = slowest)

Servo 6 position
R11 [P P P P P P P P]
P, P = Servo position 0 to 255 (0.5mS to 2.50mS)

Servo 6 control
R12 [A B C D S S S S]
A = Operate (0 - Servo disabled 1 - Servo enabled)
B = Reverse (0 - Servo normal 1 - Servo reversed)
C = Soft-start control (0 - Disabled 1 - Enabled)
D = Speed control (0 - Disabled 1 - Enabled)
S, S = Servo speed value 0 to 15 (0 = slowest)

Servo 7 position
R13

P	P	P	P	P	P	P	P	P
---	---	---	---	---	---	---	---	---

P..P = Servo position 0 to 255 (0.5mS to 2.50mS)

Servo 7 control
R14

A	B	C	D	S	S	S	S
---	---	---	---	---	---	---	---

A = Operate (0 – Servo disabled 1 – Servo enabled)
B = Reverse (0 – Servo normal 1 – Servo reversed)
C = Soft-start control (0 – Disabled 1 – Enabled)
D = Speed control (0 – Disabled 1 – Enabled)
S..S = Servo speed value 0 to 15 (0 = slowest)

Servo 8 position
R15

P	P	P	P	P	P	P	P	P
---	---	---	---	---	---	---	---	---

P..P = Servo position 0 to 255 (0.5mS to 2.50mS)

Servo 8 control
R16

A	B	C	D	S	S	S	S
---	---	---	---	---	---	---	---

A = Operate (0 – Servo disabled 1 – Servo enabled)
B = Reverse (0 – Servo normal 1 – Servo reversed)
C = Soft-start control (0 – Disabled 1 – Enabled)
D = Speed control (0 – Disabled 1 – Enabled)
S..S = Servo speed value 0 to 15 (0 = slowest)

Servo 9 position
R17

P	P	P	P	P	P	P	P	P
---	---	---	---	---	---	---	---	---

P..P = Servo position 0 to 255 (0.5mS to 2.50mS)

Servo 9 control
R18

A	B	C	D	S	S	S	S
---	---	---	---	---	---	---	---

A = Operate (0 – Servo disabled 1 – Servo enabled)
B = Reverse (0 – Servo normal 1 – Servo reversed)
C = Soft-start control (0 – Disabled 1 – Enabled)
D = Speed control (0 – Disabled 1 – Enabled)
S..S = Servo speed value 0 to 15 (0 = slowest)

Servo 10 position
R19

P	P	P	P	P	P	P	P	P
---	---	---	---	---	---	---	---	---

P..P = Servo position 0 to 255 (0.5mS to 2.50mS)

Servo 10 control
R20

A	B	C	D	S	S	S	S
---	---	---	---	---	---	---	---

A = Operate (0 – Servo disabled 1 – Servo enabled)
B = Reverse (0 – Servo normal 1 – Servo reversed)
C = Soft-start control (0 – Disabled 1 – Enabled)
D = Speed control (0 – Disabled 1 – Enabled)
S..S = Servo speed value 0 to 15 (0 = slowest)

Servo 11 position
R21

P	P	P	P	P	P	P	P	P
---	---	---	---	---	---	---	---	---

P..P = Servo position 0 to 255 (0.5mS to 2.50mS)

Servo 11 control
R22

A	B	C	D	S	S	S	S
---	---	---	---	---	---	---	---

A = Operate (0 – Servo disabled 1 – Servo enabled)
B = Reverse (0 – Servo normal 1 – Servo reversed)
C = Soft-start control (0 – Disabled 1 – Enabled)
D = Speed control (0 – Disabled 1 – Enabled)
S..S = Servo speed value 0 to 15 (0 = slowest)

Servo 12 position
R23

P	P	P	P	P	P	P	P	P
---	---	---	---	---	---	---	---	---

P..P = Servo position 0 to 255 (0.5mS to 2.50mS)

Servo 12 control
R24

A	B	C	D	S	S	S	S
---	---	---	---	---	---	---	---

A = Operate (0 – Servo disabled 1 – Servo enabled)
B = Reverse (0 – Servo normal 1 – Servo reversed)
C = Soft-start control (0 – Disabled 1 – Enabled)
D = Speed control (0 – Disabled 1 – Enabled)
S..S = Servo speed value 0 to 15 (0 = slowest)

Servo 13 position
R25

P	P	P	P	P	P	P	P	P
---	---	---	---	---	---	---	---	---

P..P = Servo position 0 to 255 (0.5mS to 2.50mS)

Servo 13 control
R26

A	B	C	D	S	S	S	S
---	---	---	---	---	---	---	---

A = Operate (0 – Servo disabled 1 – Servo enabled)
B = Reverse (0 – Servo normal 1 – Servo reversed)
C = Soft-start control (0 – Disabled 1 – Enabled)
D = Speed control (0 – Disabled 1 – Enabled)
S..S = Servo speed value 0 to 15 (0 = slowest)

Servo 14 position
R27

P	P	P	P	P	P	P	P	P
---	---	---	---	---	---	---	---	---

P..P = Servo position 0 to 255 (0.5mS to 2.50mS)

Servo 14 control
R28

A	B	C	D	S	S	S	S
---	---	---	---	---	---	---	---

A = Operate (0 – Servo disabled 1 – Servo enabled)
B = Reverse (0 – Servo normal 1 – Servo reversed)
C = Soft-start control (0 – Disabled 1 – Enabled)
D = Speed control (0 – Disabled 1 – Enabled)
S..S = Servo speed value 0 to 15 (0 = slowest)

Servo 15 position
R29

P	P	P	P	P	P	P	P	P
---	---	---	---	---	---	---	---	---

P..P = Servo position 0 to 255 (0.5mS to 2.50mS)

Servo 15 control
R30

A	B	C	D	S	S	S	S
---	---	---	---	---	---	---	---

A = Operate (0 – Servo disabled 1 – Servo enabled)
B = Reverse (0 – Servo normal 1 – Servo reversed)
C = Soft-start control (0 – Disabled 1 – Enabled)
D = Speed control (0 – Disabled 1 – Enabled)
S..S = Servo speed value 0 to 15 (0 = slowest)

Servo 16 position
R31

P	P	P	P	P	P	P	P	P
---	---	---	---	---	---	---	---	---

P..P = Servo position 0 to 255 (0.5mS to 2.50mS)

Servo 16 control
R32

A	B	C	D	S	S	S	S
---	---	---	---	---	---	---	---

A = Operate (0 – Servo disabled 1 – Servo enabled)
B = Reverse (0 – Servo normal 1 – Servo reversed)
C = Soft-start control (0 – Disabled 1 – Enabled)
D = Speed control (0 – Disabled 1 – Enabled)
S..S = Servo speed value 0 to 15 (0 = slowest)

Servo 17 position
R33

P	P	P	P	P	P	P	P	P
---	---	---	---	---	---	---	---	---

P..P = Servo position 0 to 255 (0.5mS to 2.50mS)

Servo 17 control
R34

A	B	C	D	S	S	S	S
---	---	---	---	---	---	---	---

A = Operate (0 – Servo disabled 1 – Servo enabled)
B = Reverse (0 – Servo normal 1 – Servo reversed)
C = Soft-start control (0 – Disabled 1 – Enabled)
D = Speed control (0 – Disabled 1 – Enabled)
S..S = Servo speed value 0 to 15 (0 = slowest)

Servo 18 position
R35

P	P	P	P	P	P	P	P	P
---	---	---	---	---	---	---	---	---

P..P = Servo position 0 to 255 (0.5mS to 2.50mS)

Servo 18 control
R36

A	B	C	D	S	S	S	S
---	---	---	---	---	---	---	---

A = Operate (0 – Servo disabled 1 – Servo enabled)
B = Reverse (0 – Servo normal 1 – Servo reversed)
C = Soft-start control (0 – Disabled 1 – Enabled)
D = Speed control (0 – Disabled 1 – Enabled)
S..S = Servo speed value 0 to 15 (0 = slowest)

Servo global enable register
R37

X	X	X	X	X	X	X	X	X
---	---	---	---	---	---	---	---	---

X..X = Any value

Each control register consists of four control bits and a four bit speed control value defined as follows:

Bit (A) 128_{decimal} is the operate bit which when set activates the servo being controlled.

Bit (B) 64_{decimal} is the reverse bit which reverses the position value for the servo being controlled.

Bit (C) 32_{decimal} is the soft-start bit which when set on servo first activation, see operate bit above, feeds position pulses to the servo in a ramping manner until position is attained.

Bit (D) 16_{decimal} is the speed control enable bit which when set applies the speed value 0 to 15, contained in the four bits (SSSS) 1,2,4,8_{decimal}, to the servo being controlled.

Once all the required position & control registers have been set a write to the R37 (Global enable register) must be made to activate all the new positions.

Example.
To set the first nine servos to new positions with servos 1 to 4 running at speed 0 and servos 5 to 8 running at speed 5 in reverse mode, first write:

Byte 1 (SCX18 Adr) 11101000_{binary}
Byte 2 (Register 0) 0_{decimal}

Byte 3 (Register 1) 30_{decimal}
Byte 4 (Register 2) 144_{decimal} 90_{hex}
Byte 5 (Register 3) 35_{decimal}
Byte 6 (Register 4) 144_{decimal} 90_{hex}
Byte 7 (Register 5) 40_{decimal}
Byte 8 (Register 6) 144_{decimal} 90_{hex}
Byte 9 (Register 7) 45_{decimal}
Byte 10 (Register 8) 144_{decimal} 90_{hex}
Byte 11 (Register 9) 127_{decimal}
Byte 12 (Register 10) 213_{decimal} D5_{hex}
Byte 13 (Register 11) 130_{decimal}
Byte 14 (Register 12) 213_{decimal} D5_{hex}
Byte 15 (Register 13) 140_{decimal}
Byte 16 (Register 14) 213_{decimal} D5_{hex}
Byte 17 (Register 15) 150_{decimal}
Byte 18 (Register 16) 213_{decimal} D5_{hex}

then to activate write:
Byte 1 (SCX18 Adr) 11101000_{binary}
Byte 2 (Register 0) 37_{decimal}
Byte 3 (Register 37) 0_{decimal}

To read the status registers a device write then read must be undertaken by the OOPic / I²C Master. The write consists of a Start condition, device ID ('D' bit cleared), register to start read and a Stop condition. This is followed by a read, which consists of a Start condition, device ID ('D' bit set), followed by data from the status register and terminated with a Stop condition (see Figure 1.1 for I²C read protocol).

Status registers
There are 18 registers that can be read within the SCX18 as follows:

N₁ N₂ N₃ N₄ N₅ N₆ N₇ N₈
SCX I2C Address
1.

1	1	1	1	0	1	X	X	1
---	---	---	---	---	---	---	---	---

XX = SCX18 address

Servo 1 status
R0

A	B	C	D	0	0	0	0
---	---	---	---	---	---	---	---

A = Operation (0 – Servo disabled 1 – Servo enabled)
B = Reverse (0 – Servo normal 1 – Servo reversed)
C = Soft-start (0 – Complete 1 – In-progress)
D = Movement (0 – Complete 1 – In-progress)

Servo 2 status
R1

A	B	C	D	0	0	0	0
---	---	---	---	---	---	---	---

A = Operation (0 – Servo disabled 1 – Servo enabled)
B = Reverse (0 – Servo normal 1 – Servo reversed)
C = Soft-start (0 – Complete 1 – In-progress)
D = Movement (0 – Complete 1 – In-progress)

Servo 3 status
R2

A	B	C	D	0	0	0	0
---	---	---	---	---	---	---	---

A = Operation (0 – Servo disabled 1 – Servo enabled)
B = Reverse (0 – Servo normal 1 – Servo reversed)
C = Soft-start (0 – Complete 1 – In-progress)
D = Movement (0 – Complete 1 – In-progress)

Servo 4 status
R3

A	B	C	D	0	0	0	0
---	---	---	---	---	---	---	---

A = Operation (0 – Servo disabled 1 – Servo enabled)
B = Reverse (0 – Servo normal 1 – Servo reversed)
C = Soft-start (0 – Complete 1 – In-progress)
D = Movement (0 – Complete 1 – In-progress)

Servo 5 status
R4

A	B	C	D	0	0	0	0
---	---	---	---	---	---	---	---

A = Operation (0 – Servo disabled 1 – Servo enabled)
B = Reverse (0 – Servo normal 1 – Servo reversed)
C = Soft-start (0 – Complete 1 – In-progress)
D = Movement (0 – Complete 1 – In-progress)

Servo 6 status
R5

A	B	C	D	0	0	0	0
---	---	---	---	---	---	---	---

A = Operation (0 – Servo disabled 1 – Servo enabled)
B = Reverse (0 – Servo normal 1 – Servo reversed)
C = Soft-start (0 – Complete 1 – In-progress)
D = Movement (0 – Complete 1 – In-progress)

Servo 7 status
R6

A	B	C	D	0	0	0	0
---	---	---	---	---	---	---	---

A = Operation (0 – Servo disabled 1 – Servo enabled)
B = Reverse (0 – Servo normal 1 – Servo reversed)
C = Soft-start (0 – Complete 1 – In-progress)
D = Movement (0 – Complete 1 – In-progress)

Servo 8 status
R7

A	B	C	D	0	0	0	0
---	---	---	---	---	---	---	---

A = Operation (0 – Servo disabled 1 – Servo enabled)
B = Reverse (0 – Servo normal 1 – Servo reversed)
C = Soft-start (0 – Complete 1 – In-progress)
D = Movement (0 – Complete 1 – In-progress)

Servo 9 status
R8

A	B	C	D	0	0	0	0
---	---	---	---	---	---	---	---

A = Operation (0 – Servo disabled 1 – Servo enabled)
B = Reverse (0 – Servo normal 1 – Servo reversed)
C = Soft-start (0 – Complete 1 – In-progress)
D = Movement (0 – Complete 1 – In-progress)

Servo 10 status
R9

A	B	C	D	0	0	0	0
---	---	---	---	---	---	---	---

A = Operation (0 – Servo disabled 1 – Servo enabled)
B = Reverse (0 – Servo normal 1 – Servo reversed)
C = Soft-start (0 – Complete 1 – In-progress)
D = Movement (0 – Complete 1 – In-progress)

Servo 11 status
R10

A	B	C	D	0	0	0	0
---	---	---	---	---	---	---	---

A = Operation (0 – Servo disabled 1 – Servo enabled)
B = Reverse (0 – Servo normal 1 – Servo reversed)
C = Soft-start (0 – Complete 1 – In-progress)
D = Movement (0 – Complete 1 – In-progress)

Servo 12 status
R11

A	B	C	D	0	0	0	0
---	---	---	---	---	---	---	---

A = Operation (0 – Servo disabled 1 – Servo enabled)
B = Reverse (0 – Servo normal 1 – Servo reversed)
C = Soft-start (0 – Complete 1 – In-progress)
D = Movement (0 – Complete 1 – In-progress)

Servo 13 status
R12

A	B	C	D	0	0	0	0
---	---	---	---	---	---	---	---

A = Operation (0 – Servo disabled 1 – Servo enabled)
B = Reverse (0 – Servo normal 1 – Servo reversed)
C = Soft-start (0 – Complete 1 – In-progress)
D = Movement (0 – Complete 1 – In-progress)

Servo 14 status
R13

A	B	C	D	0	0	0	0
---	---	---	---	---	---	---	---

A = Operation (0 – Servo disabled 1 – Servo enabled)
B = Reverse (0 – Servo normal 1 – Servo reversed)
C = Soft-start (0 – Complete 1 – In-progress)
D = Movement (0 – Complete 1 – In-progress)

Servo 15 status
R14

A	B	C	D	0	0	0	0
---	---	---	---	---	---	---	---

A = Operation (0 – Servo disabled 1 – Servo enabled)
B = Reverse (0 – Servo normal 1 – Servo reversed)
C = Soft-start (0 – Complete 1 – In-progress)
D = Movement (0 – Complete 1 – In-progress)

Servo 16 status
R15

A	B	C	D	0	0	0	0
---	---	---	---	---	---	---	---

A = Operation (0 – Servo disabled 1 – Servo enabled)
B = Reverse (0 – Servo normal 1 – Servo reversed)
C = Soft-start (0 – Complete 1 – In-progress)
D = Movement (0 – Complete 1 – In-progress)

Servo 17 status
R16

A	B	C	D	0	0	0	0
---	---	---	---	---	---	---	---

A = Operation (0 – Servo disabled 1 – Servo enabled)
B = Reverse (0 – Servo normal 1 – Servo reversed)
C = Soft-start (0 – Complete 1 – In-progress)
D = Movement (0 – Complete 1 – In-progress)

Servo 18 status
R17

A	B	C	D	0	0	0	0
---	---	---	---	---	---	---	---

A = Operation (0 – Servo disabled 1 – Servo enabled)
B = Reverse (0 – Servo normal 1 – Servo reversed)
C = Soft-start (0 – Complete 1 – In-progress)
D = Movement (0 – Complete 1 – In-progress)

Firmware version
R18

M	M	M	M	V	V	V	V
---	---	---	---	---	---	---	---

M.M = Firmware major revision number 1-15
V.V = Firmware minor revision number 1-15

Bit (A) 128_{decimal} is the operate bit which when set indicates that the servo is operational.

Bit (B) 64_{decimal} is the reverse bit which when set indicates that position values written to the servo will be reversed.

Bit (C) 32_{decimal} is the soft-start bit which when set indicates that soft-start is in progress.

Movement complete determination
Bit (D) 16_{decimal} is cleared to indicate if the current servo movement has completed.

This indication is not derived from mechanical or electrical feedback from the servo being controlled but is a function of the current servo speed selected and position.

When the slowest servo speed (0) is selected the determination of movement completion is at its best. This is because the positional change of the servo between its current and final position has been split into many sub-positions which must be attained before the final position is reached. These many sub-positions ensure that the mechanical position closely relates to the position requested by the pulse width and therefore the determination of final position (movement complete) will closely relate to mechanical position. As servo speed is increased the error between mechanical position and pulse width position increases and movement completion accuracy is degraded.

Electrical Characteristics (T_A = 25°C Typical)

Parameter	Minimum	Maximum	Units	Notes
Supply Voltage (Servo power)	3.8	12	V	1,2
Supply Current (Servo power)	1	2x 2800	mA	3
Supply Voltage (on-board VCC)	4.75	16	V	
Supply Current (on-board VCC)	2	25	mA	4
I ² C pull-up resistance	-	4700	Ω	
I ² C speed	-	400	kHz	

Absolute Maximum Ratings

Parameter	Minimum	Maximum	Units	Notes
Supply Voltage (Servo power)	-0.5	+30	V	5
Supply Current (Servo power)	0	4.5	A	

Environmental

Parameter	Minimum	Maximum	Units
Operating Temperature	0	70	°C
Storage Temperature	-10	80	°C
Humidity	0	80	%
Dimensions	Length 56.25mm, Width 53.5mm, Height 15mm		
Weight	25g		
Immunity & emissions	See statement on page 8		

Notes:

- 1.Servo voltage below 5V requires that the servo regulator be disabled (see above).
- 2.Voltages above 6-12V may require force cooling of the heat-sinks if servo load is high.
- 3.Values given are based on maximum and minimum loading for each regulator.
- 4.Values given are for servos being not driven and driven.
- 5.Value given is based on maximum and minimum loading.

Calculating binary bit values:

The registers used above use the binary notation to allow the control of servo operation, reversal, soft-start & speed selection. Each register is made up of eight (8) bits, which can be set or cleared to produce the desired operation, the individual bits having a value associated with them as follows:

128	64	32	16	8	4	2	1
-----	----	----	----	---	---	---	---

If we take for example one of the servo control registers we can see it is made up of four (4) separate bits A, B, C & D plus a four bit value SSSS:

Servo 1 control

R1	A	B	C	D	S	S	S	S
----	---	---	---	---	---	---	---	---

A = Operate (0 – Servo disabled 1 – Servo enabled)

B = Reverse (0 – Servo normal 1 – Servo reversed)

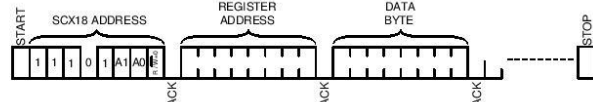
C = Soft-start control (0 – Disabled 1 – Enabled)

D = Speed control (0 – Disabled 1 – Enabled)

S..S = Servo speed value 0 to 15 (0 = slowest)

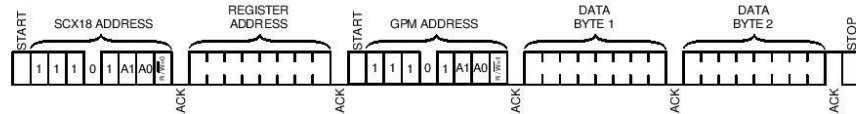
Each bit is defined to control a particular function for the servo it controls, so if for example we wanted to enable servo 1 we would need to set bit 'A' which controls the servo operation. We know from the bit values defined above that the value associated with the 'A' bit is 128, so by writing this value to register 1 we can enable servo 1. If we need to enable additional functions such as the speed control - 'D' - as well as the servo enable, the value of this bit is added to the value written to the register i.e. 128 + 16 = 144. In addition we could also add a speed value of 5 that would make the total value 128 + 16 + 5 = 149.

Figure 1.0 (I²C write protocol)



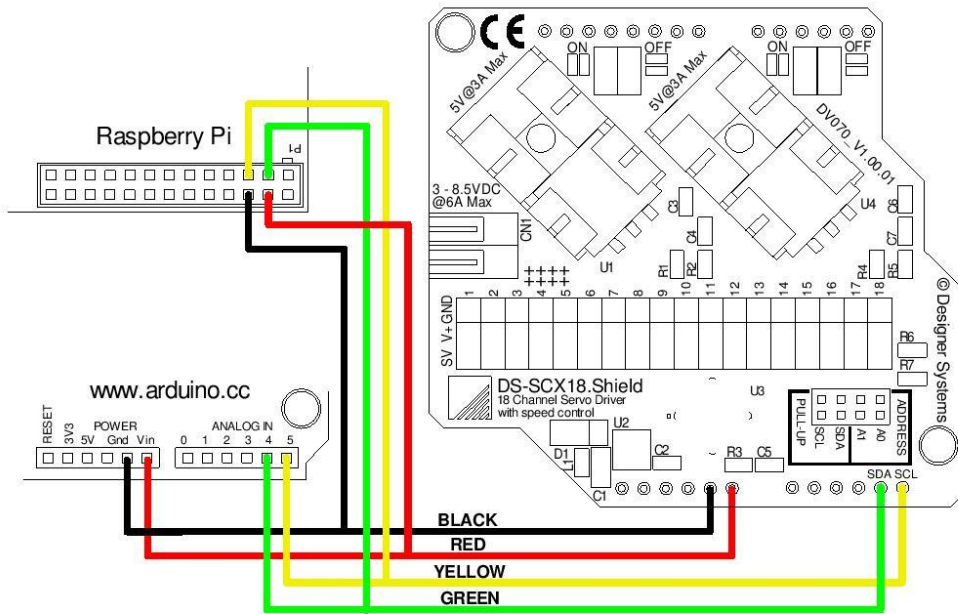
Multiple bytes may be written before the 'STOP' condition. Data is written into registers starting at 'REGISTER ADDRESS', then 'REGISTER ADDRESS' +1, then 'REGISTER ADDRESS' +2 etc. Each byte transfer is acknowledged 'ACK' by the SCX18 until the 'STOP' condition.

Figure 1.1 (I²C read protocol)

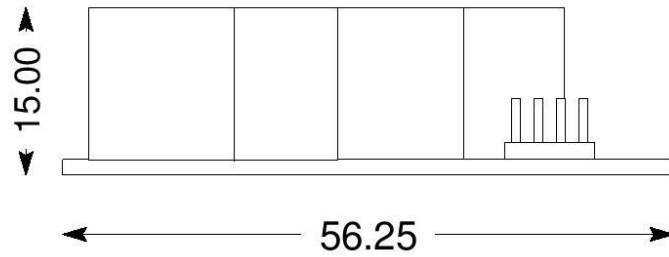
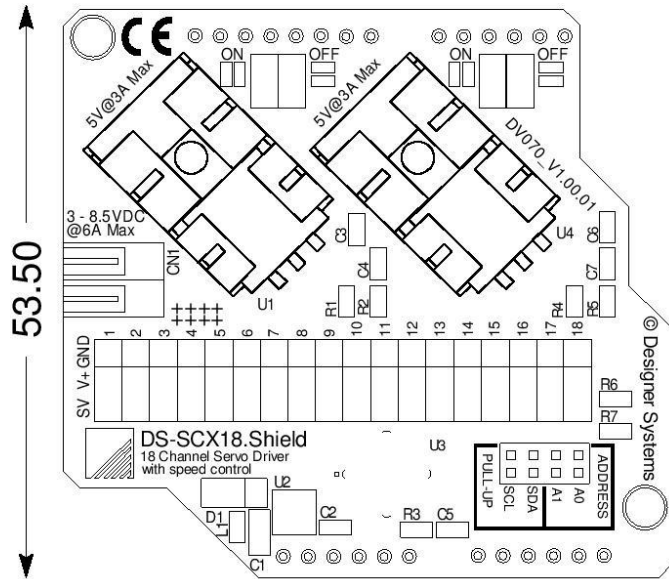


'DATA BYTE 1 & 2' are register values returned from the SCX18. Each byte written is acknowledged 'ACK' by the SCX18, every byte read is acknowledged 'ACK' by the I²C Master. A Not-acknowledge 'NACK' condition is generated by the I²C Master when it has finished reading.

Figure 2.0 (Connection Schematic for Arduino UNO or Raspberry-Pi I²C communication)



Mechanical Specifications – Units millimetres



Revision History:
1.00 Release version

**WEEE Consumer Notice**

This product is subject to Directive 2002/96/EC of the European Parliament and the Council of the European Union on Waste of Electrical and Electronic Equipment (WEEE) and, in jurisdictions adopting that Directive, is marked as being put on the market after August 13, 2005, and should not be disposed of as unsorted municipal/public waste. Please utilise your local WEEE collection facilities in the disposition and otherwise observe all applicable requirements. For further information on the requirements regarding the disposition of this product in other languages please visit www.designersystems.co.uk

**RoHS Compliance**

This product complies with Directive 2002/95/EC of the European Parliament and the Council of the European Union on the Restriction of Hazardous Substances (RoHS) which prohibits the use of various heavy metals (lead, mercury, cadmium, and hexavalent chromium), polybrominated biphenyls (PBB) and polybrominated diphenyl ethers (PBDE).

Declaration of Conformity

Apparatus name / model number DS-SCX18.S

Conformity via Generic Standard EN61000-1

Generic Standard EN61000-3

Conformity criteria For use only within commercial, residential and light industrial applications

We certify that the apparatus identified above conforms to the requirements of Council Directive 2004/108/EC & 2006/95/EC

Signed.

Date 20/6/13

Having made this declaration the CE mark is affixed to this product, its packaging, manual or warranty.

The information appearing in this data sheet is believed to be accurate at the time of publication. However, Designer Systems assumes no responsibility arising from the use of the information supplied. The applications mentioned herein are used solely for the purpose of illustration and Designer Systems makes no warranty or representation that such applications will be suitable without further modification, nor recommends the use of its products for application that may present a risk to human life due to malfunction or otherwise. Designer Systems reserves the right to alter its products without prior notification.

Copyright © 2013 by Designer Systems Ltd

Manufacturer Designer Systems, 11 Castle Street, Truro, Cornwall TR1 3AF, United Kingdom

Description of apparatus Robotic interface peripheral

22.2 TDK Lambda LS 100-5 Power Supply

LS 100

TDK Lambda

LS100 Specifications

		MODEL	LS100-3.3	LS100-5	LS100-12	LS100-15	LS100-24	LS100-36	LS100-48
Input	Voltage Range (*2)(*13)	V	AC88 - 264 or DC125 - 373 (Withstand AC300 Surge for 5 seconds)						
	Frequency (*2)	Hz	47 - 63						
	Efficiency(230VAC)(typ) (*1)	%	75	79	82	84	86		
	Current(115/230VAC)(typ) (*1)	A	2.2 / 1.2						
	Inrush Current(typ) (*3)	A	60A at 230VAC, Ta=25°C (Cold Start)						
	Leakage Current (*10)	mA	< 1mA at 230VAC, 60Hz						
Output	Nominal Voltage	VDC	3.3	5	12	15	24	36	48
	Maximum Current	A	20	16	8.5	7	4.5	3	2.3
	Maximum Power	W	66	80	102	105	108		110.4
	Maximum Line Regulation (*5)(*6)	mV	20		48	60	96	144	192
	Maximum Load Regulation (*5)(*7)	mV	40		96	120	192	288	384
	Temperature Coefficient		Less than 0.02%/°C						
	Maximum Ripple & Noise (*1)(*4)	mVp-p	80		120			150	200
	Hold-up Time(115/230VAC)(typ) (*1)	ms	25 / 150						
Voltage Adjustable Range	VDC	3 - 3.6	4.75 - 5.5	10.8 - 13.2	13.5 - 16.5	22 - 27.2	32 - 40	42 - 54	
Function	Over Current Protection (*8)	A	> 110% rated output power						
	Over Voltage Protection (*9)	VDC	3.8 - 4.45	5.75 - 6.75	13.8 - 16.2	17.25 - 20.25	27.6 - 32.4	41.4 - 48.6	55.2 - 64.8
Environment	Series Operation		Possible						
	Operating Temperature (*11)	°C	- 25 - + 70 (Refer to Output Derating Curve)						
	Storage Temperature	°C	- 40 - +85						
	Operating Humidity	%RH	20 - 90 (No dewdrop)						
	Storage Humidity	%RH	10 - 95 (No dewdrop)						
	Vibration		At no operating, 10 - 55Hz (sweep for 1min) 19.6m/s² Constant, X, Y, Z 1hour each.						
	Shock(In Package)		Less than 196.1m/s²						
	Cooling		Convection cooling						
Isolation	Withstand Voltage		Input - Output : 3.0kVAC (20mA), Input - FG : 1.5kVAC (20mA) Output - FG : 500VAC (100mA) for 1min.						
	Isolation Resistance		Input - FG, Input - Output and Output - FG: More than 100MΩ (500VDC) at 25°C and 70%RH						
Standards	Safety Standards		Approved by UL60950-1, EN60950-1, IEC60950-1						
	PFHC		Built to meet IEC61000-3-2, -3						
	EMI		Built to meet EN55011/EN55022-B, FCC-B						
	Immunity		Built to meet EN61000-4-2 (Level 2,3), -3 (Level 3), -4 (Level 3), -5 (Level 4), -6 (Level 3), -8 (Level 4), -11						
Mechanical	Weight(typ)	g	600						
	Size (W×H×D)	mm	159 x 97 x 38 (Refer to Outline Drawing)						

(*1) At Maximum Output Power, nominal input voltage, Ta = 25°C.

(*2) For cases where conformance to various safety specs (UL, CSA, EN) are required, to be described as 100 - 240VAC, 50 / 60Hz on name plate.

(*3) Not applicable for the in-rush current to Noise Filter for less than 0.2mS.

(*4) Ripple & noise are measured at 20MHz by using a 300mm twisted pair of load wires terminated with a 0.1uF film capacitor and a 47uF electrolytic capacitor.

(*5) Measure line & load regulation at output terminal M3.5 tapped point.

(*6) 88 - 264VAC, constant load.

(*7) No load - Full load (Maximum power), constant input voltage.

(*8) Current limit with automatic recovery. Avoid to operate at overload or dead short for more than 30 seconds.

(*9) OVP circuit will shutdown output, manual reset (Re-power on).

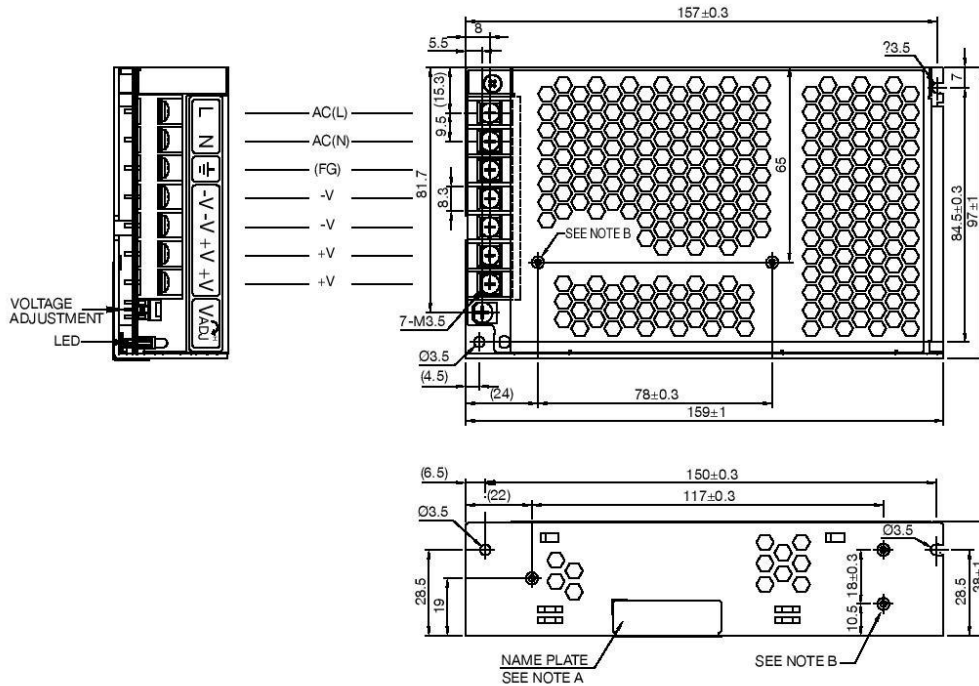
(*10) Measured by each measuring method of UL and EN (at 60Hz), Ta=25°C.

(*11) Refer to Output Derating Curve (PA577-01-02_) for details of output derating versus ambient temperature.

(*12) All parameters NOT specifically mentioned are measured at 230VAC input, rated load and Ta = 25°C.

(*13) Refer to Output Derating Curve (PA577-01-03_) for details of output derating versus input voltage.

LS100 Outline Drawing

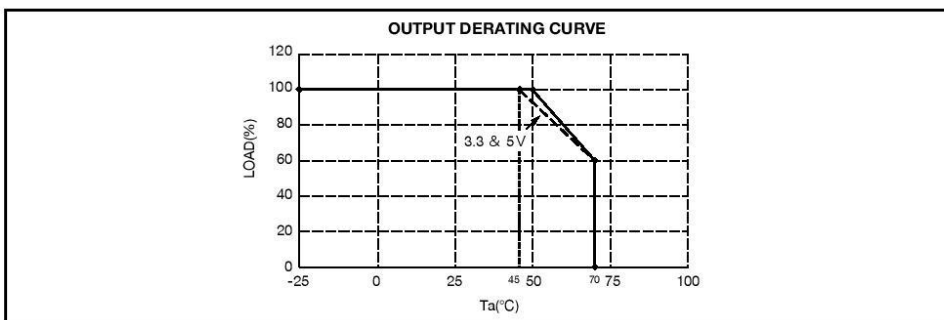


- NOTES
- A. MODEL NAME NOMINAL OUTPUT VOLTAGE AND MAXIMUM OUTPUT CURRENT ARE SHOWN IN THE NAME PLATE IN ACCORDANCE WITH THE SPECIFICATION.
 - B. M3 TAPPED & EMBOSSED & COUNTERSUNK HOLES (5) FOR CUSTOMER CHASSIS MOUNTING. SCREW MUST NOT PROTRUDE INTO POWER SUPPLY BY MORE THAN 5mm.

LS100 Output Derating

*COOLING : CONVECTION COOLING

Ta(°C)	LOAD(%)	STANDARD MOUNTING
-25 to +45	100	
50	92 (3.3 & 5V), 100 (OTHERS)	
70	60	



*All specifications are subject to change without notice.

22.3 Texas Instruments CD74HCT4015E multiplexer



Data sheet acquired from Harris Semiconductor
SCHS1221

**CD54/74HC4051, CD54/74HCT4051,
CD54/74HC4052, CD74HCT4052,
CD54/74HC4053, CD74HCT4053**

**High-Speed CMOS Logic
Analog Multiplexers/Demultiplexers**

November 1997 - Revised July 2004

Features

- Wide Analog Input Voltage Range $\pm 5V$ Max
- Low "On" Resistance
 - 70 Ω Typical ($V_{CC} - V_{EE} = 4.5V$)
 - 40 Ω Typical ($V_{CC} - V_{EE} = 9V$)
- Low Crosstalk between Switches
- Fast Switching and Propagation Speeds
- "Break-Before-Make" Switching
- Wide Operating Temperature Range . . -55 $^{\circ}C$ to 125 $^{\circ}C$
- CD54HC/CD74HC Types
 - Operation Control Voltage 2V to 6V
 - Switch Voltage 0V to 10V
 - High Noise Immunity . . . $N_{IL} = 30\%$, $N_{IH} = 30\%$ of V_{CC} , $V_{CC} = 5V$
- CD54HCT/CD74HCT Types
 - Operation Control Voltage 4.5V to 5.5V
 - Switch Voltage 0V to 10V
 - Direct LSTTL Input
Logic Compatibility . . . $V_{IL} = 0.8V$ Max, $V_{IH} = 2V$ Min
 - CMOS Input Compatibility $I_I \leq 1\mu A$ at V_{OL} , V_{OH}

Description

These devices are digitally controlled analog switches which utilize silicon gate CMOS technology to achieve operating speeds similar to LSTTL with the low power consumption of standard CMOS integrated circuits.

These analog multiplexers/demultiplexers control analog voltages that may vary across the voltage supply range (i.e. V_{CC} to V_{EE}). They are bidirectional switches thus allowing any analog input to be used as an output and vice-versa. The switches have low "on" resistance and low "off" leakages. In addition, all three devices have an enable control which, when high, disables all switches to their "off" state.

Ordering Information

PART NUMBER	TEMP. RANGE ($^{\circ}C$)	PACKAGE
CD54HC4051F3A	-55 to 125	16 Ld CERDIP
CD54HC4052F3A	-55 to 125	16 Ld CERDIP
CD54HC4053F3A	-55 to 125	16 Ld CERDIP
CD54HCT4051F3A	-55 to 125	16 Ld CERDIP

Ordering Information

PART NUMBER	TEMP. RANGE ($^{\circ}C$)	PACKAGE
CD74HC4051E	-55 to 125	16 Ld PDIP
CD74HC4051M	-55 to 125	16 Ld SOIC
CD74HC4051MT	-55 to 125	16 Ld SOIC
CD74HC4051M96	-55 to 125	16 Ld SOIC
CD74HC4051NSR	-55 to 125	16 Ld SOP
CD74HC4051PWR	-55 to 125	16 Ld TSSOP
CD74HC4051PWT	-55 to 125	16 Ld TSSOP
CD74HC4052E	-55 to 125	16 Ld PDIP
CD74HC4052M	-55 to 125	16 Ld SOIC
CD74HC4052MT	-55 to 125	16 Ld SOIC
CD74HC4052M96	-55 to 125	16 Ld SOIC
CD74HC4052NSR	-55 to 125	16 Ld SOP
CD74HC4052PW	-55 to 125	16 Ld TSSOP
CD74HC4052PWR	-55 to 125	16 Ld TSSOP
CD74HC4052PWT	-55 to 125	16 Ld TSSOP
CD74HC4053E	-55 to 125	16 Ld PDIP
CD74HC4053M	-55 to 125	16 Ld SOIC
CD74HC4053MT	-55 to 125	16 Ld SOIC
CD74HC4053M96	-55 to 125	16 Ld SOIC
CD74HC4053NSR	-55 to 125	16 Ld SOP
CD74HC4053PW	-55 to 125	16 Ld TSSOP
CD74HC4053PWR	-55 to 125	16 Ld TSSOP
CD74HC4053PWT	-55 to 125	16 Ld TSSOP
CD74HCT4051E	-55 to 125	16 Ld PDIP
CD74HCT4051M	-55 to 125	16 Ld SOIC
CD74HCT4051MT	-55 to 125	16 Ld SOIC
CD74HCT4051M96	-55 to 125	16 Ld SOIC
CD74HCT4052E	-55 to 125	16 Ld PDIP
CD74HCT4052M	-55 to 125	16 Ld SOIC
CD74HCT4052MT	-55 to 125	16 Ld SOIC
CD74HCT4052M96	-55 to 125	16 Ld SOIC
CD74HCT4053E	-55 to 125	16 Ld PDIP
CD74HCT4053M	-55 to 125	16 Ld SOIC
CD74HCT4053MT	-55 to 125	16 Ld SOIC
CD74HCT4053M96	-55 to 125	16 Ld SOIC
CD74HCT4053PWR	-55 to 125	16 Ld TSSOP
CD74HCT4053PWT	-55 to 125	16 Ld TSSOP

NOTE: When ordering, use the entire part number. The suffixes 96 and R denote tape and reel. The suffix T denotes a small-quantity reel of 250.

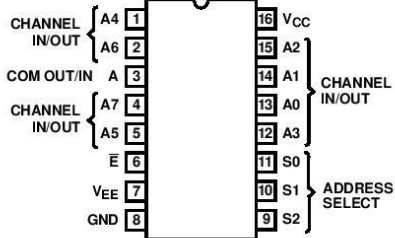
CAUTION: These devices are sensitive to electrostatic discharge. Users should follow proper IC Handling Procedures.

Copyright © 2004, Texas Instruments Incorporated

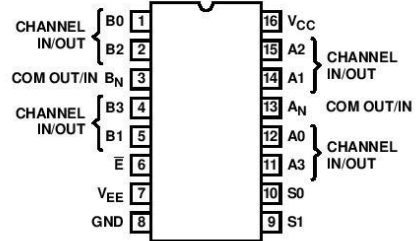
'HC4051, 'HCT4051, 'HC4052, CD74HCT4052, 'HC4053, CD74HCT4053

Pinouts

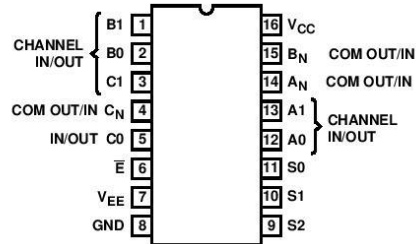
CD54HC4051, CD54HCT4051
(CERDIP)
CD74HC4051
(PDIP, SOIC, SOP, TSSOP)
CD74HCT4051
(PDIP, SOIC)
TOP VIEW



CD54HC4052
(CERDIP)
CD74HC4052
(PDIP, SOIC, SOP, TSSOP)
CD74HCT4052
(PDIP, SOIC)
TOP VIEW

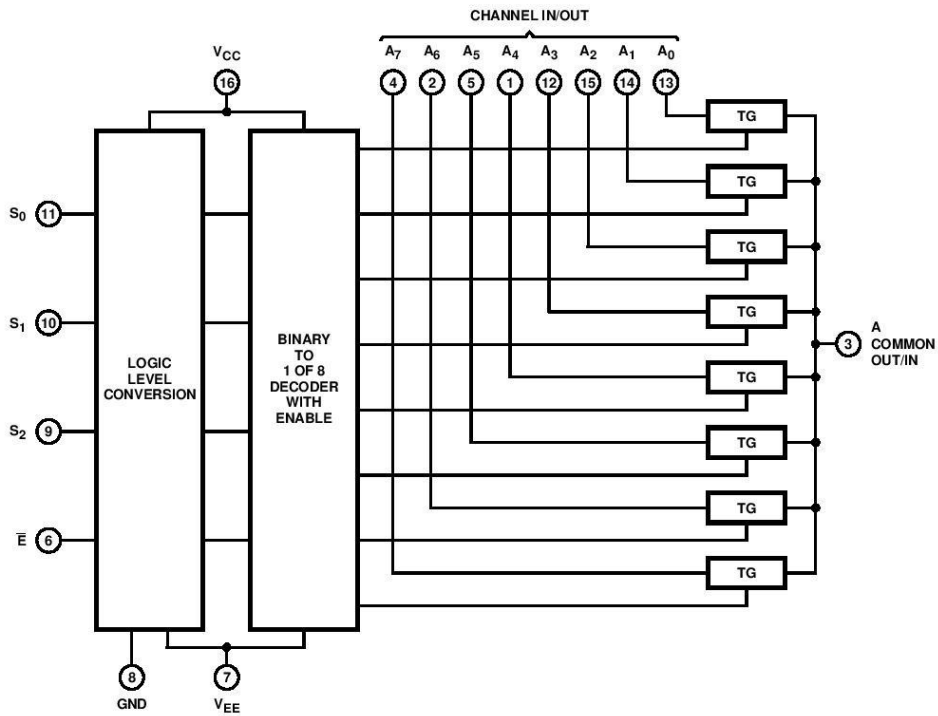


CD54HC4053
(CERDIP)
CD74HC4053
(PDIP, SOIC, SOP, TSSOP)
CD74HCT4053
(PDIP, SOIC, TSSOP)
TOP VIEW



'HC4051, 'HCT4051, 'HC4052, CD74HCT4052, 'HC4053, CD74HCT4053

Functional Diagram of HC/HCT4051



TRUTH TABLE
HC/HCT4051

INPUT STATES				"ON" CHANNELS
ENABLE	S ₂	S ₁	S ₀	
L	L	L	L	A ₀
L	L	L	H	A ₁
L	L	H	L	A ₂
L	L	H	H	A ₃
L	H	L	L	A ₄
L	H	L	H	A ₅
L	H	H	L	A ₆
L	H	H	H	A ₇
H	X	X	X	None

X = Don't care

'HC4051, 'HCT4051, 'HC4052, CD74HCT4052, 'HC4053, CD74HCT4053

Absolute Maximum Ratings (Note 2)

DC Supply Voltage, $V_{CC} - V_{EE}$	-0.5V to 10.5V
DC Supply Voltage, V_{CC}	-0.5V to +7V
DC Supply Voltage, V_{EE}	+0.5V to -7V
DC Input Diode Current, I_{IK}	
For $V_I < -0.5V$ or $V_I > V_{CC} + 0.5V$	$\pm 20mA$
DC Switch Diode Current, I_{OK}	
For $V_I < V_{EE} - 0.5V$ or $V_I > V_{CC} + 0.5V$	$\pm 20mA$
DC Switch Current, (Note 2)	
For $V_I > V_{EE} - 0.5V$ or $V_I < V_{CC} + 0.5V$	$\pm 25mA$
DC V_{CC} or Ground Current, I_{CC}	$\pm 50mA$
DC V_{EE} Current, I_{EE}	-20mA

Thermal Information

Package Thermal Impedance, θ_{JA} (see Note 1):	
E (PDIP) Package	67°C/W
M (SOIC) Package	73°C/W
NS (SOP) Package	64°C/W
PW (TSSOP) Package	108°C/W
Maximum Junction Temperature	150°C
Maximum Storage Temperature Range	-65°C to 150°C
Maximum Lead Temperature (Soldering 10s)	300°C

NOTE:

- The package thermal impedance is calculated in accordance with JESD 51-7.

Recommended Operating Conditions

For maximum reliability, nominal operating conditions should be selected so that operation is always within the following ranges

PARAMETER	MIN	MAX	UNITS
Supply Voltage Range (For T_A = Full Package Temperature Range), V_{CC} (Note 2)			
CD54/74HC Types	2	6	V
CD54/74HCT Types	4.5	5.5	V
Supply Voltage Range (For T_A = Full Package Temperature Range), $V_{CC} - V_{EE}$			
CD54/74HC Types, CD54/74HCT Types (See Figure 1)	2	10	V
Supply Voltage Range (For T_A = Full Package Temperature Range), V_{EE} (Note 3)			
CD54/74HC Types, CD54/74HCT Types (See Figure 2)	0	-6	V
DC Input Control Voltage, V_I	GND	V_{CC}	V
Analog Switch I/O Voltage, V_{IS}	V_{EE}	V_{CC}	V
Operating Temperature, T_A	-55	125	°C
Input Rise and Fall Times, t_r, t_f			
2V	0	1000	ns
4.5V	0	500	ns
6V	0	400	ns

CAUTION: Stresses above those listed in "Absolute Maximum Ratings" may cause permanent damage to the device. This is a stress only rating and operation of the device at these or any other conditions above those indicated in the operational sections of this specification is not implied.

NOTES:

- All voltages referenced to GND unless otherwise specified..
- In certain applications, the external load resistor current may include both V_{CC} and signal line components. To avoid drawing V_{CC} current when switch current flows into the transmission gate inputs, the voltage drop across the bidirectional switch must not exceed 0.6V (calculated from r_{ON} values shown in Electrical Specifications table). No V_{CC} current will flow through R_L if the switch current flows into terminal 3 on the HC/HCT4051; terminals 3 and 13 on the HC/HCT4052; terminals 4, 14 and 15 on the HC/HCT4053.

Recommended Operating Area as a Function of Supply Voltages

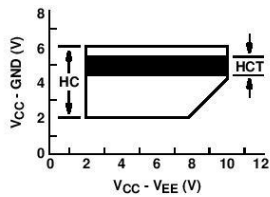


FIGURE 1.

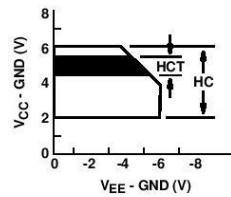



FIGURE 2.

22.4 Sunon cooling fan

SUNON

SPECIFICATION FOR APPROVAL

CUSTOMER :

MOTOR TYPE : 

DESCRIPTION : MagLev Motor Fan

DIMENSIONS : 40X40X10 mm

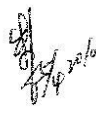
M O D E L : MB40100V2-000U-A99

SUNON SPEC. NO. : D04077770G-00

CUSTOMER APPROVAL NO. :

APPROVED BY CUSTOMER :

(AUTHORIZED)

DRAWN	<i>Emma</i> 04/22	CHECKED	<i>Cyj</i> 5/3 2010	APPROVED		SPEC.NO	D04077770G-00
	ISSUE DATE					04.22.2010	
	EDITION					0	
	REVISION DATE						
	E.SPEC					E10900343	
建準電機工業股份有限公司 SUNONWEALTH ELECTRIC MACHINE INDUSTRY CO., LTD. NO. 30, LN. 296, XINYA RD., QIANZHEN DIST., TEL:886-7-8135888 KAOHSIUNG CITY 80673, TAIWAN (R.O.C) FAX:886-7-8230505/8230606/8231010 URL:http://www.sunon.com E-mail: sunon@email.sunon.com.tw							



II. SPECIFICATION

1. MECHANICAL CHARACTERISTIC

MOTOR DESIGN	2 phases, 4-poles Brushless DC motor
BEARING SYSTEM	Vapo bearing system
DIMENSIONS	See Page 6
MATERIALS OF FRAME	Thermoplastic PBT of UL 94V-0
MATERIALS OF FAN BLADE	Thermoplastic PBT of UL 94V-0
DIRECTION OF ROTATION	Counter-clockwise viewed from front of fan blade
MOUNTING HOLES	Diameter 4.3 mm in 4 holes
WEIGHT	17 g

2. ELECTRIC CHARACTERISTIC

RATED VOLTAGE	5 VDC
RATED CURRENT	180 mA / Max. 207 mA
RATED POWER CONSUMPTION	0.90 WATTS / Max. 1.04 WATTS
OPERATING VOLTAGE RANGE	3.5~6 VDC
STARTING VOLTAGE	3.5 VDC (25 deg. C POWER ON/OFF)
OPERATING TEMPERATURE RANGE	-10 to + 70 deg. C
STORAGE TEMPERATURE RANGE	-40 to + 70 deg. C



3. PERFORMANCE CHARACTERISTIC

RATED SPEED	5800 RPM \pm 15% at rated voltage
AIR FLOW	7 CFM
STATIC PRESSURE	0.13 Inch-H₂O
ACOUSTIC NOISE	27 dB(A)
AIR FLOW V.S. PRESSURE	See Page 5
INSULATION CLASS	UL Class A
INSULATION RESISTANCE PLASTIC HOUSING	500M ohm at 500 VDC between internal stator and lead wire (+)
DIELECTRIC STRENGTH	Applied AC 500 V for one minute or AC 600 V for 2 Seconds between housing and lead wire (+)
LIFE EXPECTANCY	60,000 hours at 40 deg. C, 65% humidity, 90% CL.
PROTECTION	<input checked="" type="checkbox"/> Automatic Restart Note: In a situation where the fan is locked by an external force while the electricity is on, an increase in coil temperature will be prevented by temporarily turning off the electrical power to the motor. The fan will automatically restart when the locked rotor condition is released.
	<input type="checkbox"/> Polarity Protection

4. SAFETY

SAFETY	UL	CUR	TUV
NO.	E77551	E77551	✓



22.5 Ultimaker 2

A2. Specification of the Ultimaker 2

Printing		Physical dimensions	
Print technology	Fused filament fabrication (FFF)	Frame Dimension	X 35.7 cm Y 34.2 cm Z 38.8 cm
Build volume	23 x 22,5 x 20,5 cm	With all parts attached and the max height filament guide tube	X 49.2 cm Y 34.2 cm Z 55.8 cm
Layer resolution	20 micron (Ultra high) 60 micron (High) 100 micron (Medium) 200 micron (Low)	Shipping box	X 42.0 cm Y 42.0 cm Z 57.8 cm
Position precision	X 12,5 micron Y 12,5 micron Z 5 micron	Weight	11.2 kg
Filament diameter	2.85 mm (generally known as 3 mm filament)	Total Shipping weight	15.6 kg
Nozzle diameter	0.4 mm		
Print speed	30 mm/1 - 300 mm/s		
Travel speed	30 mm/1 - 350 mm/s		
Software		Temperature	
Software package	Cura - Official Ultimaker	Ambient Operating Temperature	15 - 32 degrees celsius
File types	STL / OBJ / DAE / AMF	Storage Temperature	0 - 32 degrees celsius
Supports	Windows (XP 32 bit/7+) Ubuntu Linux (12.04+) Mac OS X (10.6 64bit +)	Operating nozzle temperature	180 - 260 degrees celsius
		Operating heated build plate temperature	50 - 100 degrees celsius
Electrical		Sound	
AC INPUT	100 - 240 V, approx. 4 AMPS, 50 - 60 HZ 221 watt max.	Average operational noise	49 dBA.
Power Requirements	24 V DC @ 9.2 AMPS		
Connectivity	Stand-alone printing from SD-card USB (firmware) WiFi read		

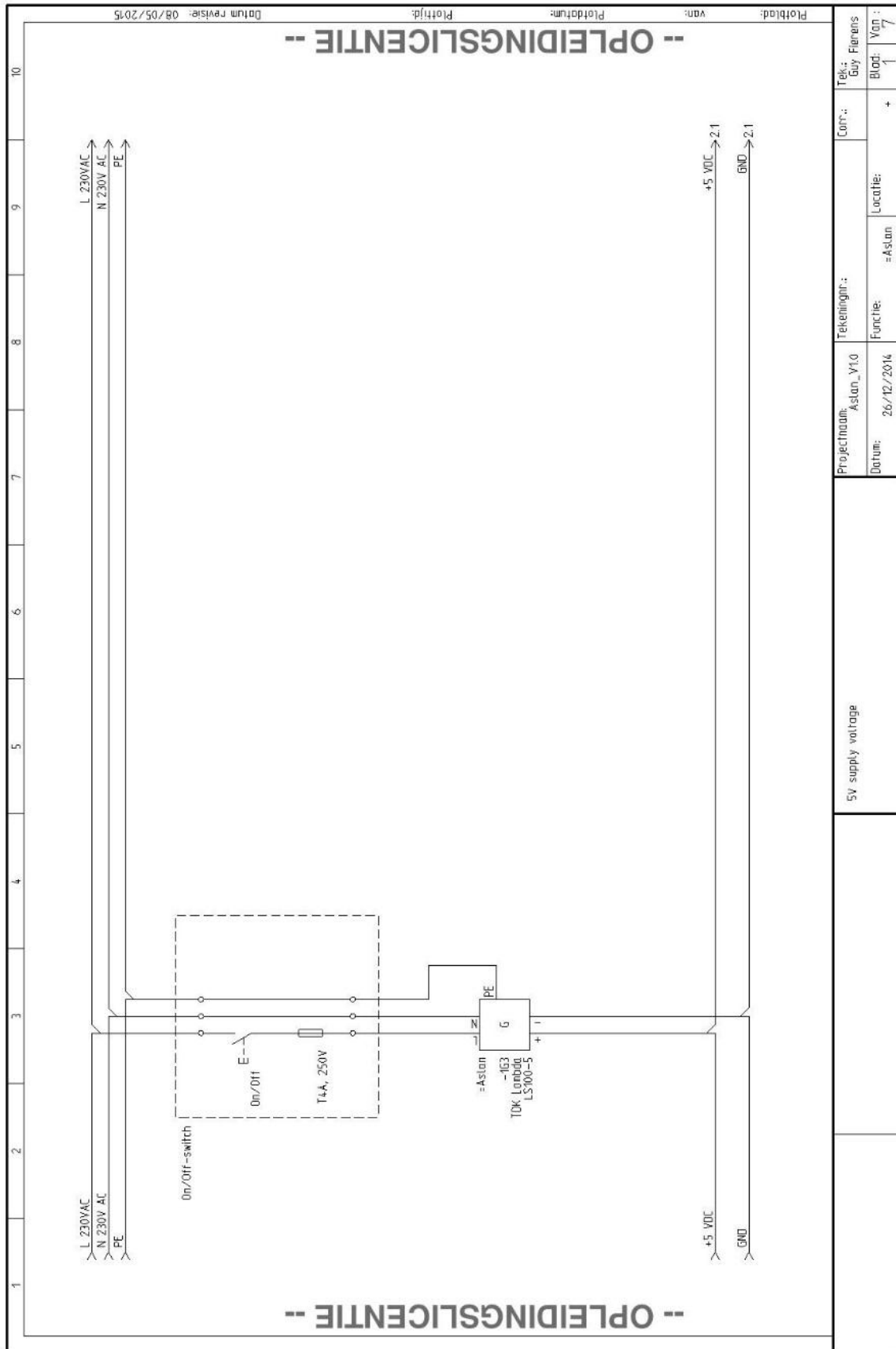
WARNING: The Ultimaker 2 generates high temperatures and has hot moving parts that can cause injury. Never reach inside of the Ultimaker 2 while it is in operation. Always control the Ultimaker 2 from the push wheel on the front or with the power-switch on the back. Allow the Ultimaker 2 to cool down for 5 minutes before reaching inside.

CAUTION: When opening the Ultimaker 2 for service, ensure that the power supply is turned off and the cord is disconnected from the wall socket.

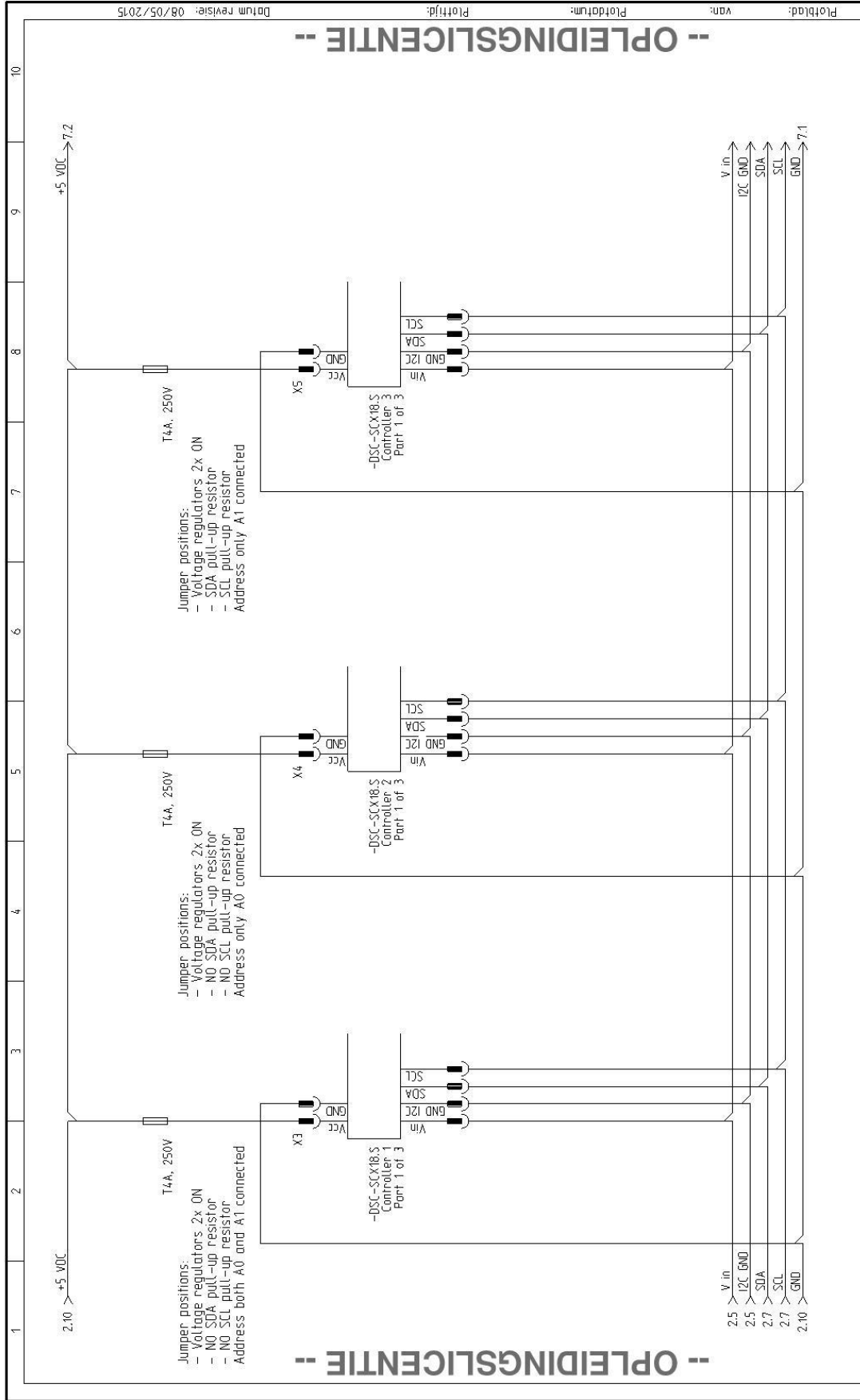
CAUTION: Only use power supply provided with your Ultimaker 2.

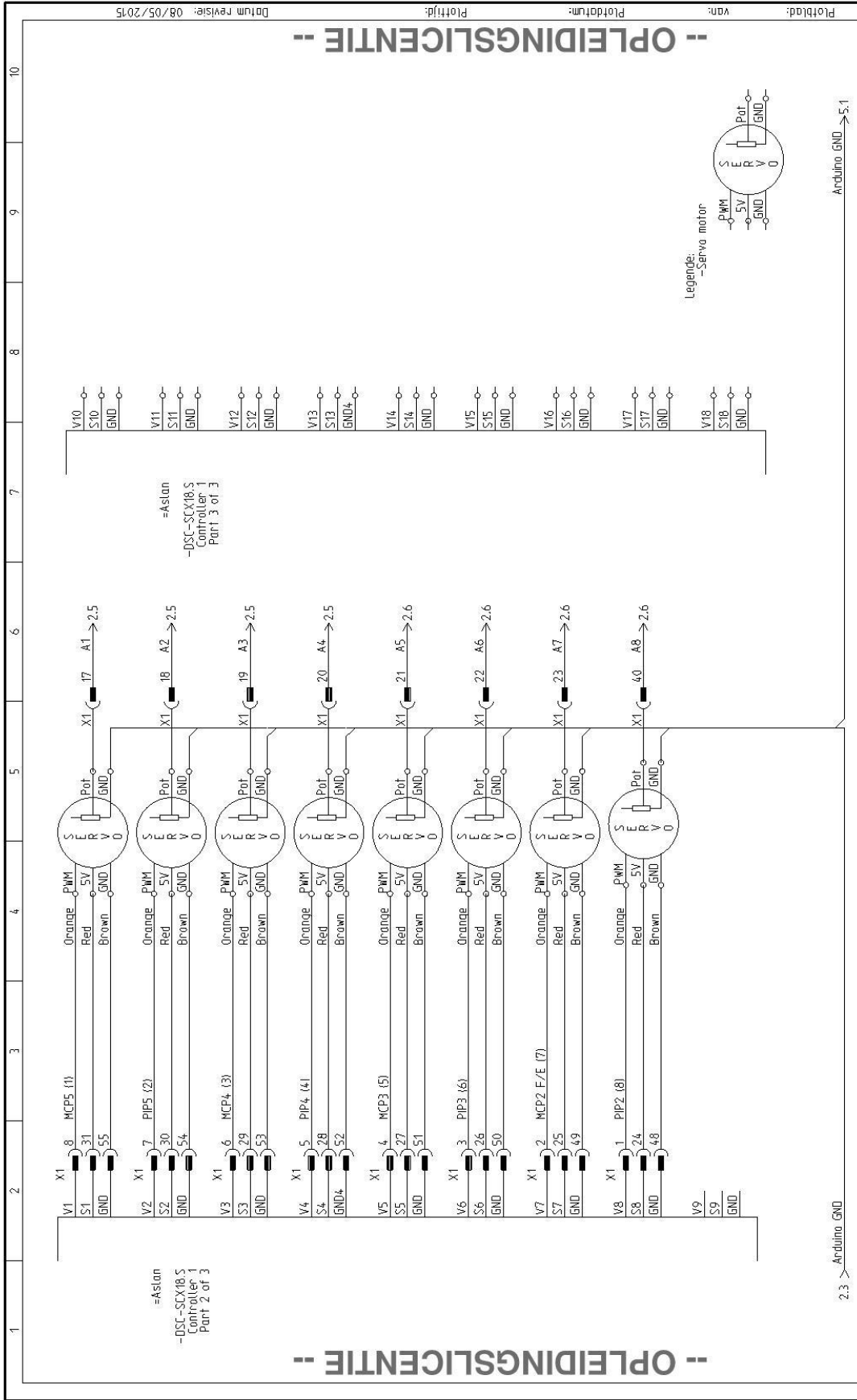


ANNEX 23: SCHEMATICS

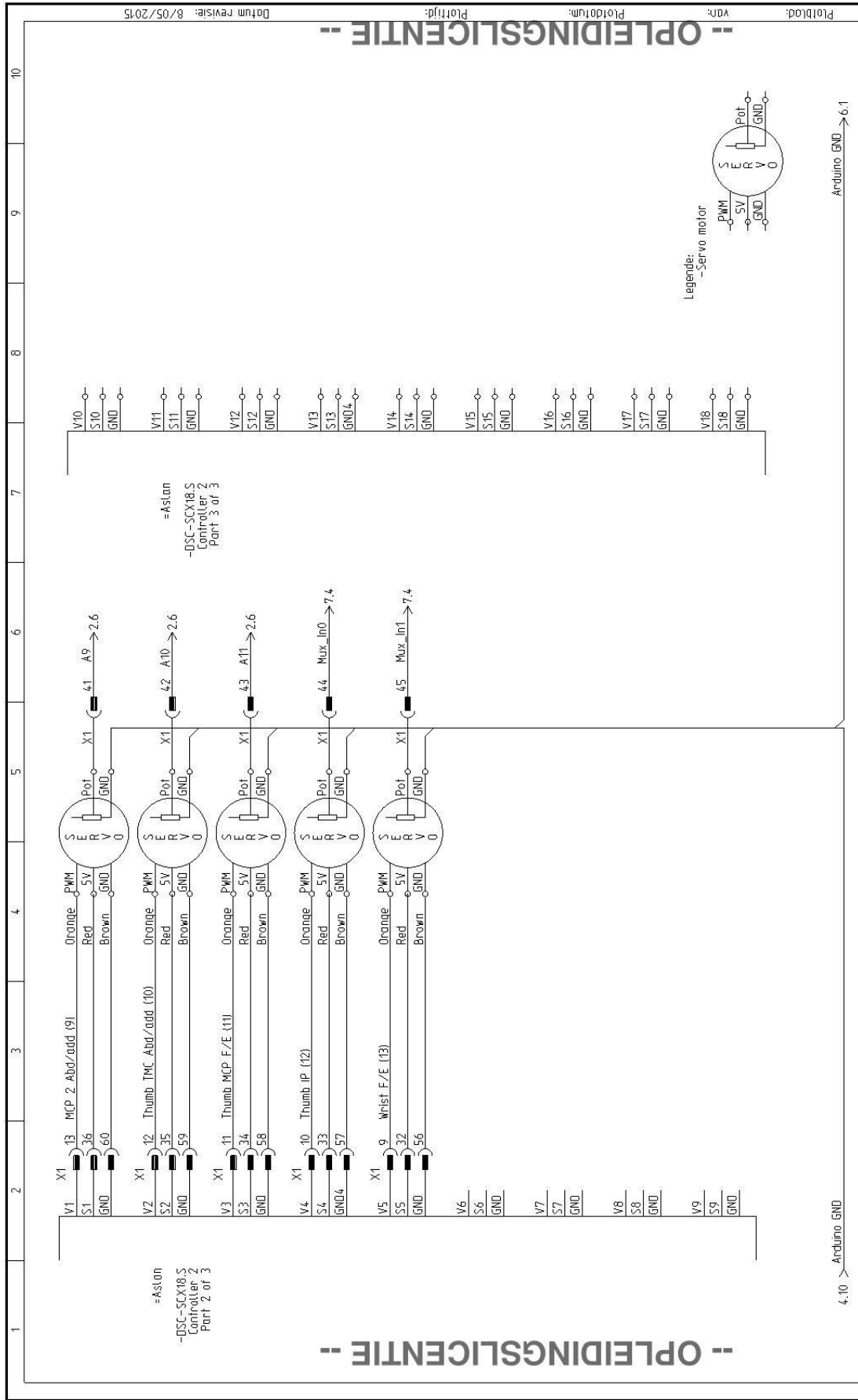


Projectnaam: Aslan_V1.0		Tekeningnr.: Tek.: Guy Fierens	
Datum: 26/12/2014		Cont.: Blad: 1	
Functie: =Aslan		Van: 7	
5V supply voltage			



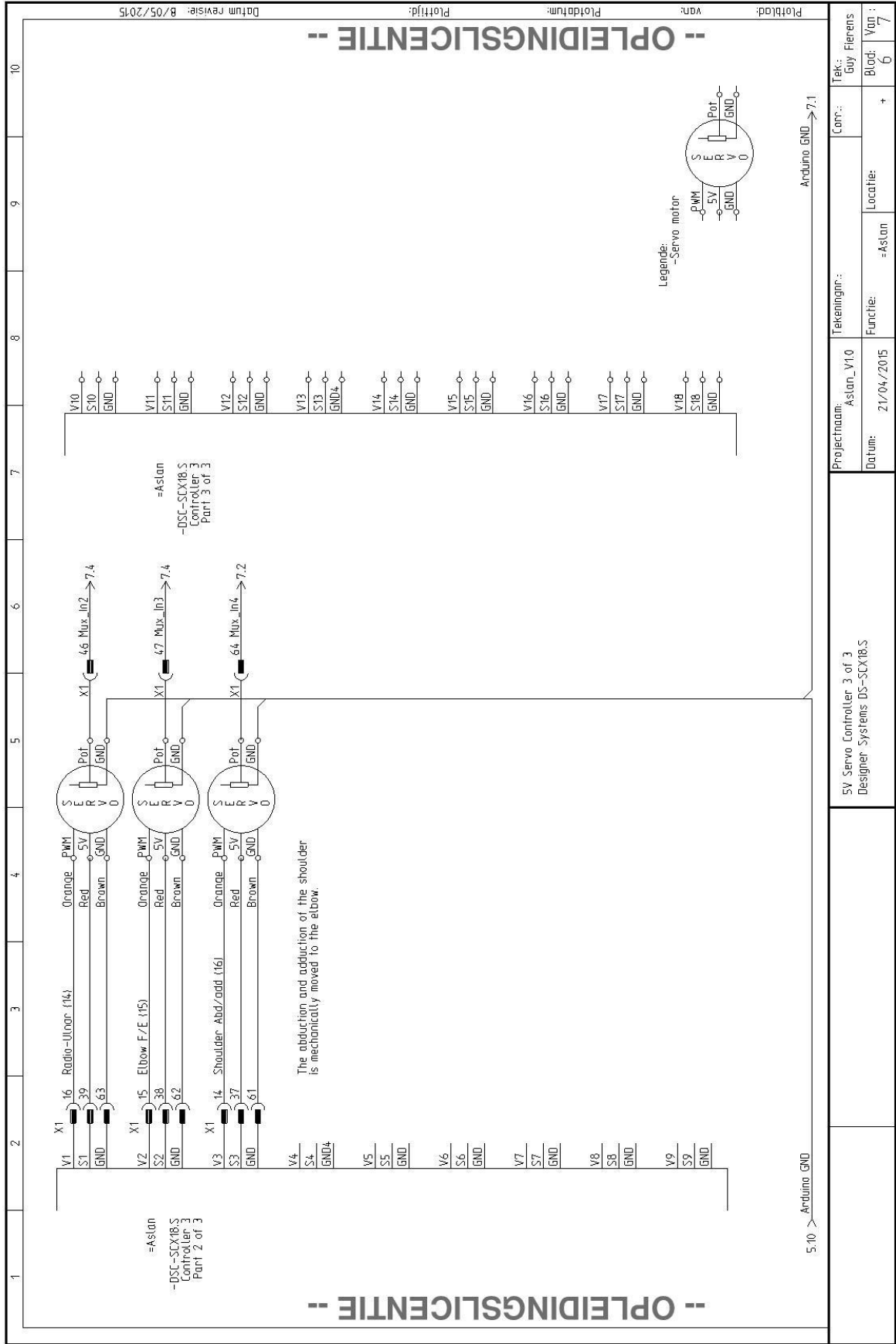


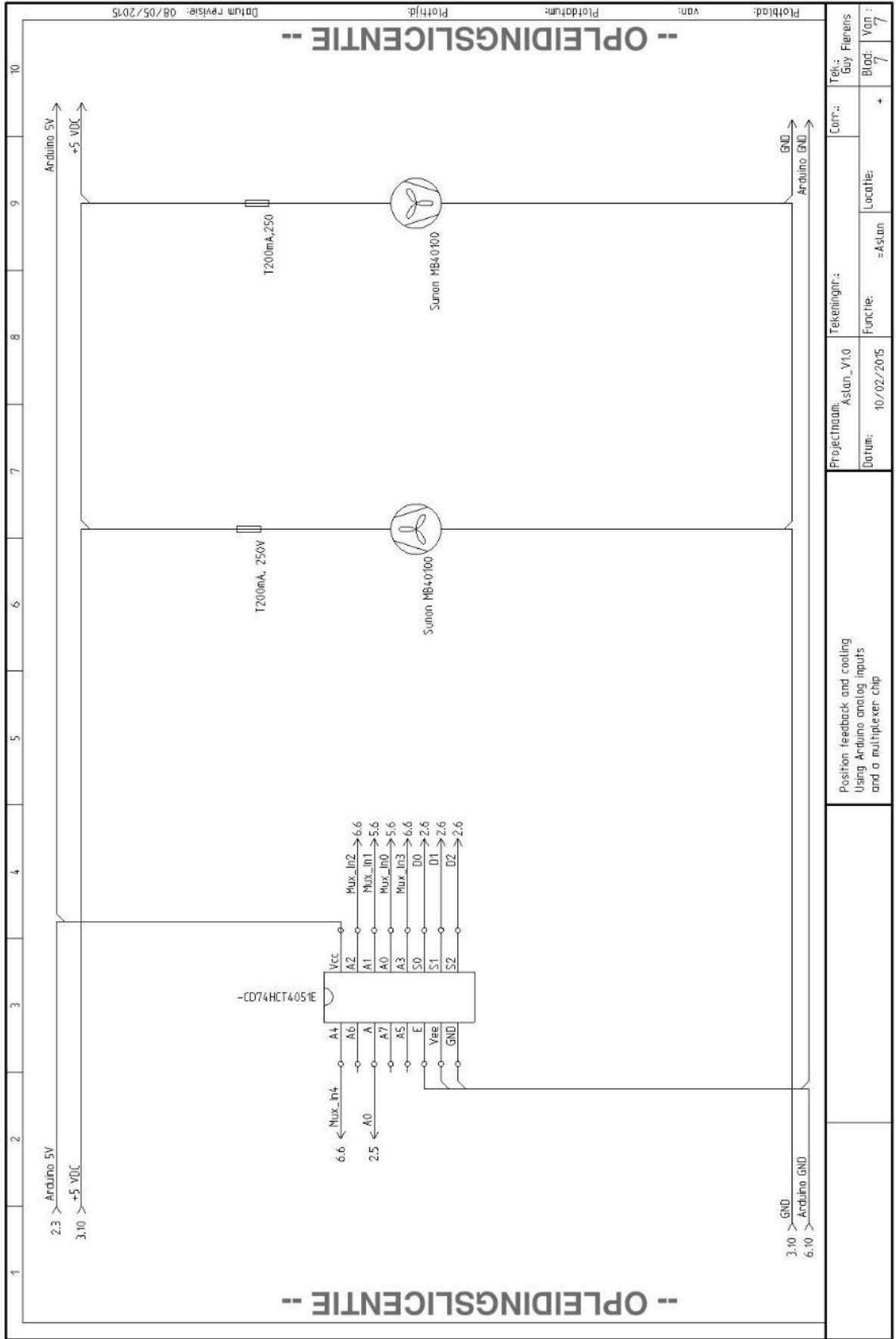
Projectnaam: Aslan_V10		Tekeningnr.: Aslan_V10	Corr.: +	Tek.: Galy Fienens
Datum: 05/01/2015		Functie: =Aslan	Locatie:	Blad: 4
				Van: 7



Projectnaam: Aslan_V1.0
Tekeningnr.:
Datum: 21/04/2015
Functie: =Aslan
Locatie:
Corr.:
Tek.: Guy Fierens
Blad: 5
Van: 7

Projectnaam: Aslan_V1.0		Tekeningnr.:	Corr.:	Tek.: Guy Fierens
Datum: 21/04/2015		Functie: =Aslan	Locatie:	Blad: 5
				Van: 7





ANNEX 24: LIMITED MOVABILITY OF BATAN MICRO SERVO MOTOR

Introduction

During the initial testing moments of the robot and the electronics system, a limited movability of the Batan micro servo motors has been observed. Although these servo motors have a mechanical movement range of 180°, the actual movement range (the movement range when actuated) is only 150°. In an attempt to resolve this movement limitation, a number of experiments have been performed.

Hypothesis 1

An incorrect pulse width is sent to the servo motor.

Background

As mentioned in paragraph 5.5.3, the frequently available analog RC servo motors are controlled with Pulse Width Modulation (PWM). This PWM signal is defined using three parameters: the minimum and maximum pulse width and the repetition rate. For RC servo motors the repetition rate is, in general defined to be 20ms. This means that the servo can read a new command every 20 ms.



Figure 215: PWM control of an analog servo motor [servocity.com]

As a part of this repetition rate, a minimum and maximum pulse width are defined. These two values are internally converted to the minimum or the maximum movement angle the servo can move to. Since there is no standard regarding the minimum and maximum pulse widths of standard RC servo motors, manufacturers are free to determine these values for their own products. The minimum pulse width varies around 1ms while the maximum pulse width varies around 2 ms.

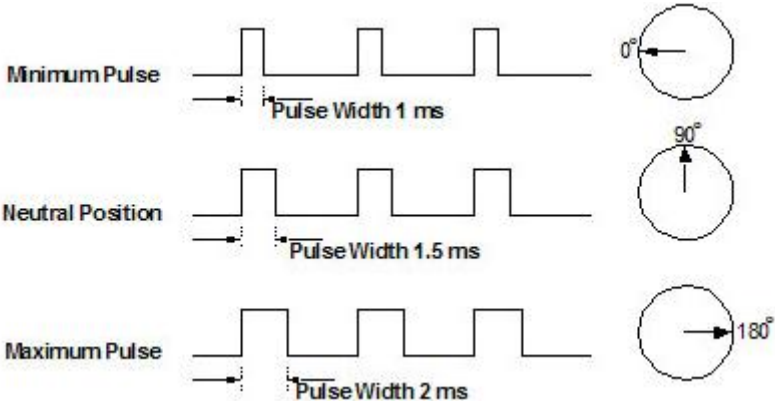


Figure 216: Minimum and maximum pulse width [servocity.com]

When using a servo driver to move RC servo motors, it is therefore important to know the minimum and maximum pulse widths in order to determine the servo’s bandwidth. The fact is that most servo drivers have a larger pulse width interval they can write just to control servo motors of different manufacturers. This should be taken into account when writing a program to move different servo motors.

Since this PWM bandwidth can vary between servo motors, different servo motors need to be tested in order to determine their bandwidth. Using the function 'writeMicroseconds()', which is a part of the Arduino servo library, the bandwidth of the servo can be determined. Using the Arduino's serial monitor a pulse width can be entered by the user.

The used code to test this hypothesis can be found in the portfolio as 'Hypothesis_1_Limited_movability.ino'.

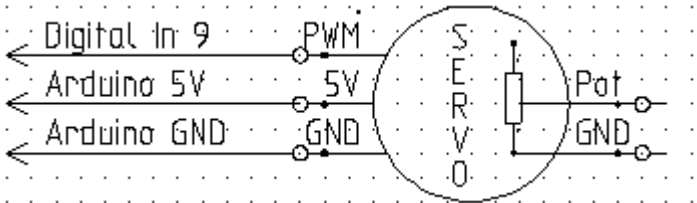


Figure 217: Hypothesis 1 Limited movability schematic

Test results

Four of the twelve available motors have been tested. Table 54 shows the observed results. The pulse length mentioned is the set pulse width using the writeMicroseconds()-function.

Table 54: Pulse width test results

Motor number	Actual zero angle (Pulse length)	Actual maximum angle (Pulse length)	Comment
1	30° (550 μs)	180° (2230 μs)	
2	30° (550 μs)	180° (2280 μs)	
3	30° (700 μs)	180° (2280 μs)	When a pulse width of 0μs is sent to Arduino, the motor returns to its mechanical 0° with the result of immediate overheating of the motor.
4	30° (550 μs)	180° (2350 μs)	

Conclusion

The measured bandwidth of the servo motors is 550 μs-2250 μs. This however does not provide the 180° movement angle but only a 150° movability. This limitation can have two possible causes:

- The mechanical safety is designed to thick.
- The servo's feedback potentiometer is wrongly placed.

The first of these two possible causes can easily be disproved by simply turning the servo's output axis. Since every servo has its mechanical movability of 180°, this hypothesis can be rejected.

Hypothesis 2

The servos feedback potentiometer is incorrectly placed.

Background

Again as mentioned in paragraph 5.5.3, the analog RC servo motors we use are equipped with a potentiometer mounted on the output axis to provide the servo system from feedback. Figure 218 shows a block diagram of the commonly used M51660L servo driver chip. Although this particular chip might not be used in the motors in our application, the images gives a clear view on the functioning of a servo controller. Internally, the potentiometer returns a certain voltage to the servo controller (pin 1). This voltage is then converted to a pulse with a certain length using a one-shot timer. The generated pulse is compared to the input pulse width (pin 5) and the error is finally amplified to a certain voltage to move the motor to the right position using pins 4, 6, 10 and 12.

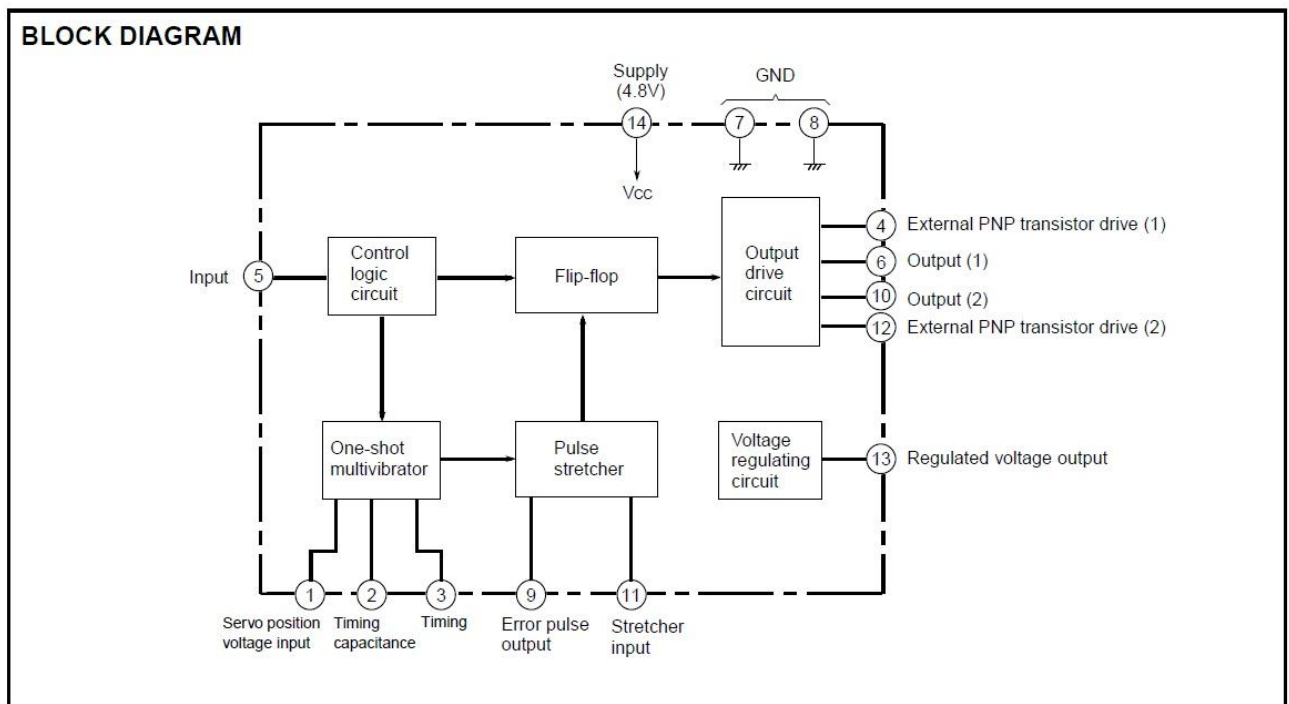


Figure 218: Servo block diagram [67]

The potentiometer is mechanically mounted on the output axis of the motor. In the case the potentiometer is mounted in the wrong position, it will measure a wrong movement angle of the output axis resulting in an incorrect controlling of the servo motor.

When the potentiometer is for example mounted with a deviation of 30° from the neutral position, the controller will interpret a mechanical movement of 30° as 0° , leading to a limited movement range.

Test results

After disassembling and examining the mechanical construction of the Batan S1123 micro servo motors, a mechanical constraint between the potentiometer's axis and the gears of the motor has been observed. This mechanical constraint prevents the option of simply dismounting the potentiometer, turn the potentiometer and mount it back in its housing.



Figure 219: Mechanical constraint on the servo potentiometer axis

Therefore the servo's feedback potentiometer has to be disconnected and replaced with an external potentiometer which can be turned manually. Using this external potentiometer, the angle position of the servo can be simulated.

This way, the servo motor can be tricked into the desired position. Thus simulating the effect of repositioning the internal potentiometer. A figure as well as a schematic can be found in Figure 221 and Figure 220: Hypothesis 2 Limited movability schematic

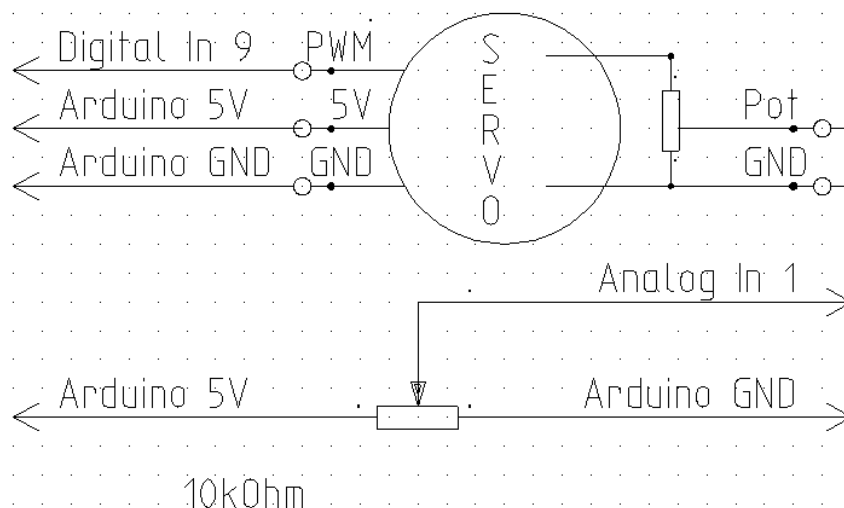


Figure 220: Hypothesis 2 Limited movability schematic

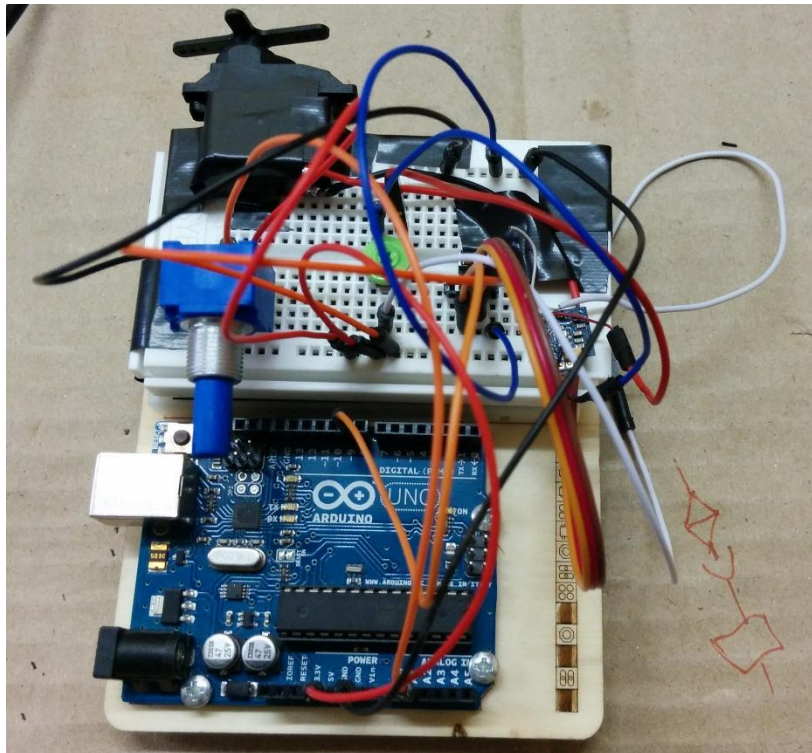


Figure 221: Hypothesis 3 limited movability

Using the blue 10k Ω potentiometer, a desired position can be entered. This analog value is mapped to a proportional pulse width and sent to the servo motor. Using the green 5k Ω potentiometer, the servo feedback can be modified in order to let the servo motor move to a stable position. Via serial communication, the user can see the desired angle and mapped values.

The code used to test this hypothesis can be found in the digital portfolio as 'Hypothesis 2 Limited movability'.

Conclusion

The performed test shows that it is possible move the feedback potentiometer in order to reach the servo's normal movement range. Using the above described technique, the servo motor is able to reach its full 180° movement range.

An additional advantage presents itself in simplifying the general control of the robot. In the current setup where every joint is remotely tendon actuated by the servo motors, the movement of other joints proximal to a specific joint also effect the movement of the joint itself. This as a result of the tendon movement along the moved proximal joints.

By dismounting the feedback potentiometer from the servo housing and mounting it directly on the actuated joint, this effect is eliminated. The servo motor will keep moving until the desired joint angle is reached, regardless the movement of proximal joints.

The implementation of the feedback potentiometers in the mechanical design of the robot will be a thesis topic for the upcoming academic year. The joints themselves have to be redesigned and a guidance for the electrical cables has to be designed as well. Another advantage of mounting the feedback potentiometers directly on the actuated joint is the simplification of the mounting of the feedback used in the software safety in the robot.

Hypothesis 3

The limited movability is proper to the Batan S1123 micro servo motors.

Test results

Four different motors have been tested. The code used repeatedly moves the motors to their minimum and maximum positions with a delay of 2s between movements. The actual movement range can then be compared visually to the mechanical movement range. Table 55 and Table 56 show the measured data for this experiment. Note that the register values or pulse widths written to the servo motors are the minimum and maximum values the servo driver is able to send to the motors. The servo specific pulse widths are neglected in this experiment.

Since four different motors have been used, the experiment was performed using the Designer Systems DS-SCX18.S servo driver. The power requirements necessary to move the motors simultaneously exceed the maximum values of the Arduino Due microcontroller, therefore the Designer Systems servo driver has been used.

Table 55: Actual minimum of different servo motors

Servo motor	Actual minimum	Used register value (Pulse width)
Batan S1123 micro servo	30°	5 (500 µs)
Batan S1213 standard servo	0°	5 (500 µs)
FS5106B standard servo	0°	5 (500 µs)
Sparkfun generic sub-micro size servo motor	0°	5 (500 µs)

Table 56: Actual maximum of different servo motors

Servo motor	Actual maximum	Used register value (Pulse width)
Batan S1123 micro servo	180°	250 (2500 µs)
Batan S1213 standard servo	180°	250 (2500 µs)
FS5106B standard servo	180°	250 (2500 µs)
Sparkfun generic sub-micro size servo motor	180°	230 (2300 µs)

Conclusion

The maximum positions of the different servos mentioned in Table 56, are the same for every tested servo motor.

The minimum positions however are not equal for the different servo motors. The Batan S1123 micro servo motors purchased to use in the Aslan robot show a limited movability whilst the other 3 models cover their whole mechanical movement range.

Further testing of the robot, in cooperation with Jasper will determine whether this limited movability of 150° will suffice for the Aslan robot. For the joints where the full 180° movability is required, new servo motors will have to be purchased.

Video footage, as well as the used code can be found in the digital portfolio as 'Hypothesis_3_Limited_Movability'.

ANNEX 25: UNEXPECTED BEHAVIOR OF SERVO MOTORS

Introduction

Besides the above mentioned limited movement range, initial testing revealed another problem. When certain commands are written to the Designer Systems DS-SCX18.S servo driver, the servo motor does not react like expected. Two irregular phenomenon's often occur:

- When a servo motor reaches a certain position, it 'vibrates' on that position. Instead of reaching a stable position the servo motor remains powered, creating a buzzing sound and constant power usage of the motor, leading to rising temperatures and eventually overheating damage.
- Certain commands cause an oscillating behavior of the servo where the servo starts moving back and forth between its movement limits instead of moving to the desired position. This oscillating behavior remains until another command is written to the servo driver.

In order to resolve this irregular behavior, and in order to create a robot able to show the right gestures without overheating or twitching, a couple of experiments have been performed.

Hypothesis 1

The received pulse width is incorrectly interpreted by the servos

Background

The same reasoning applies as in the first hypothesis of Annex 24.

Test results

The same results apply as in the first hypothesis of Annex 24, and to rule out the possibility that this behavior is specific to the Batan S1123 micro servo motors, the tests have also been performed with a FS5106B standard size servo.

Conclusion

When tested directly with the Arduino microcontroller, the unexpected behavior does not occur with both the servo motors. This means that the cause of this behavior can be found in the program using the Designer Systems DS-SCX18.S servo controller.

Since only two control registers are used to control a single servo motor, the structure of these two registers need to be examined.

Hypothesis 2

An incorrect value is written to the servos control registers.

Background

Considering the information of the DS-SCX18.S data sheet in Annex 22.1, it can be seen that in order to control a single servo motor, two registers have to be defined (Figure 222).

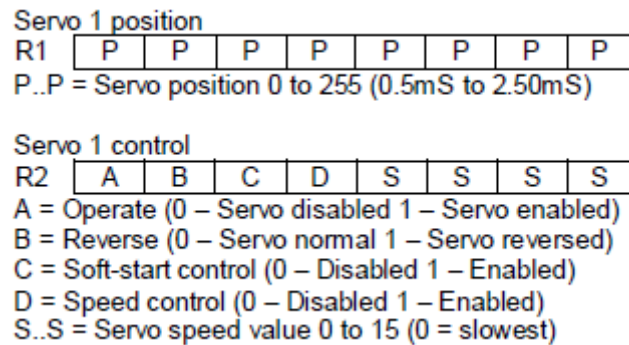


Figure 222: Control registers

For e.g. the first servo motor, registers one and two need to be defined and written to the servo driver. The first register, R1, describes the position the servo motor needs to move to and determines therefore the pulse width the driver sends to the motor.

The second register, R2, contains more information about how the servo-motor needs to reach this position. According to the datasheet, a couple of different options or features can be set using this control register:

- *Operate*: Enable or disable the servo motor
- *Reverse*: Enabling this bit reverses the respective servo. A reversed servo reacts opposite to the intended position (pulse width) [67]. This implies that for a servo motor with a bandwidth of 1000 μ s for 0° to 2000 μ s for 180° when reversed will move to 0° when a pulse width of 2000 μ s is sent to the motor.
- *Soft start control*: When soft-start control is enabled, the servo driver will send the desired pulse width to the motor in a ramping manner until the desired position is reached. Besides the obvious advantage of soft-starting the servo motor, a disadvantage is the fact that the servo driver is during a longer time occupied with the particular servo. This might compromise the movement timing for other servo motors or in the case the program does not take the delay into account, the servo will not reach the desired position before a new command is written to the driver.
- *Speed control*: enables the user to set the movement speed of the servo motor. Fifteen different speeds can be set.

In the following test, only speed control and soft-start control will be tested since both the enable bit and the reverse bit can already be ruled out as a possible cause of the described behavior.

Test results

Both soft-start control and speed control have been tested for a single servo motor, since every servo motor suffers from the same irregular behavior. Table 57 show the test results using the robots main program 'Aslan_v0_7.ino', which can be found in the digital portfolio.

Table 57: Control register test results

Soft start	Speed control	Speed	Behavior
Enabled	Disabled	/	Normal
Enabled	Enabled	13	Abnormal
Disabled	Enabled	12	Abnormal
Disabled	Enabled	11	Abnormal
Disabled	Enabled	10	Normal
Disabled	Enabled	9	Abnormal
Enabled	Enabled	9	Normal

Conclusion

As can be seen from Table 57, the abnormal behavior only occurs when speed control is enabled, for only a number of possible speeds. In combination with the soft-start control, the abnormal behavior stops occurring. Simply enabling soft-start control for every single movement is however not a possibility because the thus generated delay will compromise the cooperation and general functioning of the entire robot. Therefore, soft-start control will only be enabled for the problem cases, and speed control will be disabled with every motor.

What exactly causes this irregular behavior remains a question and an answer can not be found in literature. Therefore, Designer Systems tech support has been contacted to help solve and explain this problem.

After running the test code sent to the Designer Systems tech support in their lab, we received following answer regarding our problem:

- The test were performed with a HS311 standard servo, and the abnormal behavior occurring with speed control enabled did not occur with that type of motor. The behavior can therefore be assigned to the Batan S1123 servo motor.
- The minimum and maximum register values should be limited to respectively 32 and 210 (756 μ s to 2180 μ s).
- The soft start function requires at least five seconds to operate to a point where the servo is being driven with the constant 22 ms pulse signal. The signal ramps up from about 0.5 ms to 22 ms, taking about five seconds.
- Soft start operates in tandem with speed control. Depending upon the speed set, the servo may have already reached its final position when the soft start process completes.

According to these four remarks from Designer Systems, the following will be performed: soft start will be disabled for every motor, speed control will only be enabled for the motors in the elbow and the register limits will be altered.

ANNEX 26: BILL OF MATERIALS

Part	Amount	Unit price	Price
Arduino Due	1	€ 49,99	€ 49,99
Designer Systems DS-SCX18.S	3	€ 37,44	€ 112,32
TDK Lambda LS100-5	1	€ 41,28	€ 41,28
Jumper wires 6" F/F 10 pack	2	€ 3,95	€ 7,90
Jumper wires 6" M/M 10 pack	2	€ 3,95	€ 7,90
1,5mm ² cable	3	€ 2,43	€ 7,29
1mm ² cable	10	€ 0,55	€ 5,50
0,22mm ² cable	1	€ 9,99	€ 9,99
5x20mm fuse holder	6	€ 0,46	€ 2,76
Fuse holder shield	6	€ 0,81	€ 4,86
F0,8A, 250V 5x20 fuse	1	€ 1,67	€ 1,67
T0,2A, 250V 5x20 fuse	1	€ 2,01	€ 2,01
T4A,250V 5x20 fuse	1	€ 2,40	€ 2,40
TE Connectivity 1-963484-1	1	15,73	€ 15,73
TE Connectivity 1-968879-1	1	12,79	€ 12,79
Buscontact Micro II	90	0,35	€ 31,50
Grounded grid connector	1	€ 2,99	€ 2,99
Plug C13/C14 male	1	€ 3,66	€ 3,66
Plug C13*C14 female with power button	1	€ 2,58	€ 2,58
Tubingsset	1	€ 22,04	€ 22,04
Solder	1	€ 8,79	€ 8,79
9V DS14-M connector	1	€ 2,89	€ 2,89
Sunon cooling fan	2	€ 7,81	€ 15,62
Protective grille for cooling fans	2	€ 0,96	€ 1,92
Wire markers	1	€ 11,19	€ 11,19
Extension cables	16	€ 1,20	€ 19,20
Micro servo motor	12	€ 11,59	€ 139,08
Standard servo motor	4	€ 8,90	€ 35,60
Aluminum Channel - 3,0"	1	€ 3,57	€ 3,57
Channel bracket A	1	€ 4,47	€ 4,47
Channel bracket C	1	€ 3,57	€ 3,57
Channel Mount Gearbox Kit - Standard 7:1	2	€ 53,68	€ 107,36
ServoBlock Kit - Hitec Standard	1	€ 24,15	€ 24,15
Machine screw -Socket head (6-32;1/4")	1	€ 1,51	€ 1,51
Ultimaker filament 1 role	1	€ 41,99	€ 41,99
Mounting cabinet	1	€ 80,00	€ 80,00
Mounting plate	1	€ 16,99	€ 16,99
Dyneema fishing line	1	€ 10,00	€ 10,00
Ball chain	1	€ 4,99	€ 4,99
Polystyren plate 11m ³	1	€ 12,49	€ 12,49
Sum:			€ 892,54

ANNEX 27: PORTFOLIO

Here the structure can be found concerning the useful documents next year.

● **Portfolio**

- Alphabet
- Electrical design
 - Datasheets
 - Schematics
- General project information
 - Finances
 - Open house
- Mechanical design
 - Cables
 - Cura
 - Important components
 - Electrical motors
 - Inventor
 - Extra
 - Support piece electronics
- Programming
 - Aslan
 - Aslan
 - Aslan_V0_3
 - Aslan_V0_4
 - Aslan_V0_5
 - Aslan_V0_6
 - Aslan_V0_7
 - Aslan_V0_8
 - Aslan_V0_9
 - Aslan_V0_10
 - Calibration_V0_1
 - Lines
 - Natural
 - Original
 - Servo testing
 - Hypothesis_1_Limited_movability
 - Hypothesis_2_Limited_movability
 - Hypothesis_3_Limited_movability
 - Software safety
 - Software_safety
 - Software_safety_V0_1
 - Software_safety_V0_2

